

ISSN 0137-5075 (print)
ISSN 2300-262X (online)



P O L I S H A C A D E M Y O F S C I E N C E S
I N S T I T U T E O F F U N D A M E N T A L T E C H N O L O G I C A L R E S E A R C H
C O M M I T T E E O N A C O U S T I C S • P O L I S H A C O U S T I C A L S O C I E T Y

ARCHIVES of ACOUSTICS

QUARTERLY

Vol. 38, No. 4, 2013

WARSZAWA



ARCHIVES of ACOUSTICS

QUARTERLY, Vol. 38, No. 4, 2013

In Memoriam, <i>Professor Zbigniew Witold Engel</i>	453
Research Papers	
C. Huang, G. Chen, H. Yu, Y. Bao, L. Zhao, <i>Speech emotion recognition under white noise</i>	457
J. Yan, X. Wang, W. Gu, L. Ma, <i>Speech emotion recognition based on sparse representation</i>	465
Z. Dąbrowski, J. Dziurdź, R. Pakowski, <i>Selection of sound insulating elements in hydraulic excavators based on identification of vibroacoustic energy propagation paths</i>	471
S. Bernat, <i>Awareness of noise hazards and the value of soundscapes in Polish national parks</i>	479
G. Klekot, <i>Indicator of vibroacoustic energy propagation as a selection criterion of design solution</i>	489
T.G. Zieliński, M. Potoczek, R.E. Śliwa, Ł.J. Nowak, <i>Acoustic absorption of a new class of alumina foams with various high-porosity levels</i>	495
M. Martins, L. Godinho, L. Picado-Santos, <i>Numerical evaluation of sound attenuation provided by periodic structures</i>	503
A. Crespo, M. Recuero, G. Galvez, A. Begoña, <i>Effect of binaural stimulation on attention and EEG</i>	517
S. Wrona, M. Pawełczyk, <i>Controllability-oriented placement of actuators for active noise-vibration control of rectangular plates using a memetic algorithm</i>	529
K. Mazur, M. Pawełczyk, <i>Active Noise Control with a single nonlinear control filter for a vibrating plate with multiple actuators</i>	537
Technical Notes	
R. del Rey, J. Alba, J.P. Arenas, J. Ramis, <i>Evaluation of two alternative procedures for measuring airflow resistance of sound absorbing materials</i>	547
M. Liedtke, J. Rissler, U. Kaulbars, <i>Latest developments in international standardization of whole-body and hand-arm vibration</i>	555
B. Smagowska, <i>An objective and subjective study of noise exposure within the frequency range from 10 kHz to 40 kHz</i>	559
B. Kruk, <i>Influence of material used for the regenerator on the properties of a thermoacoustic heat pump</i>	565
In Memoriam	
Professor Marian Urbańczyk	571
Professor Mikołaj Łabowski	573
Calendar of Events	
Conferences	575

Editorial Board

Editor-in-Chief: NOWICKI Andrzej (Institute of Fundamental Technological Research PAN, Warszawa)

Deputy Editor-in-Chief: MEISSNER Mirosław (Institute of Fundamental Technological Research PAN, Warszawa)

Associate Editors

ADAMCZYK Jan (AGH University of Science and Technology, Kraków)

BATKO Wojciech (AGH University of Science and Technology, Kraków)

DANICKI Eugeniusz (Institute of Fundamental Technological Research PAN, Warszawa)

GRELOWSKA Grażyna (Polish Naval Academy, Gdynia)

GUBRYNOWICZ Ryszard (Polish-Japanese Institute of Information Technology, Warszawa)

GUDRA Tadeusz (Wrocław University of Technology, Wrocław)

KAMISIŃSKI Tadeusz (AGH University of Science and Technology, Kraków)

KUJAWSKA Tamara (Institute of Fundamental Technological Research PAN, Warszawa)

KULKA Zbigniew (Warsaw University of Technology, Warszawa)

MAKAREWICZ Rufin (Adam Mickiewicz University, Poznań)

MIŚKIEWICZ Andrzej (The Fryderyk Chopin University of Music, Warszawa)

PREIS Anna (Adam Mickiewicz University, Poznań)

RDZANEK Wojciech P. (University of Rzeszów, Rzeszów)

SNAKOWSKA Anna (AGH University of Science and Technology, Kraków)

Secretary: ŻYCHOWICZ-POKULNIEWICZ Joanna

Advisory Editorial Board

Chairman: DOBRUCKI Andrzej (Wrocław University of Technology, Wrocław)

BJØRNØ Leif (Technical University of Denmark, Lyngby)

BLAUERT Jens (Ruhr University, Bochum)

BRADLEY David (The Pennsylvania State University, Pennsylvania)

CROCKER Malcom J. (Auburn University)

DEMENKO Grażyna (Adam Mickiewicz University, Poznań)

ELLIOTT Stephen J. (University of Southampton, Southampton)

ENGEL Zbigniew (Central Institute for Labour Protection, Warszawa, retired prof. AGH)

HANSEN Collin (University of Adelaide, Adelaide)

HESS Wolfgang (University of Bonn, Bonn)

KOZACZKA Eugeniusz (Naval University of Gdynia, Gdynia)

LEIGHTON Tim G. (University of Southampton, Southampton)

LEWIN Peter A. (Drexel University, Philadelphia)

PUSTELNY Tadeusz (Silesian University of Technology, Gliwice)

RAKOWSKI Andrzej (The Fryderyk Chopin University of Music, Warszawa)

SUNDBERG Johan (Royal Institute of Technology, Stockholm)

ŚLIWIŃSKI Antoni (University of Gdańsk, Gdańsk)

TITTMANN Bernhard R. (The Pennsylvania State University, Pennsylvania)

TORTOLI Piero (University of Florence, Florence)

VORLÄNDER Michael (Institute of Technical Acoustics, RWTH Aachen)

WESOŁOWSKI Zbigniew (Polish Academy of Science, Warszawa)

ZWISŁOCKI Jozef J. (Syracuse University, Syracuse)

Editorial Board Office:

Pawińskiego 5B, 02-106 Warszawa (Poland)

fax (48-22) 826 98 15, phone (48-22) 826 12 81 ext. 206

e-mail: akustyka@ippt.pan.pl <http://acoustics.ippt.pan.pl>

PRINTED IN POLAND

Indexed and abstracted in Science Citation Index Expanded (also known as SciSearch®)
and Journal Citation Reports/Science Edition

Abstracted in Acoustics Abstracts, in Applied Mechanics Reviews
and indexed in Journal of the Acoustical Society of America

Recognised by the International Institute of Acoustics and Vibration, I IAV

Edition co-sponsored by Ministry of Science and Higher Education

Arkuszy wydawniczych 20 Arkuszy drukarskich 16

Skład i łamanie w systemie TeX: Dział Wydawnictw IPPT PAN – K. JEZIERSKA

In Memoriam

Professor Zbigniew Witold ENGEL 1933 – 2013



Professor Zbigniew Witold Engel in his element.

When we look at the history of AGH – University of Science and Technology, recognized as one of the best universities in the country, we find that for that success many people worked for several dozen years. However, the subjects, the methodology and directions of their work were shaped by units – outstanding personalities of science. Just to mention, among others Professors Stanisław Zuber, Władysław Takliński, Witold Budryk, Maksymilian Tytus Huber and Władysław Bogusz. These people have shaped our institution, marked its new path of development and permanent place in the history of Polish and world science. To belong to such a group is a great ennoblement, for which one works out for his entire life. Undoubtedly,

such personality was also Professor Zbigniew Witold Engel, to whom we said goodbye on November, 6th, 2013, in the St. Clement's church in Wieliczka.

Professor was born on April 1, 1933, in Zawady near Zhovkva in the province of Lviv. After graduating from Jan Matejko Middle and High School in Wieliczka in 1950 earned a matriculation certificate. Then he began his studies at the Department of Communications of Polytechnic Departments of Academy of Mining and Metallurgy and involved with our university for the next 63 years. October 1, 1952 the Department of Mechanics of the University of Mining and Metallurgy was created, and soon after began professor's adventure that was the work of science, education

and organization. The history and fate of our university are inextricably linked with the person of professor who practically since the very beginning of the Faculty supported it in all areas of its activities, and has always actively participated in academic life.

Scientific career

When in 1955 he graduated with the degree of Master of Engineering he already was employed for two years as a deputy assistant at the Department of Applied Mechanics. He defended his dissertation “Analysis and synthesis of planar mechanisms, especially the crank-slider” in 1962, and then in 1966 he obtained his PhD with a thesis “Some aspects of vibration technology”. He earned the degree of associate professor in 1973, and in 1978 the title of professor. Area of scientific interests of Professor Zbigniew Engel covered a very broad spectrum of issues: from analysis and synthesis of mechanisms, dynamics of machinery, selected topics of linear and non-linear mechanical vibrations, elements of vibration technology, environmental acoustics, control of noise and vibration, methods of active noise and vibration reduction, methods of research on vibroacoustical processes, reciprocity and inversion methods.

The result of these extensive interests were more than 580 publications, 15 patents and countless works, studies, expert opinions made for the industry.

Another effect of this activity was the recognition received by professor in the scientific community, reflected in a number of memberships granted to him in many prestigious organizations such as the Academy of Engineering in Poland, New York Academy of Sciences, St. Petersburg Academy of Sciences, Academie Europeenne des Sciences, des Arts et des Lettres, Institute of Noise Control Engineering, USA, Polish Society of Theoretical and Applied Mechanics, Polish Society of Technical Diagnostics, Deutsche Gesellschaft für Akustik, Gesellschaft für Angewandte Mathematik und Mechanik, Polish Acoustical Society, Noise Control League, East-European Acoustical Society of St. Petersburg, and the Union of Scientists and Engineers in Moscow. He was a chairman of the Committee on Acoustics of the Polish Academy of Sciences, Vice-President of the Central Council and Higher Education. During many years he was a Chairman of the Commission of Applied Mechanics of Krakow Department of Polish Academy of Sciences.

He also received the dignity of Honorary Professor of Warsaw University of Technology and for his exceptional achievements in and outstanding contribution to education of young researchers Professor Zbigniew Engel was honored by the University Senates of: AGH University of Science and Technology, Krakow University of Technology and the University of Kielce with the title of Honorary Doctors Causa of the University.

Also worth mentioning is his great contribution in the work related to the technological project of laboratory rooms at the Kielce University of Technology.

But undoubtedly the greatest success of professor is related to vibroacoustics, that he himself defined as a new discipline of science, and his achievements in this area are impressive. It is the result of his work and initiative that caused the consolidation of the theory of mechanical vibrations with the mechanics of acoustic phenomena in one coupled mechanical-acoustical model. Professor Engel has defined the frame, the basic goals and tasks of vibroacoustics.

Organizational and teaching abilities

As a demanding teacher he stimulated his colleagues – doctors, assistants, professors. The showed at the office promptly at 7, where every day he set an example to other employees with his diligence and thoroughness. In this way, without any discipline and rigor he set us a high standard. He supervised more than 200 theses in both engineering and masters. He has supervised 38 PhDs and reviewed more than 100 doctoral dissertations and over 50 habilitation dissertations. Has also written dozens of professors’ reviews. Through the years, we appreciate his uncommon ability to organize the environment around the current theme. He also cared for effective spreading of ideas. As a result, we can now say that he created his own Scientific School.

Taking into account the achievements of professor one can say that he pointed us the subject to work on and organized place for its implementation, since it is thanks to his efforts, that the building of the Institute of Mechanics and Vibroacoustics emerged, and now students affectionately call it a “Chocolate”.



Incorporation of the foundation stone for the building of the Institute of Mechanics and Vibroacoustics.

In that way, Professor Engel entered forever not only in the history but also in the landscape of our university. The history of the design and construction of the “Chocolate” is a record of great determination



Near Danish pavilion at the fair in Poznan in June 1975.

and strive of professor. Given the times, social relations and a number of objective difficulties involved (access to materials, formal difficulties, location etc.) that the actions of the professor managed to overcome it can be said that the building that, at that time, housed the global unique laboratories in the form of anechoic chamber and reverberation chamber is “his baby”. Thanks to the efforts of Professors Engel and Bogusz it was possible visit the plants of Sulzer in Winterthur, Switzerland, where it was possible to become acquainted with the technical documentation and work of similar laboratories.

Moreover, cooperation with foreign countries is another rich chapter in the biography of Professor Engel, who has always very actively collaborated with institutions and research organizations from around the world, including: Purdue University (USA), MIT (USA), University of Philadelphia (USA), Technical Universities in Vienna, Bratislava, Copenhagen, Tokyo, Kiev, Institute of Materials and Machine Mechanics of the Slovak Academy of Sciences, Polytechnic Institute of St. Petersburg, the Institute of Mechanical Engineering of Russian Academy of Sciences, Technical University of Lviv. Professor Zbigniew Engel was a member of many scientific committees of conferences and congresses, among others: Miami, Edinburgh, Munich, Beijing, Avignon, Newport Beach, Toronto, The Hague, Budapest, Seoul, Prague, Rio de Janeiro. He chaired the Scientific Committee of the Conference “Noise and Vibration in Transportation” in St. Petersburg. For his work in the international arena he has been awarded with, among others: Gold Medal of the Krizik’s Czechoslovak Academy of Science, Hun-

garian Medal “Pro Silentia”. The professor was also the main initiator and organizer of the International Conference on Noise Control “NOISE CONTROL”.

Another beautiful page in the professional curriculum vitae of professor is his almost fifty years of collaboration with the Central Institute for Labour Protection – National Research Institute. For over 40 years he was a member of the Scientific Council of the Institute, and for the last 15 years its president. Virtually he created from scratch the Department of Vibroacoustic Hazards, engaging and mobilizing to work fine professionals from across the Poland. Thanks to him an independent and considerate scientific and research center was established.

Wide range of interests

Professor Engel was without a doubt an outstanding mechanic, but he was also a great humanist of wide range of non-technical interests. He was passionate about history of art, and the combination of these passions has resulted in the book “Acoustics of sacred objects”.

He was also fascinated by the history of science and the history of our university. Richly documented memories and reflections of the Faculty of Mechanical Engineering and Robotics he described in the book “Sixty years have passed...” and the book, published in 2008, “Department of Mechanics and Vibroacoustics AGH University tradition – history – activity” is a record of the history of the Department, which he has co-founded. He was the author of numerous scientific publications presenting profiles of outstanding Polish scientists (among others: co-author of the book “Maksymilian Tytus Huber: biography and reprints of scientific works”).

Citizen and charity work

Despite his commitment to the scientific and academic professor was able to save more time for social activities. Such activities may include active participation in local community life. He was a member of the Club of Friends of Wieliczka, and willingly participated in various initiatives of the organization. In recent years (since 2011) he engaged himself in the work of the University of the Third Age that was created in Wieliczka, where he served as Chairman of the Program Council.

He was never indifferent to local issues and with a sense of satisfaction he involved in the social life of his nearest area, and thus tried to contribute to its development.

Professor Zbigniew Engel was the initiator and one of the founders of Engel Family Foundation, which, among others, grants the awards named after Professor Zbigniew Engel for best scientific work that includes

doctoral dissertations, habilitation dissertation, monograph or a series of articles. The awards are granted to young scientific-didactic workers of AGH University of Science and Technology, Krakow University of Technology and Kielce University of Technology.

For his activities professor was granted numerous awards and designations: Golden Cross of Merit, Knight's Cross of the Order of Polonia Restituta and Officer's Cross of the Order of Polonia Restituta, Commander's Cross of the Order of Polonia Restituta, Medal of the National Education Commission. He was also the winner of many awards, including: Award of the Minister of Higher Education, Ministry of National Education, the Ministry of Construction and Awards of Royal Capital City of Krakow in the field of science and technology.

Family and friends

Professor Engel was a great man of family. His wife and children have always been the center of his world, in them he had his support and refuge. With



Professor with his wife Maria.

his wife Maria, whom their friends called the Masia, were an inseparable pair. They were married for 57 years and all these years Masia together with professor participated in countless conferences and business trips.

In recent years, during the fight with the Professor's disease, she was a source of support and strength for him. Like the sons Jacek and Zbigniew Junior, who were always his joy and pride. They both have achieved great professional success and started their families, bringing another inexhaustible source of joy for professor – four grandchildren.



Professor with his family.

His love and care for home and family were exceptional. It is significant also that the activity, which he was very fond of and which relaxed him most was the gardening.

Professor was a wonderful, kind friend, he was very sociable. His house was always open, and friendships lasted for long years. He and his wife were the organizers and hosts of regular meetings with colleagues from professor's Middle School.

The professor was a multi-dimensional man, man-institution. All of us who knew him, were impressed by his steadfastness, diligence, strength and almost legendary perseverance. Especially in recent years, when with the incredible fortitude he fought with severe disease. He still worked, wrote, participated in conferences. He never gave up.

It is said that there are no irreplaceable people. Professor Zbigniew Engel is proof that's not true. He was a person of such outstanding achievements in so many fields, with such a rich scientific legacy and social impact so huge that no one can take his place.

Kraków, 20.11.2013

*Jan Adamczyk
Wojciech Batko*

Speech Emotion Recognition under White Noise

Chengwei HUANG⁽¹⁾, Guoming CHEN⁽¹⁾, Hua YU⁽¹⁾, Yongqiang BAO⁽²⁾, Li ZHAO⁽¹⁾

⁽¹⁾ *School of Information Science and Engineering
Southeast University*

2# Sipailou, Nanjing 210096, Jiangsu Prov., China; e-mail: huang.chengwei1@gmail.com

⁽²⁾ *School of Communication Engineering
Nanjing Institute of Technology*

1# Hongjing Ave., Nanjing 211167, Jiangsu Prov., China

(received April 30, 2012; accepted February 6, 2013)

Speaker's emotional states are recognized from speech signal with Additive white Gaussian noise (AWGN). The influence of white noise on a typical emotion recognition system is studied. The emotion classifier is implemented with Gaussian mixture model (GMM). A Chinese speech emotion database is used for training and testing, which includes nine emotion classes (e.g. happiness, sadness, anger, surprise, fear, anxiety, hesitation, confidence and neutral state). Two speech enhancement algorithms are introduced for improved emotion classification. In the experiments, the Gaussian mixture model is trained on the clean speech data, while tested under AWGN with various signal to noise ratios (SNRs). The emotion class model and the dimension space model are both adopted for the evaluation of the emotion recognition system. Regarding the emotion class model, the nine emotion classes are classified. Considering the dimension space model, the arousal dimension and the valence dimension are classified into positive regions or negative regions. The experimental results show that the speech enhancement algorithms constantly improve the performance of our emotion recognition system under various SNRs, and the positive emotions are more likely to be miss-classified as negative emotions under white noise environment.

Keywords: speech emotion recognition; speech enhancement; emotion model; Gaussian mixture model.

Notations

$x(t)$ – clean speech signal,
 $n(t)$ – noise signal,
 $y(t)$ – speech signal contained noise,
 ω – Fourier frequency,
 $X(\omega)$ – Fourier transformation of $x(t)$,
 $Y(\omega)$ – Fourier transformation of $y(t)$,
 $N(\omega)$ – Fourier transformation of $n(t)$,
 $P_x(\omega)$ – power spectral density of $x(t)$,
 $P_y(\omega)$ – power spectral density of $y(t)$,
 $P_n(\omega)$ – power spectral density of $n(t)$,
 m – index of speech signal frame,
 k – discrete Fourier frequency,
 $X(m, k)$ – discrete Fourier Transformation of the m -th frame,
 $\hat{X}(m, k)$ – enhanced speech from $X(m, k)$,
 G_{SP} – transfer function,
 $\xi_{m|m'}$ – priori SNR,
 γ_m – posterior SNR,
 $T(m, k)$ – masking threshold,
 $\alpha(m, k)$ – parameter in the second speech enhancement algorithm (10),
 M – symbol for simplicity of presentation,
 σ_s^2 – speech signal power,

σ_n^2 – noise signal power,
 B – symbol for simplicity of presentation,
 C – symbol for simplicity of presentation,
 \mathbf{S} – feature vector of the input sample,
 λ – parameters of GMM,
 q – index of the Gaussian mixtures,
 Q – the mixture number,
 a_i – the mixture weight,
 b_i – Gaussian distribution function,
 j^* – index of the target emotion,
 N – number of emotions,
 j – index of emotions,
 μ_q – mean of q -th Gaussian distribution,
 Σ_q – covariance matrix of q -th Gaussian distribution,
 K – class number in the K-mean clustering.

1. Introduction

Emotions in vocal communication are very important for understanding speaker's intention, mood, and attitude. Unlike linguistic information, affective information is expressed even without the notice of the

speaker (JOHNSTONE *et al.*, 2005; SCHERER, 2003). These emotions are naturally expressed and uneasy to disguise or control, which makes speech emotion recognition very important in natural human-computer interaction.

There are many challenges in the real world applications. In the in-car environment, driver's emotional stability is a crucial problem for driving safety. C.M. JONES and I. JONSON studied an in-car emotion recognition system which may help the driver to respond appropriately (JONES, JONSON, 2005). C. CLAVEL *et al.* studied the fear-type emotions in an audio-based surveillance system (CLAVEL *et al.*, 2008). Fear-type emotions may be a sign of potential threats. J. ANG *et al.* used the prosodic features to detect frustration and annoyance in natural human-computer dialog (ANG *et al.*, 2002).

Oriented to the real world applications, the noise problem is considered in our research. Noise is an important factor which affects the performance of most speech recognition systems (VARGA, STEENEKEN, 1993). However, it has rarely been studied in speech emotion recognition, since most of the researches were carried out in an ideal lab environment (HUANG *et al.*, 2011; HUANG *et al.*, 2009; JOHNSTONE *et al.*, 2005; NEIBERG, 2006; TRUONG, 2009). SCHULLER *et al.* first studied the noise problem in automatic speech emotion recognition (SCHULLER *et al.*, 2006). TAWARI *et al.* then proposed a framework to improve the speech emotion recognition under noisy environment (TAWARI, TRIVEDI, 2010). In their framework the noise cancellation was based on the adaptive thresholding in wavelet domain. However there are still more speech enhancement methods to be explored in order to work properly with the emotion recognition module.

Emotion model is another important problem in emotion recognition. Emotion class model was used in the most attempts to classify emotions in the early researches (AYADIA *et al.*, 2010; SCHERER, 2003; ZENG *et al.*, 2009). Basic human emotions like happiness, sadness, fear, anger, disgust, surprise were detected from speech signals under controlled conditions. However, in the real world applications we need to deal with various emotions which may not be recognized using the pre-trained emotion class models. M. WÖLLMER *et al.* suggested abandoning the emotion classes (WÖLLMER *et al.*, 2008). They proposed to detect the arousal dimension and the valence dimension instead. In this paper we adopt both the emotion class model and the dimension space model to evaluate our speech emotion recognition system under a noisy environment.

2. The database

A Chinese speech emotion database built in our lab is adopted in this paper, which includes two data

sources, the acted speech and the induced speech, as shown in Table 1. The acted speech data contains six emotions, which are fear, surprise, anger, happiness, sadness and neutral (CAI, 2005). Six professional male actors and six professional female actresses were required to simulate the emotions. Subjects who didn't participate in the recording were asked to carry out a listening test to verify the emotional data. A majority vote method was used for selecting the utterances with good quality.

Table 1. Emotion types and data collection method.

Emotions	Collecting method	Number of speakers
fear, surprise, anger, happiness, sadness and neutral	Acted	12
anxiety, hesitation and confidence	Induced	1

The induced speech data contains three emotions, anxiety, hesitation and confidence. These emotions were induced in a cognitive task (ZOU, 2011). One male subject was required to work on a series of math calculations and report the answers orally. Negative emotions are not easy to induce in a lab environment, and the subject is generally more cooperative to express his or her positive emotions, like happiness, confidence, etc. Therefore noise stimulations and sleep deprivation were used for inducing the negative emotions (anxiety and hesitation). The subject was required to wear a headset and heavy noise recorded from construction sites and other real world environment is played for inducing the negative emotions. Sleep deprivation is a common method in emotion eliciting and cognitive related experiments, which was also used in our experiment. The subject was required to stay up in a separate room for 36 hours. After the recording, a listening test was carried out to verify the emotional data.

3. Speech enhancement

In real world applications, such as mobile phones, call-centers and interactive toys, speech signals are often corrupted by acoustic background noise. In these applications, speech enhancement is a necessary module for the emotion recognition system. In this section we present a basic spectral subtraction method and an advanced method based on masking properties.

3.1. Speech enhancement based on spectral subtraction

Spectral subtraction is a widely used speech enhancement algorithm first proposed by BOLL (1979). Let $x(t)$ be the clean speech signal, $n(t)$ be the noise

signal following a zero-mean Gaussian distribution, and $y(t)$ be the speech signal with noise:

$$y(t) = x(t) + n(t), \quad (1)$$

where $Y(\omega)$, $X(\omega)$, and $N(\omega)$ are the Fourier transformations of $y(t)$, $x(t)$, and $n(t)$, thus we have:

$$Y(\omega) = X(\omega) + N(\omega) \quad (2)$$

and the power spectral density:

$$|Y(\omega)|^2 = |X(\omega)|^2 + |N(\omega)|^2 + X^*(\omega)N(\omega) + X(\omega)N^*(\omega). \quad (3)$$

Suppose the speech signal and noise signal are independent, we have:

$$|Y(\omega)|^2 = |X(\omega)|^2 + |N(\omega)|^2. \quad (4)$$

Let $P_y(\omega)$, $P_x(\omega)$, and $P_n(\omega)$ be the power spectral density of $y(t)$, $x(t)$ and $n(t)$:

$$P_y(\omega) = P_x(\omega) + P_n(\omega). \quad (5)$$

The estimation of noise power spectral $P_n(\omega)$ is achieved from the silent duration:

$$P_x(\omega) = P_y(\omega) - P_n(\omega). \quad (6)$$

To ensure the non-negativity, when $P_y(\omega) < P_n(\omega)$, let $P_x(\omega) = 0$:

$$P_x(\omega) = \begin{cases} P_y(\omega) - P_n(\omega) & P_y(\omega) \geq P_n(\omega), \\ 0 & P_y(\omega) < P_n(\omega). \end{cases} \quad (7)$$

In the spectral subtraction method, the phase information for IFFT to recover speech signal in time domain is directly obtained from the original speech signal with noise, since human listening perception is not sensitive to phase changes.

3.2. Speech enhancement based on masking properties

The spectral subtraction method is a low computational complexity algorithm, and it may effectively improve the signal-to-noise ratio (SNR). However, the speech signal after spectral subtraction enhancement usually contains musical noise, which may affect the speech quality. Therefore we adopt a more sophisticated speech enhancement algorithm proposed by CHEN *et al.* (2007), which is based on the masking properties and short-time spectral amplitude estimation. Masking properties of human auditory system were first introduced by JOHNSTON (1988) and later used in the speech enhancement by TSOUKALAS *et al.* (1997) and VIRAG (1999). Generally speaking

the speech signal is the stronger signal than the background noise is the weaker signal. The frequency domain masking can be modeled by a noise masking threshold, below which all components are inaudible. Therefore when the residual noise after speech enhancement is below the noise masking threshold, it cannot be perceived by human auditory system.

The enhanced speech signal should satisfy:

$$\widehat{X}(m, k) = \arg \min_{\widehat{X}} E \left\{ d \left| X(m, k), \widehat{X}(m, k) \right| \left| Y^{m'} \right. \right\}, \quad (8)$$

where m stands for the frame index, k stands for the discrete frequency and $Y^{m'}$ is the Fourier transform of the m' -th frame of the speech signal, and $d \left| X(m, k), \widehat{X}(m, k) \right|$ is the distance measurement between the original speech signal $X(m, k)$ and the enhanced speech signal $\widehat{X}(m, k)$.

Let G_{SP} denotes a transfer function, we have:

$$\begin{aligned} \widehat{X}_m &= G_{SP}(\xi_{m|m'}, \gamma_m) Y_m \\ &= \sqrt{\frac{\xi_{m|m'}}{1 + \xi_{m|m'}} \left(\frac{1}{\gamma_m} + \frac{\xi_{m|m'}}{1 + \xi_{m|m'}} \right)} Y_m, \end{aligned} \quad (9)$$

where $\xi_{m|m'}$ is the priori SNR and γ_m is the posterior SNR, details can be found in (COHEN, 2005).

We propose a parameterized spectral estimation of the speech signal in the following form (CHEN *et al.*, 2007):

$$\widehat{X}_m = \sqrt{\frac{\xi_{m|m-1}}{a^*} \left(1 + \frac{\xi_{m|m-1} \gamma_m}{a^*} \right)} Y_m, \quad (10)$$

where $a^* = \alpha(m, k) + \xi_{m|m-1}$.

Let $T(m, k)$ denotes the masking threshold, considering the masking property we have (VIRAG, 1999):

$$E \left\{ \left| X^2(m, k) - \widehat{X}^2(m, k) \right| \right\} \leq T(m, k). \quad (11)$$

Let $M = \frac{\xi_{m|m-1}}{\alpha(m, k) + \xi_{m|m-1}}$, σ_s^2 denotes the speech signal power, and σ_n^2 denotes the noise power. Subject (10) to (11). Notice $E \{ X^2(m, k) \} = \sigma_s^2$ and $E \{ N^2(m, k) \} = \sigma_n^2$, we have:

$$\begin{aligned} \sigma_s^2 - T(m, k) &\leq M(1 + M\gamma_m)(\sigma_s^2 + \sigma_n^2) \\ &\leq \sigma_s^2 + T(m, k). \end{aligned} \quad (12)$$

When the speech signal power is below the masking threshold ($\sigma_s^2 - T(m, k) \leq 0$) let $\alpha(m, k) = 1$. Otherwise we have:

$$\begin{aligned} \frac{2\gamma_m \xi_{m|m-1}}{-1 + \sqrt{4C}\gamma_m} - \xi_{m|m-1} &\leq \alpha(m, k) \\ &\leq \frac{2\gamma_m \xi_{m|m-1}}{-1 + \sqrt{4B}\gamma_m} - \xi_{m|m-1}, \end{aligned} \quad (13)$$

where

$$B = \frac{\sigma_s^2 - T(m, k)}{\sigma_s^2 + \sigma_n^2}$$

and

$$C = \frac{\sigma_s^2 + T(m, k)}{\sigma_s^2 + \sigma_n^2}.$$

Therefore the parameter $\alpha(m, k)$ can be determined by the auditory masking threshold, the estimated speech power spectral and the noise power spectral (CHEN *et al.*, 2007). It may dynamically adjust the transfer function, and an optimized tradeoff among the reduction of noise, the speech distortion and the level of musical residual noise may be achieved. This speech enhancement method based on masking properties of human auditory system may be suitable for emotional speech, in the experimental section we will carry out a set of emotion recognition tests using the two different speech enhancement methods for comparison.

4. Recognition methodology

4.1. Emotional feature extraction

Various acoustic features have been studied for speech emotion recognition. The prosodic features may be related to arousal dimension and the voice quality features may be related to valence dimension (GOBL, CHASAIDE, 2003; JOHNSTONE *et al.*, 2005). Both temporal features and static features can be used for speech emotion recognition. Typically the temporal features may be used with Hidden Markov Model (HMM) while the static features may be used with GMM. Since the static features are considered less dependent on phoneme information, we adopt the static features including maximum, minimum, mean, standard deviation and range for the construction of the emotional features. A total of 372 features are generated, as shown in Table 2. Basic Linear Discriminant Analysis (LDA) is then adopted for feature dimension reduction.

When searching for the emotional features, it may be better to exclude the influence of the text variations. In a good emotion data set, the text should be well designed so that its proportion among various emotion classes is balanced. However the uncontrolled naturalistic data is often unbalanced in text, consequently the selected emotional features may be influenced by the phonetic information.

The utterances are categorized according to their time durations, since time duration is an important character of emotional expression in speech. For a balanced data set, we compared the statistics on the time duration and selected the training samples to reduce the variations among different emotion classes, as shown in Table 3.

Table 2. Feature extraction (“dev” is short for deviation; “MFCC” stands for Mel-Frequency Cepstral Coefficients and “BBE” stands for Bark Band Energy).

Feature Index	Feature Description
1–10	max, min, mean, std, range of pitch and dev pitch
10–11	Jitter, Shimmer
12–52	max, min, mean, std, range of F1 to F4 and dev of F1 to F4
52–62	max, min, mean, std, range of intensity and dev intensity
62–192	max, min, mean, std, range of MFCC1 to MFCC13 and dev of MFCC1 to MFCC13
192–372	max, min, mean, std, range of BBE1 to BBE18 and dev of BBE1 to BBE18

Table 3. The text length balance of each emotion class (number of characters in each utterance).

Emotion class	Max of duration	Min of duration	Mean of duration
Happiness	13	2	6.3
Sadness	11	2	7.1
Anger	13	2	6.8
Surprise	12	2	6.9
Fear	14	2	7.0
Neutral	13	2	6.8
Anxiety	13	2	6.8
Hesitation	14	2	7.0
Confidence	11	2	6.7

4.2. Gaussian Mixture Model

Gaussian Mixture Model (GMM) is successfully applied to speaker and language identification. And recently GMM has shown its promising performance in speech emotion recognition (KOCKMANN *et al.*, 2011). It can be seen as a HMM of one state. The probability density function of an m -order GMM is consist of weighted summation of m Gaussian probability density function, which can be expressed as (REYNOLDS *et al.* 1995; REYNOLDS, 1997):

$$p(\mathbf{S}|\boldsymbol{\lambda}) = \sum_{q=1}^Q a_q b_q(\mathbf{S}), \quad (14)$$

where \mathbf{S} is the feature vector of the input sample, $\boldsymbol{\lambda}$ denotes the parameters of GMM, q is the index of the Gaussian mixtures, Q stands for the mixture number, a_q is the mixture weight and b_q stands for the Gaussian distribution function.

Bayes method is used in the identification of emotion. Among the N unknown models, the emotion class whose corresponding model gets the maximum likelihood probability is the target emotion:

$$j^* = \arg \max_{1 \leq j \leq N} \log P(\mathbf{S}|\lambda_j), \quad (15)$$

where j^* denotes the index of the target emotion.

We adopt the EM (expectation-maximization) algorithm in GMM parameter estimation. GMM parameters can be presented as:

$$\lambda = \{a_q, \mu_q, \Sigma_q\}, \quad q = 1, 2, \dots, Q, \quad (16)$$

where Q is the mixture number, μ_q is the mean of each Gaussian distribution, and Σ_q is the covariance matrix.

K-mean clustering is used for initialization where K equals to the GMM mixture number, and EM procedure is used for parameter estimation. The EM equations for training a GMM can be found in (REYNOLDS *et al.* 1995; REYNOLDS, 1997).

5. Experimental results

Based on two types of emotion model theories (the basic emotion theory and the dimension space theory), we adopted two types of classification tasks for the evaluation of the classification system: i) the emotion class classification, and ii) the arousal-valence dimension region classification.

In the training and testing stages, 400 utterances of each emotion class were used for training and 100 utterances of each emotion class were used for testing, including nine emotion types. For the dimension region classification, both the arousal dimension and the valence dimension were classified into positive and negative. We took four training sets for training the positive and the negative model in arousal dimension and valence dimension respectively, each training set contained 800 samples. We also took four testing set, each contained 200 samples. The arousal classifier and the valence classifier were trained separately. Both classifiers classify the input sample into positive dimension or negative dimension.

5.1. Parameter settings

To study the noise influence on speech emotion recognition, we adopted the clean condition training. The training dataset contains clean speech while the noise levels (SNR) of the testing dataset are different. The clean speech was mixed with AWGN at various signal-to-noise ratios (15 dB, 10 dB and 5 dB). Before testing, we apply two types of speech enhancement algorithms to the noisy speech.

The sampling rate was 11.025 kHz, the digitalizing bit was 16 bit. Hamming window was used on the

speech data, the frame length was 256, with an overlap of 128.

The GMM mixture number was set to 32 for emotion classification, and 64 for dimension region classification. The maximum iteration in the EM algorithm was set to 50. K-mean cluster algorithm was used for the initialization in the GMM parameter estimation, and k equals to GMM mixture number.

5.2. Classification results

The classification rates under various noise levels are shown in Fig. 1 through Fig. 2. Two speech enhancement algorithms were evaluated separately on both emotion-class classification task and arousal-valence dimension classification task. As the SNR drops from 15 dB to 5 dB, the classification rates decrease subsequently through all emotion classes and both valence and arousal dimension.

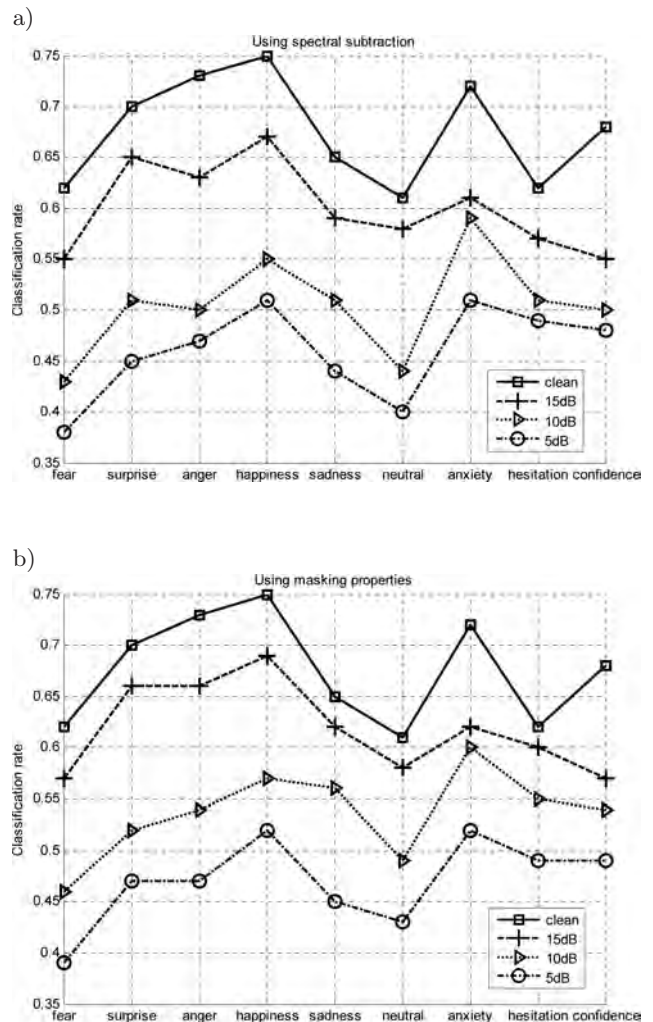


Fig. 1. Emotion-class classification rate under various noise levels: a) using speech enhancement algorithm based on spectral subtraction; b) using speech enhancement algorithm based on masking properties.

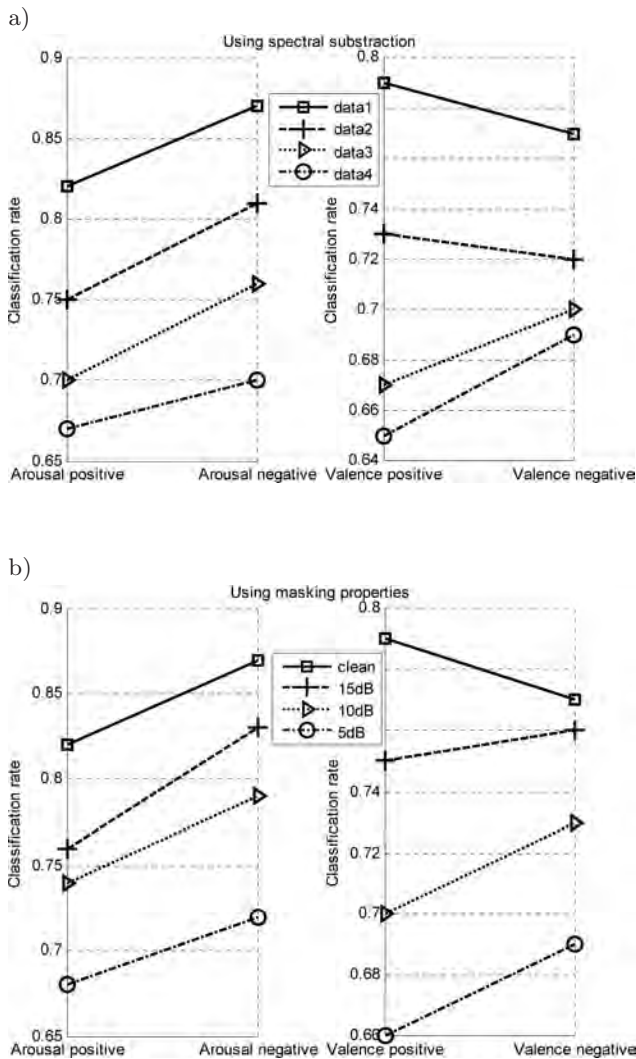


Fig. 2. Arousal-Valence region classification rate under various noise levels: a) speech enhancement based on spectral subtraction; b) speech enhancement based on masking properties.

The advantage of the second algorithm (masking properties based speech enhancement) is obvious, it constantly over-perform the first algorithm (basic spectral subtraction method). The second algorithm takes advantage of human auditory properties, which provides a better tradeoff between the amount of noise reduction and the emotion feature distortion. By an automatic adaptation based on human perception criteria it may be more suitable for emotion recognition tasks.

In the emotion class classification experiment, when tested with clean speech “happiness” is the highest recognized emotion type. However when the SNR drops to 10 dB, “anxiety” becomes better detected than other emotions. As shown in Fig. 1. This accuracy shift is caused by noise influence, and it may be classifier dependent. Similar results are observed in the dimension classification experiment, the classification

rate of negative emotions becomes higher than the classification rate of positive emotions as the noise level increase, as shown in Fig. 2. Since “anxiety” and other negative emotions are most related to valence dimension, the voice quality features may be distorted by the noise, and caused the miss-classification of the positive emotions.

6. Conclusions

In this paper we evaluated the speech emotion recognition system from two points of views, the emotion class view and the arousal-valence dimensional view. From the former one we built GMM based models for each individual emotion class, from the later one we classified the positive and the negative regions of the arousal-valence space also using GMM based models.

The noise influence is an important factor to many of the automatic speech recognition systems, especially when it comes to real world applications. In our study we investigated the speech emotion recognition problem under various white noise conditions. To deal with the AWGN we applied two existing speech enhancement algorithms, the spectral subtraction based algorithm and the algorithm based on masking properties.

The experimental results show that the second algorithm is better than the first algorithm when applied to the speech emotion recognition problem. Speech enhancement is a necessary procedure for speech emotion recognition systems working in a noisy field environment. When increasing the noise level, the overall classification rate dropped, and the positive emotions were more likely to be miss-classified as negative emotions (in valence dimension).

In our study on the speech enhancement, we only compared two existing algorithms, and considered only under AWGN condition. Verifying our emotion recognition system on different databases and various noise types other than white noise may be an interesting future topic. In the feature selection stage we used the same feature set constantly, it is also interesting to select noise robust features for future practical systems.

Acknowledgments

The authors would like to thank the anonymous reviewers for their valuable suggestions on improving this paper. This work is supported by the Natural Science Foundation of China (No. 60872073; No. 60975017; No. 51075068), the Doctoral Fund of Ministry of Education of China (No. 20110092130004), and the Natural Science Foundation of the Jiangsu Higher Education Institutions of China (No. 10KJB510005).

References

1. ANG J., DHILLON R., KRUPSKI A., SHRIBERG E., STOLCKE A. (2002), *Prosody-based automatic detection of annoyance and frustration in human-computer dialog*, 7th International Conference on Spoken Language Processing, pp. 2037–2040, Denver, Colorado, USA.
2. AYADIA M.E., KAMELB M.S., KARRAY F. (2010), *Survey on speech emotion recognition: Features, classification schemes, and databases*, Pattern Recognition, **44**, 3, 572–587.
3. BOLL S. (1979), *Suppression of acoustic noise in speech using spectral subtraction*, IEEE Transactions on Acoustics, Speech and Signal Processing, **27**, 2, 113–120.
4. CAI L. (2005), *Speech emotion analysis and recognition based on data fusion*, Master Thesis, Department of Radio Engineering, Southeast University, China.
5. CHEN G., ZHAO L., ZHOU C. (2007), *Speech Enhancement Based on Masking Properties and Short-Time Spectral Amplitude Estimation*, Journal of Electronics & Information Technology, **29**, 4, 863–866.
6. CLAVEL C., VASILESCU I., DEVILLERS L., RICHARD G., EHRETTE T. (2008), *Fear-type emotion recognition for future audio-based surveillance systems*, Speech Communication, **50**, 487–503.
7. COHEN I. (2005), *Relaxed statistical model for speech enhancement and a priori SNR estimation*, IEEE Transactions on Speech and Audio Processing, **13**, 5, 870–881.
8. GOBL C., CHASAIDE A.N. (2003), *The role of voice quality in communicating emotion, mood and attitude*, Speech Communication, **40**, 189–212.
9. HUANG C., JIN Y., ZHAO Y., YU Y., ZHAO L. (2009), *Speech emotion recognition based on re-composition of two-class classifiers*, 3rd International Conference on Affective Computing and Intelligent Interaction and Workshops, pp. 1–3, Amsterdam, Netherlands.
10. HUANG C., ZHAO Y., JIN Y., YU Y., ZHAO L. (2011), *A Study on Feature Analysis and Recognition for Practical Speech Emotion*, Journal of Electronics & Information Technology, **33**, 1, 112–116.
11. JOHNSTON J.D. (1988), *Transform coding of audio signals using perceptual noise criteria*, IEEE Journal on Selected Areas in Communications, **6**, 2, 314–323.
12. JOHNSTONE T., VAN REEKUM C.M., HIRD K., KIRSNER K., SCHERER K.R. (2005), *Affective speech elicited with a computer game*, Emotion, **5**, 4, 513–518.
13. JONES M.C., JONSON I.M. (2005), *Automatic recognition of affective cues in the speech of car drivers to allow appropriate responses*, Proceedings of the 17th Australia conference on Computer-Human Interaction: Citizens Online: Considerations for Today and the Future, Canberra, Australia.
14. KOCKMANN M., BURGET L., CERNOCKY J.H. (2011), *Application of speaker- and language identification state-of-the-art techniques for emotion recognition*, Speech Communication, **53**, 1172–1185.
15. NEIBERG D., ELENUS K., LASKOWSKI K. (2006), *Emotion recognition in spontaneous speech using GMMs*, International Conference on Spoken Language Process, pp. 809–902, Pittsburgh, Pennsylvania, USA.
16. REYNOLDS D.A., ROSE R.C. (1995), *Robust text-independent speaker identification using Gaussian mixture speaker models*, IEEE Transactions on Speech Audio Process, **3**, 72–83.
17. REYNOLDS D.A. (1997), *Comparison of background normalization methods for text-independent speaker verification*, European Conference on Speech Communication and Technology, pp. 963–966, Rhodes, Greece.
18. SCHULLER B., ARSIC D., WALLHOFF F., RIGOLL G. (2006), *Emotion recognition in the noise applying large acoustic feature sets*, 3rd International Conference on Speech Prosody, Dresden, Germany.
19. SCHERER K.R. (2003), *Vocal communication of emotion: A review of research paradigms*, Speech Communication **40**, 227–256.
20. TAWARI A., TRIVEDI M. (2010), *Speech emotion analysis in noisy real-world environment*, International Conference on Pattern Recognition, pp. 4605–4609, Istanbul, Turkey.
21. TRUONG K. (2009), *How does real affect affect affect recognition in speech?* Ph.D. Thesis, Department of Electrical Engineering, Mathematics and Computer Science, University of Twente.
22. TSOUKALAS D.E., MOURJOPOULOS J.N., KOKKINAKIS G. (1997), *Speech enhancement based on audible noise suppression*, IEEE Transactions on Speech and Audio Processing, **5**, 6, 497–514.
23. VARGA A., STEENEKEN H.J.M. (1993), *Assessment for automatic speech recognition: II. NOISEX-92: A database and an experiment to study the effect of additive noise on speech recognition systems*, Speech Communication, **12**, 3, 247–251.
24. VIRAG N. (1999), *Single Channel Speech Enhancement Based on Masking Properties of the Human Auditory System*, IEEE Transactions on Speech and Audio Processing, **7**, 2, 126–137.
25. WÖLLMER M., EYBEN F., REITER S., SCHULLER B., COX C., DOUGLAS-COWIE E., COWIE R. (2008), *Abandoning emotion classes – Towards continuous emotion recognition with modeling of long-range dependencies*, 9th Annual Conference of the International Speech Communication Association, pp. 597–601, Brisbane, Australia.
26. ZENG Z., PANTIC M., ROISMAN G.I., HUANG T. (2009), *A survey of affect recognition methods: audio, visual and spontaneous expressions*. IEEE Transactions on Pattern Analysis and Machine Intelligence, **31**, 1, 39–58.
27. ZOU C., HUANG C., HAN D., ZHAO L. (2011), *Detecting practical speech emotion in a cognitive task*, 20th International Conference on Computer Communications and Networks, Maui, Hawaii, USA.

Speech Emotion Recognition Based on Sparse Representation

Jingjie YAN⁽¹⁾, Xiaolan WANG⁽²⁾, Weiyi GU⁽²⁾, LiLi MA⁽²⁾

⁽¹⁾ *The School of Information Science and Engineering, Southeast University*
No.2 Sipailou, Nanjing, P.R.China; e-mail: yanjingjie2012@gmail.com

⁽²⁾ *Research Center for Learning Science, Southeast University*
No.2 Sipailou, Nanjing, P.R.China

(received November 29, 2012; accepted April 16, 2013)

Speech emotion recognition is deemed to be a meaningful and intractable issue among a number of domains comprising sentiment analysis, computer science, pedagogy, and so on. In this study, we investigate speech emotion recognition based on sparse partial least squares regression (SPLSR) approach in depth. We make use of the sparse partial least squares regression method to implement the feature selection and dimensionality reduction on the whole acquired speech emotion features. By the means of exploiting the SPLSR method, the component parts of those redundant and meaningless speech emotion features are lessened to zero while those serviceable and informative speech emotion features are maintained and selected to the following classification step. A number of tests on Berlin database reveal that the recognition rate of the SPLSR method can reach up to 79.23% and is superior to other compared dimensionality reduction methods.

Keywords: speech emotion recognition, sparse partial least squares regression (SPLSR), feature selection and dimensionality reduction.

1. Introduction

It is common knowledge that accurate and dependable speech emotion recognition can provide with quite momentous affect for achieving or consummating intelligent, efficient, and reliable human-computer interaction. Consequently, a great number of investigators centralize their attention and energy on this intractable and unmanageable issue, and a great quantity of tremendous advance has been gained to probe, analyze, and exploit speech emotion more informative, meaningful, convenient, and efficient during the past decades (AYADI *et al.*, 2011; CEN *et al.*, 2008; SER *et al.*, 2008).

How to pick up the most beneficial and serviceable speech emotion features which can accessibly and accurately represent the speech emotion information is the pivotal problem for speech emotion recognition (CHEN *et al.*, 2012; JIN *et al.*, 2013; AYADI *et al.*, 2011). Among all speech emotion features, prosodic feature and spectral feature are the most representative types of speech emotion features that are comprehensively employed in speech emotion recognition (WU *et al.*, 2011; JIN *et al.*, 2013). The frequently adopted prosodic feature contains pitch, formants, energy, speed, and so

on (CHEN *et al.*, 2012; AYADI *et al.*, 2011). The spectral feature is deemed to offer certain supplementary and various speech emotion features comparing with the prosodic feature and mel-frequency cepstral coefficients (MFCC), linear predictive cepstral coefficients (LPC) and log-frequency power coefficients (LFPC) are three most classic spectral features that are broadly adopted in a number of speech emotion recognition approaches (WU *et al.*, 2011; AYADI *et al.*, 2011; JIN *et al.*, 2013).

In the time of dealing with the above extracted speech emotion features, we may find out that the dimension of obtained speech emotion features can be as high as several hundred or more than one thousand, and each extracted speech emotion feature owns disparate effect on speech emotion recognition (ZHOU *et al.*, 2012; CEN *et al.*, 2008; JIN *et al.*, 2013; LAI *et al.*, 2012). For instance, some features can promote and increase the recognition performance of speech emotion recognition, but some redundant and invalid features are harmful and unhelpful for final emotion classification.

Over the last several decades, plenty of investigators burgeon a mass of dimensionality reduction and feature selection approaches for working out those su-

ervised and unsupervised studying issues (BISHOP, 2006; LAI *et al.*, 2012; JIN *et al.*, 2013). Among those approaches, principle component analysis (PCA) (TURK, PENTLND, 1991) and linear discriminant analysis (LDA) (BELHUMEUR, HESPANHA, 1997; CHEN *et al.*, 2000) are the two outstanding methods and they already have been triumphantly exploited to speech emotion recognition and other relevant research domains (JIN *et al.*, 2013; BISHOP, 2006).

It is noted that PCA and LDA can only deal with and analyze one group of data, whereas canonical correlation analysis (CCA) (HOTELLING, 1936) and partial least squares regression (PLSR) (ROSOPAL, KAMER, 2008) are investigated to deal with two groups of data at the same time (PARKHOMENKO *et al.*, 2009). Akin to PCA and LDA, CCA also has been addressed and applied in speech emotion recognition (CEN *et al.*, 2008). The application of PLSR is also comprehensive and efficient in various important spheres such as vehicle detection (KEMBHAVI *et al.*, 2011), neuroimaging (KRISHNAN *et al.*, 2011) and human detection (SCHWARTZ *et al.*, 2009). But when making use of the PLSR method in speech emotion recognition, we will discover one main weakness of the PLSR method analogous to PCA, LDA, and CCA, and this weakness is that the weight vectors of PLSR are the linear combination of the whole extracted speech emotion features, therefore it is unable to clear away those redundant and insignificant speech emotion features (CAO *et al.*, 2008; CHUN, KELES, 2010; MCWILLIAMS, MONTANA, 2010; QIAO *et al.*, 2009; CAI *et al.*, 2007; LAI *et al.*, 2012).

In the last few years, a number of sparse versions of PLSR approach have been established to resolve the above-mentioned shortcoming of PLSR method. CAO *et al.* (2008; 2009) presented a novel bilateral sparse partial least squares regression based on the SVD decomposition and sparse PCA approach (SHEN, HUANG, 2008) that can achieve data fusion and variable selection simultaneously when applied to biology. Similar to the work of CAO *et al.* (2008; 2009), a unilateral sparse partial least squares regression (MCWILLIAMS, MONTANA, 2010; MA, 2010; CAO *et al.*, 2011; CAO, GALL, 2011) based on unilateral sparse SVD approach has been developed. Moreover, MCWILLIAMS and MONTANA (2010) apply this unilateral sparse partial least squares regression method for increment learning task. CHUN and KELES (2010) propose a new sparse partial least squares approach in which the objective function is rewritten as SPCA's optimization formula (ZOU *et al.*, 2006). Based on the work of CHUN and KELES (2010), CHUNG and KELES (2010) have developed two classification-based methods including SPLS discriminant analysis (SPLSDA) and sparse generalized PLS (SGPLS), and then applied them to conduct variable selection on high-dimension datasets. Moreover, HUANG *et al.* (2012)

utilized the SPLSR method to conduct intelligibility detection tests. In this paper, we exploit the unilateral sparse partial least squares regression method (MCWILLIAMS, MONTANA, 2010; MA, 2010; CAO *et al.*, 2011; CAO, GALL, 2011) to implement the feature selection and dimension reduction of obtained speech emotion features in speech emotion recognition.

In this paper, we investigate speech emotion recognition based on sparse partial least squares regression (SPLSR) approach. The whole of acquired speech emotion features have available implemented the feature selection and dimensionality reduction with the sparse partial least squares regression method whose basic idea is to receive sparse projections by means of calculating a sparse singular value decomposition issue (MCWILLIAMS, MONTANA, 2010; MA, 2010; CAO *et al.*, 2008; SHEN, HUANG, 2008). By introducing the properties of sparsity on the whole acquired speech emotion features with SPLSR method, the component parts of redundant and meaningless speech emotion features are lessened to zero while those serviceable and informative speech emotion features are maintained for the next classification step.

We organize the remaining part of this paper as follows. We roughly provide the description of the PLSR method in Sec. 2. Section 3 introduces the SPLSR approach in detail and its specific algorithm. The speech emotion classification via SPLSR method is illustrated in Sec. 4. Section 5 introduces the adopted speech emotion databases and describes a number of experiments. Ultimately, Sec. 6 concludes the paper and gives some discussion on the future work.

2. Partial Least Squares Regression

Consider a pair of sample data matrices $X \in R^{N \times n_x}$ and $Y \in R^{N \times n_y}$ which indicate the extracted speech emotion feature matrices and its speech emotion category feature matrices respectively, where N expresses the number of samples. The fundamental purpose of PLSR method is exploring a cluster of vectors ϕ_r and ζ_r which are achieved by maximizing the under optimization formulation in the form of alleged latent vectors $X\phi_r$ and $Y\zeta_r$ (CAO *et al.*, 2008; ROSOPAL, KAMER, 2008; GU, 2010; MA, 2010; YAN *et al.*, 2013)

$$\{\phi_r; \zeta_r\} = \arg \max_{\phi^T \phi = \zeta^T \zeta = 1} \text{cov}(X\phi_r, Y\zeta_r). \quad (1)$$

As we all know, X and Y can be resolved into the following pattern (ROSOPAL, KAMER, 2008; CAO *et al.*, 2008)

$$\begin{aligned} X &= WP_x^T + E_x, \\ Y &= WP_y^T + E_y, \end{aligned} \quad (2)$$

where P_x and P_y are matrices of coefficient which are expressed as $p_x = X^T w / w^T w$ and $p_y = Y^T w / w^T w$,

respectively. Besides, E_x and E_y are the corresponding residuals matrices of X and Y , respectively (ROSOPAL, KAMER, 2008; CAO *et al.*, 2008).

Suppose $R_{XY} = X^T Y$, $R_{XY} = R_{YX}^T$. Then, the formula (1) can be changed into the following optimization problem (GU, 2010; MA, 2010) (we seek the first cluster of vectors ϕ_r and ζ_r here):

$$\arg \max_{\phi, \zeta} \phi^T R_{XY} \zeta, \quad (3)$$

subject to $\phi^T \phi = 1$ and $\zeta^T \zeta = 1$.

Then we can receive the Lagrangian of formula (3) as the following pattern (GU, 2010; MA, 2010; ZHOU *et al.*, 2012):

$$L(\phi, \zeta, \lambda, \mu) = \phi^T R_{XY} \zeta - \frac{\lambda}{2} (\phi^T \phi - 1) - \frac{\mu}{2} (\zeta^T \zeta - 1). \quad (4)$$

Further, the following two equations can be obtained by calculating the partial derivatives of $L(\phi, \zeta, \lambda, \mu)$ with respect to ϕ and ζ (MA, 2010):

$$\begin{aligned} R_{XY} \zeta &= \lambda \phi, \\ R_{YX} \phi &= \mu \zeta. \end{aligned} \quad (5)$$

Ultimately, we are capable of receiving the first desired cluster of projection vectors ϕ and ζ by figuring up the next eigenvalue equations of (6) and (7), respectively:

$$R_{XY} R_{YX} \phi = \lambda \mu \phi, \quad (6)$$

$$R_{YX} R_{XY} \zeta = \lambda \mu \zeta. \quad (7)$$

3. Sparse Partial Least Squares Regression

On the basis of the antecedent discussion and analysis, we can note that the PLSR approach is not capable of carrying out the feature selection on the whole extracted speech emotion features. Moreover, it should be noted that X and Y signify the whole extracted speech emotion features and its speech emotion category feature respectively, and the speech emotion category feature contains only category information. Therefore we only need to carry out the feature selection on the whole extracted speech emotion feature X . Consequently in the following section, we will introduce the unilateral sparse partial least squares regression method (MCWILLIAMS, MONTANA, 2010; MA, 2010; CAO *et al.*, 2011; CAO, GALL, 2011) and then employ it to carry out the feature selection on X in the form of solving sparse projection ϕ . The conventional PLSR method can be solved by means of PLSR-SVD pattern in the light of the literature of CAO *et al.* (2008). In the PLSR-SVD form, the matrix $R_{XY} = X^T Y$ of the conventional PLSR method can be expressed in the following singular value decomposition

(SVD) form (CAO *et al.*, 2008; MCWILLIAMS, MONTANA, 2010; SHEN, HUANG, 2008; YAN *et al.*, 2012):

$$R_{XY} = X^T Y = \sum_{t=1}^h d_t u_t v_t^T. \quad (8)$$

It is noted that the eigenvalues of $R_{XY}^T R_{XY}$ and $R_{XY} R_{XY}^T$ are d_1, d_2, \dots, d_h , and the eigenvectors of $R_{XY}^T R_{XY}$ and $R_{XY} R_{XY}^T$ are equivalent to u_i and v_i , respectively. In accordance with the nature of the above PLSR-SVD approach, the pair of desired vectors α and β of the conventional PLSR are just equivalent to u_i and v_i in the above SVD form, and it indicates $\phi = u_i$ and $\zeta = v_i$ in other words (CAO *et al.*, 2008; MCWILLIAMS, MONTANA, 2010; MA, 2010; YAN *et al.*, 2013). Consequently, the cluster of vectors ϕ and ζ that are received by the conventional PLSR solving approach can be transformed to calculate the cluster of vectors of u_i and v_i in the above PLSR-SVD form.

On the basis of the work of SHEN and HUANG (2008) and CAO *et al.* (2008), a unilateral sparse partial least squares regression method (MCWILLIAMS, MONTANA, 2010; MA, 2010; CAO *et al.*, 2011; CAO, GALL, 2011) is developed to obtain only one cluster of sparse projection and is different from the method of CAO *et al.* (2008) in which two sets of sparse projections can be obtained. The optimization formulation of unilateral SPLSR is adapted as the following pattern by introducing the lasso penalty on the vector u (MCWILLIAMS, MONTANA, 2010; MA, 2010; CAO *et al.*, 2011; CAO, GALL, 2011):

$$\min_{u, v} \|R_{XY} - uv^T\|_F^2 + \lambda_u \sum_{j=1}^p |u_j|, \quad (9)$$

where $\lambda_u \sum_{j=1}^p |u_j|$ stands for the lasso function, and $\lambda_u \geq 0$ signifies a positive value for deciding the sparse degree of u .

For the sake of calculating the optimization problem of (9) efficiently, MCWILLIAMS and MONTANA (2010) have developed an iterative algorithm with respect to solving u and v . The process of this iterative algorithm consists in that u is achieved by optimizing (9) through fixing v , and then v is achieved by optimizing (9) through fixing u (ZHOU *et al.*, 2012).

By means of repeating the above iterative process, the desired optimal projection v and sparse projection u are acquired finally from the following Eqs. (10) and (11), respectively, after the iterative algorithm achieves convergence (MCWILLIAMS, MONTANA, 2010; MA, 2010):

$$v^* = \frac{R_{XY}^T u}{\|R_{XY}^T u\|}, \quad (10)$$

$$u^* = \text{sign}(R_{XY} v) (|R_{XY} v| - \lambda_u / 2)_+. \quad (11)$$

For details of the above solving procedure of the unilateral SPLSR, please see the paper of MCWILLIAMS and MONTANA (2010). At last, we can project the whole extracted speech emotion feature X onto the above sparse projection u (u is equivalent to ϕ) received by the unilateral SPLSR to implement feature selection.

4. Emotion Recognition via Sparse Partial Least Squares Regression

Assuming that a cluster of the sparse projection matrix $\phi_X = (\phi_x^1, \phi_x^2, \dots, \phi_x^h)$ are received conclusively via the above unilateral SPLSR method, where h denotes the number of the above extracted sparse projection matrix ϕ_X , then on the basis of the Eq. (2) we can get the following two regression equations (GU, 2010; MA, 2010; MCWILLIAMS, MONTANA, 2010):

$$\begin{aligned} X &= w_1 P_{x1}^T + w_2 P_{x2}^T + \dots + w_h P_{xh}^T \\ &+ E_x^h = W P_x^T + E_x^h, \\ Y &= w_1 P_{y1}^T + w_2 P_{y2}^T + \dots + w_y P_{yh}^T \\ &+ E_y^h = W P_y^T + E_y^h, \end{aligned} \quad (12)$$

where $W = (w_1, w_2, \dots, w_h)$, $p_X = (p_{X1}, p_{X2}, \dots, p_{Xh})$, $p_Y = (p_{Y1}, p_{Y2}, \dots, p_{Yh})$.

In the light of (MANNE, 1987; GU, 2010; MA, 2010), we obtain the next equation by simple approximately calculation:

$$W = X \phi_X (p_X^T \phi_X)^{-1}. \quad (13)$$

Form Eqs. (12) and (13), we are able to receive the following formula (GU, 2010; MA, 2010)

$$Y = W P_y^T + E_y^h = X \phi_X (p_X^T \phi_X)^{-1} P_y^T + E_y^h. \quad (14)$$

At last, if providing a test speech emotion feature sample X_{test} , we are able to calculate the homologous speech emotion category feature Y_{test} in the light of the following formula (GU, 2010; MA, 2010; MCWILLIAMS, MONTANA, 2010):

$$Y_{\text{test}} = X_{\text{test}} \phi_X (p_X^T \phi_X)^{-1} P_y^T. \quad (15)$$

5. Experiments

In the following section, we will simply introduce the adopted speech emotion database, the detailed experiment design and show results of the experimental test. In this study, we assess the property of our speech emotion recognition approach based on the SPLSR algorithm by carrying out certain tests on the Berlin database (BURKHARDT *et al.*, 2005; ZHENG *et al.*, 2012; JIN *et al.*, 2013; GU, 2010). In our experiment, from a number of samples representing different speech emotion categories, we select and utilize a subset of the Berlin dataset which contains 260 speech samples and

five speech emotion categories including anger, boredom, fear, joy, and sadness.

In the speech emotion feature extraction procedure, two sorts of speech emotion features consisting of prosodic features and spectral features are picked up in our experiment (GU, 2010; WU *et al.*, 2011; ZHENG *et al.*, 2012; JIN *et al.*, 2013). The details of extracted speech emotion feature in our test included pitch, formant frequency, the logarithmic form of energy, and so on (GU, 2010; ZHENG *et al.*, 2012).

Apart from the SPLSR method, we also conduct other classic dimensionality reduction methods for speech emotion recognition, i.e. the principal component analysis (PCA) method, the linear discriminant analysis (LDA) method, the gaussian mixture model (GMM) method, and the partial least squares regression (PLSR) method. For PCA and LDA, we adopt the K-nearest neighbor (KNN) classifier to classify five different emotion categories, whereas PLSR and SPLSR exploit the classification method introduced in Sec. 4. Besides, in our experiments, we employ the thirteen-fold cross-validation strategy to the above five methods (GU, 2010; ZHENG *et al.*, 2012).

The average recognition rates of the above five methods are exhibited in Table 1. It is noted that the disparate number of the reduced dimension will produce a certain influence concerning the final property, therefore we also implement the tests with the disparate dimension. Figure 1 displays the recognition rates of three methods with disparate reduced dimension.

Table 1. The average recognition rate of each method.

Method	Recognition rate
PCA	64.23
LDA	75.00
GMM	69.62
PLSR	78.46
SPLSR	79.23

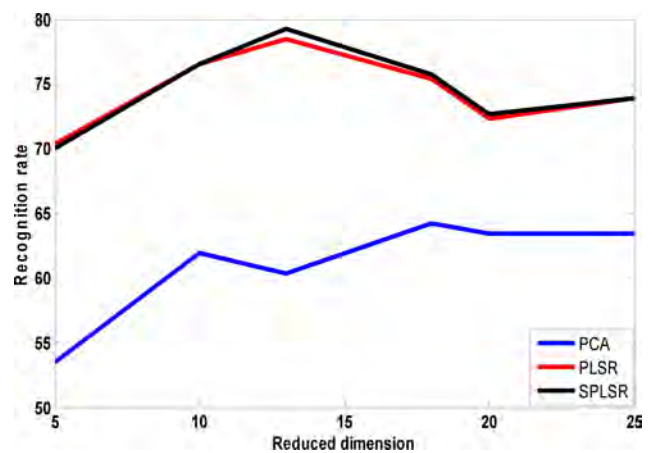


Fig. 1. Recognition rates of each method for different number of reduced dimensions.

To distinctly display the test results of different emotion category, the confusion matrices of PLSR method and SPLSR method are shown in Fig. 2 and Fig. 3, respectively. Moreover, we also implement the experiment of SPLSR method with different values of the sparse parameter. Table 2 shows the recognition rates of SPLSR method versus different values of the sparse parameter.

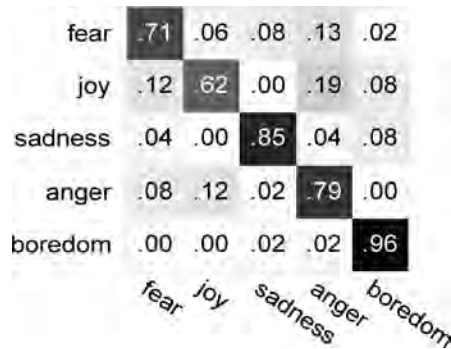


Fig. 2. Confusion matrix for the PLSR method.

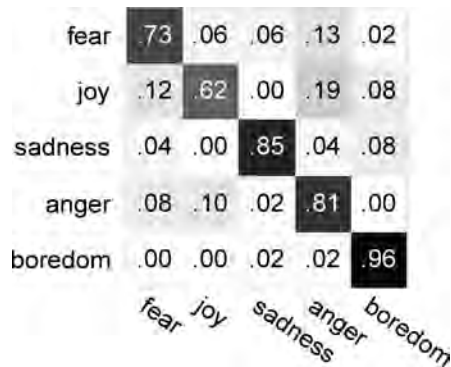


Fig. 3. Confusion matrix for the SPLSR method.

Table 2. Recognition rates of SPLSR for the different values of sparse parameter.

Sparse parameter	Recognition rate
0.1	78.85
0.08	78.85
0.05	79.23
0.01	78.46

In accordance with the above test results, we can note that the recognition rate of the SPLSR method can reach up to 79.23% and it is superior to other compared methods such as PCA, LDA, GMM, and PLSR. This test result indicates that the SPLSR method may provide more serviceable and informative speech emotion information than those compared methods. Moreover, in line with Table 2, we can see that the sparse parameter λ can produce the effect on the recognition rate of the SPLSR approach to some degree and the best recognition rate of SPLSR is achieved when the sparse parameter λ is 0.05.

6. Conclusion and discussion

In this paper, we study speech emotion recognition based on the partial least squares regression (SPLSR) approach. We make use of the sparse partial least squares regression method to implement the feature selection and dimensionality reduction on the whole acquired speech emotion features. Moreover, a number of experimental tests on the Berlin database certify the validity and meaning of the speech emotion recognition approach based on the SPLSR method. In the future study, we can import those sparse kernel approaches onto speech emotion recognition which may allow to obtain nonlinear discriminative speech emotion information to some degree.

Acknowledgments

This work was supported in part by the National Natural Science Foundation of China under Grant 61231002 and Grant 61073137, the Natural Science Foundation of Jiangsu Province under Grant BK20130020, and the Program for Distinguished Talents of Six Domains in Jiangsu Province of China under Grant 2010-DZ088.

References

1. AYADI M.E., KAMEL M.S., KARRAY F. (2011), *Survey on speech emotion recognition: features, classification schemes, and databases*, Pattern Recognition, **44**, 572–587.
2. BELHUMEUR P.N., HESPANHA P. (1997), *Eigenfaces vs. Fisherfaces: recognition using class specific linear projection*, IEEE Trans. Pattern Anal. Mach. Intell, **19**, 711–720.
3. BAEK J.S., KIM M. (2004), *Face Recognition using partial least squares components*, Pattern Recognition, **37**, 1303–1306.
4. BURKHARDT F. *et al.* (2005), *A database of german emotional speech*, Interspeech, 1517–1520.
5. BISHOP C. (2006), *Pattern recognition and machine learning*, Springer, United States of America.
6. CHEN L.F., MARK H.Y., KO M.T. (2000), *A new LDA-based face recognition system which can solve the small sample size problem*, Pattern Recognition, **33**, 1713–1726.
7. CEN L., SER W., LIANG Z. (2008), *Speech emotion recognition using canonical correlation analysis and probabilistic neural network*, International Conference on Machine Learning and Applications, 859–862.
8. CAI D., HE X.F., HAN J.W. (2007), *Spectral Regression: A Unified Approach for Sparse Subspace Learning*, IEEE International Conference on Data Mining, 73–82.

9. CAO K.A., ROSSOUWY D., GRANI C.R., BESSE P. (2008), *A sparse PLS for variable selection when integrating omics data*, *Statistical Applications in Genetics and Molecular Biology*, **7**, 35–45.
10. CAO K.A., MARTIN P.G.P., ROBERT-GRANIÉ C., BESSE P. (2009), *Sparse canonical methods for biological data integration: application to a cross-platform study*, *BMC Bioinformatics*, **10**.
11. CAO K.A., BOITARD S., C.R., BESSE P. (2011), *Sparse PLS Discriminant Analysis: biologically relevant feature selection and graphical displays for multi-class problems*, Technical report, University of Queensland.
12. CAO K.A., GALL G.L. (2011), *Integration and variable selection of 'omics' data sets with PLS: a survey*, *Journal de la Société Française de Statistique*, **152**, 77–96.
13. CHEN L.J., MAO X., XUE Y.L., CHENG L.L. (2012), *Speech emotion recognition: features and classification models*, *Digital Signal Processing*, **2**, 154–1160.
14. CHUN H., KELES S. (2010), *Sparse partial least squares regression for simultaneous dimension reduction and variable selection*, *Journal of the Royal Statistical Society: Series B (Statistical Methodology)*, **72**, 3–25.
15. CHUNG D., KELES S. (2010), *Sparse Partial Least Squares Classification for High Dimensional Data*, *Statistical Applications in Genetics and Molecular Biology*, **9**.
16. GU W.Y. (2010), *A Study on Speech Emotion Recognition*, master thesis, Research Center for Learning Science, Southeast University (in chinese).
17. HOTELLING H. (1936), *Relations between two sets of variates*, *Biometrika*, **28**, 312–377.
18. HUANG D.Y., ZHU Y.W., WU D.J., YU R.S. (2012), *Detecting Intelligibility by Linear Dimensionality Reduction and Normalized Voice Quality Hierarchical Features*, *Interspeech*, 546–549.
19. JIN Y., ZHENG W.M., ZHAO L., YAN J.J. (2013), *Generalized maximal margin discriminant analysis for speech emotion recognition*, *Electrical review*.
20. KEMBHAVI A., HARWOOD D., DAVIS L.S. (2011), *Vehicle detection using partial least squares*, *IEEE Transactions on Pattern Analysis and Machine Intelligence*, **33**, 1250–1265.
21. KRISHNAN A., WILLIAMS L.J., MCINTOSH A.R., ABDI H. (2011), *Partial Least Squares (PLS) methods for neuroimaging: A tutorial and review*, **56**, 455–475.
22. LAI Z.H., WAN M.H., JIN Z., YANG J. (2012), *Sparse two-dimensional local discriminant projections for feature extraction*, *Neurocomputing*, **74**, 629–637.
23. LONG N., GIANOLA D., ROSA G.J.M., WEIGEL K.A. (2011), *Dimension reduction and variable selection for genomic selection: application to predicting milk yield in Holsteins*, *Journal of Animal Breeding and Genetics*, **128**, 147–257.
24. MA L.L. (2010), *The Research and Application of Facial Expression Recognition based on Semantic Feature*, master thesis, Research Center for Learning Science, Southeast University (in chinese).
25. MANNE R. (1987), *Analysis of Two Partial-Least-Squares Algorithms for Multivariate*, *Calibration Chemometrics and Intelligent Laboratory Systems*, **2**, 187–197.
26. MCWILLIAMS B., MONTANA G. (2010), *Sparse partial least squares regression for on-Line variable selection with multivariate data streams*, *Statistical Analysis and Data Mining*, **3**, 170–193.
27. PARKHOMENKO E., TRITCHLER D., BEYENE J. (2009), *Sparse canonical correlation analysis with application to genomic data integration*, *Statistical Applications in Genetics and Molecular Biology*, **8**, 55–61.
28. QIAO Z., ZHOU L., HUANG J.Z. (2009), *Sparse linear discriminant analysis with application to high dimensional low sample size data*, *International Journal of Applied Mathematics*, **39**, 48–60.
29. ROSOPAL R., KAMER N. (2008), *Overview and recent advances in partial least squares. subspace latent structure and feature selection*, *Statistical and Optimization Perspectives Workshop*, **3940**, 34–51.
30. SHEN H., HUANG J. (2008), *Sparse principal component analysis via regularized low rank matrix approximation*, *Journal of Multivariate Analysis*, **99**, 1015–1034.
31. SER W., CEN L., YU Z.L. (2008), *A Hybrid PNN-GMM classification scheme for speech emotion recognition*, *International Conference on Pattern Recognition*, 1–4.
32. SCHWARTZ W.R., KEMBHAVI A., HARWOOD D., DAVIS L.S. (2009), *Human detection using partial least squares analysis*, *IEEE International Conference on Computer Vision*, 24–31.
33. TURK M., PENTLAND A.P. (1991), *Face recognition using eigenfaces*, *IEEE Conference on Computer Vision and Pattern Recognition*, 586–591.
34. WU S.Q., TIAGO H., FALK, CHAN W.Y. (2011), *Automatic speech emotion recognition using modulation spectral features*, *Speech Communication*, **53**, 768–785.
35. YAN J.J., ZHENG W.M., ZHOU X.Y., ZHAO ZHI.J. (2012), *Sparse Two-dimensional Canonical Correlation Analysis via Low Rank Matrix Approximation for Feature Extraction*, *IEEE Signal Processing Letters*, **19**, 51–54.
36. YAN J.J., ZHENG W.M., XIN M.H., QIU WEI (2013), *Bimodal Emotion Recognition based on Body Gesture and Facial Expression*, *Journal of Image and Graphics*, **18**, 1101–1106 (in chinese).
37. ZOU H., HASTIE T., TIBSHIRANI R. (2006), *Sparse principal component analysis*, *Journal of Computational and Graphical Statistics*, **15**, 265–286.
38. ZHOU X.Y., ZHENG W.M., XIN M.H. (2012), *Improving CCA via spectral components selection for facial expression recognition*, *IEEE International Symposium on Circuits and Systems (ISCAS)*, 1696–1699.
39. ZHENG W.M., ZHOU X.Y. (2012), *Speech Emotion Recognition Based on Kernel Reduced-rank Regression*, *International Conference on Pattern Recognition (ICPR 2012)*, 1972–1976.

Selection of Sound Insulating Elements in Hydraulic Excavators Based on Identification of Vibroacoustic Energy Propagation Paths

Zbigniew DĄBROWSKI, Jacek DZIURDŹ, Radosław PAKOWSKI

The Institute of Machine Design Fundamentals, Warsaw University of Technology
Narbutta 84, 02-524 Warszawa, Poland; e-mail: zdabrow@simr.pw.edu.pl

(received April 23, 2013; accepted May 23, 2013)

In spite of the fact that standardizing operations and increased awareness of hazards led to a significant improvement of vibroacoustic climate of operator's stands of new machines, their long-term operation – often under difficult conditions – leads to a fast degradation of acoustic qualities of machines. Temporary operations performed during surveys and periodical overhauls are rarely effective, due to the lack of any guidelines. In this situation the authors propose the algorithm for selection of eventual screens or sound absorbing and sound insulating partitions, utilizing the measuring procedure aimed at identification, at the operator's stand, of main noise components originated from various sources. On the basis of this procedure, the vibroacoustic energy propagation paths in the machine was estimated.

Keywords: noise and vibration, propagation path, coherence function.

1. Introduction

A lot of emphasis is currently put on the employees protection at work stands. It concerns, among others, operators of earth work machines. Since driving systems of this type of machines are characterised with high vibroactivity, minimising noise and vibration hazards belongs to the most important structural problems and modernisation programs of existing machines. The applied methods of suppression noises and vibrations can be divided into two groups: active and passive methods.

A principle of operation of active damping methods can be generally described as generation of signal components of time waveforms being phase-shifted by a half of a period in relation to noise and vibration components subjected to damping. In this case the waves decay effect as a result of interferences is utilised. Such technique can be only successful in case of time synchronisation which in case of random effects requires a system with a very short reaction time as well as maintaining the same (opposite) propagation directions. These difficulties are the cause for which active methods are used only in certain specific applications.

Passive techniques of noise and vibration damping can be divided, from the point of view of the physics of the effect, into the following groups:

- minimisation of noise and vibration sources;
- changing vibroacoustic energy into another form (e.g. thermal);
- changing the propagation direction of acoustic field and dissipating its energy outside the noise protected area.

The last two groups consist in designing structures to be put on the vibroacoustic energy propagation path. The methodology of machine noise and vibrations damping can be put in order according to the following scheme:

- localisation and description of basic sources;
- identification of the model of the vibroacoustic energy propagation;
- determination frequency characteristics of the designed damping systems;
- designing damping elements according to the determined characteristics.

In search for effective tools of the computer-aided designing of structures minimising vibroacoustic hazards caused by earth work machines, the present authors assumed the following:

1. The basis of computational algorithms of insulating structures should be the determination of main

propagation paths of the vibroacoustic energy between noise and vibration sources and the operator's work stand – on the grounds of the identified mathematical model.

2. The proposed mathematical model of the vibroacoustic energy propagation in a machine should be identifiable by a simple measurement procedure and should constitute the basis for the computer-aided selection of vibroinsulating elements.
3. The model identification should be performed by means of a procedure allowing for the separation components originated from individual sources from the signals recorded at the system output (noise and vibrations in the operator's cabin) – under the assumption that the investigated system can be non-linear.

The investigated problem is widely analysed and discussed in the world literature, especially by scientific research groups related to the automotive industry (e.g. Society of Automotive Engineers, SAE). Some commercial programs analysing signals in time and/or frequency domains were also developed. They are using the method of modal analysis or the Finite Element Method (FEM) for modelling and determination of parameters characterising propagation of vibroacoustic energy. Several methods described in the literature are based on the energy propagation analysis using measurements of the acoustic particle velocity, including:

- Source Path Contribution (SPC) consists in performing a phased summation of partial responses from all noise and vibration paths to give total tactile and acoustic responses under specific operating loads at a given frequency or RPM (Source Path Contribution software, 2010). A similar principle of operation has the Transfer Path Analysis (TPA).
- Statistical Energy Analysis (SEA) is used to predict the sound transmission loss, the radiation resistance and the vibration amplitude of a partition. Conformity between theory and experiment is shown to be good. The “mass-law” sound transmission is seen to be due to non-resonant modal vibration, while the increased transmission in the coincidence region is

due to resonant modal vibration (CROCKER, PRICE, 1969). To solve a noise and vibration problem with the SEA, the system is divided into a number of components (such as plates, shells, beams, and acoustic cavities) that are coupled together in various combinations. Each component can support a number of different propagating wave types (e.g. bending, longitudinal, and shear wave fields in a thin isotropic plate). From the SEA point of view, the reverberant field of each wave field represents an orthogonal store of energy and thus is represented as a separate energy degree of freedom in the SEA equations.

2. Theoretical considerations

Vibration-noise effects occurring in real systems, such as e.g. machines for earth works, can be presented as a continuous exchange of the mechanical vibrations energy into noise and vice versa. The energy originated from correlated and non-correlated sources of vibrations and noises passes through the complicated machine structure undergoing linear (and often non-linear) transformations. This energy arrives to various points, e.g. machine operator stand, as a sum in which fractions of individual sources do not have to be proportional (and usually are not) to their power.

The structural model describing these effects is presented in Fig. 1.

The most important issue in the realised task is determination of the influence of individual factors (localised and identified vibroacoustic energy sources) on noise and vibrations influencing the operator. This is a difficult task, since we analyse recorded signals of effects occurring in a complicated, non-linear, inner machine field with several independent sources of vibroacoustic energy. From the point of view of the need of decreasing vibrations and noise levels, it is necessary to estimate fractions of individual sources in the total energy at the machine point of interest or in its vicinity by determining propagation paths properties.

Because of the above-mentioned non-linear effects, disturbances, and hardly identifiable (invisible) changes of a vibroacoustic machine structure during

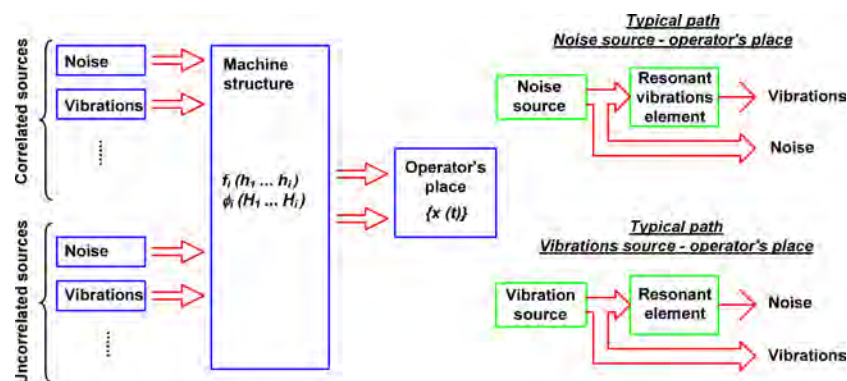


Fig. 1. Structural model describing vibroacoustic energy propagation in machines.

operation, detailed models are far from the reality and difficult to identify. According to the authors, much better effects can be achieved by building a simplified model (partially of a ‘black box’ type) well identified on the grounds of input and output values (BATKO *et al.*, 2008). Therefore the authors have proposed their own method of investigating the vibroacoustic energy propagation in machines for earth works.

In order to determine the propagation paths properties, the acoustic pressure changes in the vicinity of identified sources of vibroacoustic energy should be recorded (in case of propagation in air) as well as the accelerations of vibrations at points of attaching these sources to the carrying system (in case of a propagation in the machine structure). Simultaneously, the acoustic pressure changes and accelerations of vibrations influencing the machine operator should be recorded.

The proposed method of analysis is based on the application of the autocorrelation and ordinary coherence functions. Correlation and coherence functions belong to the classic analytical methods used, among other things, in investigation of determined signals disturbed by random noises. In the time domain, the autocorrelation function allows to determine the time cohesion between neighbouring fragments of the analysed process, shifted by various time values. The ordinary coherence function is a spectral measure of the cohesion of processes in the frequency domain. However, these are not the only properties of these functions. The autocorrelation function is a superposition of the determined process and random noise being the result of disturbances from other processes or from the measurement. Due to that, it is possible to determine the fraction related to random disturbances and to the determined part in the total signal energy. The auto-coherence value depends, among other things, on the random disturbance value and on non-linearity of the analysed system.

In order to limit the influence of harmonics of similar frequencies and originated from various vibroacoustic energy sources, application of an algorithm using the given standard signal was proposed. One of the essential advantages of the proposed method is improving the resolution analysis in the frequency domain in comparison with classic spectral methods.

The simplest description of the vibroacoustic energy propagation path can be supplemented by presenting the total effect of weakly non-linear disturbances in the form of one or a few unknown functions determined in the identification process and taken into account in the model, either in an additive or a multiplicative way. For one dominating source, it is reduced to the following description, in the frequency domain:

$$Y(f) = \mathfrak{F}\{y(t)\} = X(f) \cdot H(f) + \Phi(f) + \Psi(f) \quad (1)$$

or

$$Y(f) = \mathfrak{F}\{y(t)\} = (X(f) \cdot H(f)) * \Phi(f) + \Psi(f), \quad (2)$$

where $Y(f)$ – Fourier transform of the output signal $y(t)$, $X(f)$ – excitation process (Fourier transform of the input signal $x(t)$), $H(f)$ – transmittance of the propagation path, $\Phi(f)$ – a function being the result of non-linear disturbance and determined in the identification process, $\Psi(f)$ – influence of external disturbances (random effects).

After simple transformation, Eq. (1) can be brought to the product form (DĄBROWSKI, 1992; CROCKER *et al.*, 2007):

$$Y(f) = X(f) \cdot H(f) \cdot \Phi^*(f) \cdot \Psi^*(f). \quad (3)$$

This form allows to subject both sides of Eq. (3) to the operator changing the component amplitudes of spectra into values expressed in decibels. Assuming that the total transmittance can be presented as the product of transmittances of individual elements of series systems (elements causing a vibroacoustic energy decrease), reduces the task to the equation of level decreases:

$$L_c(f) = L_s(f) + \sum \Delta L_i(f) + \Delta \Phi^*(f) + \Delta \Psi^*(f), \quad (4)$$

where $L_c(f)$ – signal level at the output, $L_s(f)$ – signal level originated from the dominating source of the vibroacoustic energy, $\Delta L_i(f)$ – signal level changes at individual elements of the series system, $\Delta \Phi^*(f)$ – signal level change at the output, caused by non-linear disturbances and determined in the identification process, $\Delta \Psi^*(f)$ – error of the description caused by various random disturbances.

The problem becomes complicated when there are several vibroacoustic energy sources. In this case, the main aim of modelling is obtaining the independent description of each propagation path. Mutual couplings, resulting, among other things, from the system non-linearity, usually make it impossible to uncouple equations and thus the problem becomes much more complex when the number of the described paths increases.

Let us consider the case of two weakly correlated vibroacoustic energy sources (Fig. 2). In such model we have to assume three unknown functions to be introduced into the model in one of the two ways,

$$Y(f) = X_1(f) \cdot H_1(f) * \Phi_1(f) + X_2(f) \cdot H_2(f) * \Phi_2(f) + \Phi_{12}(f) + \Psi(f) \quad (5)$$

or

$$Y(f) = (X_1(f) \cdot H_1(f) + \Phi_1(f) + X_2(f) \cdot H_2(f) + \Phi_2(f)) * \Phi_{12}(f) + \Psi(f), \quad (6)$$

where $\Phi_1(f)$ – correction for the non-linear disturbance for the first source, $\Phi_2(f)$ – correction for the non-linear disturbance for the second source, $\Phi_{12}(f)$ – correction for the mutual dependence of the determined transmittances $H_1(f)$ and $H_2(f)$ resulting, among other things, from the system non-linearity.

Before we set about discussing the latter possibility, let us try to simplify the model by assuming that the mutual influence of vibrations of one of the sources on noises of the second source is negligible. The model simplified in such a way is presented in Fig. 5.

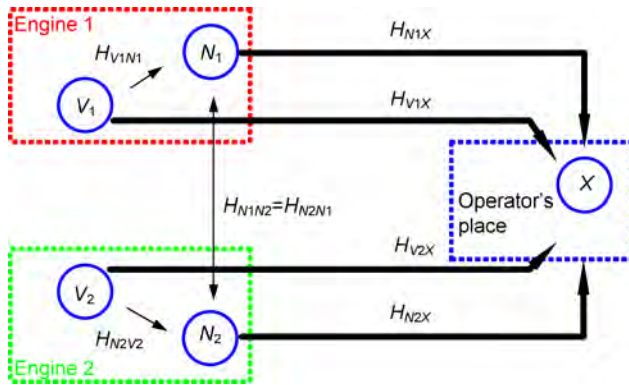


Fig. 5. Simplified model of the vibroacoustic energy propagation for a two-motor machine.

Individual propagation paths can be described as follows:

$$\begin{aligned}
 N_1^* \cdot H_{N1X} &= (N_1 + N_2 \cdot H_{N2N1} \\
 &\quad + V_1 \cdot H_{V1N1}) \cdot H_{N1X} = Y_{N1X}, \\
 N_2^* \cdot H_{N2X} &= (N_2 + N_1 \cdot H_{N1N2} \\
 &\quad + V_2 \cdot H_{V2N2}) \cdot H_{N2X} = Y_{N2X}, \\
 V_1 \cdot H_{V1X} &= Y_{V1X}, \\
 V_2 \cdot H_{V2X} &= Y_{V2X}, \\
 \sum_i Y_{NiX} + \sum_j Y_{VjX} + \sum_i \Phi_{NiX} \\
 &\quad + \sum_j \Phi_{VjX} + \Psi = X.
 \end{aligned} \tag{8}$$

After rearranging Eq. (8) and taking into account that

$$\sum_{i,j} Y_{i,j} = \sum_{i,j} U_{i,j} \quad (Y_{i,j} \neq U_{i,j}),$$

equation of energy fractions from individual sources in the total energy of the signal measured at the operator's stand will be as follows:

$$\begin{aligned}
 N_1 \cdot (H_{N1X} + H_{N1N2} \cdot H_{N2X}) &= U_{N1X} + \Phi_{N1X}, \\
 N_2 \cdot (H_{N2X} + H_{N2N1} \cdot H_{N1X}) &= U_{N2X} + \Phi_{N2X}, \\
 V_1 \cdot (H_{V1X} + H_{V1N1} \cdot H_{N1X}) &= U_{V1X} + \Phi_{V1X}, \\
 V_2 \cdot (H_{V2X} + H_{V2N2} \cdot H_{N2X}) &= U_{V2X} + \Phi_{V2X}, \\
 \sum_i U_{NiX} + \sum_j U_{VjX} + \sum_i \Phi_{NiX} \\
 &\quad + \sum_j \Phi_{VjX} + \Psi = X,
 \end{aligned} \tag{9}$$

where U_{NiX} – energy fraction of the noise source in the noise measured in the operator's cabin, U_{VjX} – energy

fraction of the vibration source in the noise measured in the operator's cabin, and other symbols have the same meaning as in Eq. (7).

In spite of introduced simplifications there are still too many unknowns in Eq. (9). Thus, the only possibility of obtaining a reliable model is looking for new relationships.

As the solution to this problem, the authors assumed the precise identification of high-energy harmonic components of the investigated vibroacoustic signals. In order to do that, application of the normal coherence function was proposed for the determination of energy fractions originated from individual sources for the selected harmonic components. Decomposing functions $\sum U_{NiX}$ and $\sum U_{VjX}$ into individual components allows to reduce each equation from the system (9) to the form (4).

4. Application of the normal coherence function

As it follows from previous considerations, the problem of separation of components representing vibroacoustic processes originated from various sources is the crucial problem solution of which enables the mathematical model identification.

Values of the normal coherence function $\gamma_{xy}^2(f)$ can be interpreted as a part of the output signal energy derived from harmonic components of the input signal for successive frequencies f . This function is often applied in tasks involving identification of energy propagation paths by means of the spectral method (together with the multiple coherence function) (BENDAT, PIERSOL, 1993; 2010). Each of the energy propagation paths, in the system with n independent sources, can be treated as the single-input independent series system. The function of normal coherence for such system can be written as

$$\gamma_{xy}^2(f) = \frac{|G_{xy}(f)|^2}{G_{xx}(f) \cdot G_{yy}(f)}, \tag{10}$$

where $G_{xy}(f)$ – cross-spectral function density of the input $x(t)$ and output $y(t)$ signal, $G_{xx}(f)$ – autospectral density function of the input signal $x(t)$, $G_{yy}(f)$ – autospectral density function of the output signal $y(t)$. Since $|G_{xy}(f)|^2 \leq G_{xx}(f) \cdot G_{yy}(f)$, the normal coherence function can take values from the range $\langle 0, 1 \rangle$.

However, such application of the normal coherence function does not allow to solve the task. The description of the paths of the vibroacoustic energy propagation, even in the simplified form, contains too many unknowns. Moreover, the coherence function value depends on several other factors, including non-linear disturbances, random effects, and frequency components coming from very close frequency values (differences are comparable with resolution Δf of the spectral analysis).

If, in the course of the model identification, we focus on the analysis of harmonic components of the highest energies, we will be able to use properties of the coherence function in a different way. The principle of the proposed computational algorithm is based on the determination the coherence function between individual investigated signals and the harmonic signal which was generated with the assumed parameters (among other things, the frequency value). Treating the signal generated this way as the reference one, we can look for harmonic components in the investigated signals originated from energy sources and recorded at the machine operator’s stand (Fig. 6). Frequency values of the sought harmonic components can be found by analysing operation of individual elements of the driving system.

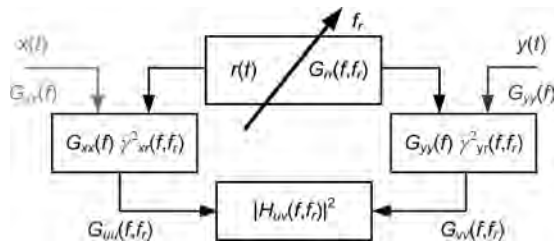


Fig. 6. Schematic presentation of the algorithm for determination of the coherence function with the intermediate signal (reference).

Let us analyse the operation of the proposed algorithm (DZIURDZ, 2000; 2013). The measured signals are represented by spectral densities $G_{xx}(f)$ and $G_{yy}(f)$. By calculating coherence functions between the recorded signals and the reference signal of a spectral density $G_{rr}(f)$,

$$\begin{aligned} \gamma_{xr}^2(f) &= \frac{|G_{xr}(f)|^2}{G_{xx}(f) \cdot G_{rr}(f)}, \\ \gamma_{yr}^2(f) &= \frac{|G_{yr}(f)|^2}{G_{yy}(f) \cdot G_{rr}(f)}, \end{aligned} \quad (11)$$

it is possible to determine the energy being transferred by harmonic components of real signals (accurately at least for the part related to the linear response of the system):

$$\begin{aligned} G_{uu}(f) &= G_{xx}(f) \cdot \gamma_{xr}^2(f), \\ G_{vv}(f) &= G_{yy}(f) \cdot \gamma_{yr}^2(f). \end{aligned} \quad (12)$$

Dividing the obtained values by each other we obtain the coefficient of amplification squared:

$$\frac{G_{vv}(f)}{G_{uu}(f)} = |H_{uv}(f)|^2. \quad (13)$$

Moreover, this algorithm allows, by the controlled change of the reference signal frequency, for a more accurate determination of frequencies of harmonic components of the investigated signals and separation of harmonic components of similar frequencies.

The verification of the operation effectiveness of the proposed method was carried out for signals recorded in a real object (hydraulic excavator) in which the driving motor was working at a constant rotational speed of approx. 2000 rpm. This corresponds to the rotational frequency of approx. 33.33 Hz. Accelerations of vibrations recorded at the motor support and on the operator’s cabin floor were the analysed signals.

At first, let us determine the actual rotational frequency of the motor (with an accuracy possible to obtain when the algorithm is applied). Determination of more accurate rotational frequency is essential insofar as the knowledge of kinematic relations allows for better determination of frequencies of vibroacoustic signals components originated from the driving system.

Narrow-band spectra of accelerations of vibrations at selected points of the machine are presented in Fig. 7. Based on them, the preliminarily determined rotational frequency of the motor was 33.57 Hz (approx. 2014 rpm).

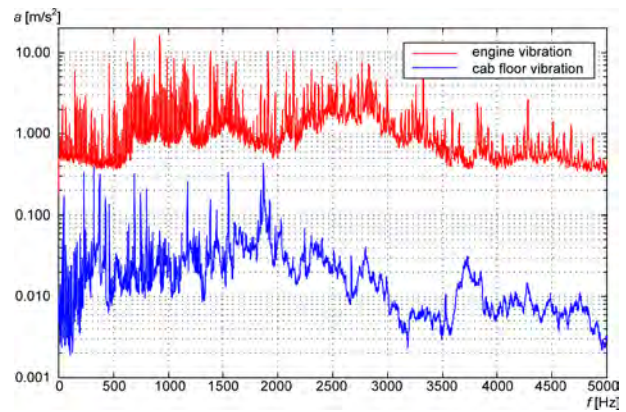


Fig. 7. Spectra of acceleration of vibrations at selected points of the machine.

The results of more accurate analysis of the rotational frequency signal component are presented in Fig. 8. Overall results of the performed calculations are presented in Table 1.

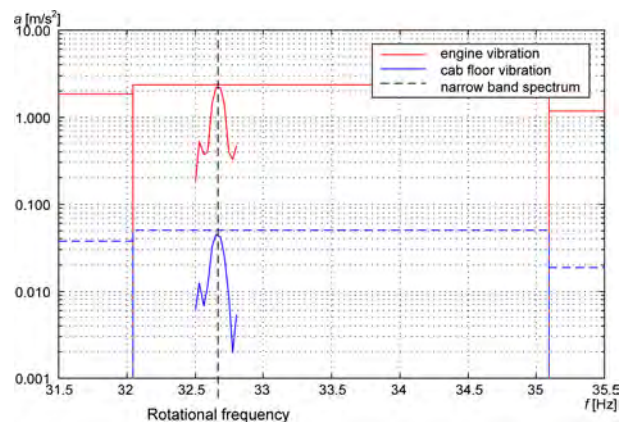


Fig. 8. Example of the vibration accelerations analysis for the signal component of the rotational frequency.

Table 1. Analytical results for the signal component of the rotational frequency.

	Spectral line	Determined harmonic component
Signal frequency [Hz]	33.57	32.65
Accelerations of vibrations of the motor support [m/s ²]	2.339	2.211
Accelerations of vibrations of the operator's cabin floor [m/s ²]	0.051	0.045
Coefficient of amplification [-]	21.8·10 ⁻³	20.4·10 ⁻³
Damping [dB]	approx. 33.2	approx. 33.8

The applied algorithm allowed for more accurate determination of the harmonic component signal frequency. For the parameters applied, the accuracy of analysis of the obtained rotational frequency was ±0.015 Hz (while the value obtained from the narrow-band spectrum was ±1.53 Hz). Differences in the coefficients of amplification values were above 6%. This more accurate analysis allowed to limit the influence of the lower-energy signal components which in the classical analysis are taken into account in the total energy represented by the spectral line.

5. Uncoupling equations of the vibroacoustic energy propagation

The proposed algorithm can be utilised in two ways. When we have a possibility of performing a certain number of partial measurements (including possibility to switch off temporarily some vibroacoustic energy sources), determination of unknowns from the system of Eqs. (9) is possible and thus also the relatively accurate model description (Fig. 5). When we do not have such possibility, more accurate determination of parameters of harmonic components allows to replace the relatively complicated non-linear model with the parallel linear model. In such case, maintaining constant excitation, i.e. stationary motion of the system, is indispensable (it results from the general theory of non-linear systems) (BATKO *et al.*, 2008). Equations (9) are then reduced to the form

$$\begin{aligned}
 S[N_1] \cdot |H_{N1X}^*| &= S[X]_{N1} \cdot \Phi_{N1X}, \\
 S[N_2] \cdot |H_{N2X}^*| &= S[X]_{N2} \cdot \Phi_{N2X}, \\
 S[V_1] \cdot |H_{V1X}^*| &= S[X]_{V1} \cdot \Phi_{V1X}, \\
 S[V_2] \cdot |H_{V2X}^*| &= S[X]_{V2} \cdot \Phi_{V2X}, \\
 \sum_i S[X]_{Ni} + \sum_j S[X]_{V1j} + \sum_i \Phi_{NiX} & \\
 + \sum_j \Phi_{VjX} + \Psi &= X,
 \end{aligned} \tag{14}$$

where S – operator denoting operations performed according to the proposed algorithm, S [N_i] – dominating signal harmonic components of the source N_i, S [N_j] – dominating signal harmonic components of the source V_j, S [X]_{N_i} = U_{N_iX} – fraction of dominating har-

monic components of the source N_i in the observed process measured at the system output within an accuracy of the value of function Φ_{N_iX}, S [X]_{V_j} = U_{V_jX} – fraction of dominating harmonic components of the source V_j in the observed process measured at the system output within an accuracy of the value of function Φ_{V_jX},

$$\begin{aligned}
 |H_{N1X}^*| &= |H_{N1X} + H_{N1N2} \cdot H_{N2X}|, \\
 |H_{N2X}^*| &= |H_{N2X} + H_{N2N1} \cdot H_{N1X}|, \\
 |H_{V1X}^*| &= |H_{V1X} + H_{V1N1} \cdot H_{N1X}|, \\
 |H_{V2X}^*| &= |H_{V2X} + H_{V2N2} \cdot H_{N2X}|,
 \end{aligned}$$

and meaning of the remaining symbols is the same as in Eq. (7).

Equations (14) are uncoupled within an accuracy of the value of function Φ_{ijX}, and after transferring into the logarithmic scale (values in decibels), they can be reduced to equations representing balancing out the level decreases on each of the propagation paths and the equation determining the total level in the cabin:

$$\begin{aligned}
 L_{N1} + L_{HN1X} &= L_{UN1} + \Delta_{N1X}, \\
 L_{N2} + L_{HN2X} &= L_{UN2} + \Delta_{N2X}, \\
 L_{V1} + L_{HV1X} &= L_{UV1} + \Delta_{V1X}, \\
 L_{V2} + L_{HV2X} &= L_{UV2} + \Delta_{V2X}, \\
 \log_{10} \left(\sum_i 10^{L_{UNiX}} + \sum_j 10^{L_{UVjX}} \right) + \Delta_X &= L_X,
 \end{aligned} \tag{15}$$

where L_{N_i} – level of dominating harmonic components of the source N_i, L_{V_j} – level of dominating harmonic components of the source V_j, L_{HN_iX} – decrease of the signal level between the source N_i and system output X, L_{HV_iX} – decrease of the signal level between the source V_j and system output X, L_{UN_i} – fraction level of dominating harmonic components of the source N_i in the observed process measured at the system output within an accuracy of the value of Δ_{N_iX}, L_{UV_i} – fraction level of dominating harmonic components of the source V_j in the observed process measured at the system output within an accuracy of the value of Δ_{V_jX}, L_X – signal level at the system output, Δ_{N_iX} – relative error of separating the propagation path between the source N_i and the system output, Δ_{V_jX} – relative error of separating the propagation path between the

source V_j and the system output, Δ_X – total error of separating the propagation paths between the sources and the system output.

6. Conclusions

On the basis of the performed investigations it can be stated that the proposed algorithm utilising the normal coherence function allows to solve the identification problem of the general model of the noise and vibrations in non-linear multi-source system, at least for harmonic components. It is possible ‘to assign’ to a process, observed at the output, the components originated from individual sources with a high accuracy, even in the most difficult case of two twin-type driving systems operating with the same nominal rotational speed. Thus, it allows to calculate the coefficients of amplification on the source-system output path.

The application of the intermediate method (with a reference signal) allows to eliminate or reduce errors of the correlation function estimations which could be caused by:

- presence of external disturbances affecting input or output signals;
- non-linearity of the system binding signals at inputs and outputs;
- occurrence of feedbacks in the investigated system;
- interactions between the sources;
- correlation between input processes (presence of identical or similar harmonic components in various input processes).

The identified model provides a simple tool for assessing the impact of additional sound- and vibration-isolating elements on the noise in the cabin, and thus the selection of suitable insulating structures. Then one can use Eqs. (15) by adding level decreases resulting from characteristics of those structures to the levels L_{HNiX} and L_{HViX} (DĄBROWSKI, 1992).

Acknowledgments

This paper has been compiled on the grounds of results obtained in the 2nd stage of the long-term

program “Improvement of safety and work conditions” financed in the years 2011–2013 in the framework of research and development works from the resources of the Ministry of Science and Higher Education/National Research and Development Centre. The Program Co-ordinator was the Central Institute of Labour Protection – National Research Institute.

References

1. BATKO W., DĄBROWSKI Z., KICINSKI J. (2008), *Non-linear Effects in Technical Diagnostics*, Publishing and Printing House of the Institute for Sustainable Technologies – NRI.
2. BENDAT J.S., PIERSOL A.G. (1993), *Engineering Applications of Correlation and Spectral Analysis*, 2nd ed., John Wiley, New York.
3. BENDAT J.S., PIERSOL A.G. (2010), *Random data: Analysis and Measurement Procedures*, 4th ed., John Wiley, New York.
4. CROCKER M.J., PRICE A.J. (1969), *Sound transmission using statistical energy analysis*, Journal of Sound and Vibration, **9**, 3, 469–486.
5. CROCKER M.J. [Ed.], (2007), *Handbook of Noise and Vibration Control*, John Wiley & Sons.
6. DĄBROWSKI Z. (1992), *The Evaluation of the Vibro-acoustic Activity for the Needs of Constructing and use of Machines*, Machine Dynamics Problems, **Vol. 4**, Warsaw.
7. DZIURDZ J. (2000), *Minimize noise and vibration for the operator working machine (proposed method)*, [in Polish: *Minimalizacja hałasu i drgań na stanowisku operatora maszyny roboczej (propozycja metody)*], PhD Dissertation, Warsaw University of Technology.
8. DZIURDZ J. (2013), *Application of Correlation and Coherence Functions in Diagnostic Systems*, Selected, peer reviewed papers from the Symposium on Mechatronic Systems, Mechanics and Materials, Solid State Phenomena, **196**, 3–12.
9. Brüel & Kjær Sound & Vibration Measurement A/S (2010), Source Path Contribution software, SPC Pulse User Manual, ver. 14.1.

Awareness of Noise Hazards and the Value of Soundscapes in Polish National Parks

Sebastian BERNAT

*Department of Environmental Protection, Faculty of Earth Sciences and Spatial Management
Maria Curie-Skłodowska University*

Al. Kraśnicka 2cd, 20-718 Lublin, Poland; e-mail: sebastian.bernat@poczta.umcs.lublin.pl

(received March 20, 2013; accepted August 12, 2013)

The goal of the studies undertaken in Polish national parks was to determine noise threats, examine the resources, assess the quality of soundscapes and identify the possibilities of their protection. The questionnaire method used in the studies made it possible to identify the awareness of noise threats and the value of soundscapes according to the park service staff. In addition, the semantic differential and description methods were used to learn how students assessed the soundscape quality of Polish national parks. Finally, avenues of further research on soundscape in environmentally valuable areas were indicated.

The research findings indicate that each national park in Poland is characterised by diverse and unique soundscapes and is subject to the pressure of road traffic and tourism resulting in noise hazards. The conservation of the acoustic values of parks is necessary and possible.

Keywords: landscape perception, noise, soundscape, quiet zone, national parks.

1. Introduction

As early as the 1960s, the Canadian composer and musicologist R. Murray Schafer observed the need for a change in how we consider noise abatement and suggested a positive approach to the sounds around us. According to Schafer, “a fascinating macro cosmic symphony is being played ceaselessly around us”. It is a symphony of the soundscapes of the world and we are its listeners, performers and composers at the same time. It is essential to recognize which sounds we wish to preserve, develop, and multiply in order to isolate harmful and wearisome sounds that must be eliminated (SCHAFER, 1976). The invasion of all-pervading noise can be countered by developing auditory sensitivity and improving the aesthetic quality of the acoustic environment through soundscape design. It is important to restore order in the soundscape, to improve, modify and eliminate undesirable sounds or to move them to other sites, and to preserve the sounds of the past. In 1970, at the Simon Fraser University, R. Murray Schafer founded his own research group, the World Soundscape Project, guided by the idea to thoroughly examine the soundscape in all its aspects, giving particular consideration to its determinants associated with human beings. The Project

sought to build a scientific foundation for acoustic design and discipline proposing ecological solutions for improving the aesthetics of the sonic environment. As part of the Project, studies were initially conducted in Vancouver (Vancouver Soundscape) and five European villages (Five Village Soundscapes). Schafer’s initiative has led to the development of an international acoustic ecology movement whose activity includes soundscape studies conducted in many countries as well as a collaboration within the World Forum for Acoustic Ecology. Increasingly often, interdisciplinary projects concerned with soundscapes are being implemented, e.g. Soundscape of European Cities and Landscapes, with 18 countries represented by 35 specialists being involved (BOTELDOOREN *et al.*, 2011; BROWN, 2012). At the intersection of acoustic ecology, bioacoustics, ecology of space and psychoacoustics, a new research field is developing dynamically: soundscape ecology, concentrating on the relationships between sound and landscape from the structural and functional perspective (PIJANOWSKI *et al.*, 2011). The sustainable development of cities depends on the soundscape design and protection of tranquil areas (BROWN, 2012; Designing Soundscape for Sustainable Urban Development; WEBER, 2012). Since 2010, the European Soundscape Award has been awarded to highlight creative solu-

tions to noise problems (the city of Stockholm has been awarded in 2010, the Gerderland Province in 2011 and the city of Berlin in 2012). The role of soundscapes in the modern world has been recognized in the Careggi Landscape Declaration on Soundscapes that emphasizes, among other things, the need to protect soundscapes and consider the acoustic dimension in landscape planning as well as to expand education in terms of developing auditory sensitivity.

In recent years, the subject of soundscapes has been addressed by representatives of various branches of science in Poland (ref. BERNAT, 2008; LOSIAK, TAŃCZUK, 2012) including geographers conducting research on the perception of landscape where sonic stimuli play an important role alongside the visual ones (e.g. PIECHOTA, 2006). So far, however, there have been no comprehensive studies undertaken on the quality of soundscapes in areas of environmental value in Poland, even though these areas are increasingly threatened by noise that, for example, degrades the quality of the environment, leads to the loss of biodiversity, deterioration of health and a distorted perception of attractive landscapes. Although Article 15 of the Act on Environmental Protection (2004) prohibits noise nuisance in national parks and nature reserves, it is doubtful whether the ban is observed and whether the soundscape resources of national parks in Poland are recognized and protected.

The goal of the studies undertaken in Polish national parks was to determine noise threats, examine the resources, assess the quality of soundscapes and identify the possibilities for their protection. The questionnaire method used in the studies made it possible to identify the awareness of noise threats and the value of soundscapes according to the park service staff. In addition, the semantic differential and the description methods were used to learn how students assessed the soundscape quality of Polish national parks. Finally, avenues of further research on soundscape in environmentally valuable areas were indicated.

2. Soundscapes as the object of environmental protection

The soundscape, perceived as an “acoustic event”, is formed through the overcrowding and intermingling of many and various sound fields, each of which has a single source. According to SCHAFER (1976), soundscapes consist of a background, referred to as “keynote sounds”, and “sound events” that can be ascribed certain meanings by a specific community. Sound events can be analysed from the perspective of their source (e.g. nature, human beings), function and social context (warning, internal, landmark, relaxing, stress-inducing, status-indicating sounds) as well as associations and symbolism. Certain sound events

are sound signals, i.e. sounds that one pays special attention to. Schafer as a soundmark referred to a sound signal that, for some reason, is unique, or possesses qualities of particular value to a local community. Each sound event has its spatial range, described as a sound profile or acoustic space. It is an “area over which it may be heard before it drops below the level of the ambient noise” (TRUAX, 1999). Azimuth denotes the direction of a sound in the horizontal plane. The acoustic horizon is “the farthest distance in each direction from which sounds may be heard” (TRUAX, 1999). Sound events have a temporal dimension, i.e. a specific rhythm and tempo. Rhythms can assume periodic patterns, isorhythms, or, still wider, cycles. A soundscape can also have a hi-fi or lo-fi quality. Hi-fi refers to an environment “where all sounds may be heard clearly without being crowded or masked”, whereas lo-fi refers to a soundscape where sounds “are overcrowded, resulting in masking and lack of clarity” and perspective (TRUAX, 1999).

Soundscapes are an important element of the natural and cultural heritage, particularly sensitive to changes associated with the development of civilisation. They can also be a significant distinguishing feature of places and regions. Sounds that are unique, or of particular value to a local community, occur in nearly every environment. Soundscapes are a carrier of content, associations and symbolism. Evoked by remembered sounds, particularly sequences of sounds (a tune, piece of music), such associations bind the perceived scenery with the information that one has about a given region. Soundscape research usually makes use of sociological methods (semantic differential, sonic preference test, mental map, questionnaire, interviews, free description) that complement observations (soundwalks) and acoustic measurements carried out in the field (BERNAT, 2008). In soundscape ecology, biophones, geophones and anthropophones are distinguished, the spatial and temporal dynamics of soundscapes are analysed, and human impact on natural soundscapes is evaluated. Within the various types of soundscapes (natural, sensitive, endangered, unique, recreational, representative, cultural, and everyday soundscapes), values, threats, management objectives and monitoring directions are identified as the basis for planning protection (DUMYAHN, PIJANOWSKI, 2011).

The soundscape is a very delicate resource. According to the report “Environmental Quality Objectives. Noise in Quiet Areas”, natural soundscapes are an indicator of environment quality, important for the preservation of biodiversity (WAUGH *et al.*, 2003). Noise intrusions are detrimental to the functioning of nature (e.g. BARBER *et al.*, 2011) and the aesthetic experiences of tourists. Therefore, proper monitoring and management of soundscapes, including the protection of their natural and cultural values, is essential. This

necessity has been recognised in national parks in the U.S. where soundscapes play a major part of the conservation strategy (Management Policies 2006). The restoration of natural soundscapes is part of the national park services' responsibilities, aimed at improving the functioning of the natural environment system. The measures taken include establishing quiet zones, evaluating human impact on the soundscape, surveying the expectations of tourists, monitoring, and educational campaigns. There is some awareness that the above measures should be integrated with road traffic management schemes. Numerous indicators are used in order to evaluate the quality of soundscape, e.g. maximum volume of single sound events (in dB), percent time of human-caused sounds remaining audible above natural ambience, noise-free interval, and number of noise intrusions (ROSSMAN, 2005). Studies are conducted to determine the acoustic quality standards and identify aspects of soundscapes that impact the tourists' experience and nature (e.g. AMBROSE, BURSON, 2004; PILCHER *et al.*, 2009). An important role is played by educational work, supported by an educational programme for listening and recording soundscapes (wild soundscapes in the national parks). Soundscape management plans are developed based on detailed perception and acoustic analyses (sound sources and levels, indicators, and standards).

3. National parks in Poland

In Poland, national parks (NP) are regarded as the primary and most effective form of nature and landscape protection despite the fact that they only account for 1% of the country's territory. At present, there are 23 national parks in Poland, representing the main geographical regions and landscape zones. Mountain parks predominate: two in the Sudetes (Tatra Mountains NP and Karkonosze NP) and six in the Carpathians (Babia Góra NP, Gorce NP, Pieniny NP, Tatra NP, Magura NP and Bieszczady NP). Furthermore, there are two coastal parks (Wolin NP and Slovinski NP), four lake district parks (Wigry NP, Bory Tucholskie NP, Drawa NP and NP of Wielkopolska), six in the Central-Polish Lowland (Białowieża NP, Biebrza NP, Narew NP, Polesie NP, Kampinos NP and Ujście Warty NP) and three in the uplands (Ojcowski NP, Roztocze NP and Świętokrzyski NP). The average size of a national park in Poland, at 13 673 hectares (statistical data from Environmental Protection Yearbook 2009), is considerably lower than the average around the world. The smallest park, Ojcowski NP, is 27 times smaller than the largest, Biebrza NP. Forests are the dominant landscape feature in most of the national parks (Table 1); altogether they cover about 60% of the total area of all parks.

Each national park is characterised by its own unique landscape, such as sand dunes, marshes, peat

bogs, primeval forests, lakes, or alpine landscapes with altitudinal vegetation zones. According to a natural environment assessment carried out by the Polish Academy of Sciences Institute of Nature Conservation (DENISIUK, 1992), the Tatra and the Bieszczady national parks are the most comprehensive in terms nature and landscapes (landscape variety and occurrence of unique landscape features). The Ujście Warty and the Gorce national parks are the least attractive in this respect. What is striking is the poor rating of most of the recently established parks: the inhabitants of Poznań regarded the Tatra as the most attractive, while the Polesie, Narew and Magura parks as the least attractive (ADACH, ADACH, 2010).

Studies conducted by ZGŁOBICKI *et al.* (2005) on seven national parks representing different types of landscape (3 mountain, 2 lowland and 2 coastal parks) show that areas with vast landscapes are the most visually attractive. Hence, at the top of the list are the Tatra, Karkonosze and Bieszczady national parks, i.e. mountain parks characterised by very intense tourism traffic. The Narew and the Slovinski parks received the lowest rating. Furthermore, the perception of national parks (the aesthetic evaluation of landscape) was found to correspond to their actual environmental value (ecological evaluation of the landscape).

Being the most attractive areas in terms of nature and landscape, parks are subject to intensive tourism pressure. In 2009, the Tatra and the Karkonosze parks were the most popular among tourists (each attracting more than 2 million visitors). In comparison, the Narew NP was only visited by 8 600 tourists in 2009. As shown by the survey of the inhabitants Poznań, the attractiveness of a given park is most considerably reduced due to a large number of visitors (ADACH, ADACH, 2010).

As regards the tourism-to-park size ratio, the Karkonoski and the Pieniński parks are under the greatest strain (Table 1). The smallest number of tourists was recorded in the Narwiański, Biebrzański, Poleski, Drawieński and Ujście Warty national parks. A network of tourist trails, particularly well-developed in the Biebrzański and the Kampinoski parks, is conducive to large numbers of visitors. The shortest total length of tourist trails exists in the Ujście Warty park. However, the availability of a dense network of tourist trails is not the key factor attracting tourists to a particular national park. Studies conducted by PIETRZAK *et al.* (1999) along the Cyryl Ratajski tourist trail in the NP of Wielkopolska indicated that sound had a considerable impact on the actual visual attractiveness of the landscape.

As studies by LEBIEDOWSKA (2009) indicate, the Kampinoski NP is troubled by transport noise pollution propagated along national roads. According to acoustic measurements carried out in the Tatra National Park, the noise levels in some places, frequented

Table 1. National Parks in Poland. Source: Environmental Protection Yearbook 2009.

National Parks	Year of Foundation	Area in hectares	Area of forest land in %	The number of tourist in th. / in number/hectares	Tourist routes in km
Biebrzański	1993	59223.0	26.2	32.0/0.5	483.1
Kampinoski	1959	38548.5	73.1	1000.0/26.0	360.0
Bieszczadzki	1973	29176.5	84.6	273.0/0.9	245.0
Słowiński	1967	21572.9e	28.7	275.4/12.8	144.3
Tatrzański	(1947)b,1954	21197.3	71.8	2078.7/98.0	275.0
Magurski	1995	19438.9	95.5	50.0/2.6	85.0
Wigierski	1989	14999.5	62.8	120.0/8.0	245.4
Drawieński	1990	11342.0	84.2	23.0/2.0	101.0
Białowiecki	(1932)c,1947	10517.3	94.8	82.3/7.8	38.5
Poleski	1990	9764.3	49.0	15.4/1.6	67.5
Roztoczański	1974	8482.8	95.5	120.0/14.1	61.1
Woliński	1960	8133.1	42.5	1500.0/137.0	50.1
Ujście Warty	2001	8074.0	1.0	20.0/2.5	12.6
Świętokrzyski	1950	7626.4	94.6	210.5/27.6	41.0
Wielkopolski	1957	7583.9	62.0	1200.0/158.2	215.0
Narwiański	1996	7350.0	1.3	8.6/1.2	58.0
Gorczański	1981	7030.8	93.8	60.0/8.5	105.1
Gór Stołowych	1993	6340.4	91.1	354.0/55.8	175.1
Karkonoski	1959	5580.5	72.1	2000.0/358.0	117.6
Bory Tucholskie	1996	4613.0	85.3	60.0/13.0	75.0
Babiogórski	1954	3390.5	95.3	52.0/15.0	53.0
Pieniński	(1932)d,1954	2346.2	71.0	756.0/322.0	35.2
Ojcowski	1956	2145.6	71.2	400.0/186.4	40.7

b – The National Forest Unit “Tatra Parki”, c – Forestry National Park in Białowieża, d – The National Forest Unit “National Park in Pieniny”, e – Excluding coastal water of the Baltic Sea

by numerous tourists (e.g. Wyżnia Kira Miętusia in Kościeliska Valley), corresponded to those of a rather busy street, which compromised the opportunity for people to relax and created adverse living conditions for wild animals (WAGNER *et al.*, 2006). According to studies on the perception of sound in the landscape of the Tatra NP, the sounds most frequently recognised by students were the voices of their colleagues and tourists, the rustle of the wind, the sound of a stream or waterfall, and the singing of birds (MADUROWICZ, SZUMACHER, 2007). The Masurian Lake District (in this proposed Masurian National Park) is described as a “noise zone” due to the roar of boat engines as from May to October as about 60 thousand people per day sail on the lakes.

4. Questionnaire survey

In 2010, a pilot survey was conducted using electronic mail (BERNAT, 2010). The services of all the national parks in Poland were asked: Have any noise measurements been carried out in the ... National Park? Do

the Park Service staff believe there exist noise hazards, and if yes, what are the sources of the noise?

According to the replies received (no replies were received from the Narew, Świętokrzyski and Ujście Warty national parks), noise hazards occur in the majority of national parks (no hazards were found in the Białowieża, Biebrza, Polesie and Słowiński national parks). However, noise measurements were carried out rarely, only in the following parks: Drawa, Gorce, Karkonosze, Ojcowski, Roztocze, Tatra, Wielkopolska and Wolin (most often along roads, as part of tests conducted by the Inspection of Environmental Protection, and as part of environmental impact assessments for investment projects). In addition, general information on noise sources was obtained.

The results of this survey were used to prepare a detailed questionnaire on the perception of sound in the landscape, addressed to the authorities of 23 national parks in Poland. In addition, a separate questionnaire was prepared for students of geography and of tourism and recreation (potential tourists) at Maria Curie-Skłodowska University (UMCS) in Lublin. Both

surveys were conducted at the start of 2011 (BERNAT, 2011). The replies from the national park authorities (the questions were answered by the national park directors themselves or nature conservation experts, scientific research experts, etc.) were compared to the replies from students (87 persons, in this 54 women and 33 men, participated in the survey; 46 respondents were residents of Lublin while the remainder lived mostly in other towns of the Lublin Province) in order to show the similarities and differences in the perception of sound in the landscape of Polish national parks.

The questionnaire for national park authorities consisted of 12 (mostly open) questions concerning noise hazards and the values in soundscapes as well as noise abatement methods. The individual questions involved the importance of sound in experiencing the landscape of a park, characteristic sounds (sounds characteristic of a given park, i.e. typical, representative or distinguishing, unique, special, peculiar, dominant or key sounds), noise sources, degree of noise hazard, places where pleasant and unpleasant soundscapes occurred, the time of day when noise was the least tiresome, changes in acoustic conditions over the previous 10 years, the previous presentation of acoustic values, social conflicts associated with noise nuisance prohibition, attitudes towards the conservation of acoustic values, proposals for noise abatement measures, preservation of noise-free areas and soundscapes.

The questionnaire for students consisted of two tasks. The first one was the evaluation of the soundscape of the selected park (known to the respondent) with regard to two features: the kind of impressions (pleasant/unpleasant) and the noise level (noisy/quiet). The semantic differential method was used (semantic scale 1–10). The analysis included parks that received more than 30 replies, i.e.: Roztocze, Tatra, Ojcowski, Bieszczady, Świętokrzyski, Pieniny, Polesie, Białowieża and Slovinski. The Magura, Narew, Wigry, Biebrza, Drawa and Ujście Warty national parks turned out to be the least known. The second task concerned the characteristics of the soundscape of the selected national park. It was assumed that the free description method would enable, among other things, the identification of characteristic sounds and sources of noise hazards, as perceived by the students, and the overall experience of the national park's soundscape. The selection of a specific park by the respondents was also significant because it reflected their familiarity and thus the frequency of their visits there and/or the degree of the landscape's impressiveness. The tasks for the students complemented the survey for the national park authorities, although it was assumed that the answers given in both questionnaires might correspond with each other.

Sounds were recognised as being very important or important for experiencing the landscape in a consid-

erable majority of the parks (14 and 9 parks respectively). Characteristic sounds, mainly the sounds of nature, were indicated in nearly all the parks (20), e.g. “the howling of wolves”, “the wind blowing in mountain pastures” (Bieszczady NP), “the mating calls of black grouse”, “the clanging of cranes” (Polesie NP), “the hooting of the Ural owl in early spring” (Magura NP), “the grunting of the bison” (Białowieża NP), “the sound of water dripping on the floor of a cave and echoes in the caves” (Ojcowski NP), and “the roar of foehn winds, the rumble of waterfalls, the squishing sound of walking on peat” (Karkonosze NP). In some parks, tranquillity was also indicated as a characteristic sound (Ojcowski NP – “the peace and quiet of the caves”, Karkonosze NP – “the quiet of the peat bogs”, Tatra NP – “the tranquillity of the high mountains” off the tourist trails). A few parks share the same sounds of nature (e.g. the rutting of deer, the sounds of specific bird species). In the case of the Wigry park, the sound of mining machines was mentioned (the facilities of the Suwałki Mineral Materials Mines are located about 2 km from the western boundary of the Park). This sound is not typical of environmentally valuable areas and not desirable though discernible. In the case of four parks (Roztocze NP, Świętokrzyski NP, Ujście Warty NP and NP of Wielkopolska), no characteristic sounds were identified because it is actually difficult to tell to what extent the sounds occurring in a given park “cannot be found anywhere else”.

The perception of the above sounds is mainly disrupted by car traffic and groups of noisy visitors (Fig. 1). Other threats mentioned included mass events, discos in localities close to the park's border (Table Mountains and Białowieża NP), the sounds of neighbouring towns and villages (Polesie NP, Białowieża NP, Karkonosze NP, and Tatra NP), trains (Narew and Biebrza NP), agricultural activity (Biebrza NP), motorised hang gliders (Gorce NP), snowmobiles (Karkonosze NP), sports and recreational events using a PA system (Pieniny and Tatra NP), events at hostels in the Tatras, religious ceremonies and other events at the Święty Krzyż mountain (Świętokrzyski NP), and the sound of mineral aggregate mining machines (Wigry NP). As well as these, a grow-

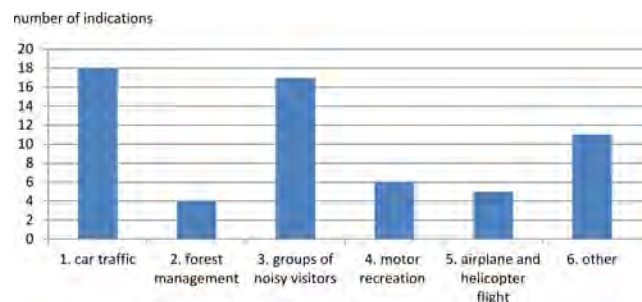


Fig. 1. Threats sources connected with noise in Polish national parks according to services of parks.

ing threat was observed in some parks as a result of the uncontrolled use of quads and motorcycles (individual rallies or company events) in breach of all kinds of regulations. The roar of these vehicles causes panic among walkers, scares away animals, and generally disturbs the peace. In consequence, places that should provide relaxation and rest are deprived of their environmental and aesthetic value, while people's health and even life are endangered.

The noise hazard was most often rated as medium. However, in the case of four parks it was rated as high (Drawa, Ojcowski and Karkonosze NP) or very high (Tatra NP). The greatest noise nuisance occurs in the daytime, particularly in the "rush hours". In most of the parks (14), the acoustic conditions deteriorated over the last 10 years due to an increased number of tourists and increased vehicle traffic on the roads surrounding the park.

According to the park service staff, locations can be identified in the park where the noise is a particular nuisance as well as places with particularly pleasant soundscapes (21 parks). The former are places with considerable vehicle traffic and those having the greatest concentration of tourists. Places with particularly pleasant soundscapes are characterised by a high degree of naturalness (e.g. old alder carrs and other ancient tree stands, hollows between dunes, valleys of streams, banks of permanent and periodic water reservoirs in the Kampinos NP, large forest complexes, valleys of rivers and streams in the Roztocze NP, open peat bogs and wet meadows in the Polesie NP, and mountain top areas in the Gorce NP). In some cases, specific locations are indicated, e.g. the area of Śnieżne Kotły or Wielki Staw in the Karkonosze park (the moraines are barrier to the disturbing urban sounds from Karpacz and Jagniątków).

The need to display the acoustic values is recognised in 14 parks, and museum exhibitions are typically used for this purpose. An example worth mentioning is the Bieszczady park, where sounds characteristic of typical ecosystems are presented as part of spherical panoramas.

In most of the parks, the noise nuisance ban did not cause social conflict. That being said, in as many as 16 parks, interventions and disputes were mentioned concerning, for example, the use of cars, including traffic restrictions (Bory Tucholskie, Roztocze, Gorce and Świętokrzyski parks) and the noisy behaviour of visitors (Wolin, Magura, Drawa and Pieniny parks). Disputes over noise-free zones (acc. to the Act on Environmental Protection Law noise-free zones usually encompass lakes where the use of motorboats and other motor equipment as well as the practicing of water and motor sports are totally prohibited due to the need to maintain suitable acoustic conditions in areas designated for relaxation and recreation; the establishment of noise-free zones through a county council resolution

is binding for spatial planning and development instruments, which means that such an area may not be used for activities that might cause increased noise levels) were mentioned in the case of the Bory Tucholskie park (Lake Charzykowskie) and Pieniny park (Lake Czorsztyńskie). It was discussed for two years whether Lake Czorsztyńskie (part of it being within the park's buffer zone) should be a noise-free zone or whether motorboats could be used on it. The arguments by nature conservationists and enthusiasts of quiet water sports clashed with the interests of motorboat users and owners of the local guesthouses. However, in 2009, the councillors of Nowy Targ County passed a resolution sanctioning a noise-free zone and banning water vessels powered by combustion engines.

In the vast majority of the parks (22), the need to protect the park's acoustic values, including tranquility, was acknowledged. Finally, possible noise abatement measures were proposed, e.g. banning general traffic on some road stretches and introducing transport based on electric vehicles or horse-drawn carriages; moving traffic outside the park (a bypass); eliminating heavy-load vehicle transit; introducing lower speed limits and load weight limits on roads; banning quads, cross-country motorcycles and motorised hang gliders; establishing hedges and noise barriers along roads (subject to an assessment of their impact on the landscape); channelling tourism traffic; limiting the number of tourists; and constant monitoring of tourist trails.

The soundscapes of the national parks in Poland were rated by students as pleasant and tranquil, although there are discernible differences in the evaluation of particular parks (Figs. 2 and 3), as exemplified by a comparison of the Białowieża and the Tatra parks. In the case of the "noisy/quiet" characteristics, nearly 80% of ratings for Białowieża NP were within the range from 7 to 10, i.e. the park's soundscape was rated as tranquil. The rating was similar for Bieszczady NP.

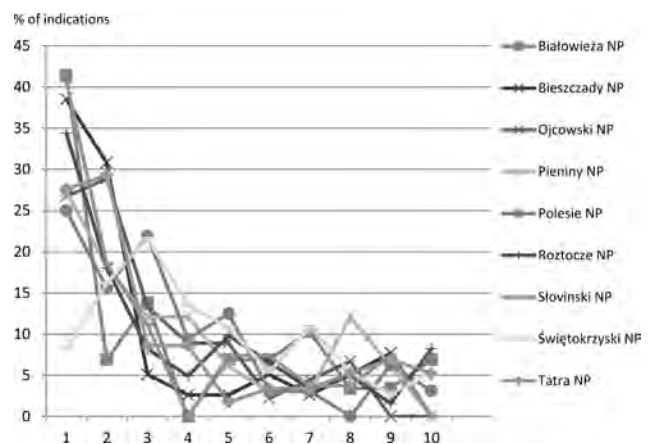


Fig. 2. Soundscape evaluation of Polish national parks in terms of index "pleasant-unpleasant" according to students (scale 1–10); 1 – pleasant, 10 – unpleasant.

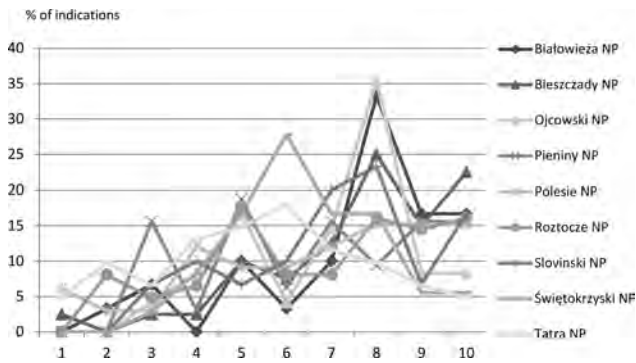


Fig. 3. Soundscape evaluation of Polish national parks in terms of index “noisy-quiet” according to students (scale 1–10); 1 – noisy, 10 – quiet.

The Tatra park was different though: ratings from 7 to 10 accounted for nearly 33% while those from 1 to 4 represented nearly 35% of the responses. These results correspond to the responses of the park service staff about the degree of noise hazard.

The most frequently described parks were the Roztocze (16 respondents), Tatra (12), Bieszczady (11) and Białowieża (6) national parks. Other parks described included Polesie (3 respondents), Słowiński (3), Wolin (2), Ojcowski, Narew, Pieniny, Karkonosze, Świętokrzyski and Bory Tucholskie national parks (one respondent each). The descriptions are of varying quality, although they form a very important source of information about the impressions of the students (potential visitors). For example, the author of a description of the Tatra park emphasised that “in autumn, when most of the tourists have gone, you can hear the wind beating against the rocks higher up the mountains. From below you can hear the sound carried along with the smell of the soil and the forest, the moisture that you can see and hear among the trees. Sometimes you can hear the monophonic sound of a falling stone, disappearing into the silence, a silence that expresses more than many a symphony”. A description of the Karkonoski park mentions “the sounds of the forests and wind rustling in the forest and whistling over open ground, but they are disturbed by relatively large numbers of people who are unable to behave suitably (the excessive use of phones, iPods and other gadgets is irritating)”.

The present survey identified the awareness of noise hazards and the value of soundscapes in particular national parks in Poland, as well as the need to protect soundscapes and possible ways of achieving this. The questionnaire for the national park authorities and the questionnaire for students (potential tourists) complemented one another and gave a more complete picture of the phenomenon. Both groups of respondents were quite consistent in their evaluation of the noise hazards. However, some responses in the questionnaires vary.

The author is aware of the limitations of the research methods used due to their subjectivity. The present findings should be treated as a basis for field research and detailed analysis, also acoustic research. It is the preliminary attempt of assessment the quality of soundscapes of Polish national parks.

To supplement the questionnaire survey, the draft conservation plans for the Bieszczady NP and the Tatra Mountains NP were analysed. These draft plans acknowledge the noise hazards, mainly linked to transport and tourism traffic. The proposed solutions include restricting road traffic crossing the park. Unfortunately, the draft plans make no mention of the perception of sound in the landscape.

5. Conclusions and final remarks

The research findings indicate that each national park in Poland is characterised by diverse and unique soundscapes and is subject to the pressure of road traffic and tourism, resulting in noise hazards. The least attractive soundscapes (though not devoid of any value) occur in the most visually attractive parks (in the mountains) and parks most frequented by tourists (Tatra and Karkonoski NP). The most attractive soundscapes are characteristic of parks not subject to intense tourism pressure and located far from transport routes (e.g. Ujście Warty NP, Poleski NP, Narew NP and Białowieża NP). The conservation of the acoustic values of parks is necessary and possible.

It is essential to conduct studies on the perception of sound in the landscape because increased noise has a considerable disruptive effect on the perception of the natural landscape typified by tranquillity, construed as the audibility of the subtle sounds of nature. In environmentally valuable areas, even the distant reverberating drone of heavy vehicles can be perceived as a nuisance, distorting the perception of the landscape to an inadmissible extent. This was the argument for including the impact of noise on the perception of landscape in the environmental impact assessment of the Augustów bypass, that had originally been planned to cross the Rospuda valley. It also is worth noting that the construction of noise barriers along roads may cause a deterioration of the visual aspects of landscapes besides decreasing the noise levels. In order to prevent the excessive use of noise barriers, in September 2012 the Ministry of the Environment raised the permitted noise levels. Therefore, it can be surmised that the soundscapes of environmentally valuable areas will be subject to increasing threat due to road construction.

It is also necessary to eliminate factors threatening the perception of the landscape so that the high acoustic quality can be preserved (valuable/characteristic sounds must be discernible). It is also important to continue studies on soundscapes (e.g. the preferences of tourists by social groups), supported by acoustic

monitoring, field observations and educational activities. The studies require an interdisciplinary approach (combining acoustics, geography, ornithology, psychology, sociology, etc.) as well as the collaboration of park services, inhabitants, tourists and local governments.

The soundscape may be a factor that increases the attractiveness of environmentally valuable areas, including the least visually attractive parks, and it is particularly important in view of the uneven distribution of tourism traffic. Viewing soundscapes as a resource can make the public more attuned to the beauty of tranquillity (the subtle sounds of nature), essential to preserve the values represented by environmentally valuable areas.

It is worth noting the need to take care of green and open areas in cities as they are potential tranquil areas. The protection of tranquil areas has been consistently implemented in London as part of the city's noise strategy (City of London Noise Strategy 2012–2016). Furthermore, attention is paid to the acoustic design of public spaces, e.g. exposing iconic sounds. Since 2012 an international scientific project has been carried out, focussed on developing coherent methods of assessing and managing tranquil areas in cities (WEBER, 2012). In many Polish cities, efforts aimed at designating noise-free zones have been futile.

Noise abatement cannot be limited to observing acoustic standards; it should also include the shaping of high quality soundscapes. The severity of noise nuisance is determined not only by the intensity of sound but also by its perception. Sound in a particular space cannot be evaluated only negatively, as a nuisance, but should also be viewed positively, as a resource and value.

References

- ADACH O., ADACH J. (2010), *Attractiveness of the polish national parks among the citizens of the city of Poznan* [in Polish: *Atrakcyjność polskich parków narodowych w oczach mieszkańców Poznania*], *Problemy Ekologii Krajobrazu*, **27**, 15–21.
- AMBROSE S., BURSON S. (2004), *Soundscape studies in National Parks*, *The George Wright Forum*, **21**, 29–38.
- BARBER J.R., BURDETT C.L., REED S.E., CROOKS K.R., THEOBALD D.M., FRISTRUP K.M. (2011), *Anthropogenic noise exposure in protected natural areas: estimating the scale of ecological consequences*, *Landscape Ecol.*, **26**, 1281–1295.
- BERNAT S. [Ed.] (2008), *Sound in landscape as a subject of interdisciplinary research* [in Polish: *Dźwięk w krajobrazie jako przedmiot badań interdyscyplinarnych*], *Prace Komisji Krajobrazu Kulturowego PTG*, **11**, Lublin.
- BERNAT S. (2010), *Valuable natural areas – refuges of silence or temples of noise?* [in Polish: *Obszary cenne przyrodniczo – ostoje ciszy czy świątynie hałasu?*], *Prądnik, Prace i Materiały Muzeum im. Prof. Władysława Szafera, Ojców*, **20**, 105–114.
- BERNAT S. (2011), *Soundscape attractiveness of Polish national parks* [in Polish: *Atrakcyjność dźwiękowa polskich parków narodowych*], *Studia i Materiały CEPL*, **13**, 3(28), 83–88.
- BOTELDOOREN D., LAVANDIER C., PREIS A., DUBOIS D., ASPURU I., GUSTAVINO C., BROWN L., NILSSON M., ANDRINGA T.C. (2011), *Understanding urban and natural soundscapes*, *Forum Acusticum 2011, Aalborg* [http://www.lam.jussieu.fr/Publications/Conferences/FA_2011_Dubois.pdf].
- BROWN L. (2012), *A Review of Progress in Soundscapes and an Approach to Soundscape Planning*. *International Journal of Acoustics and Vibration*, **17**, 2, 73–81.
- Careggi Landscape Declaration on Soundscapes (2012) [<http://www.uniscape.eu/allegati/Ref%20UNISCAPE%20CD2-14-06-12%20-Second%20Careggi%20Declaration%20on%20Soundscapes%20draft%20new.pdf>].
- City of London Noise Strategy 2012–2016 [<http://www.cityoflondon.gov.uk/business/environmental-health/environmental-protection/Documents/CoL%20Noise%20Strategy%202012-2016.pdf>].
- DENISIUŁ Z. (1992), *Natural values of the national parks in Poland* [in Polish: *Walory przyrodniczo-krajobrazowe parków narodowych w Polsce*], *Parki Narodowe i Rezerваты Przyrody*, **11**, 2–3, 5–16.
- Designing Soundscape for Sustainable Urban Development (2011) [<http://www.soundscape-conference.eu/>].
- DUMYAHN S.L., PIJANOWSKI B.C. (2011), *Soundscape conservation*, *Landscape Ecology*, **26**, 1327–1344.
- Environmental Protection Yearbook 2009 [in Polish: *Ochrona Środowiska 2009*], GUS Warszawa [Central Statistical Office Warsaw].
- European Soundscape Award, [<http://www.eea.europa.eu/themes/noise/the-european-soundscape-award>].
- LEBIEDOWSKA B. (2009), *Silence as a competitive tourist product*, *Polish Journal of Sport and Tourism*, **16**, 176–183.
- LOSIĄK R., TAŃCZUK R. [Ed.] (2012), *The audiosphere of the city* [in Polish: *Zarządzanie krajobrazem dźwiękowym miast*], *Acta Universitatis Wratislaviensis no 3366*, *Prace Kulturoznawcze XIII*, Wrocław.
- MADUROWICZ M., SZUMACHER I. (2007), *Comparative Workshop on Space Perception: Warsaw-Tatra Mountains. A Research Report*, [in Polish: *Warsztaty porównawcze z percepcji przestrzeni: Warszawa – Tatry. Raport z badania*], [in:] *Perception of contemporary city space*, [in Polish: *Percepcja współczesnej przestrzeni miejskiej*], MADUROWICZ M. [Ed.], *Wyd. WGiSR UW Warszawa*, 309–328.
- Management Policies 2006, National Park Services, US Government Official.

20. PIECHOTA S. (2006), *Perception of recreational landscape in Pszczewski Landscape Park* [in Polish: *Percepcja krajobrazu rekreacyjnego Pszczewskiego Parku Krajobrazowego*], Bogucki Wyd. Nauk., Poznań.
21. PIJANOWSKI B.C., VILLANUEVA-RIVERA J., DUMYAHN S.L., FARINA A., KRAUSE B.L., NAPOLITANO B., GAGE S.H., PIERETTI N. (2011), *Soundscape Ecology: The science of sound in the landscape*, *BioScience*, **61**, 3, 203–216.
22. PIETRZAK M., MIEDZIŃSKA I., STYPEREK J. (1999), *The “real” visual attractiveness of a landscape with tourist routes (the case of the Cyryl Ratajski route in WNP)*, [in Polish: *“Rzeczywista” atrakcyjność wizualna krajobrazu szlaku turystycznego (na przykładzie szlaku im. Cyryla Ratajskiego) w Wielkopolskim Parku Narodowym*], *Problemy Ekologii Krajobrazu*, **5**, 113–121.
23. PILCHER E., NEWMAN P., MANNING R.E. (2009), *Understanding and Managing Experiential Aspects of Soundscapes at Muir Woods National Monument*, *Environmental Management*, **43**, 425–435.
24. ROSSMAN B. (2005), *The importance of soundscapes in National Park Management*, The George Wright Society Conference Proceedings, 335–340.
25. SCHAFER R.M. (1976), *The tuning of the world*, McClelland and Stewart, Toronto.
26. Soundscape Management Plan. Zion National Park, NPS 2010 [<http://www.nps.gov/zion/zion-soundscape-management-plan-available-for-review.htm>].
27. Soundscape of European Cities and Landscapes [<http://soundscape-cost.org/>].
28. TRUAX B. [Ed.] (1999), *Handbook for Acoustic Ecology*, Cambridge Street Publishing, online version [<http://www.sfu.ca/sonic-studio/handbook/>].
29. *Act on Environmental Protection* [in Polish: *Ustawa o ochronie przyrody*] (Dz. U. 2004.92.880 z dnia 30 kwietnia 2004 r.).
30. WAGNER M., NOWAKOWSKI W., CZARNOWSKA K. (2006), *Noise in Tatra National Park* [in Polish: *Zanieczyszczenie hałasem Tatrzańskiego Parku Narodowego*], *Aura*, **9**, 32–34.
31. WAUGH D., DURUCAN S., KORRE A., HETHERINGTON O., O’REILLY B. (2003), *Environmental Quality Objectives. Noise in Quiet Areas. Synthesis Report*, Environmental Protection Agency Wexford, Ireland.
32. WEBER M. (2012), *Quiet Urban Areas: repositioning local noise policy approaches – questioning visitors on soundscape and environmental quality*, *Internoise 2012*, [<http://project.quadmap.eu/wp-content/uploads/2012/09/InterNoise2012-quiet-urban-areas-figures-vdef140-512.pdf>].
33. Wild soundscapes in the national parks. An Educational Program Guide to Listening and Recording, Wild Sanctuary Bernard L. Krause. National Park Service 2002.
34. ZGŁOBICKI W., BARAN-ZGŁOBICKA B., ZIÓLEK M., ZIÓLEK G. (2005), *Scenic beauty of Polish National Parks landscape and their natural values* [in Polish: *Atrakcyjność wizualna krajobrazu polskich parków narodowych a ich wartości przyrodnicze*], *Parki Narodowe i Rezerваты Przyrody*, **24**, 1–4, 135–151.

Indicator of Vibroacoustic Energy Propagation as a Selection Criterion of Design Solution

Grzegorz KLEKOT

*Faculty of Automotive and Construction Machinery Engineering
Warsaw University of Technology
Narbutta 84, 02-524 Warszawa, Poland; e-mail: gkl@simr.pw.edu.pl*

(received July 11, 2013; accepted September 2, 2013)

Contemporary tools which help to design technical objects refer to the conclusions drawn from studying the changes of physical processes accompanying the exploitation, especially to vibroacoustic processes. The main problem is to define such vibroacoustic measures, where their changes would model the analyzed physical phenomena in the best way. Basing on simple indicators which refer to occurring phenomena, it is possible to obtain accurate solutions with a satisfactory reliance level without using complex computing techniques needing detailed descriptors. According to the author, the indicators which are based on the analysis of vibroacoustic energy propagation are very useful in solving engineering problems. These indicators are useful while diagnosing the condition of technical systems, identifying and minimizing the vibroacoustic risks. The possibilities of using such indicators in order to find design solution are illustrated by sample results of the research of the structures with vibroacoustic elements which reduce the noise of rail vehicles by the rail vibration damping.

Keywords: vibration damping, vibroacoustic energy propagation.

1. Introduction

One of the conditions of comfortable, safe, and fail-safe exploitation of technical objects is an appropriate choice of conceptions of constructional solutions which are directed to specific needs and applications. Engineering works which aim to obtain established utility values are determined by assumptions from the concept stage. They are used to specify these assumptions, develop the number of possible options and the choice of the best one in specific conditions.

Today, two extreme approaches to solving engineering problems are worth paying attention. The first direction which results from the dynamic development and almost infinite possibilities of modern computing tools is connected with modeling which is based on very detailed descriptions of phenomena and processes which can be observed in technical objects. Numerical methods allowing to obtain the solutions of systems with several unknowns make it possible to do complex simulation analyses. The multitude of performed operations is no longer the barrier for modeling with a vast number of parameters. In some scientific communities

there is an opinion that it is possible to solve any complicated problem through numerical simulations, and the conclusions from calculations are reflected in technical realities. As a rule, results of the most precise simulation calculations cannot be transferred directly to practical applications: they usually need empirical verification. The reliability of obtained solutions increases after identification of correct parameters of the adopted computing model – if such identification is based on the results of the research of real objects (DĄBROWSKI, 1992).

The second approach stresses the need of theoretical analyses of phenomena taking place during the exploitation processes referring mainly to algorithms including outlines present in the norms, directives, and other acts. Such outlines are often based on empirical indicators supported by the experiment in developing and exploiting the technical objects. Algorithms of progress have the form of procedural records and use simple qualifying criteria (often considered by the protagonists of simulations to be unreliable and leading to serious errors). They allow different people to accomplish repetitive activities and obtain

comparable and satisfactory results – making themselves the part of philosophy of management systems which are gaining a greater recognition in various fields of human activity. Improving the effectiveness of such procedures is possible through applying indicators sensitive to changes of specific features of considered objects, these indicators relate to fundamental physics laws and a sense of analyzed phenomena.

According to the author, there are a lot of situations when, while solving specific engineering problems, there is no need to use sophisticated and complex computing techniques which are based on particular descriptors, and the use of uncomplicated indicators which refer to occurring phenomena allows to make precise conclusions (KLEKOT, 2012). Particularly, the problem of recognizing and minimalizing vibroacoustic threats or evaluation of objects' technical state (KLEKOT, 1992) can be analyzed on the basis of the value of defined indicators taking into account the phenomena accompanying vibroacoustic energy propagation.

2. Comments on the use of vibroacoustic signal

It is generally known that the vibroacoustic signal carries a series of information potentially useful in making conclusions about the state of a technical object and recognizing and minimalizing the threats of vibration and noise. The analysis of changes of vibroacoustic energy propagation, in particular, the analysis of the signal features reflecting these changes (RANDALL, 2009; MARUYAMA *et al.*, 2011) has an important role in the process of a proper exploitation and for improvement of devices' ergonomics (in the range of low noise and vibration level). Because of the dynamic character and complexity of vibroacoustic processes, such problems should be solved in a complex, with taking into account the series of factors which shape the signal form. The tool will be effective under the condition of defining features in the form of measurable parameters whose weight will depend on the solved problem.

The starting point for further considerations will be a signal which is recorded at least by two measurement converters. We should notice that two synchronously recorded signals make it possible to examine the vibroacoustic energy flow between the points (ADAMCZYK *et al.*, 1999). A greater number of places where the signal is recorded, results in wider possibilities to make conclusions in relation to the whole object (DĄBROWSKI *et al.*, 2007a). However, not always the increase in number of measuring points is purposeful, since it inevitably leads to an uncontrolled increase in the number of obtained information,

whose multidimensionality will result in small usefulness in implementation of established goals (NATKE, CEMPEL, 1997). During the analysis of mutual relations, each subsequent recorded signal increases dimensionality of observation space, which consequently leads to information chaos (BOLC *et al.*, 1991). Thus, in order to formulate a proper problem, it is important to adjust the number and kind of recorded signals to an engineering problem which is being solved.

On the basis of executed analyses it is possible to try to make preliminary proposition of vibroacoustic characteristics of the object (considered in time and frequency domains). Such characteristics will be improved with the use of modeling and with special stress on main excitations. Modeling supported by an experiment allows i.a. to optimize the location of measuring converters in terms of realization of particular problems (DĄBROWSKI *et al.*, 2007b; DEUSZKIEWICZ *et al.*, 2009; KLEKOT, 2011).

The next step which simplifies the solution of the problem is decomposition. On the one hand, this concept is about division of the object into assemblies and components generating vibroacoustic processes and responsible for their propagation; on the other hand, the concept of decomposition covers decomposition of a signal into harmonics (i.a. with the spectrum analysis use) which enables one to assign particular features to specified exploiting parameters. Numerical values of particular harmonics will make a space which characterizes vibroacoustic process, and consequently – characterizing the considered technical object.

At this stage we have a big number of partially grouped data ready for further processing or direct use. It is experimentally proved that the process of making effective conclusions can be occasionally carried out without additional classification tools. The choice of classifiers is the absolute minimum, this choice is usually preceded by the design of descriptors which are based on the parts of the space which characterizes the vibroacoustic process.

Verification of usefulness of the indicators and proposed classifiers is possible under the condition of carrying out experiments on real objects, which on the one hand will allow to execute the identification of the parameters of model, on the other hand they will narrow the area of the value of the object parameters represented by particular descriptors.

The final result of all described stages is the presentation of the state of the considered object in the form (from the viewpoint of a task) of complete information about its exploitation properties.

The scheme (Fig. 1) depicts a generalized procedure with pointing at mutual relations between particular stages. Precise description of a particular stage is possible after taking into account the nature of concrete technical objects and problems being solved. The ele-

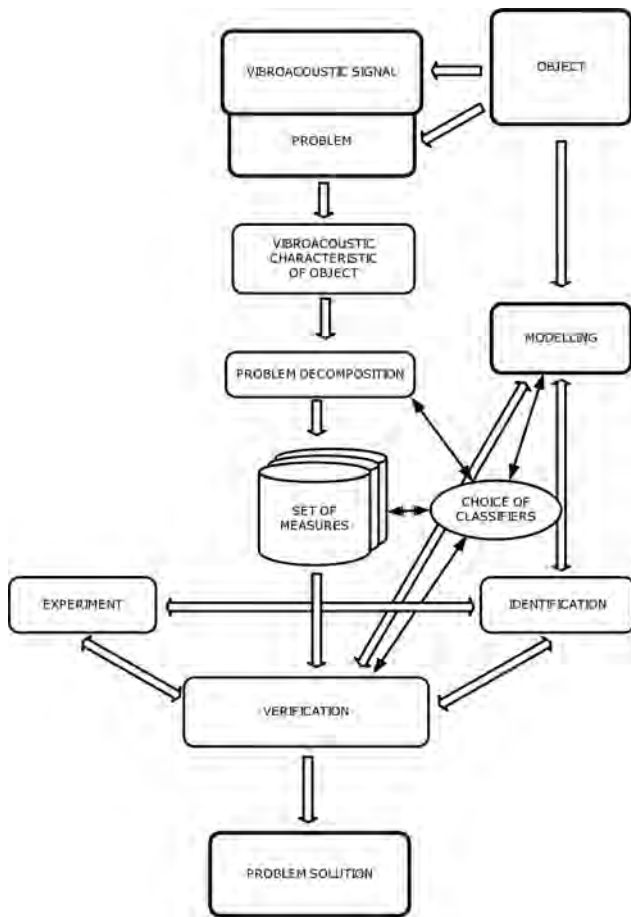


Fig. 1. Scheme of using features of the vibroacoustic signal as tools in the design process and exploitation of technical objects.

ments of the block scheme map the actions adequate to a detailed engineering issue.

3. Indicators of vibroacoustic energy propagation

In order to compare dynamic signals, root mean square value is commonly used as an uncomplicated parameter directly proportional to the energy signal which is variable in time (CROCKER, 1998; KLEKOT, 2003), thus, directly connected with examined processes. Linking root mean square values of signal amplitudes which are recorded at the input and output of the system enables the proposition of indicator H which is directly connected with energy propagation in the form of:

$$H = \frac{\int_0^T (x(t))^2 dt}{\int_0^T (P(t))^2 dt}, \quad (1)$$

where $x(t)$ is the initial signal, and $P(t)$ – extortion.

In order to compare numerical values in view of a large range of amplitudes of vibroacoustic signals the logarithmic scale is useful:

$$H_{[\log]} = \log(H). \quad (2)$$

Such recording is one of the ways of data compression into values in a form of one number. It does not exclude analysis of the results written in a matrix form with the use of many indicators calculated e.g. by integration in different intervals or after the transformation of signals – which creates further big potential research opportunities.

The conception of indicator of vibroacoustic energy propagation naturally refers to Parseval's theorem (Bendat, Piersol, 2010) from which the sameness of the signal energy presented in time and frequency domain results:

$$\int_{-\infty}^{\infty} x^2(t) dt = \int_{-\infty}^{\infty} |X(f)|^2 df. \quad (3)$$

It is possible, thus, to formulate an analogical indicator of vibroacoustic energy propagation also in the frequency domain. Equation (1) will replace relation (4):

$$H_f = \frac{\int_{-\infty}^{\infty} |X(f)|^2 df}{\int_{-\infty}^{\infty} |P(f)|^2 df}. \quad (4)$$

In relation (4) $X(f)$ stands for the spectral density of the signal power, $P(f)$ stand for the spectral density of the forcing signal power, and f is the frequency (expressed in hertz).

The measure defined in such a way truly corresponds in the frequency domain to the squared gain (square transmittance module) of a linear system with constant parameters. A subtle difference can be noticed that the gain coefficient refers to the spectral density, and the measures of vibroacoustic energy propagation depend on the energy of the process reflected by the spectrum or time course, treating equivalently calculations in time and frequency domain.

Proposed energy indexes, which use rms amplitudes in both domains, are calculated with the use of multiplication operation. The undeniable value is the possibility of their selective use: by the choice of integration interval the measure can be sensitized for low-energy changes which are unnoticeable while observing complete process accomplishment.

4. The choice of constructional solution

The implementation of indicator of vibroacoustic energy propagation in order to choose a constructional

solution is illustrated by the example of noise minimization of the tramway. The properties of a structure with four variants of damping elements are compared on the basis of the results of experimental studies of vibration accelerations of impulsively forced steel profile and changes of vibroacoustic pressure in a direct neighbourhood of the structure. The values of indicators linking the RMS amplitude values of vibration acceleration and vibroacoustic pressure with the driving force were calculated. Four constructional solutions are illustrated by Fig. 2.

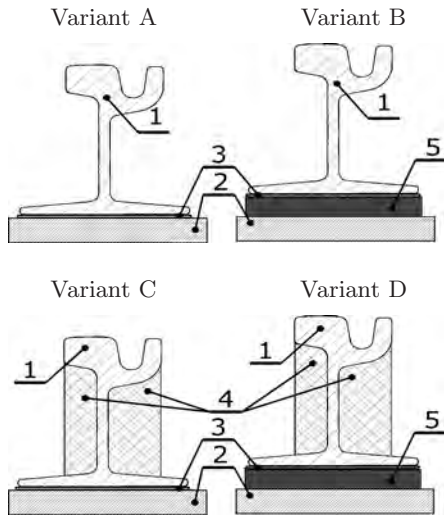


Fig. 2. Constructional solutions of the damping elements: 1 – rail profile, 2 – fundamental, 3 – rubber liner, 4 – damping inserts, 5 – vibroinsulating mat.

Each time the forcing pulse and accelerations of the profile vibration and changes of vibroacoustic pressure over the station were recorded. Vibrations were forced with an impact hammer equipped with a force transducer, the impulses of driving force were reaching 3–5 kN. The indicator values of vibrations' propagation efficiency H_a were calculated according to the dependency (5) as the average for series of 10 of subsequent impulses; analogically, according to dependency (6) the indicator values of sound propagation efficiency H_p :

$$H_a = \frac{\int_0^T (a(t))^2 dt}{\int_0^T (P(t))^2 dt}, \tag{5}$$

$$H_p = \frac{\int_0^T (p(t))^2 dt}{\int_0^T (P(t))^2 dt}. \tag{6}$$

In dependencies (5) and (6) $a(t)$ is the signal of vibration accelerations, $p(t)$ is the signal of the vibroacoustic pressure, and $P(t)$ is the driving force.

The results obtained after the transformation of the recorded time signal for four sets of damping elements is illustrated in the charts. Low values of indicators represent small vibroacoustic energy propagation, which corresponds to a better effectiveness of particular solutions.

The comparison of values presented in Fig. 3 allows to note an important role of rail rubber inserts and vibroinsulating mat for limitation of the energy flow of mechanical vibrations to the environment. The use of rubber damping elements directly glued to the profile is justified because it substantially changes dynamic properties of the steel elastic element.

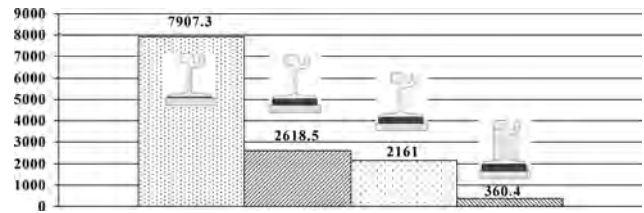


Fig. 3. Values of the efficiency indicator of sound propagation to the environment.

While computing (according to dependency (5)) the indicator which illustrates the effectiveness of vibration propagation by the examined steel profile, the signal of vibration accelerations recorded by the accelerometer fixed to the rail and extortion made with an impact hammer were used. The value analysis from the chart in Fig. 4 confirms an important limitation of vibration transformation owing to the inserts.

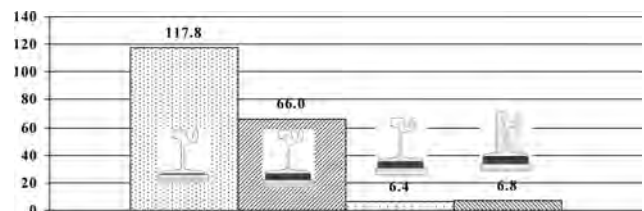


Fig. 4. Values of the efficiency indicator of vibration propagation by the rail.

The inserts are less important for the reduction of transmitting the vibration from the profile into the fundamental: in this case, the vibroinsulating mat which is fixed between the steel profile and the fundamental acts as the vibration isolator. In order to evaluate the effectiveness of transmitting the vibrations into the fundamental in accordance with (5), the recorded accelerations of fundamental vibrations were used. The chart from Fig. 5 allows for the comparison.

Conclusions concerning the effectiveness of particular damping elements are similar if we use a different parameter of a global nature: expressed in seconds by

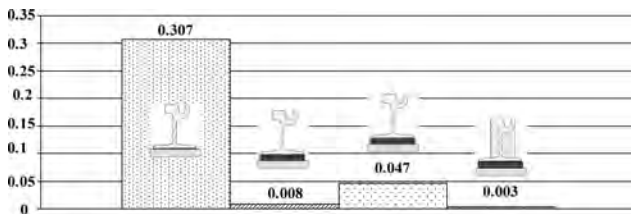


Fig. 5. Values of the efficiency indicator of vibration propagation between the rail and fundamental.

the time after which a decaying amplitude decreases thousand times (known as reverberation time). A little longer time of the sound decay in the neighbourhood of the profile placed on the vibroinsulating mat than without the mat (Fig. 6) can be justified by little stiffness of the elements separating the rail from the fundamental. The nature of the graphs in Fig. 7 and Fig. 8 reflect the damping properties of the various constructional solutions in analogy to the diagrams in Fig. 4 and Fig. 5.

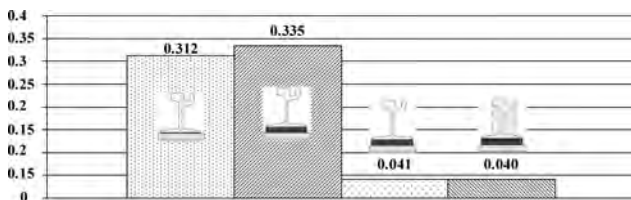


Fig. 6. Time of the sound decay (in seconds) in the neighbourhood of the examined objects.

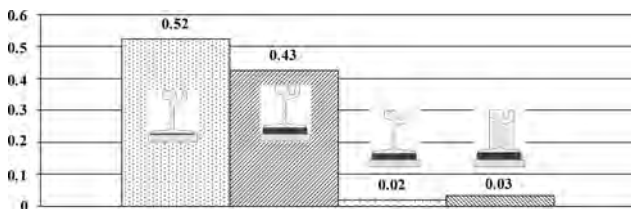


Fig. 7. Time of the rail vibration decay (in seconds).

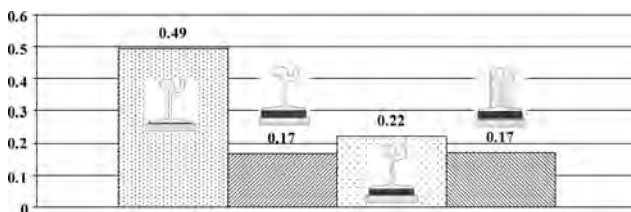


Fig. 8. Time of the fundamental vibration decay (in seconds).

To conclude, vibroinsulation of the designed tramway was made in accordance with variant D presented in Fig. 1.

5. Conclusion

The research technique used during the recognition and minimization of vibroacoustic risks and during the

evaluation of the state of objects allows to use identically defined indicators in design problems and for exploitation diagnostics needs. The indicators referring to the physical basis of the described phenomena are characterized by a large versatility of applications. The computing algorithm from the point of view of usefulness for engineering applications should satisfy two basic conditions: have the features of an object or phenomena and guarantee that the space of founded descriptors is metric; the fulfillment of these two conditions allows to execute some calculations on the indicators.

Energy indicators work well in various domains, even for low-energy processes with an average energy process established in sufficiently long time it is possible (basing on the noticed changing shape of instantaneous spectrums) to take into account appropriately chosen frequency bands and examine the energy changes in these bands. Since in many cases the vibroacoustic energy propagation determines the functional values of an object, and the part of this energy always scatters, it is reasonable to use the descriptors which take into account the role of structural and internal damping and individual properties of considered objects. The example of a choice of a constructional solution of tramway vibroinsulation on the basis of the evaluated effectiveness of damping structures illustrates one of the possibilities of specific engineering applications of this kind of indicators.

References

- ADAMCZYK J., KRZYWORZEKA P., ŁOPACZ H. (1999), *Systems for synchronic processing of diagnostic signals* [in Polish: *Systemy synchronicznego przetwarzania sygnałów diagnostycznych*], Collegium Columbinum, Kraków.
- BENDAT J.S., PIERSOL A.G. (2010), *Random Data: Analysis and Measurement Procedures*, 4th ed., Wiley-Interscience, New Jersey.
- BOLC L., BORODZIEWICZ W., WÓJCIK M. (1991), *The basis of incomplete and uncertain information processing* [in Polish: *Podstawy przetwarzania informacji niepełnej i niepewnej*], PWN, Warszawa.
- CROCKER M.J. (1998), *Handbook of Acoustics*, John Wiley & Sons Inc., New York.
- DĄBROWSKI Z. (1992), *The Evaluation of the Vibroacoustic Activity for the Needs of Constructing and Use of Machines*, Machine Dynamics Problems, **4/1992**, 3–98.
- DĄBROWSKI Z., DZIURDŹ J., KLEKOT G. (2007a), *Studies on propagation of vibroacoustic energy and its influence on structure vibration in a large-size object*, Archives of Acoustics, **32**, 231–240.
- DĄBROWSKI Z., DZIURDŹ J., SKÓRSKI W.W. (2007b), *The vibrations of composite masts* [in Polish: *Drgania masztów kompozytowych*], ITE PIB, Warszawa–Radom.

8. DEUSZKIEWICZ P., DOBROCIŃSKI S., DZIURDŹ J., FLIS L., GRZĄDZIELA A., PAKOWSKI R., SPECHT C. (2009), *Vibroacoustic diagnostics of vessel's turbine engines* [in Polish: *Diagnostyka wibroakustyczna okrętowych silników spalinowych*], ITE PIB, Radom,.
9. KLEKOT G. (1992), *Simplified Kinematic Model of a Spur Gear with Involute Teeth Elaborated for Analysis of Gear Vibroactivity*, *Machine Vibration*, **1**, 261–267.
10. KLEKOT G. (2003), *The choice of damping elements in the task of reduction of noise and vibration of the rails* [in Polish: *Dobór elementów tłumiących w zadaniu minimalizacji drgań i hałasu torowiska*], *Przegląd Mechaniczny*, **4/03**, 40–46.
11. KLEKOT G. (2011), *The measure of propagation of vibration for assessment of damages in concrete beam*, *Scientific Problems of Machines Operation and Maintenance*, **46**, 105–112.
12. KLEKOT G. (2012), *The use of measures of propagation of vibroacoustic energy for condition monitoring and as a tool for noise management* [in Polish: *Zastosowanie miar propagacji energii wibroakustycznej do monitorowania stanu obiektów oraz jako narzędzie w zarządzaniu hałasem*], ITE PIB, Warszawa – Radom.
13. MARUYAMA M., KUNO K., SONE T. (2011), *New Mathematical Model to Estimate Road Traffic Noise in View of the Appearance Rate of Heavy Vehicles*, *International Journal of Acoustics and Vibration*, **16**, 64–71.
14. NATKE H.G., CEMPEL C. (1997), *Model-Aided Diagnosis of Mechanical Systems*, Springer-Verlag, Berlin Heidelberg New York.
15. RANDALL R.B. (2009), *The Application of Fault Simulation to Machine Diagnostics and Prognostics*, *International Journal of Acoustics and Vibration*, **14**, 81–89.

Acoustic Absorption of a New Class of Alumina Foams with Various High-Porosity Levels

Tomasz G. ZIELIŃSKI⁽¹⁾, Marek POTOCZEK⁽²⁾, Romana E. ŚLIWA⁽³⁾, Łukasz J. NOWAK⁽¹⁾

⁽¹⁾ *Institute of Fundamental Technological Research
Polish Academy of Sciences*

Pawińskiego 5B, 02-106 Warszawa, Poland; e-mail: tzielins@ippt.pan.pl

⁽²⁾ *Faculty of Chemistry, Rzeszow University of Technology
al. Powstańców Warszawy 12, 35-959 Rzeszów, Poland*

⁽³⁾ *Faculty of Mechanical Engineering and Aeronautics, Rzeszow University of Technology
al. Powstańców Warszawy 12, 35-959 Rzeszów, Poland*

(received May 7, 2013; accepted October 2, 2013)

Recently, a new class of ceramic foams with porosity levels up to 90% has been developed as a result of the association of the gelcasting process and aeration of the ceramic suspension. This paper presents and discusses original results advertising sound absorbing capabilities of such foams. The authors manufactured three types of alumina foams in order to investigate three porosity levels, namely: 72, 88, and 90%. The microstructure of foams was examined and typical dimensions and average sizes of cells (pores) and cell-linking windows were found for each porosity case. Then, the acoustic absorption coefficient was measured in a wide frequency range for several samples of various thickness cut out from the foams. The results were discussed and compared with the acoustic absorption of typical polyurethane foams proving that the alumina foams with high porosity of 88–90% have excellent sound absorbing properties competitive with the quality of sound absorbing PU foams of higher porosity.

Keywords: sound absorption, porous materials, alumina foams.

1. Introduction

Sound absorptivity of porous media is determined by its total and open porosity, flow resistivity, tortuosity, characteristic sizes of pores and windows linking the pores. In the case of soft materials – like polyurethane (PU) foams – the elasticity of skeleton plays an important role in the lower frequency range. Although PU foams are lightweight materials and some of them have excellent sound absorbing and insulating properties, they cannot be used in many applications, especially, under extreme conditions such as high temperatures, high intensity sound and velocity flow of air, oil contamination and humidification – in such applications (for example, as a material for acoustical liner in turbofan engines) metal foams (BO, TIANNING, 2009) or ceramic foams are adequate.

Ceramic foams are light-weight materials with unique properties such as low density, low thermal conductivity, low dielectric constant, low thermal mass,

high specific strength, high permeability, high thermal shock resistance, high porosity, high specific surface area, high resistance to chemical corrosion, making them indispensable for various engineering applications (COLOMBO, 2006; GREEN, COLOMBO, 2003). These materials are being considered for a whole range of potential aerospace applications, including sound absorbers, thermal insulation, and light-weight structures.

It is well known that many of the above mentioned parameters (like porosity, flow resistivity, pore dimensions, etc.) may be controlled during the production processes in ceramics, and their effects on sound absorption capability of porous ceramics should therefore be studied. Thus, for example, TAKAHARA (1994) investigated sound absorption of porous ceramic material $\text{Al}_2\text{O}_3\text{-SiO}_2$ with porosity from 49 to 55% (although most of the presented results are for the highest value of 55%). For samples with 55% porosity he determined and compared sound absorption with respect

to the sample thickness, namely, 50 mm or 10 mm. In the case of the 50 mm thick sample the absorption coefficient exceeded 0.6 at frequencies above 500 Hz. For the 10 mm thick sample the absorption was much inferior – it exceeded 0.4 above 1 kHz; to improve it an air gap may be added between the sample and the reverberant enclosure (rigid wall). Therefore, the influence of such backing cavity of 85 mm depth on the absorption of the combined (95 mm thick) system of porous ceramic layer and air gap was also shown. For 50 mm thick samples the effect of flow resistivity and porosity was illustrated by comparing results obtained for three different values of these parameters. Sound insulating characteristics of porous ceramics $\text{Al}_2\text{O}_3\text{-SiO}_2$ were also investigated by TAKAHARA (1982) in his earlier work where he presented transmission loss and absorption coefficient for 25 mm-thick sample of porous ceramics with 55% porosity.

Effects of surfactants on some intrinsic properties of porous building ceramics were investigated by FUJI *et al.* (2006). They measured the sound absorption coefficient in the frequency range from 0.5 to 6.5 kHz for porous ceramics fabricated by gelcasting using different surfactants, namely: (a) ammonium lauryl sulphate, (b) fatty alcohol ethoxy sodium, and (c) poly-(oxyethylene)-sorbitan monolaurate. The best results were achieved for the first two surfactants, however, they seem to be rather mediocre when comparing with typical PU foams (although this cannot be clearly stated, since unfortunately, the thickness of ceramic samples is not given). The acoustic absorption coefficient is app. 0.3 at lower frequencies, exceeding 0.4 in the higher frequency range, reaching 0.5 in the case of ammonium lauryl sulphate. For this surfactant the absorption is the best and the total porosity of porous ceramics is 64.7%, whereas the open porosity is 53.4%; in the case when the alcohol ethoxy sodium was used they are 52.3% and 38.6%, respectively. In another work (ZHANG *et al.*, 2006) the authors show that the acoustic absorption can be improved when the porous ceramics is fabricated by gelcasting using a continuous process. By this new method a better pore size distribution is achieved, which improves the total and open porosities (to 68.3% and 73.5%, respectively), and that has its effect on the acoustic absorption which now exceeds 0.5 at 3.3 kHz, reaching 0.7 at 6.4 kHz.

GIESE *et al.* (2011) presented a new processing technique – combining the freeze gelation process with sacrificial templating – to create porous sound absorption ceramics for high-temperature applications. The process leads to near-net shape components with open-cell porosity which can be increased up to 74% by adding expanded perlite as melting filler. Sound absorption was measured in the frequency range from 250 to 1400 Hz for three samples made up of ceramics with different open porosity, namely, 74, 73, and 67%, and various corresponding flow resistance; each of the sam-

ples had the same thickness of 30 mm. The absorption results were very good for two samples of higher porosities, exceeding 0.4 at frequencies above 200 Hz (the maximum value for the sample with porosity 74% was above 0.6 at app. 400 Hz), however, the configuration involved a 50 mm air gap behind the sample, which generally increases the frequency range with a high absorption coefficient towards lower frequencies (notice that the total thickness to the reverberant enclosure was 70 mm); therefore, these results cannot be directly compared with standard tests performed with no gap.

Sound absorption capabilities of porous zeolite with macropores – which is a ceramic material fabricated by high-temperature sintering – were recently investigated by CUIYUN *et al.* (2012). They measured acoustic absorption coefficient in the frequency range from 200 Hz to 4 kHz for 8 ceramic samples with various porosity, bulk density, flow resistivity, and thickness. For three samples the porosity was 60%, for another three it was app. 70%, for one sample it was 64%, and it was 76% for yet another one. The mean pore size varied from 1.1 to 2.9 mm, while it was 6.2 mm for one sample. The sample thickness was: 15, 20, 25, or 28 mm. The measurements showed excellent sound absorbing properties of this ceramics: for most of the samples the acoustic absorption exceeded 0.7 at frequencies over 1.5 kHz, often with some peak/maximum value exceeding 0.9 at 2 or 2.5 kHz. Two analytical models – a simple two-parameter model by Delany and Bazley, and more advanced Johnson-Allard model (ALLARD, ATALLA, 2009), were applied to calculate the absorption coefficient. The latter one showed a better fit to the experimental results, however, the analytical curves were in general very approximative: they were very smooth (the Delany-Bazley curves were even nearly monotonic) and no characteristic peaks were represented.

Corrundum materials have been subject to some acoustical measurements, like acoustic emission (see, for example, RANACHOWSKI *et al.* (2009)) or sound absorption (see some references above), however, in the case of the corrundum or other ceramic foams their porosity was always significantly inferior than the porosity of the recently developed corrundum foam tested in the present paper. It will be shown below that this high porosity ratio together with some microstructural features described in this paper (like typical size of pores and windows linking the pores) contribute to the excellent acoustical properties comparable only with the best of PU foams.

2. Characterization of a new class of alumina foams

In recent years, a new class of ceramic foams with porosity levels up to 90% has been developed as a re-

sult of the association of the gelcasting process and aeration of the ceramic suspension containing foaming agents and gelling agents (SEPULVEDA, BINNER, 1999; SEPULVEDA, 1997). The in situ polymerisation of gelling agents, led to fast solidification, resulting in strong porous bodies. The next step is calcination followed by sintering at high temperature.

Ceramic suspensions of alumina powder (CT 3000 SG, Alcoa Chemie, Ludwigshafen, Germany) were prepared to a solid loading of 55 vol.% by dispersing them with 0.5 wt.% of dispersant (Darvan 821A, R.T. Vanderbilt, U.S.A.). Next, the agarose solution as a gelling agent was added to the slurry maintaining the temperature of all constituents at 60°C. Foaming was conducted through agitation, with the help of a double-blade mixer at 60°C. Addition of non-ionic surfactants (Tergitol TMN-10, Aldrich, Germany) was necessary to stabilise the foam. Gelation was performed by cooling the foam to 15°C. The green body was then de-molded and left in room conditions to dry. Sintering was performed at 1575°C for 2 hours. The details are described in the paper by POTOCZEK (2008). The Al₂O₃ foams were manufactured in that way in the form of cylinders of various height (thickness; see below) in three main cases of porosity levels, namely: 72%, 88%, and 90% (also 89.5%). Ceramic samples were cut out from the cylinders and served for acoustic measurements described in the next Sections.

The density of porous bodies was calculated from the mass and dimensions of a minimum of five samples with regular shapes. The theoretical density of fully densified alumina (3.98 g/cm³) was used as a reference to calculate the total volume fraction of porosity. The microstructure of ceramic foams was observed by scanning electron microscopy (SEM), (Jeol JSM-5500 LV). The fractured samples first were coated with a thin layer of gold. Pictures for monitoring the cellular structure were taken for estimation of cell and window sizes. This allowed window and cell size to be estimated from cells which presented an equator in the fracture surface and from windows by taking the major axis of oblique windows as the true diameter. The diameter of minimum 150 cells and 350 windows was measured for each sample and the pore and window size distributions were calculated.

The densities of alumina foams were found to be between 0.40 and 1.11 g/cm³, and the calculated total porosity varied between 90 and 72%, respectively. It is important to notice that the foam porosity is strongly related to the typical microstructural sizes, like, for example, their pore (or cell) diameters. The microstructure of the sintered foams is presented in Fig. 1 for the three considered cases of porosity, namely: 90, 88, and 72%. The alumina foams are typically composed of approximately spherical cells interconnected by circular windows. The cell size and the window size decrease

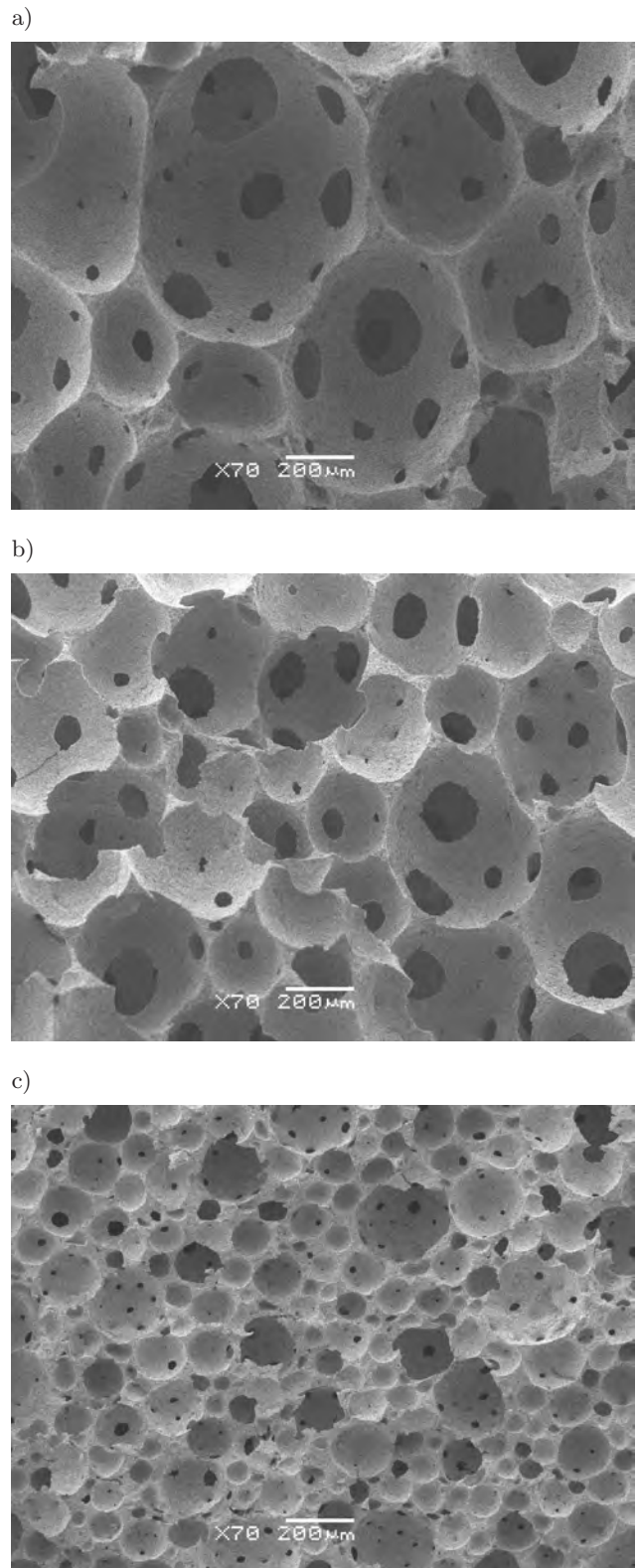


Fig. 1. SEM cross-section of alumina foams having porosity of: a) 90%, b) 88%, and c) 72%.

with increasing of porosity in alumina foams. This is illustrated in Figs. 2 and 3 where the cumulative fractions of cell and window diameters are shown for the

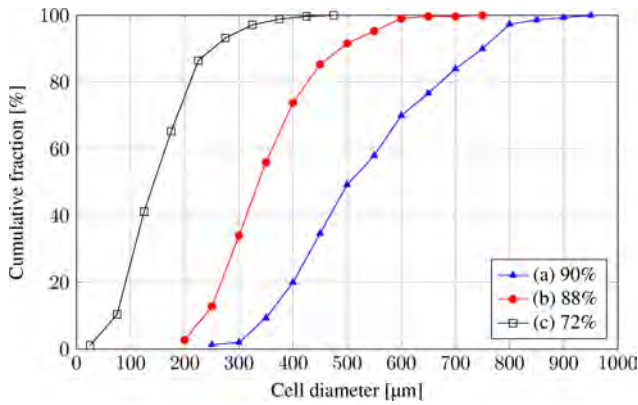


Fig. 2. Cumulative fraction of cell diameters of alumina foams with porosity of: a) 90%, b) 88%, and c) 72%.

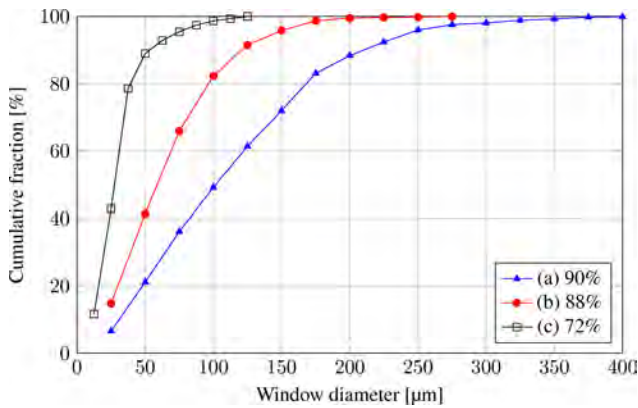


Fig. 3. Cumulative fraction of window diameters of alumina foams with porosity of: a) 90%, b) 88%, and c) 72%.

three cases of porosity. Table 1 provides the median value of cell and window sizes for these three types of alumina foam.

Table 1. Average diameters of cells and windows for alumina foams with particular porosity.

Porosity [%]	Average diameter [μm]	
	of cells	of windows
90	505	101
88	380	60
72	135	28

3. Acoustical testing

All acoustical measurements of ceramic samples were performed using the so-called transfer function method (see, for example, CHUNG, BLASER (1980); DALMONT (2001); BOONEN, SAS (2004)) according to the ISO 10534-2 standard (ISO, 1998). To this end two-microphone configuration of impedance tube was used – the whole experimental setup is shown in Fig. 4. A sample is set at the rigid-wall termination (or, sometimes, leaving an air gap of known thickness, between



Fig. 4. Experimental setup for measurement of acoustic absorption coefficient of materials.

the wall and the sample) at one end in the impedance tube. At the other end, a loudspeaker is mounted which is driven by a broadband, stationary random signal to generate plane acoustic waves which arrive at the sample, penetrate it, and are reflected by the wall. A standing-wave interference pattern results due to the superposition of forward and backward-travelling waves inside the tube. Basing on measurements of the sound pressure at two fixed locations, the so-called complex transfer function is calculated, which can be used to determine acoustical properties of the sample, namely: the normal acoustic impedance, the complex reflection coefficient, and the sound absorption coefficient. Operating frequency range of the instrument depends on the spacing between the microphone positions and on the sample size. The correctness and accuracy of the method strongly depend on the calibration of microphones, which requires measurements of the transfer function for two configurations of the microphones, in their normal and interchanged positions. If the improved calibration procedure proposed by BOONEN, SAS (2004) is used the temperature and ambient pressure measurements are superfluous since then the exact estimation of the actual speed of sound in air is not necessary.

Sound absorption capability was determined for corundum ceramic foams with various porosity, namely: 90%, 88%, 72%, and again also for 89.5%. For each of these porosities two samples were manufactured in the form of cylinders with 29 mm diameter and various thickness (height), see Fig. 5; the cor-



Fig. 5. Ceramic samples prepared for measurements in the impedance tube with diameter 29 mm; the samples 5 and 6 are made up with plaster, whereas the samples 7 and 8 are wrapped up in a thin tape in order to fit well in the tube.

responding data for all samples are given in Table 2. For such sample diameter the valid frequency range for measurements in the impedance tube was from 500 Hz to 6.4 kHz.

All samples with porosity 90% or 88% fitted very well in the measurement tube, while the lateral surfaces of samples with porosity 72% were additionally made up with plaster, and the samples with porosity 89.5% were wrapped up in a thin (transparent) tape in order to fit well. Nevertheless, the fitting was done accordingly to the standard procedure and it should not affect the testing results.

Table 2. Porosity and thickness of cylindrical samples of ceramics Al_2O_3 .

No.	Label	Porosity [%]	Thickness [mm]
1	p90h18	90	18
2	p90h24	90	24
3	p88h14	88	14
4	p88h17	88	16.5
5	p72h16	72	16
6	p72h22	72	22
7	p89h18	89.5	18
8	p89h22	89.5	22

4. Discussion of the results

Figures 6, 7, and 8 show the curves of the acoustic absorption coefficient determined for ceramic samples with porosity 90%, 88%, and 72%, respectively. Additionally, on each of these graphs absorption curves for typical polyurethane (PU) foams are shown for com-

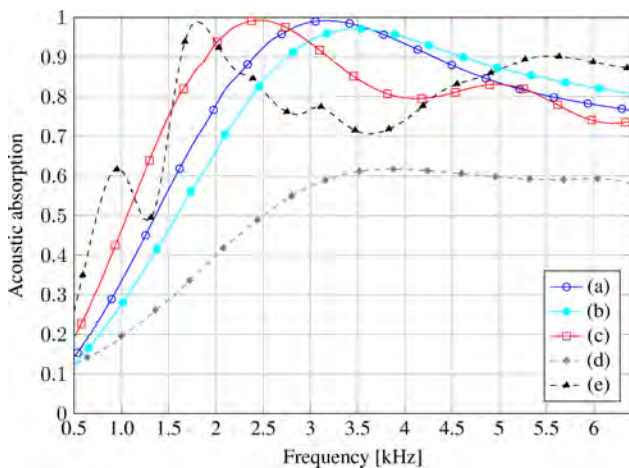


Fig. 6. Acoustic absorption of ceramic samples with porosity 90%: (a, b) thickness 18 mm, face 'A' and 'B', (c) thickness 24 mm. Acoustic absorption of PU foams with porosity app. 98%: (d) stiff PU foam, thickness 26 mm, (e) soft PU foam, thickness 21 mm.

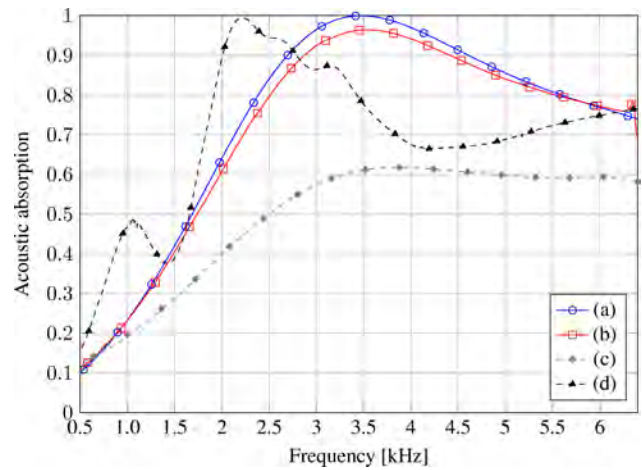


Fig. 7. Acoustic absorption of ceramic samples with porosity 88%: (a) thickness 14 mm, (b) thickness 16.5 mm. Acoustic absorption of PU foams with porosity app. 98%: (c) stiff PU foam, thickness 26 mm, (d) soft PU foam, thickness 16 mm.

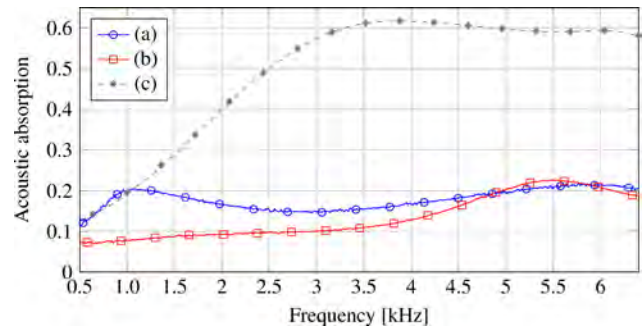


Fig. 8. Acoustic absorption of ceramic samples with porosity 72%: (a) thickness 16 mm, (b) thickness 22 mm. Acoustic absorption of stiff PU foam with porosity app. 98%: (c) thickness 26 mm.

parison. The porosity of PU foams was approximately 98% (as declared by the producer) and the thickness of samples was taken to be in some correspondence with the thickness of relevant ceramic samples. All acoustical measurements were carried out for both sides (faces) of all porous samples. In general, the opposite-side measurements were (nearly) identical, because of the macroscopic homogeneity of the examined porous materials; thus, instead of showing two almost overlapping curves only one of them (or the average result) is presented. The both opposite-side absorption curves are shown only for one sample p90h18 – see curves (a) and (b) in Fig. 6 – those curves do not overlap and are slightly different because of some distinct imperfections on one of the sample faces (curve (b), face 'B').

One should observe that the acoustic absorption is very good for ceramic samples with open-cell porosity of 90% and 88% (Figs. 6 and 7, respectively),

while it is poor for ceramics with closed-cell porosity of 72% (see Fig. 8). Results for the open-cell ceramic foams should be compared with acoustic absorption of typical polyurethane foams which are considered very good sound absorbing and insulating materials. From Fig. 6 one can see that the acoustic absorption of ceramic samples with porosity 90% (and thickness 18 mm or 24 mm) is comparable with the absorption of soft PU foam – thickness 21 mm, curve (e) in Fig. 6; in some frequency ranges it is even superior. Notice that at lower frequencies (app. at 0.9 kHz and 1.8 kHz) acoustic resonances resulting from the motion of elastic skeleton of the soft PU foam are visible; at higher frequencies the skeleton behaviour tends to be rigid even for the soft PU foam. This is a typical situation for soft PU foams: the low-frequency resonances and anti-resonances of elastic skeleton significantly influence sound propagation and absorption; the flexibility of elastic skeleton may also be utilized in order to improve the acoustic absorption in semi-active (ZIELINSKI, RAK, 2010) or active way (ZIELINSKI, 2008; 2010; 2011). The sound absorption properties of PU foams may also be improved passively by changing the skeleton density and stiffness – this can be attained by adding some inclusions in the foam matrix, for example, rice hull (WANG *et al.*, 2013), or tea-leaf-fibres (EKICI, 2012). The acoustic absorption curve for a stiff PU foam – thickness 26 mm, curve (d) in Fig. 6 – does not manifest any skeleton resonances and is inferior in the whole frequency range. Similar conclusions can be drawn when comparing the acoustic absorption of ceramic samples of 88% porosity with the absorption of soft and stiff PU foams. Apart from some lower frequency resonances, the sound absorption performance for a 16 mm high sample of soft PU foam – illustrated by the absorption curve (c) in Fig. 7 – tend to be comparable with the absorption performance obtained for ceramic samples of similar thickness; however, it is distinctly superior around the elastic skeleton resonances at 1.1 kHz and 2.2 kHz. The absorption coefficient for the stiff PU foam – curve (c) in Fig. 7 – is inferior in the whole frequency range.

It is important to notice that changes between the absorption curves obtained for ceramic samples of the same porosity but different thickness result mainly (if not only) from that difference in thickness, and not from some subtle local variations in morphology which can be neglected on the macroscopic scale, especially at lower frequencies. For example, notice that the absorption curves (a) and (b) from Fig. 7 are fairly similar since the thickness difference between these samples with porosity 88% is not significant. This observation is also confirmed in Fig. 9, where absorption curves are presented for all ceramic samples, and additionally, for samples with 89.5% porosity: notice that absorption coefficients measured for samples p90h18

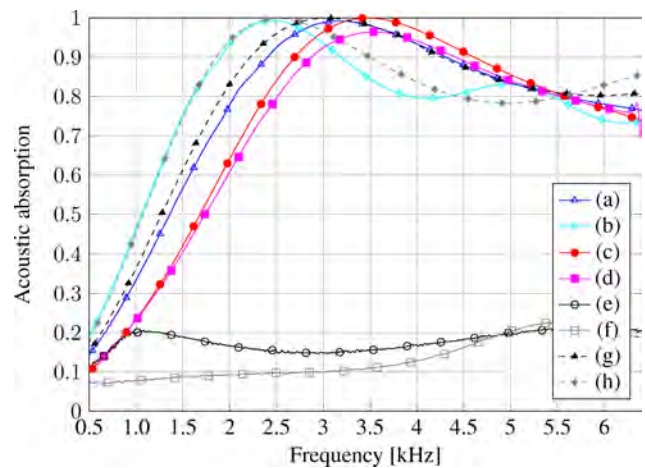


Fig. 9. Acoustic absorption of Al_2O_3 ceramic samples with porosity: (a,b) 90%, (c,d) 88%, (e,f) 72%, (g,h) 89.5%; and thickness: (a) 18 mm, (b) 24 mm, (c) 14 mm, (d) 16.5 mm, (e) 16 mm, (f) 22 mm, (g) 18 mm, (h) 22 mm.

and p89h18, namely, curves (a) and (g) in Fig. 9, are very similar (and, as a matter of fact, identical in the lower frequency range) since the samples have exactly the same thickness (18 mm) and nearly identical porosity (90% and 89.5%, respectively); similarly, the results obtained for samples p90h24 and p89h22 – curves (b) and (h) in Fig. 9 – are also very close to each other, since the samples have similar thickness (24 mm and 22 mm) and nearly identical porosity (90% and 89.5%, respectively). All this shows that alumina foams are manufactured with repeatable micro-morphology, and moreover, they are macroscopically homogeneous and for a given porosity should manifest typical values of average macroscopic parameters relevant for sound propagation, like permeability or tortuosity.

5. Conclusions

- The microstructure of alumina foams is typically composed of approximately spherical cells interconnected by circular windows. Depending on the porosity (72–90%) the median cell size ranged from 135 to 505 μm , while the median window size varied from 28 to 101 μm .
- Such foams are highly porous ceramics. In case of fully open-cell porosity of 88–90% the alumina foams exhibit excellent sound absorbing properties comparable with the best sound insulating polyurethane foams.
- The repeatability of results obtained for samples cut out from foams (with the porosity of app. 90%) produced at different times shows that alumina foams are manufactured with recurrent micro-morphology which is correlated with the parameter of the total

porosity. They can be considered as macroscopically homogeneous and isotropic.

- A typical character of the frequency-dependent curves of the acoustic absorption coefficient confirms that (from the modelling perspective) they can be treated as porous media with rigid skeleton. These curves may be utilised for some parametric estimation, for example, using procedures for inverse identification of parameters for sound absorption modelling of porous ceramics and other rigid porous media proposed recently by ZIELINSKI (2012).

Acknowledgments

Financial support of Structural Funds in the Operational Programme – Innovative Economy (IE OP), financed from the European Regional Development Fund – Project “Modern Material Technologies in Aerospace Industry”, No. POIG.0101.02-00-015/08, is gratefully acknowledged. Mr. Nowak also would like to acknowledge the financial support of the National Science Centre (NCN) within the framework of his PhD project No. UMO-2011/01/N/ST8/07755.

References

1. ALLARD J.F., ATALLA N. (2009), *Propagation of Sound in Porous Media: Modelling Sound Absorbing Materials*, Second Edition, Wiley.
2. BO Z., TIANNING C. (2009), *Calculation of sound absorption characteristics of porous sintered fiber metal*, Appl. Acoust., **70**, 337–346.
3. BOONEN R., SAS P. (2004), *Calibration of the two microphone transfer function method to measure acoustical impedance in a wide frequency range*, Proceedings of ISMA 2004: International Conference on Noise and Vibration Engineering, SAS P., DEMUNCK M. [Eds.], Leuven (Belgium), 325–336.
4. CHUNG J.Y., BLASER D. (1980), *Transfer function method of measuring in-duct acoustic properties*, J. Acoust. Soc. Am., **68**, 3, 907–921.
5. COLOMBO P. (2006), *Conventional and novel processing for cellular ceramics*, Philosophical Transaction of the Royal Society A, **364**, 109–124.
6. CUIYUN D., GUANG C., XINBANG X., PEISHENG L. (2012), *Sound absorption characteristics of a high-temperature sintering porous ceramic material*, Appl. Acoust., **73**, 865–871.
7. DALMONT J.-P. (2001), *Acoustic impedance measurement, Part I: A review. Part II: A new calibration method*, J. Sound Vib., **243**, 3, 427–459.
8. EKICI B., KENTLI A., KÜÇÜK H. (2012), *Improving sound absorption property of polyurethane foams by adding tea-leaf fibers*, Archives of Acoustics, **37**, 4, 515–520.
9. FUJI M., KATO T., ZHANG F.-Z., TAKAHASHI M. (2006), *Effects of surfactants on the microstructure and some intrinsic properties of porous building ceramics fabricated by gelcasting*, Ceram. Int., **32**, 797–802.
10. GIESE F., EIGENBROD C., KOCH D. (2011), *A novel production method for porous sound-absorbing ceramic material for high-temperature applications*, Int. J. Appl. Ceram. Technol., **8**, 3, 646–652.
11. GREEN D.J., COLOMBO P. (2003), *Cellular ceramics: intriguing structures, novel properties, and innovative applications*, Materials Research Bulletin, **28**, 296–300.
12. ISO 10534-2 (1998), *Determination of sound absorption coefficient and impedance in impedance tubes*, International Standard Organisation.
13. POTOCZEK M. (2008), *Gelcasting of alumina foams using agarose solutions*, Ceramics International, **34**, 661–667.
14. RANACHOWSKI P., REJMUND F., RANACHOWSKI Z., PAWELEK A., PIATKOWSKI A. (2009), *Comparison of acoustic emission and structure degradation in compressed porcelain and corundum materials*, Archives of Acoustics, **34**, 4, 655–676.
15. SEPULVEDA P. (1997), *Gelcasting of foams for porous ceramics*, American Ceramic Society Bulletin, **76**, 61–65.
16. SEPULVEDA P., BINNER J.G.P. (1999), *Processing of cellular ceramics by foaming and in situ polymerisation of organic monomers*, Journal European Ceramic Society, **19**, 2059–2066.
17. TAKAHARA H. (1982), *Sound insulating characteristics of porous ceramic Al₂O₃-SiO₂*, Appl. Acoust., **15**, 2, 111–116.
18. TAKAHARA H. (1994), *The sound absorption characteristics of particulate porous ceramic materials*, Appl. Acoust., **41**, 3, 265–274.
19. WANG Y., ZHANG C., REN L., ICHCHOU M., GALLAND M.-A., BAREILLE O. (2013), *Influences of rice hull in polyurethane foam on its sound absorption characteristics*, Polymer Composites, article in press, published online in Wiley Online Library, doi:10.1002/pc.22590.
20. ZHANG F.-Z., KATO T., FUJI M., TAKAHASHI M. (2006), *Gelcasting fabrication of porous ceramics using a continuous process*, J. Eur. Ceram. Soc., **26**, 667–671.
21. ZIELINSKI T.G. (2008), *Active porous composites for wide frequency-range noise absorption*, Proceedings of ISMA2008: International Conference on Sound and Vibration, Leuven (Belgium), 89–103.
22. ZIELINSKI T.G. (2010), *Fundamentals of multiphysics modelling of piezo-poro-elastic structures*, Archives of Mechanics, **62**, 5, 343–378.

23. ZIELINSKI T.G. (2011), *Numerical investigation of active porous composites with enhanced acoustic absorption*, Journal of Sound and Vibration, **330**, 5292–5308.
24. ZIELINSKI T.G. (2012), *Inverse identification and microscopic estimation of parameters for models of sound absorption in porous ceramics*, Proceedings of International Conference on Noise and Vibration Engineering (ISMA2012)/International Conference on Uncertainty in Structural Dynamics (USD2012), SAS P., MOENS D., JONCKHEERE S. [Eds.], Leuven (Belgium), 95–107.
25. ZIELINSKI T.G., RAK M. (2010), *Acoustic absorption of foams coated with MR fluid under the influence of magnetic field*, J. Intell. Mater. Syst. Struct., **21**, 125–131.

Numerical Evaluation of Sound Attenuation Provided by Periodic Structures

Mário MARTINS⁽¹⁾, Luís GODINHO⁽²⁾, Luís PICADO-SANTOS⁽³⁾

⁽¹⁾ *I.P.C., Instituto Superior de Engenharia de Coimbra*
R. Pedro Nunes, 3030-199 Coimbra, Portugal

CIEC — Departamento de Engenharia Civil da Universidade de Coimbra
R. Luís Reis Santos, 3030-788 Coimbra, Portugal; e-mail: mariomm@isec.pt

⁽²⁾ *CICC, Departamento de Engenharia Civil, Universidade de Coimbra*
R. Luís Reis Santos, 3030-788 Coimbra, Portugal; e-mail: lgodinho@dec.uc.pt

⁽³⁾ *DECivil, Instituto Superior Técnico, Universidade Técnica de Lisboa*
Av. Rovisco Pais, 1049-001 Lisboa, Portugal; e-mail: picado.santos@civil.ist.utl.pt

(received March 22, 2013; accepted October 10, 2013)

The use of periodic structures as noise abatement devices has already been the object of considerable research seeking to understand its efficiency and see to what extent they can provide a functional solution in mitigating noise from different sources. The specific case of sonic crystals consisting of different materials has received special attention in studying the influence of different variables on its acoustic performance.

The present work seeks to contribute to a better understanding of the behavior of these structures by implementing an approach based on the numerical method of fundamental solutions (MFS) to model the acoustic behavior of two-dimensional sonic crystals. The MFS formulation proposed here is used to evaluate the performance of crystals composed of circular elements, studying the effect of varying dimensions and spacing of the crystal elements as well as their acoustic absorption in the sound attenuation provided by the global structure, in what concerns typical traffic noise sources, and establishing some broad indications for the use of those structures.

Keywords: traffic noise, sonic crystals, numerical methods.

1. Introduction

Among different types of environmental noise sources for which the national and European legislation established maximum noise exposure levels, the traffic noise, with special focus on road traffic, assumes a clear prevalence.

The World Health Organization (2011) estimates that, considering the different impacts associated with noise, the losses, expressed in Disability-Adjusted Life Year (DALY), reach a value between 1.0 and $1.6 \cdot 10^6$, i.e. at least a million years of healthy life are lost annually as a result, mostly due to traffic noise.

Another study on the situation held in the Netherlands (DEN BOER, SCHROTEN, 2007) indicates that the annual loss (in 2000) due to traffic noise was approximately $40 \text{ DALY} \times 1000$ inhabitants, and this value already accounted for about half of the total result of traffic accidents. Moreover, the same study mentions

the growing trend of the effects of traffic noise, whereas on traffic accidents the tendency is to decrease.

Being relatively consensual as for the need to invest in interventions that can offset the negative effects of this type of noise, generically one can distinguish between interventions at three different levels: at the generation (the vehicle-tire-pavement interaction), at the propagation medium (the area surrounding the roads), and at the reception of noise (the characteristics of the facades of buildings in the vicinity of roads).

Fitting into the second of the above types of interventions, the use of ‘classical’ noise barriers is usually considered an effective solution to reduce sound levels, by between 5 and 10 dB, but whose performance depends essentially on the geometry and the sound absorption characteristics of their surfaces.

This work intends to contribute to the analyses of a different approach in the use of these barriers which consists in using a periodic arrangement of vertical

cylindrical elements organized in a geometric configuration such as to attenuate the incident sound levels, with particular emphasis on certain frequencies. This solution is commonly known as “sonic crystal”.

Sonic crystals get their name by analogy with ordered structures of semiconductor materials such as silicon crystals whose feature of allowing certain energy waves to pass through and block others is transposed, in sonic crystals, into the capacity to prevent or limit the propagation of certain sound frequencies. The shape of these structures corresponds to a “grid” or “lattice” consisting of a base element which is repeated regularly in one, two, or three dimensions.

It is generally considered that the first evidence that it was possible to achieve some effect of acoustic obstruction using structures in periodic arrays was derived fortuitously from a sculptural element, in the gardens of the *Fundación Juan March* in Madrid, consisting of a number of vertical metal tubes arranged in a rectangular grid. A series of measurements conducted in 1995 by placing a set of microphones along this sculpture revealed clear effects in attenuating certain frequency bands of sounds which were a function of the direction of incident sound waves (MARTINEZ-SALA *et al.*, 1995).

Since then, different aspects of the behavior of sonic crystals have been studied, some of which were essentially theoretical, while others focused on some potential practical applications. In the first group, aspects such as the influence of so called point defects (WU *et al.*, 2009) or the existence of waveguides in which the sound propagates with low attenuation (VASSEUR *et al.*, 2008) can be mentioned. In the field of the practical uses of sonic crystals, one which may be regarded perhaps as the most promising is their precise use for the selective attenuation of sound, for example as traffic noise barriers (SÁNCHEZ-PÉREZ *et al.*, 2002). A very recent work on this topic (CASTIÑEIRA-IBÁÑEZ *et al.*, 2012) has addressed the classification of sonic crystal barriers in terms of relevant European standards for the determination of the intrinsic characteristics of acoustic barriers. Although a limited set of tests was performed in that work, the results have shown that the sonic crystal barriers can be acoustically competitive when compared with classic noise barriers used to mitigate traffic noise.

The underlying principle behind the latter case has to do with the aforementioned fact that these periodic structures have an attenuation capacity in certain frequency bands of sounds and with the fact that the dominant frequencies in road traffic noise can also be identified. Thus, by being designed to match those frequencies, such structures could provide a very effective way to mitigate traffic noise.

This application presents some advantages when compared to conventional noise barriers such as the fact that it does not require foundations as significant

as the latter, due to its comparatively small mass, and the relatively small action of the wind, as it is a fairly “open” structure (CASTIÑEIRA-IBÁÑEZ *et al.*, 2012). Another important benefit is the ability to adapt its attenuation capabilities to a specific site’s requirements through an appropriate “fine tuning” of geometrical configuration of the elements in its periodic structure.

As a disadvantage, it should be noted that to achieve an attenuation level similar to that of a traditional noise barrier, a structure with a significant thickness may be required. A possible solution could arise by combining different effects, such as multiple scattering resonances or sound absorption capabilities in the sonic crystal (ROMERO GARCÍA, 2010). There are, moreover, some experiments in this direction, for example the use of porous coatings on individual cylindrical of elements sonic crystals (UMNOVA *et al.*, 2006) or the use of trees arranged in different periodic geometrical configurations in order to achieve noise attenuation outdoor (MARTÍNEZ-SALA *et al.*, 2006).

A relatively consensual aspect, from the available published literature, is that these periodic structures provide a certain level of sound attenuation due to two different mechanisms: the geometry of the structure itself and also the acoustic properties of the scatterers, for example their sound absorption. What is also apparently clear is that the study of the combined effect of these two aspects, in order to correctly predict the level of sound attenuation results, is not a trivial procedure.

Although a significant number of works has been published, the subject of sonic crystals is still under development and there are several issues that need further studying. In what concerns the numerical modeling of these structures, some benefits can be taken from adapting concepts inherited from other areas of acoustics and wave propagation, namely in what concerns the theoretical and numerical treatment of the problem. This paper is, thereby, intended as a contribution to the development of the study in this area, proposing a general numerical strategy based on the Method of Fundamental Solutions (MFS) to model a 2D sonic crystal noise barrier subjected to the incidence of acoustic waves generated by a line source. First, the theoretical formulation in which the numerical analysis methodology is based will be presented; the proposed model will then be verified against reference solutions; a set of results will be further laid out, depicting different combinations of geometrical and acoustic absorption characteristics, followed by main conclusions and some indications regarding further work.

2. Mathematical formulation

In the present work, MFS is adopted to perform numerical simulations. Essentially, MFS is a collocation

technique which requires only the definition of a set of points along the physical boundaries of the problem to establish an approach to its solution. Based on these points and making use of a linear combination of fundamental solutions of the differential equation governing the problem, the method allows to obtain, in a simple manner, an approximation to the solution. As in the better-known Boundary Element Method, MFS requires previous knowledge of the fundamental solutions which are not always known to the type of the problem involved; obtaining these solutions is mathematically complex and can be extremely difficult in the case of nonlinear problems with moving boundaries or time dependence. Still, the mathematical approach of MFS is much simpler than that of the BEM, since its formulation does not require performing any kind of integrations, analytically or numerically, within the domain or along the boundary. This method has been discussed in the literature by various authors. Noteworthy are the works of FAIRWEATHER and KARAGEORGHIS (1998), FAIRWEATHER *et al.* (2003), or GOLBERG and CHEN (1999). It should be noted that, despite its simplicity, many of the published works show that MFS can provide a very accurate calculation of solutions for different physical problems, including those related to the field of acoustics (ALVES, VALTCHEV, 2005; GODINHO *et al.*, 2007; ANTÓNIO *et al.*, 2008) and wave propagation (GODINHO *et al.*, 2009).

The following sections summarize the main aspects of the method when applied to solving acoustical problems in the frequency domain.

2.1. Governing equation

It is usual to consider that the propagation of sound in a two-dimensional space, in the frequency domain, can be represented mathematically by the Helmholtz equation. This equation has the usual form

$$\nabla^2 p + k^2 p = 0, \quad (1)$$

where $\nabla^2 = \frac{\partial}{\partial x^2} + \frac{\partial}{\partial y^2}$, p is the acoustic pressure, $k = \omega/c$, $\omega = 2\pi f$, f is the frequency, and c is the propagation velocity within the acoustic medium.

2.2. Fundamental solution

Given the differential equation (1), it becomes possible to define analytical solutions that satisfy the equation under certain conditions. One such situation corresponds to free-field conditions in which the medium is considered infinite and for which a two-dimensional pressure field is generated by a sound source located at point \mathbf{x}_0 of coordinates (x_0, y_0) . This solution, known as the fundamental solution, allows to define the acoustic field in terms of pressure and par-

ticle velocities generated by the source at any receiver located at point \mathbf{x} of coordinates (x, y) as

$$G^{2D}(\mathbf{x}, \mathbf{x}_0, k) = -\frac{i}{4} H_0^{(2)}(kr), \quad (2)$$

$$H^{2D}(\mathbf{x}, \mathbf{x}_0, k, \mathbf{n}) = \frac{k}{-4\rho\omega} H_1^{(2)}(kr) \frac{\partial r}{\partial \mathbf{n}}, \quad (3)$$

where $r = \sqrt{(x - x_0)^2 + (y - y_0)^2}$, and \mathbf{n} represents the direction along which the particle velocity is to be calculated.

2.3. MFS formulation

In MFS, the solution of the problem is approximated by a linear combination of fundamental solutions. To formulate the method, consider a generic problem governed by Eq. (1) where the problem's physical boundary $\Gamma = \Gamma_1 \cup \Gamma_2$ (see Fig. 1) can be subjected to either Dirichlet or Neumann boundary conditions defined, respectively, by:

$$p = p_K \quad \text{at} \quad \Gamma_1, \quad (4)$$

$$-\frac{1}{i\rho\omega} \frac{\partial}{\partial \mathbf{n}} p = v_K \quad \text{at} \quad \Gamma_2. \quad (5)$$

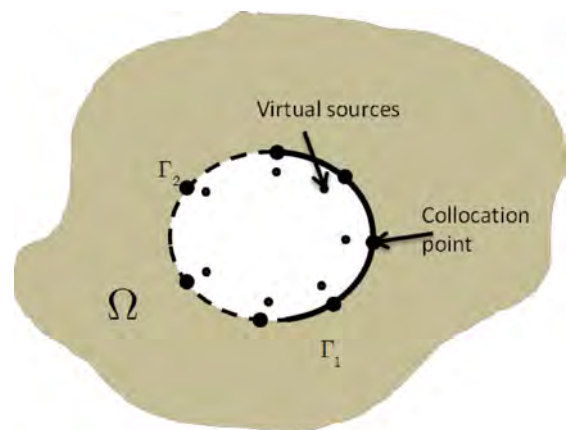


Fig. 1. Schematic representation of the problem.

In the general case, it is not a trivial task to compute a solution that simultaneously satisfies these prescribed boundary conditions together with Eq. (1). To allow obtaining one such solution, consider a set of NS virtual sources located outside the field of analysis, and assume that the pressure field at any domain point \mathbf{x} can be represented by a linear combination of the effects of NS sources positioned at points \mathbf{x}_j , so that

$$p(\mathbf{x}, k) = \sum_{j=1}^{NS} Q_j G(\mathbf{x}, \mathbf{x}_j, k), \quad (6)$$

where Q_j is an amplitude factor associated with each of the virtual sources and which is, *a priori*, unknown.

For the problem under study, and given such representation of the pressure field, consider, additionally, a set of NC collocation points distributed along the boundary (see Fig. 1). Imposing the desired boundary conditions (Eqs. (4) and (5)) at each of the NC collocation points, two sets of equations can be written:

$$\sum_{j=1}^{NS} Q_j G(\mathbf{x}_i, \mathbf{x}_j, k) = p_{K,i} \text{ for each } \mathbf{x}_i \text{ at } \Gamma_1, \quad (7)$$

$$\sum_{j=1}^{NS} Q_j H(\mathbf{x}_i, \mathbf{x}_j, k, \mathbf{n}) = v_{K,i} \text{ for each } \mathbf{x}_i \text{ at } \Gamma_2, \quad (8)$$

where $p_{K,i}$ and $v_{K,i}$ are the sound pressure and the normal particle velocity values, respectively, to be prescribed at each collocation point i .

Establishing these equations, a system with NC equations for NS unknowns can be written, allowing the calculation of the unknown amplitude factors Q_j . If $NS = NC$, a linear equation system is obtained for which the solution can be calculated making use of common solution procedures such as the Gauss elimination.

It is worth noting that besides the two boundary conditions indicated in Eqs. (4) and (5), it is sometimes useful to impose mixed, or Robin, boundary conditions. In acoustics, this can be the case of absorbing boundaries to which surface impedance Z is ascribed. In that situation, the boundary condition can be written as

$$\frac{p}{i/\rho\omega \times \partial p/\partial \mathbf{n}} = Z. \quad (9)$$

To enforce this boundary condition, a combination of Eqs. (7) and (8) must be written for the relevant collocation points, which becomes

$$\sum_{j=1}^{NS} [Q_j G(\mathbf{x}_i, \mathbf{x}_j, k) - Z Q_j H(\mathbf{x}_i, \mathbf{x}_j, k, \mathbf{n})] = 0. \quad (10)$$

3. Model verification

To verify and assess the accuracy of the proposed MFS model described in the previous section, two different configurations will be here analyzed corresponding to systems with one or multiple inclusions.

As a first test, consider that the system includes just a single circular inclusion placed within an infinite fluid medium with density of 1.22 kg/m^3 and allowing sound to propagate at 340 m/s . The circular inclusion has a rigid surface and exhibits a radius of 0.1 m , being centered at $(x = 0.0 \text{ m}; y = 0.0 \text{ m})$; this inclusion is illuminated by a source located at $(x = -0.5 \text{ m}; y = 0.0 \text{ m})$, and the response is determined at a set of receivers located over a circumference of radius 0.2 m , with the same center as the inclusion. This configuration is illustrated in Fig. 2a.

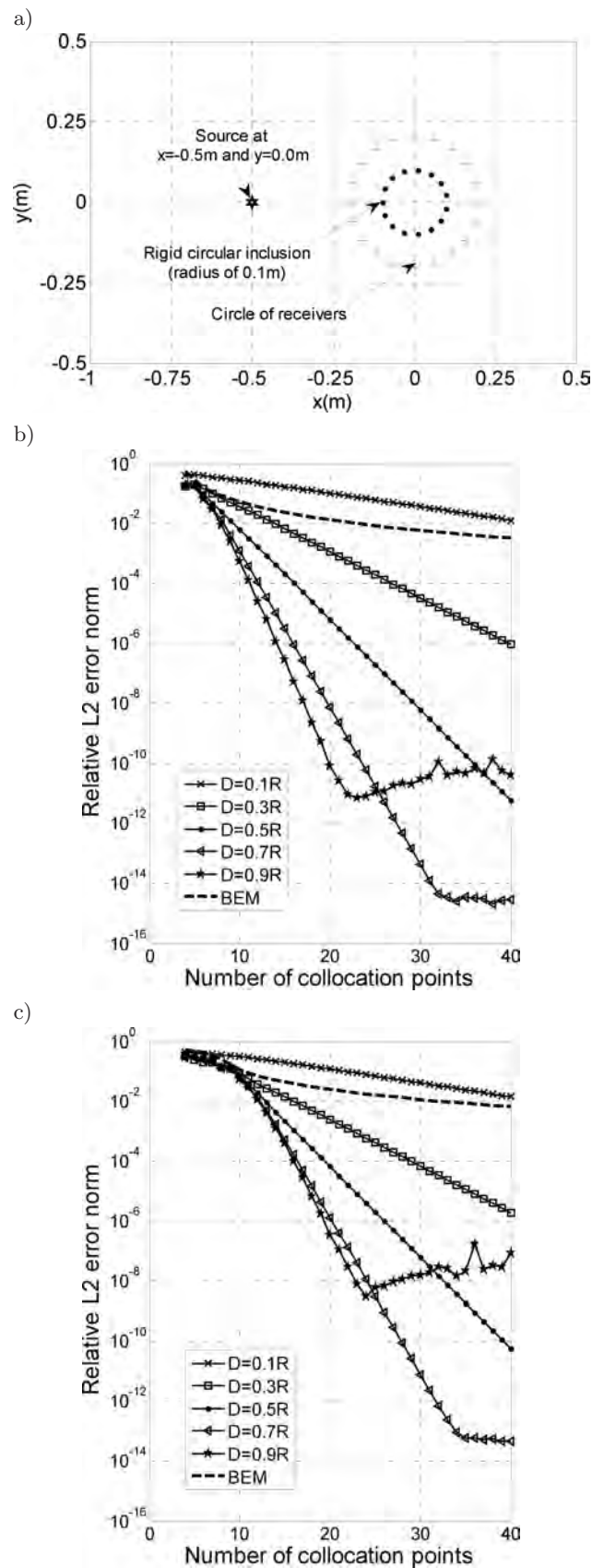


Fig. 2. Geometry of the model (a) and convergence results when analyzing a single rigid circular inclusion with a radius of 0.1 m . Results are shown for 1 kHz (b) and 2 kHz (c).

To analyze the proposed configuration, MFS is here used, positioning the virtual sources inside the inclusion, equally spaced along a circumference; different distances between these sources and the boundary are tested ranging from $0.1R$ to $0.9R$. Figures 2b and 2c illustrate the relative L2 error norm computed for frequencies of 1 kHz and 2 kHz, for different numbers of collocation points; as a reference for the calculation of this error, an analytical solution of this problem is used based on works of TADEU *et al.* (2001). In addition, a similar curve is presented for the more classic BEM model, also for increasingly refined discretizations. It should be noted that each of these plots can be viewed as a set of convergence curves computed for each of the considered distances, and thus gives important information related to numerical behavior of the method.

Analyzing the two figures, it can be observed that MFS presents very good convergence rates for all analyzed distances, clearly surpassing the behavior of the BEM for this test case. Moreover, one can conclude that by positioning the sources at larger distances from the boundary leads to increasingly better results, reaching excellent convergence rates for distances equal or larger than $0.5R$. The best convergence rates are obtained when the sources are positioned as far from the boundary as possible (e.g. concentrated near the center); however, for this case, the convergence curve reaches a point above which the results do not improve with the increase in the number of collocation points, since the equation system becomes progressively more ill-conditioned, affecting the quality of the results.

A second test case was analyzed to verify the proposed model, corresponding to a more complex configuration in which eight circular inclusions, each of them with a radius of 0.1 m, are illuminated by a source located at the same position as indicated above; in addition, Robin boundary conditions (as defined in Eq. (9)) with $Z = 1000$ Pa·s/m are imposed along all boundaries. For this case, results are computed using MFS with 15 collocation points (and positioning the virtual sources at a distance $0.5R$) and BEM with 30 boundary elements. The response is computed at a line of receivers located at $x = 1.0$ m. Figure 3a illustrates the proposed configuration.

Figure 3b exhibits the calculated results for a frequency of 2 kHz, over the indicated line of receivers. Here, a perfect match between the two numerical methods can be seen, revealing the excellent behavior of MFS in the analysis of this specific type of problem, even when Robin conditions are considered. It should also be noted that the finer discretization required by BEM, together with the need to perform integrations over each boundary element, leads to a much higher computational effort of this method when compared with MFS.

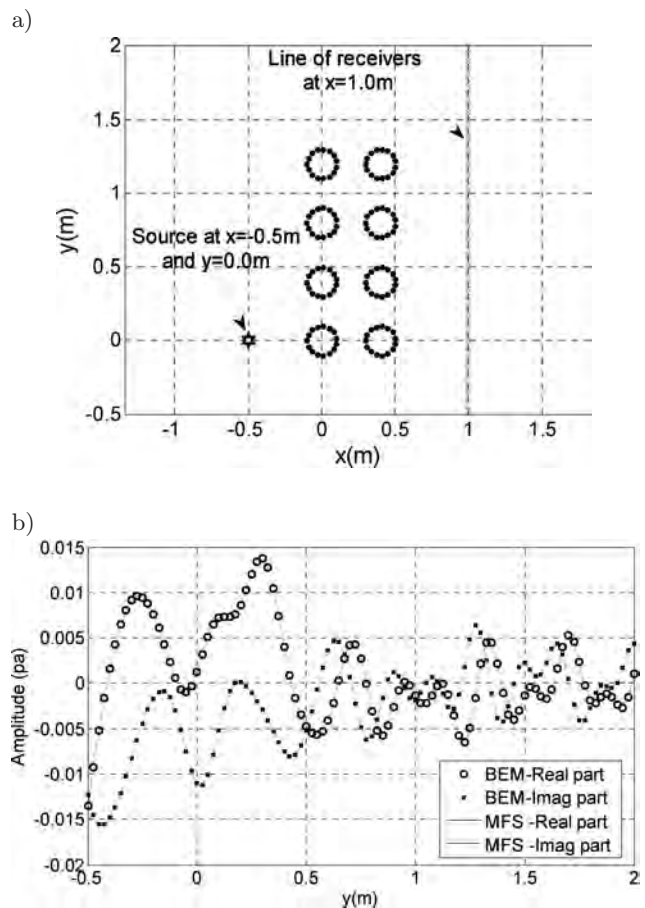


Fig. 3. Comparison with the results computed using a BEM model for 2 kHz when the geometry consists of eight circular inclusions (a) with Robin boundary conditions. The results (b) are computed using 30 boundary elements (BEM) or 15 collocation points (MFS) to discretize each circle.

4. Discussion of numerical results

As previously mentioned, the main mechanisms by which sonic crystals provide specific levels of sound attenuation or insertion loss, are the geometry of its basic periodic structure, or lattice, and the acoustic properties of its individual scatterer elements. In what follows, the proposed MFS formulation is applied to analyze the influence of different combinations of those aspects when a periodic structure is used as a noise barrier alongside a road, as illustrated in Fig. 4.

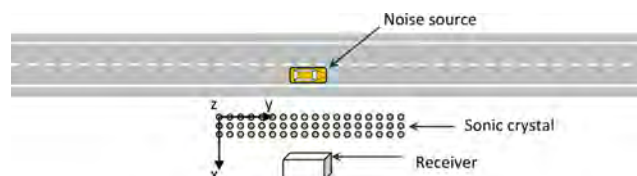


Fig. 4. General configuration for the studied cases.

For this purpose, the traffic assumes the role of the noise source, a small area (a window for exam-

ple) of a nearby house shall correspond to the receiver, and a sonic crystal noise barrier will be located between them, materialized by a set of vertical cylinders, either rigid or with some level of acoustic absorption. Those cylinders are considered to be arranged in two distinct lattice configurations, typical of sonic crystals, namely square or triangular, as shown in Fig. 5.

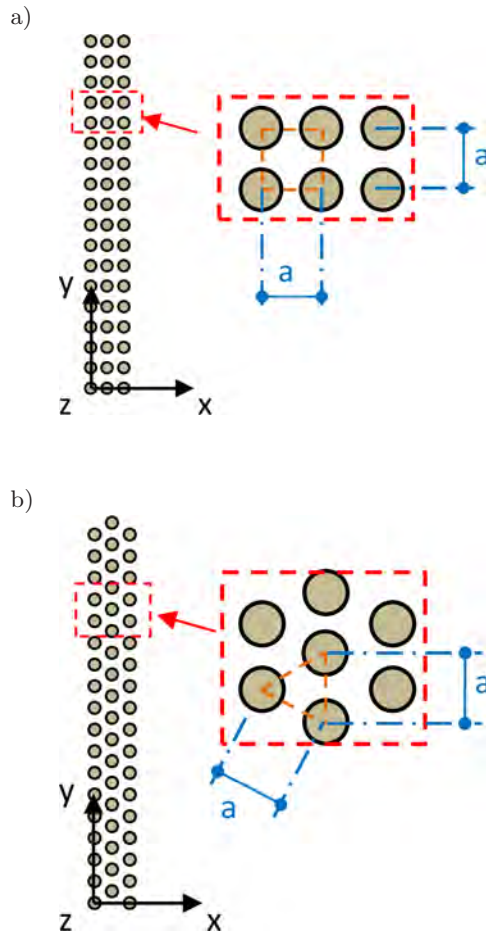


Fig. 5. Square (a) and triangular (b) lattice configurations of the sonic crystal.

Throughout the different analyses presented in the following, the situation shown above is studied by means of frequency domain responses calculated on a horizontal plane, as the geometry of the problem can be considered constant along the z -axis (vertical). For such a case, the MFS model described in the previous sections can be used to simulate the pressure field around the structure of the sonic crystal.

In order to replicate a realistic situation, based on the usual dimensions from a typical cross section of a road, the positions of the source and receivers will correspond, in the axis system shown in Fig. 4, respectively, to values of $x = -6.5$ m and $x = 7.5$ m. As for the y -axis values, the analyses were made considering the receiver close to the center of the barrier along that

axis (consisting of five distinct receiver points along a length of 0.80 m). The source was initially assumed to be located in front of the receiver (at half the length of the crystal), although in further calculations its location will additionally be considered in other positions.

The analysis carried out sought to evaluate the influence in the sonic crystal's sound attenuation features for different geometrical parameters (the number of cylinders in the sonic crystal, the diameter of the cylinders, the spacing between cylinders, the position of the noise source and also the random variability of the diameter of the cylinders) as well as the acoustic absorption characteristics of the scatterers.

4.1. Influence of the number of cylinders

As the intention is to examine the attenuation related to road traffic noise, given that it is usual to consider that this noise exhibits a maximum sound level near 1000 Hz (SANDBERG, 2003), at this stage the attenuation values evaluated corresponded to five individual frequencies in the region of this maximum, specifically 600, 800, 1000, 1200, and 1400 Hz.

In analyzing the influence of the number of cylinders, the purpose is to establish the minimum number of scatterers that can provide nearly stable levels of attenuation at those frequencies, for each of the two lattice configurations previously mentioned. Along the y -axis, that number will correspond to the smallest "length" along that direction so that the diffraction effect near the extremities of the structure becomes negligible. In trying to keep the solutions as economical as possible, the "width" of the sonic crystals, along the x -axis, will be kept at two or three cylinders.

Consequently, N being the number of cylinders along the y -axis, we will have arrangements for each of the cases of $2N$ cylinders or $3N$ cylinders.

As for the other geometrical parameters of the sonic crystals, given that they are supposed to embody road noise barriers, to avoid very dense structures and ensure the cylindrical elements are sufficiently robust but have a plausible dimension if obtained from trees, the diameter of the cylinders was assumed to be 0.20 m, and the distance between the centers of cylinders, i.e. the lattice constant, $a = 0.40$ m.

The sound attenuation was then evaluated for each of the five frequencies already mentioned, for increases in the number of cylinders along the y -axis, in multiples of five, until the values of the sound attenuation can be perceived stabilizing for the various frequencies, indicating that negligible diffraction phenomena occur at edges of the sonic crystals. The results are summarized in Figs. 6 and 7.

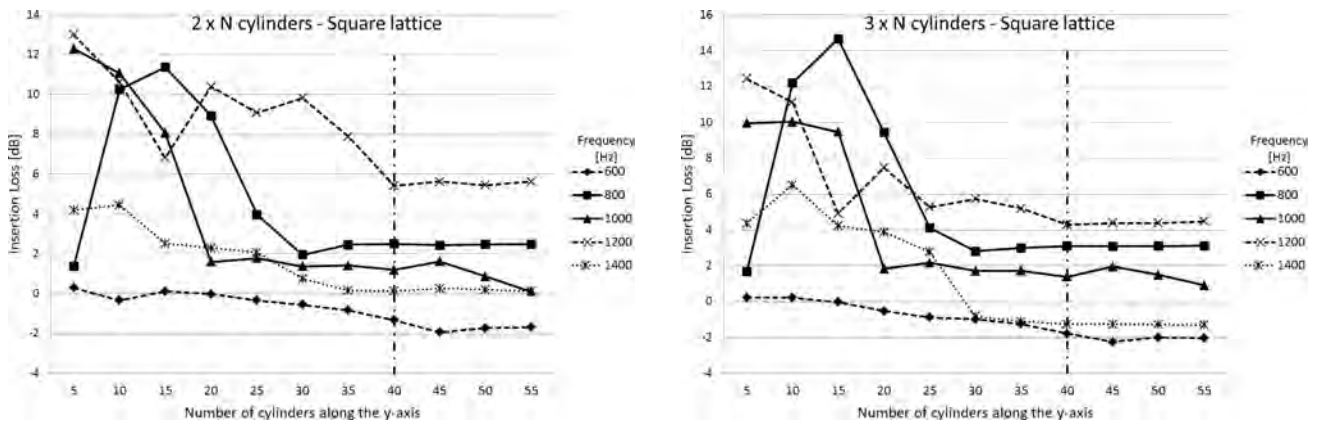


Fig. 6. Insertion Loss (in dB) vs number of cylinders (square configuration).

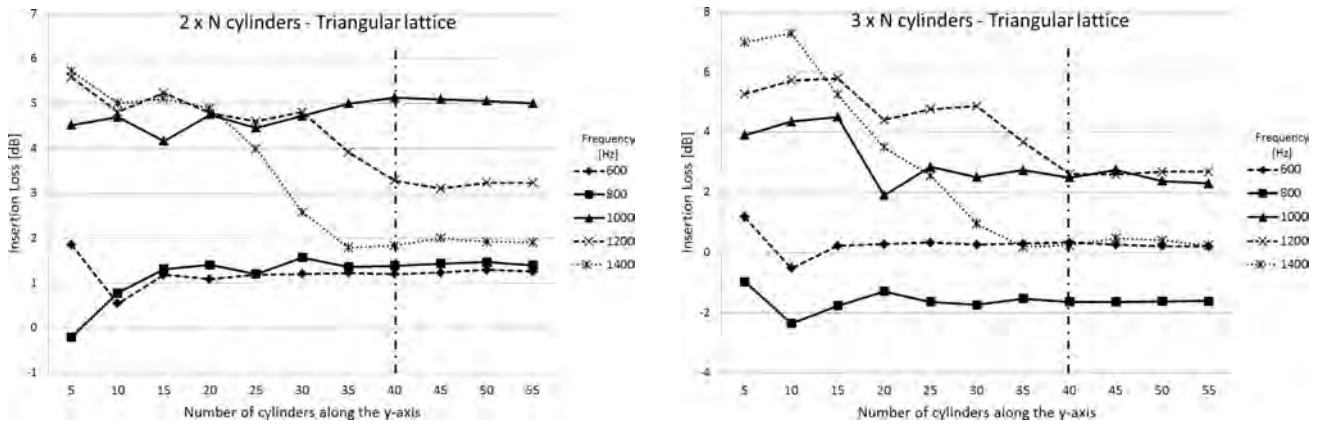


Fig. 7. Insertion Loss (in dB) vs number of cylinders (triangular configuration).

In view of these results, the minimum numbers of cylinders along the y -axis for the different configurations under consideration were established as follows:

- Square configuration:
 $2N = 40$ cylinders / $3N = 40$ cylinders;
- Triangular configuration:
 $2N = 40$ cylinders / $3N = 40$ cylinders.

From this point on, the attenuation values are obtained by means of an energetic average within each of five 1/3 octave frequency bands with centers at 630, 800, 1000, 1250, and 1600 Hz. For this purpose, fre-

quencies between 562.5 Hz and 1777.5 Hz, with an increment of 7.5 Hz, were analyzed.

4.2. Influence of the diameter of the cylinders

In this case, assuming sonic crystals with the number of cylinders established in the preceding section for different lattice configurations and maintaining $a = 0.40$ m, the attenuation values were calculated considering diameters of 0.20, 0.15, and 0.10 m. The results are shown in Figs. 8 and 9, referring to the center frequency of the five 1/3 octave frequency bands defined above.

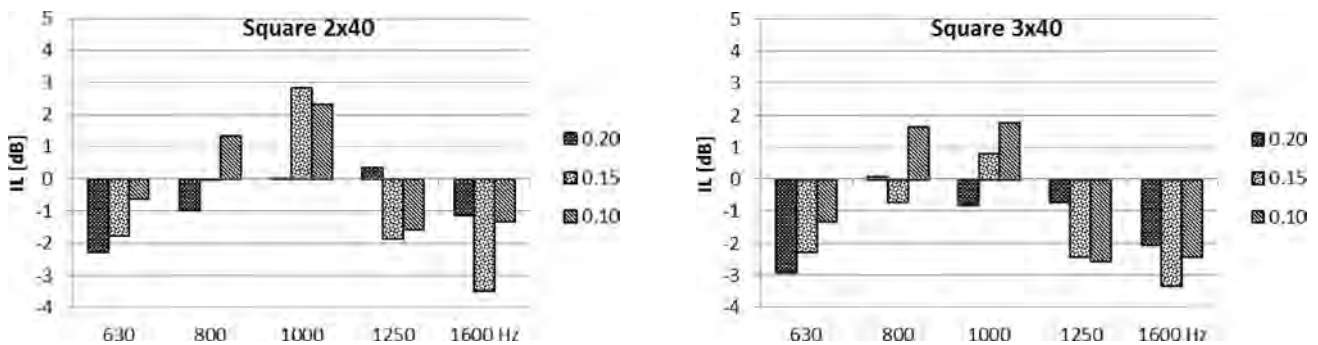


Fig. 8. Insertion Loss (in dB) vs diameter of cylinders (square configuration).

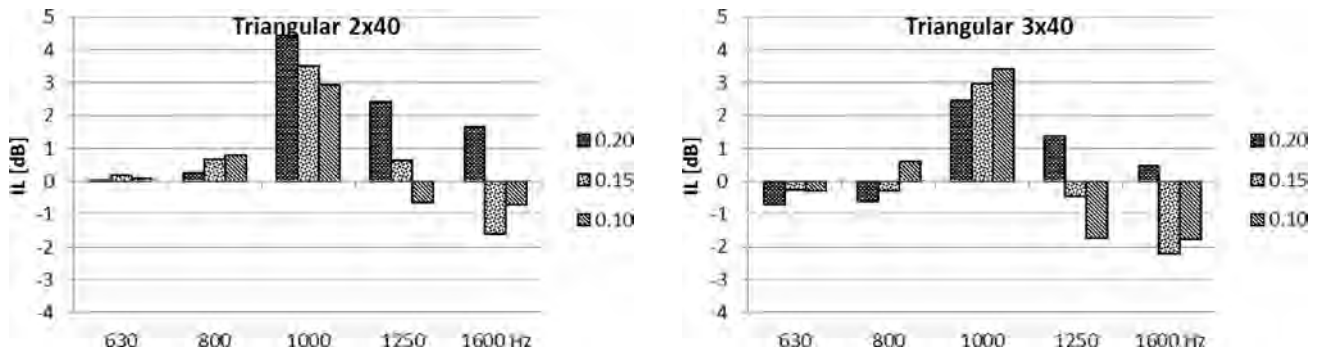


Fig. 9. Insertion Loss (in dB) vs diameter of cylinders (triangular configuration).

From these values, a noticeably higher attenuation can be seen to occur when the triangular lattice configurations (particularly the one with 2×40 cylinders) are used. Indeed, for those configurations, peak attenuation values at the frequency band of 1000 Hz are observable, with insertion loss values as high as 4.5 dB. Interestingly, and mostly for the square lattice configuration, negative values of the *IL* (amplification) may be observable which can be strongly related to the fact that the source and the receivers are at similar positions in the *y*-axis. For that case, the sound may travel directly through the gap between cylinders which could have a waveguide-type effect generating some amplification.

4.3. Influence of the spacing between the cylinders

Assuming, once again, sonic crystals with the dimensions used in the preceding point and cylinders with a diameter of 0.20 m, the influence of the distance between the centers of cylinders, i.e. the lattice constant *a*, was analyzed. The sound attenuation corresponding to values for that spacing of 0.50, 0.40, and 0.30 m, for the different configurations, was determined, and the results are shown in Figs. 10 and 11.

The main conclusion that can be drawn from these figures is that variation of the lattice constant induces

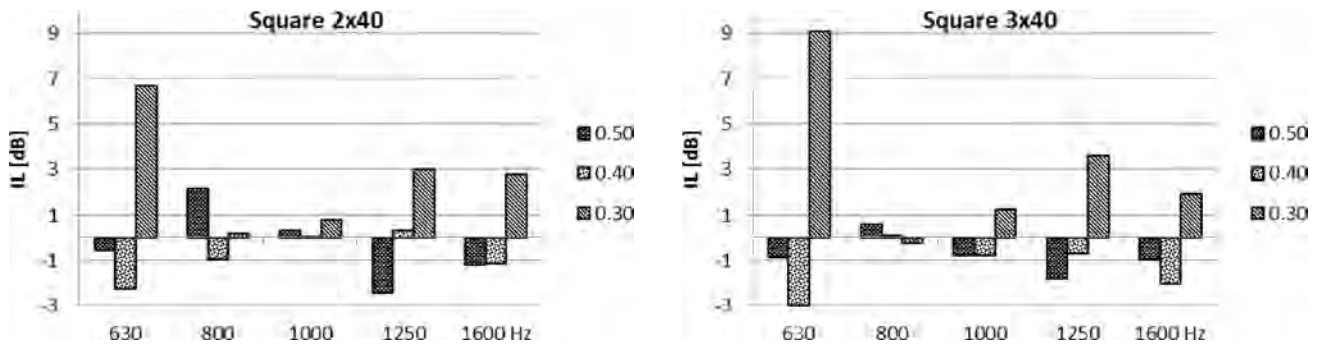


Fig. 10. Insertion Loss (in dB) vs lattice constant *a* (square configuration).

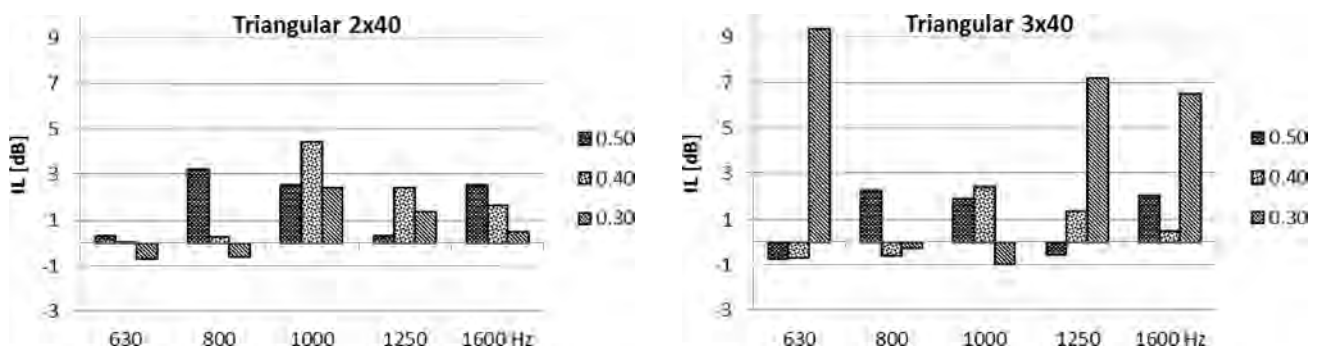


Fig. 11. Insertion Loss (in dB) vs lattice constant *a* (triangular configuration).

very pronounced variations of performance in terms of attenuation. There is no clear advantage of any of the tested scenarios, which makes it difficult to identify the best choice. However, it can be stated that, in these results, the smaller attenuation provided by the square configuration compared to the triangular one is again very clear.

Comparing the results computed for the three values of the lattice constant it can be seen that strong variations occur between the tested cases. Indeed, although the smaller value (0.3 m) seems to provide better results when the square lattice is used, in some cases it seems to be outperformed by other values of this spacing. As an example, observing the results for the triangular lattice with 3×40 elements, it is possible to conclude that this spacing is clearly inadequate when analyzing the 800 Hz and 1000 Hz frequency bands; by contrast, on the lower and higher frequency bands, the results reveal a very good efficiency, with high values of the *IL*.

4.4. Influence of the random variability of the cylinders' diameter

The possibility of using natural resources, such as timber logs, to build a sonic crystal noise barrier could

mean using scatterers that are not entirely identical concerning their diameter.

Therefore, in the present section the aim is to investigate if small diameter variations can produce a substantial difference in terms of the sound attenuation provided by the structure. In the presented results, a lattice constant of 0.40 m is assumed.

For each of the lattice configurations under study, a possible maximum random variation of 10 and 20% of the reference diameter (0.20 m) is analyzed. The computed sound attenuation values are presented in Figs. 12 and 13. In the cases where random variations of the diameters are assumed, the results correspond to an average of three separate computations. One should note that the random variation in those cases is applied separately for each element of the structure, thus generating structures with heterogeneous elements. From the presented results, only small differences of sound attenuation seem to occur when random variations of the diameter of the scatterer elements exist. Indeed, even when a maximum 20% diameter variation is assumed, the calculated insertion loss values are only very slightly changed, with maximum variations of less than 0.5 dB in all analyzed frequency bands.

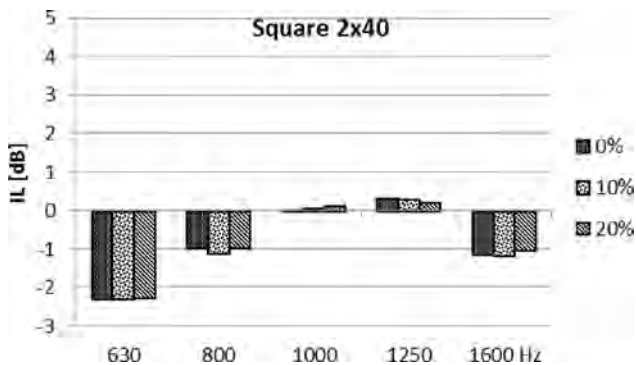


Fig. 12. Insertion Loss (in dB) vs diameter variability (square configuration).

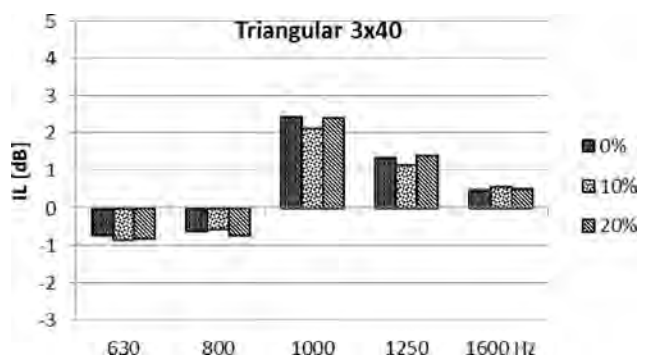
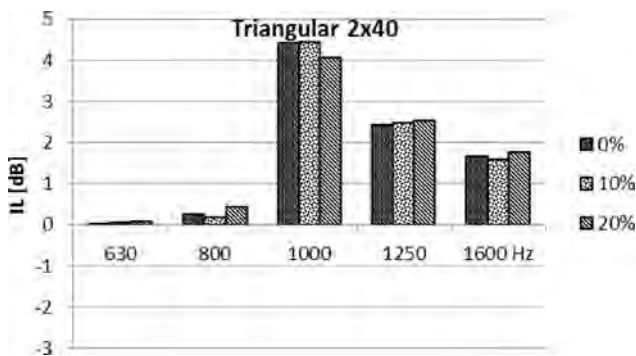
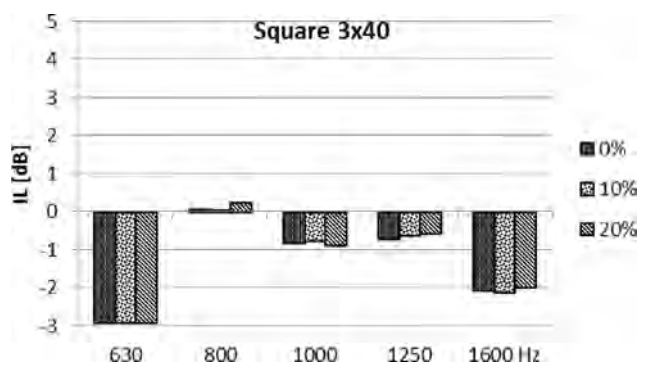


Fig. 13. Insertion Loss (in dB) vs diameter variability (triangular configuration).

4.5. Influence of the incidence angle of the sound waves

As stated above, the relative position of source and receivers can generate significant changes in the sound attenuation results. This topic is addressed in the present section by trying to find out how a longer path and different obstructions from the scatterers affect the sound attenuation at the receiver. The noise source was considered in three different positions, related to the “length” L of the sonic crystal, namely $y = 0$, $y = 1/4L$, and $y = 1/2L$ (which was the position assumed in the preceding sections), as shown in Fig. 14.

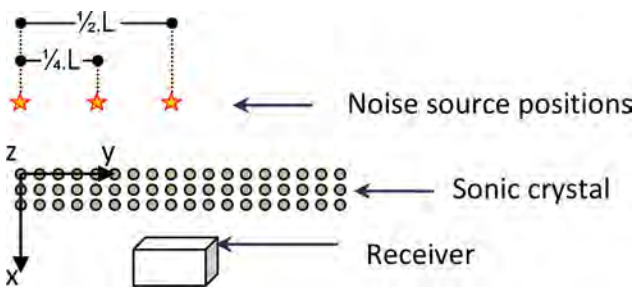


Fig. 14. Different positions of the noise source.

For each of the three positions of the source, the sound attenuation values for the five frequency bands were calculated. The resulting calculations, related to

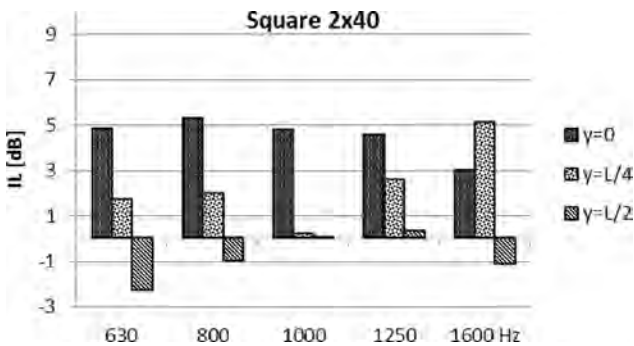


Fig. 15. Insertion Loss (in dB) vs noise source position (square configuration).

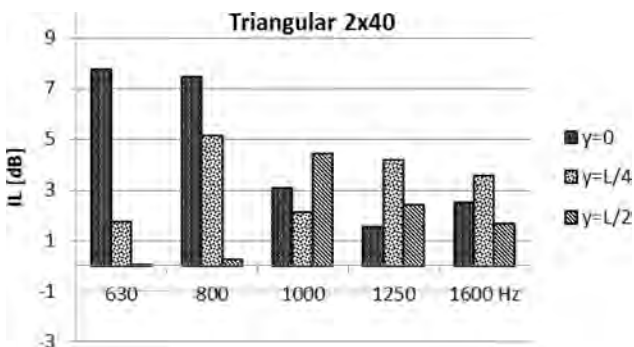


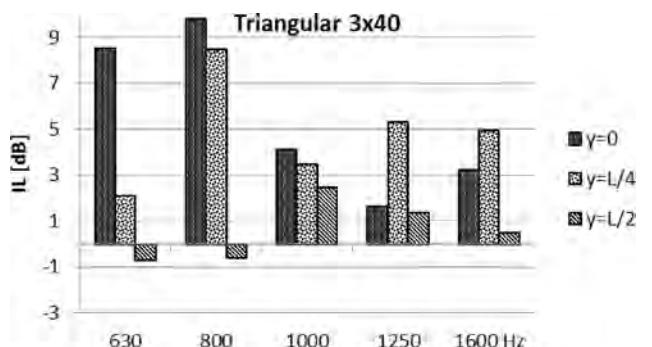
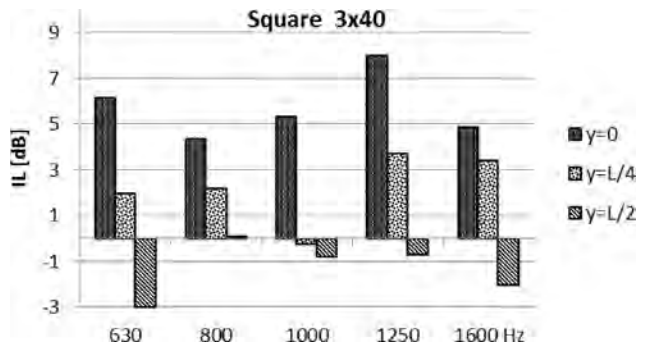
Fig. 16. Insertion Loss (in dB) vs noise source position (triangular configuration).

the different lattice configurations, with $a = 0.40$ m and cylinders with 0.20 m in diameter, are presented in Figs. 15 and 16.

The presented results clearly reveal the strong influence of the relative position of source and receivers. As the source is positioned nearer to the extremity of the sonic crystal (further away from the receiver), the insertion loss computed for the square lattice becomes progressively higher. As stated before, when the source and receivers are aligned around the same y -coordinates, a direct travel path may exist and almost no attenuation is observed. This path no longer seems to exist when the source is positioned further from the receivers' position, and thus higher attenuation values are generated. In the presence of triangular lattices, a similar, but less evident, effect is also seen. For that case, the most prominent feature is that the attenuation reaches higher values for the lower frequency bands, for which insertion loss values of more than 8 dB (for the 3×40 triangular configuration) may be observed.

4.6. Influence of the acoustic absorption of the cylinders

Taking into consideration the possible use of cylinders made of different materials, the effect of different sound absorption coefficients (α) was also studied. Attenuation values were computed for each of the three



positions of the noise source discussed in the previous section. The results are presented in Figs. 17 and 18, for $\alpha = 0.1, 0.3, \text{ and } 0.5$. To implement these values of the absorption coefficient, Robin boundary conditions are considered at boundaries of each cylinder. A real-valued impedance given by

$$Z = \rho c \frac{1 + \sqrt{1 - \alpha}}{1 - \sqrt{1 - \alpha}}, \quad (11)$$

with $c = 340 \text{ m/s}$ and $\rho = 1.22 \text{ kg/m}^3$, is then considered.

In Fig. 17, corresponding to results computed for the square lattice, it can be observed that by progressively increasing the sound absorption coefficient, increased values of the insertion loss are obtained throughout the studied frequency bands. This fact was very much expected, since the presence of an absorbing surface allows sound energy to be progressively dissi-

pated whenever one of those surfaces is hit by acoustic waves. Curiously, the effect of those absorbing surfaces is also quite significant when the source and the receivers are aligned, which indicates that the waveguide effect referred before is strongly attenuated by those absorbent materials. Indeed, observing the results for the higher absorption coefficient ($\alpha = 0.5$) it can be seen that interesting values of the insertion loss are computed for all source positions, representing a marked improvement when compared with the results computed for $\alpha = 0.1$. For this case ($\alpha = 0.5$), peak insertion loss values are reached at 1000 Hz (for the 2×40 structure) and 1250 Hz (for the 3×40 structure), for which IL values of 10 dB and 15 dB are reached when the source is further away from the receivers, and of 4 dB and 6 dB when the source is aligned with those receivers. These attenuation values can be seen as noteworthy in what concerns traffic noise attenuation.

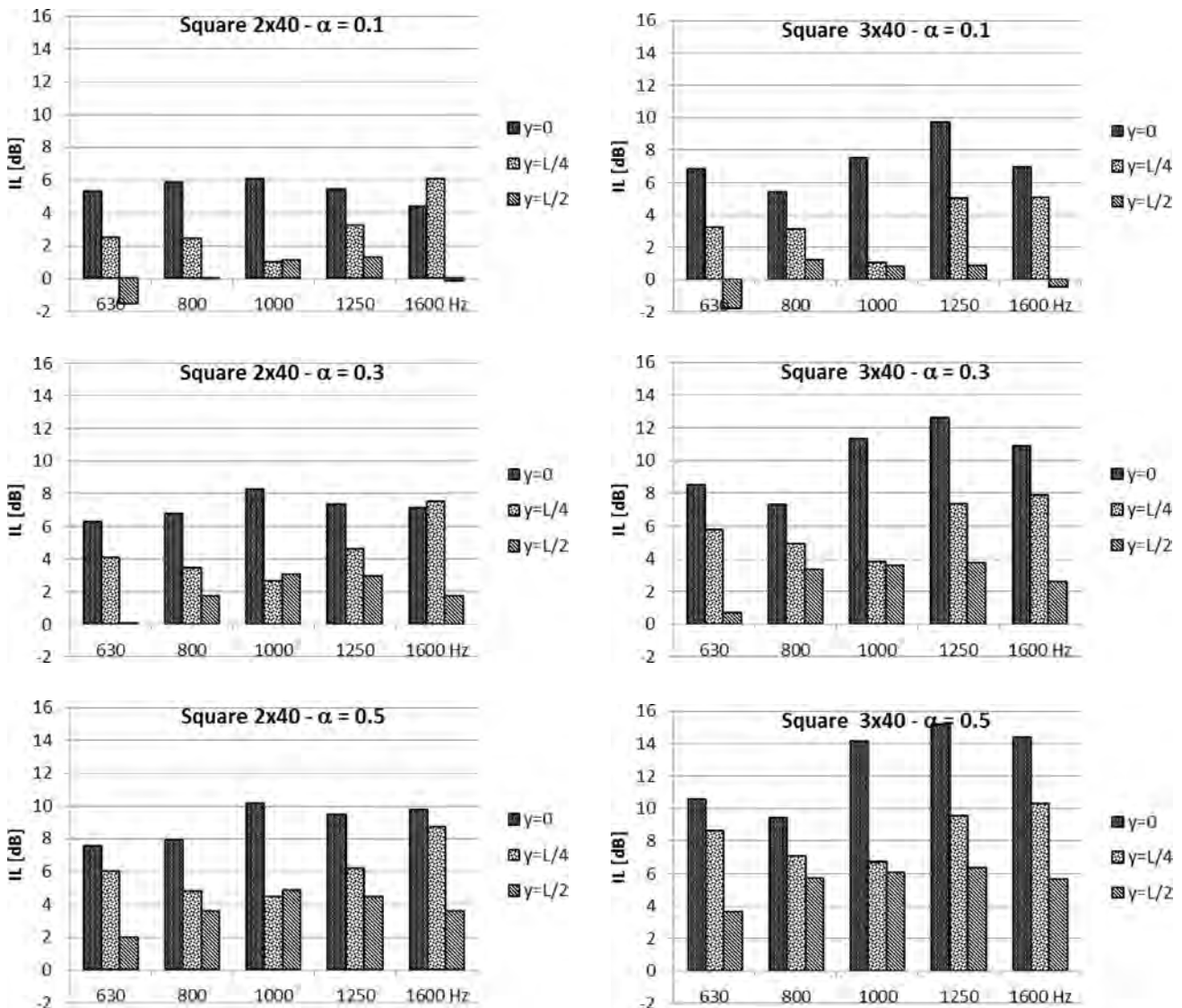


Fig. 17. Insertion Loss (in dB) vs noise source position (square configuration) for varying values of the absorption coefficient.

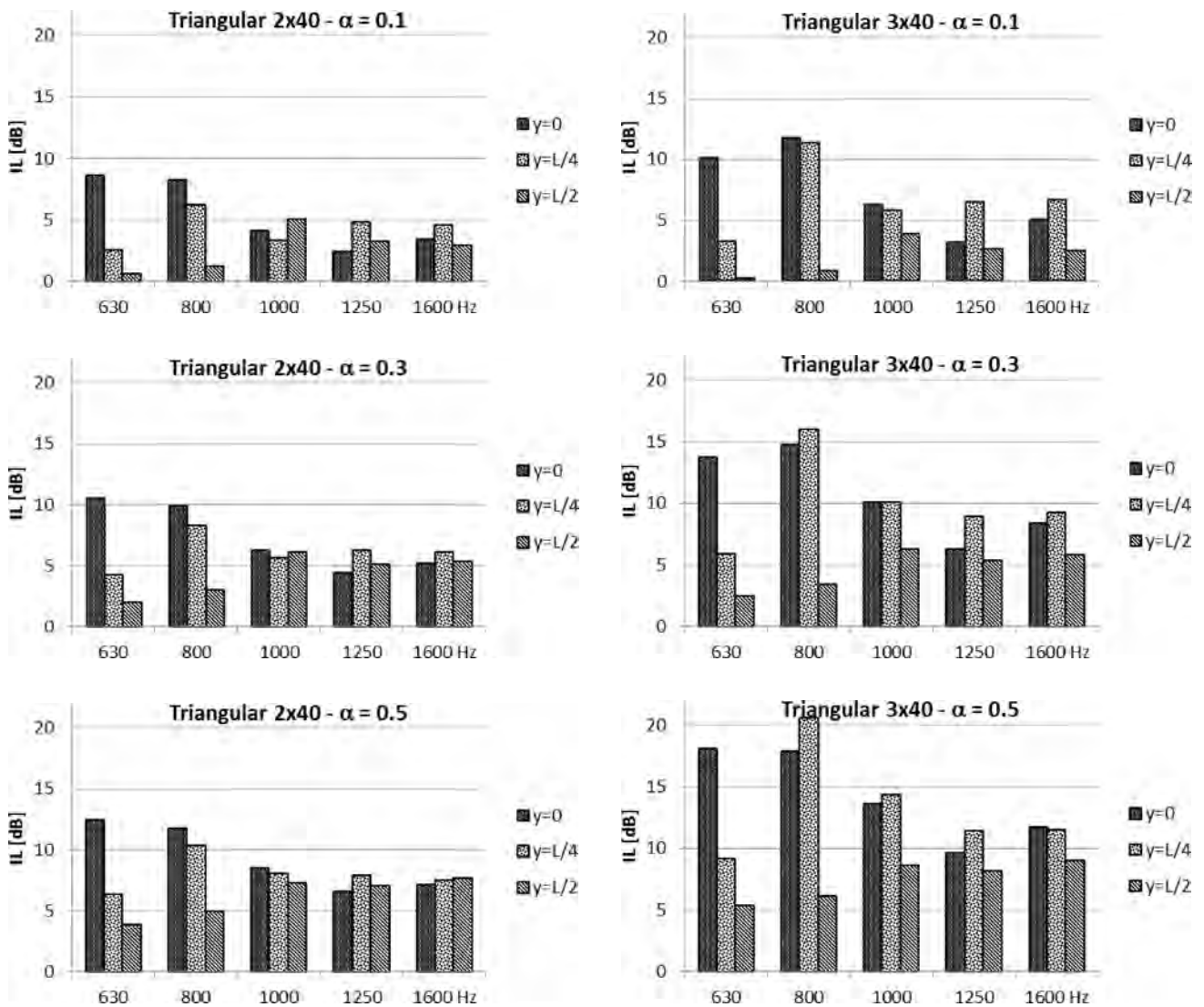


Fig. 18. Insertion Loss (in dB) vs noise source position (triangular configuration) for varying values of the absorption coefficient.

Finally, the results in Fig. 18 illustrate the evolution of the attenuation for the case of the triangular lattice. For this case, the conclusions that may be drawn are, globally, very similar to those stated for the square lattice. However, as the computed values of the insertion loss are, generally, higher for this configuration, this seems to suggest that in an actual road barrier application, the triangular configuration might be considered more adequate.

5. Final remarks

The present work addressed the use of sonic crystals as noise barriers to mitigate road traffic noise by means of an approach based on a numerical technique called the Method of Fundamental Solutions. This technique was adopted, as it appeared to be par-

ticularly well suited to the requirements of the topic being studied, largely due to the geometric characteristics of the structures employed.

The accuracy of the model in evaluating the sound pressure in the presence of multiple cylindrical inclusions is analyzed by benchmarking the results against those computed using the better known Boundary Element Method. The comparison yielded very favorable indications in favor of MFS, namely regarding discretization of the problem and computation times, compared with those when BEM was used.

Several arrangements were studied, covering different combinations of geometrical and acoustic absorption characteristics, and the influence of those aspects in the resulting attenuation values provided by the sonic crystals was analyzed, allowing some broad indications to be established. For example, when comparing the effect of using a triangular or square lattice, the

results seem to show a trend for better performance, in terms of the calculated insertion loss, when structures with a triangular lattice configuration are used.

Another apparently clear implication of the results is the influence of the location of the noise source on the overall sound attenuation. When assuming the source's position in different locations, noticeable variations of the insertion loss are registered at the receiver's position, which appears to suggest the possible existence of some sort of waveguide action. As this can lead to highly divergent outcomes, from the receiver's point of view, such possibility should be thoroughly examined by carrying out additional analyses.

The results presented in this work appear to indicate that the use of MFS may have a good potential to be employed in further research in this subject. Future developments will predictably include the analysis of more complex arrangements, regarding both the geometrical parameters of the periodic structure and acoustical properties of the scatterers. Another relevant topic for further development is related with the three-dimensional effect of the sonic crystal which, in a real configuration, has a limited height and thus may also be affected by diffraction effects occurring at its top. From a more experimental point of view, further investigation will certainly be required in terms of laboratory and field tests, using physical models, to allow the validation of the numerical results.

Acknowledgments

The research work presented herein was supported by FEDER funds through the Operational Programme for Competitiveness Factors – COMPETE and by national funds through the FCT (Portuguese Foundation for Science and Technology), under research project PTDC/ECM-COM/1438/2012.

This paper represents a development with increased detail of a paper presented at the VIII Iberomeric Acoustics Congress, VII Iberian Acoustics Congress, XLIII Spanish Acoustics National Congress – TECNIACÚSTICA® 2012 and Acoustics European Symposium, organized by the Sociedade Portuguesa de Acústica (SPA) and the Sociedad Española de Acústica (SEA), with the support of the European Acoustics Association (EAA), the Federação Iberoamericana de Acústica (FIA), the International Commission for Acoustics (ICA), the Laboratório Nacional de Engenharia Civil (LNEC), and the University of Évora.

References

- ALVES C.J.S., VALTCHEV S.S. (2005), *Numerical comparison of two meshfree methods for acoustic wave scattering*, Engineering Analysis with Boundary Elements, **29**, 4, 371–382.
- ANTÓNIO J., TADEU A., GODINHO L. (2008), *A three-dimensional acoustics model using the method of fundamental solutions*, Engineering Analysis with Boundary Elements, **32**, 525–531.
- DEN BOER L.C., SCHROTEN A. (2007), *Traffic noise reduction in Europe – Health effects, social costs and technical and policy options to reduce road and rail traffic noise*, Delft.
- CASTIÑEIRA-IBÁÑEZ S., RUBIO C., ROMERO-GARCÍA V., SÁNCHEZ-PÉREZ J.V., GARCÍA-RAFFI L.M. (2012), *Design, Manufacture and Characterization of an Acoustic Barrier Made of Multi-Phenomena Cylindrical Scatterers Arranged in a Fractal-Based Geometry*, Archives of Acoustics, **37**, 4, 455–462.
- FAIRWEATHER G., KARAGEORGHIS A. (1998), *The method of fundamental solutions for elliptic boundary value problems*, Adv. Comput. Math., **9**, 69–95.
- FAIRWEATHER G., KARAGEORGHIS A., MARTIN P. (2003), *The method of fundamental solutions for scattering and radiation problems*, Engineering Analysis with Boundary Elements, **27**, 759–769.
- GODINHO L., AMADO MENDES P., TADEU A., CADENA-ISAZA A., SMERZINI C., SÁNCHEZ SESMA F., MADEC R., KOMATITSCH D. (2009), *Numerical Simulation of Ground Rotations along 2D Topographical Profiles under the Incidence of Elastic Plane Waves*, Bulletin of the Seismological Society of America, **99**, 2B, 1147–1161.
- GODINHO L., TADEU A., AMADO MENDES P. (2007), *Wave propagation around thin structures using the MFS*, Computers Materials, Continua (CMC), **5**, 2, 117–127.
- GOLBERG M., CHEN C.S. (1999), *The method of fundamental solutions for potential, Helmholtz and diffusion problems. Boundary Integral Methods: Numerical and Mathematical Aspects*, Computational Engineering, vol. 1. Boston, MA: WIT Press/Computational Mechanics Publications, pp. 103–176.
- MARTINEZ-SALA R., RUBIO C., GARCIA-RAFFI L.M., SANCHEZ-PEREZ J.V., SANCHEZ-PEREZ E.A., LLINARES J. (2006), *Control of noise by trees arranged like sonic crystals*, Jour. Sound Vib., **291**, 100.
- MARTÍNEZ-SALA R., SANCHO J., SÁNCHEZ J.V., GÓMEZ V., LLINARES J., MESEGUER F. (1995), *Sound attenuation by sculpture*, Nature, **378**, 241.
- ROMERO GARCÍA D. (2010), *On the control of propagating acoustic waves in sonic crystals: analytical, numerical and optimization techniques*, Doctoral Thesis.
- SÁNCHEZ-PÉREZ J.V., RUBIO C., MARTÍNEZ-SALA R., SÁNCHEZ-GRANDIA R., GÓMEZ V. (2002), *Acoustic barriers based on periodic arrays of scatterers*, Appl. Phys. Lett., **81**, 5240.

14. SANDBERG U. (2003), *The Multi-Coincidence Peak around 1000 Hz in Tyre/Road Noise Spectra*, Euro-noise, Naples.
15. TADEU A., GODINHO L., ANTÓNIO J. (2001), *Benchmark Solution for 3D Scattering from Cylindrical Inclusions*, Journal of Computational Acoustics, **9**, 4, 1311–1328.
16. UMNVA O., ATTENBOROUGH K., LINTON C.M. (2006), *Effects of porous covering on sound attenuation by periodic arrays of cylinders*, J. Acoust. Soc. Am., **119**, 1.
17. VASSEUR J.O., DEYMIER P.A, DJAFARI-ROUHANI B., PENNEC Y., HLADKY-HENNION A-C. (2008), *Absolute forbidden bands and waveguiding in two-dimensional phononic crystal plates*, Phys. Rev. B, **77**, 085415.
18. World Health Organization – Regional Office for Europe (2011), *Burden of disease from environmental noise*, Frank Theakston [Ed.], ISBN: 978 92 890 0229 5.
19. WU L.-Y., CHEN L.-W., LIU C.-M. (2009), *Acoustic pressure in cavity of variously sized two-dimensional sonic crystal with various filling fraction*, Phys. Lett. A, **373**, 1189–1195.

Effect of Binaural Stimulation on Attention and EEG

Adela CRESPO⁽¹⁾, Manuel RECUERO⁽¹⁾, Gerardo GALVEZ^{(1),(2)}, Adrián BEGOÑA⁽¹⁾

⁽¹⁾ *Centro de Acústica Aplicada y Evaluación no Destructiva,
Consejo Superior de Investigaciones Científicas (CAEND-CSIC)
C/ Serrano 144, 28005 – Madrid, Spain;*

e-mail: adela.crespo@csic.es; manuel.recuero@upm.es; gerardo.galvez@csic.es; adrian.begona@csic.es

⁽²⁾ *Centro de Tecnología Biomédica,
Universidad Politécnica de Madrid (CTB-UPM)
Campus de Montegancedo, 28223 – Pozuelo de Alarcón, Spain;
e-mail: gerardo.galvez@ctb.upm.es*

(received December 4, 2012; accepted November 2, 2013)

When two pure tones of slightly different frequency are presented separately to each ear, the listener perceives a third single tone with amplitude variations at a frequency that equals the difference between the two tones; this perceptual illusion is known as the binaural auditory beat (BB). There are anecdotal reports that suggest that the binaural beat can entrain EEG activity and may affect the arousal levels, although few studies have been published.

There is a need for double-blind, well-designed studies in order to establish a solid foundation for these sounds, as most of the documented benefits come from self-reported cases that could be affected by placebo effect. As BBs are a cheap technology (it even exists a free open source programmable binaural-beat generator on the Internet named Gnaural), any achievement in this area could be of public interest. The aim in our research was to explore the potential of BBs in a particular field: tasks that require focus and concentration. In order to detect changes in the brain waves that could relate to any particular improvement, EEG recordings of a small sample of individuals were also obtained.

In this study we compare the effect of different binaural stimulation in 7 EEG frequency ranges. 78 participants were exposed to 20-min binaural beat stimulation. The effects were obtained both qualitative with cognitive test and quantitative with EEG analysis. Results suggest no significant statistical improvement in 20-min stimulation.

Keywords: binaural auditory beats, attention, frequency following response.

PACS no.: 43.66.Pn

1. Introduction

Binaural waves stimulation at different frequencies has been used in the past two decades in the treatment of many diseases and also to modify different states such as pain, relaxation, meditation, anxiety, and also to improve attention and memory.

Binaural tones are subjective auditory sensations which occur as a result of receiving two tones of slightly different frequencies, each in a different ear. Binaural waves were discovered by Heinrich Wilhelm Dove in 1839.

The binaural hearing beats occur in the brain stem in response to auditory stimulation produced by two

pure tones of slightly similar frequency, each in a different ear. The upper groove located in the brainstem is responsible for interpreting the frequency difference, which is called the binaural tone (OSTER, 1973). For example, if we issue a 110 Hz tone in the right ear and another 115 Hz tone in the left ear, the frequency difference between the two will be 5 Hz, and this is the binaural tone (LANE *et al.*, 1998).

The ability of a human to hear binaural beats seems to be a result of evolutionary assimilation. Many advanced species can detect binaural beats, depending on a skull size (KASPRZAK, 2011).

The binaural tones are the result of neuronal firing overlapping at an appropriate level of the auditory

path, coming from the right and left ear. The binaural tones show how neuronal firing in the auditory nerve maintains the phase information of the received signal (KASPRZAK, 2011; OZIMEK *et al.*, 2008). The route of the auditory nerve to the brain allows the exchange of information coming from both sides, before the sound reaches the cortex, ensuring conscious listening. This exchange occurs at least in two areas of the auditory nerve: in the upper olive grove body, small mass of gray matter located in the ventral pontine reticular system (in charge of contralateral integration of auditory system), and transfers it to other area, the inferior colliculus (SCHWARZ, TAYLOR, 2005). The two signals arriving from different ears are connected in the brain, resulting in a third signal called the binaural tone (KASPRZAK, 2011; PADMANABHAN *et al.*, 2005).

Listening to binaural beats provides the information to the network system, also called the diffuse activation system, a large area of the brain that looks like a network, which makes decisions about the clarity, concentration, and awareness. If either internal (feelings, behaviors, or beliefs) or external (perceived by the senses) stimuli are not in conflict with information willing, the reticular system modifies the activity of brain waves, adjusting these to the frequency binaural tone. This is a natural function of homeostasis. The brain regulates automatic body functions to maintain homeostasis. The reticular system tries to maintain homeostasis in a natural way, controlling and maintaining sustainable states of brain wave activity all the time (unless you get external or internal information). Thanks to the fact that the frequency characteristics of the auditory signal and the frequency of brain waves are similar, the reticular system begins processing the information coming from the auditory signal, believing that the information coming in binaural tone comes of brain wave activity (SMITH *et al.*, 1975; WAHBEH *et al.*, 2007). The term used for this synchronization process in the literature is “entrainment”.

With the development of EEG, it became increasingly clear that certain frequencies can induce changes in the EEG, for instance binaural waves in the delta range (1–4 Hz) are associated with sleep, those in the theta range (4–8 Hz) relate to a slow brain activity, while those that are in the alpha range are associated with awake states (8–13 Hz). The binaural beats in the beta range (16–24 Hz) occur in states of alertness and concentration (LANE *et al.*, 1998).

FOSTER (1991) examined the effects of stimulation in the alpha range (FOSTER, 1990), combined with neurofeedback in this range. The results of this study suggest that the combination of binaural tones with neurofeedback result in increased production of alpha comparing with application of neurofeedback only, but also the group receiving only binaural stimulation waves had higher alpha production than any of the groups. LANE *et al.* (1998) provide evidence on the fre-

quency response of runoff to 7 Hz and its direct effect on psychomotor development and mood.

C. Kasprzak examined experimentally the effect of a binaural wave in 20 subjects (KASPRZAK, 2011). The carrier frequency was 100 Hz, 73 dB SPL, with 20 minutes of binaural stimulation. In this study, positive statistical results are obtained on the modification of cortical arousal with binaural frequencies. Also an entrainment at 10 Hz for 4 of the subjects was found.

Among many applications that are commercial, binaural waves seem to help achieve deeper and faster meditative states. Meditation techniques are used to achieve altered states of consciousness, developing awareness and perception, reduce stress, and increase a positive attitude (BARUŠS, 2001). We found specific patterns in the EEG of meditators when compared with subjects who have never meditated as well when compared against baseline state (AFTANAS, GOLOCHEIKINE, 2002).

LAVALLEE and KOREN (2011) conducted a study with 8 subjects, of whom half were expert meditators and half rookies, subjected to two different binaural stimulation, 7 Hz to facilitate meditation and the other 15 Hz to hinder meditation (LAVALLEE *et al.*, 2011). The results evidenced that novices had less power theta and increased gamma in 15 Hz condition. This result suggest experienced meditators have developed techniques, over the years of practice, to maintain a deep state of meditation while blocking external stimuli (LAVALLEE *et al.*, 2011).

Susan KENNEL (2010) studied the effectiveness of binaural stimulation to reduce symptoms of inattention in teenagers. The study confirmed the utility of binaural waves. It was a randomized, double blind and placebo control study with 20 young people who listened to 20 min stimulation, 3 times per weeks during 3 weeks. They used TOVA, Color Trails test and Homework Problem Checklist to evaluate the cognitive change. They didn't find any significant attention results despite the feedback from parents was very positive (KENNEL *et al.*, 2010).

There were similar studies that found positive results on attention tasks (LANE *et al.*, 1998).

There is a need for double-blind, well-designed studies in order to establish a solid foundation for these sounds, as most of the documented benefits come from self-reported cases that could be affected by placebo effect. As BBs are a cheap technology (it even exists a free open source programmable binaural-beat generator on the internet named Gnaural), any achievement in this area could be of public interest. The aim in our research was to explore the potential of BBs in a particular field: tasks that require focus and concentration. In order to detect changes in the brain waves that could relate to any particular improvement, EEG recordings of a small sample of individuals were also obtained.

2. Materials and methods

2.1. Study design

This study is a randomized, double blind, placebo controlled exploratory pilot investigation in order to determine the effect of two different binaural beat stimulations in the theta and beta ranges and therefore establish the start methodology to continue research in this area of interest.

We have divided experiments into two parts, A and B; in **Experiment A** we measured the improvement in attention with different tests, while in **Experiment B** we measured EEG modifications.

2.2. Setting a sample

Experiment A: We have recruited 60 members of general public from Madrid, included men and women (28 females and 32 males; mean (\pm s.d.) aged 28.9 ± 4.3 years) who were new to binaural beat stimulation and who consented to participate. Exclusion criteria were neurological diseases and left-handedness. They were informed about the general goal of the research and rules of their particular experiment, and completed an audiometric test to assure they suffered no major hearing loss.

Experiment B: We have recruited 18 members of general public from Madrid (5 females and 13 males, aged 26.6 ± 7.49 years), who were new to binaural beat stimulation and who consented to participate. Exclusion criteria were neurological diseases and right-handedness. They were informed about the general goal of the research and rules of their particular experiment, and completed an audiometric test to assure they suffered no major hearing loss.

2.3. Procedures

Experiment A: Participants were blindly allocated to one of three groups according to a predetermined computer-generated random sequence. They listened for 20 minutes via standard headphones to a commercial binaural audio beat (Binaural commercial Group, $n = 20$), an identical soundtrack without these tones (Placebo Group, $n = 20$), or a self-made audio including several layers of BBs (Binaural experimental Group, $n = 20$). The commercial beat audio had the BBs embedded in a fluctuating pink noise that was used also in the self-made audio (the noise that all the Placebo Group listened to). All were instructed to relax and listen with closed eyes in a comfortable position. After 20 minutes, the participants were asked to open their eyes and, without removing the headphones, were requested to complete three different tasks: the test on differences perception (REPÁRAZ *et al.*, 1996), used to evaluate attention and perceptive skills; the 5 digit test, used to measure the processing speed of the subjects and their ability to direct and switch their

attention control; and the EMAV-2, used to measure sustained attention and quality of attention.

When the three tests were completed, headphones were removed and participants were questioned about any unusual feeling during the course of the experiment.

Experiment B: Participants were blindly allocated to one of three groups according to a predetermined computer-generated random sequence. They listened for 20 minutes via standard headphones to a commercial binaural beat audio (Binaural commercial Group, $n = 6$), an identical soundtrack without these tones (Placebo Group, $n = 6$), or a self-made audio including several layers of BBs (Binaural experimental Group, $n = 6$). EEG was used in this study, as we were interested in changes evoked by BBs, and data from 3-min period prior to listening were firstly recorded (baseline). After that, participants listened for 20 minutes via standard headphones to one of the same three audios as described in the first experiment. All were instructed to relax and listen with closed eyes in a comfortable position. After that, headphones were removed and participants were questioned about any unusual feeling during the course of the listening.

2.4. Instrumentation

2.4.1. Stimulation

20-min stimulation with sampling frequency of 44100 and 16 bits. The commercial audio consisted in 2 binaural beats on theta (4 Hz) and beta (16 Hz) at 200 Hz and 250 Hz carrier tones with 13 dB dynamic range; self-made audio consisted in 4 binaural beats in theta (4 Hz) at 100 Hz, 200 Hz, 250 Hz, and 300 Hz carrier tones with another four binaural beats in beta (16 Hz) at 500 Hz, 650 Hz, 750 Hz, and 900 Hz carrier tones with 18 dB dynamic range. We selected those particular frequencies of the binaural tones because we wanted to test the effects of commercial audio aimed at improving concentration and this worked for these frequencies binaural, both have pink noise because it is more comfortable to listen binaural beats, the placebo signal consist in the pink noise with 15 dBs All developed with MATLAB.

Acoustic pressure levels of the applied acoustic stimuli are given in Table 1.

Table 1. Acoustic Pressure Levels of applied stimuli.

	Commercial audio	Self-made audio	Placebo audio
Channel L			
Leq,1min	83.2 dB	78.3 dB	83.2 dB
LAeq,1min	75.3 dBA	72.9 dBA	75.3 dBA
Channel R			
Leq,1min	84.6 dB	80 dB	84.6 dB
LAeq,1min	76 dBA	73 dBA	76 dBA

For the application of sound we used Philips SHH9567 headphones.

2.4.2. EEG

EEG was recorded by a Brainvision Braimnamp EEG at 29 scalp points (International 10/20 system) with simultaneous registration of ECG during 20 min. Sampling rate was 1000 Hz. Mid-forehead electrode was the ground and Nuprep cream was placed on each electrode.

Spectral analysis of the EEG was calculated offline. A 30-second time interval free of artifacts was extracted from the baseline resting state and at 5, 10, 15, and 20 minutes of listening. The extracted intervals were notch-filtered at 50 Hz and band pass filtered between 1 Hz and 70 Hz. EEG power was computed by FFT for the following frequency bands: delta (1–4 Hz), theta (4–8 Hz), alpha (8–12 Hz), beta (12–30 Hz), gamma (30–40 Hz), and for two narrow bands (0.2 Hz width) centered at 4 Hz and 16 Hz. Entrainment was defined for each band and electrode as the ratio of power between stimulation and pre-stimulation (baseline).

Therefore, we calculated four matrixes of 29×7 entrainment values for every subject in the experiment.

As the number of entrainment values was very high (29 electrodes \times 7 bands \times 4 moments), we considered results significant for $p < 0.01$, in order to minimize type I errors. A non-parametric Kruskal-Wallis analysis of variance was performed.

2.4.3. Perception test of differences

The perception test of differences was developed to assess the speed and hits in partially ordered stimulation pattern similarities and differences. It is a discrimination test based on the similarities and differences principles. This type of testing have been shown positive correlations with general intelligence (REPARAZ *et al.*, 1996).

The test consists of 60 graphic elements, in blocks of three elements each; the task is to determine which of the three faces is different from the other two.

2.4.4. EMAV test

The EMAV test assesses the attention capacity and effectiveness in children and adults. This test provides evidence on sustained attention in simple tasks of visual analysis and synthesis. It provides two levels of focus: Sustained Attention (AS) and Quality of Attention (CA) (PÉREZ, LAGO, 2000).

2.4.5. Five Digit Test

The Five Digit Test is a tool to evaluate cognitive processing speed, the ability to focus and refocus at-

tention, and ability to cope with interference. Based on the known Stroop effect, but instead of using words and colors as stimulus, figures or digits are employed in this test, allowing for a greater variety of tasks and possibility to be used with less educated people, even those who do not know the language or cannot read (SEDÓ, 2004).

3. Results

Experiment A: There was no significant difference in scores between groups for any of the three tests (Table 2). A non-parametric Kruskal-Wallis analysis of variance was performed. Data are presented in Table 1 as the mean \pm s.d. $p < 0.05$ was considered significant.

Table 2. Statistic analysis results.

Test	Placebo	Binaural commercial group	Binaural experimental group	p
Perception of differences				
Score	51.5 \pm 6.9	49.6 \pm 6.6	49.1 \pm 7.9	0.52
5 digit				
Reading time	19.6 \pm 3.5	21.5 \pm 5.0	19.4 \pm 3.6	0.36
Counting time	20.9 \pm 2.7	21.9 \pm 3.3	20.9 \pm 3.4	0.38
Election time	31.9 \pm 7.0	31.3 \pm 4.5	29.0 \pm 4.9	0.43
Alternation time	37.2 \pm 9.1	38.6 \pm 5.0	37.2 \pm 7.3	0.23
EMAV-2				
Inhibition	12.3 \pm 6.7	9.8 \pm 5.5	9.5 \pm 4.3	0.54
Flexibility	17.5 \pm 8.3	17.1 \pm 5.5	17.7 \pm 7.1	0.77

Experiment B: As the number of entrainment values was very high (29 electrodes \times 7 bands \times 4 moments), we considered results significant for $p < 0.01$, in order to minimize type I errors. A non-parametric Kruskal-Wallis analysis of variance was performed but we could not find any significant differences between the three groups for any electrode, band, or moment of stimulation. The results of KruskalWallis analysis of variance are given for commercial audio (Tables 3–6), for self-made audio (Tables 7–10), and placebo audio (Tables 11–14).

- *Commercial Audio,*
- *Self-made Audio,*
- *Placebo Audio.*

Table 3. Entrainment at **5 min** (*Commercial Audio*). Kruskal-Wallis p -significance.

Electrode	Bands						
	Delta	Theta	Alpha	Beta	Gamma	Narrow 4 Hz	Narrow 14 Hz
Fp1	0.03	0.46	0.03	0.17	0.46	0.60	0.60
Fp2	0.03	0.60	0.05	0.12	0.60	0.75	0.35
F3	0.17	0.46	0.05	0.07	0.60	0.17	0.46
F4	0.03	0.12	0.03	0.07	0.75	0.25	0.35
C3	0.07	0.17	0.05	0.17	0.75	0.03	0.60
C4	0.25	0.05	0.03	0.75	0.35	0.07	0.35
P3	0.03	0.07	0.03	0.60	0.05	0.03	0.35
P4	0.03	0.03	0.03	0.92	0.07	0.05	0.35
O1	0.03	0.05	0.03	0.75	0.05	0.05	0.03
O2	0.04	0.35	0.04	0.35	0.08	0.04	0.35
F7	0.17	0.60	0.03	0.25	0.60	0.03	0.75
F8	0.17	0.60	0.03	0.25	0.60	0.03	0.75
T7	0.17	0.46	0.03	0.46	0.46	0.03	0.75
T8	0.07	0.60	0.05	0.07	0.75	0.12	0.35
P7	0.03	0.25	0.03	0.92	0.05	0.03	0.07
P8	0.03	0.05	0.03	0.75	0.07	0.03	0.05
Fz	0.25	0.12	0.05	0.35	0.46	0.60	0.75
Cz	0.12	0.75	0.03	0.60	0.46	0.46	0.60
Pz	0.03	0.07	0.03	0.17	0.05	0.03	0.75
FC1	0.75	0.35	0.03	0.92	0.60	0.07	0.46
FC2	0.75	0.05	0.03	0.75	0.75	0.03	0.92
CP1	0.05	0.25	0.03	0.12	0.07	0.03	0.60
CP2	0.05	0.03	0.03	0.35	0.07	0.12	0.35
FC5	0.12	0.17	0.03	0.60	0.46	0.03	0.92
FC6	0.46	0.92	0.03	0.25	0.46	0.17	0.35
CP5	0.07	0.46	0.03	0.75	0.05	0.03	0.60
CP6	0.07	0.46	0.03	0.75	0.05	0.03	0.60
TP9	0.05	0.60	0.03	0.12	0.92	0.03	0.60
TP10	0.05	0.92	0.03	0.03	0.92	0.07	0.92

Table 4. Entrainment at **10 min** (*Commercial Audio*). Kruskal-Wallis p -significance.

Electrode	Bands						
	Delta	Theta	Alpha	Beta	Gamma	Narrow 4 Hz	Narrow 14 Hz
Fp1	0.92	0.12	0.17	0.75	0.25	0.46	0.46
Fp2	0.92	0.35	0.12	0.46	0.25	0.75	0.92
F3	0.75	0.92	0.17	0.75	0.35	0.75	0.92
F4	0.46	0.12	0.12	0.75	0.35	0.92	0.75
C3	0.46	0.12	0.05	0.60	0.46	0.07	0.25
C4	0.46	0.03	0.07	0.03	0.46	0.46	0.03
P3	0.17	0.05	0.03	0.35	0.12	0.05	0.17
P4	0.07	0.05	0.03	0.60	0.12	0.12	0.75
O1	0.05	0.03	0.03	0.75	0.07	0.03	0.46
O2	0.08	0.08	0.08	0.69	0.14	0.04	0.35
F7	0.75	0.46	0.12	0.60	0.35	0.75	0.92
F8	0.75	0.46	0.12	0.60	0.35	0.75	0.92
T7	0.75	0.46	0.07	0.46	0.60	0.35	0.46
T8	0.35	0.17	0.05	0.75	0.92	0.75	0.75
P7	0.12	0.12	0.03	0.92	0.12	0.07	0.46
P8	0.25	0.05	0.03	0.92	0.07	0.05	0.46
Fz	0.75	0.75	0.35	0.92	0.75	0.35	0.60
Cz	0.25	0.05	0.12	0.75	0.35	0.60	0.60
Pz	0.35	0.05	0.03	0.46	0.05	0.03	0.35
FC1	0.60	0.05	0.12	0.03	0.60	0.05	0.07
FC2	0.60	0.05	0.12	0.07	0.60	0.92	0.17
CP1	0.35	0.12	0.05	0.35	0.17	0.03	0.12
CP2	0.60	0.05	0.05	0.35	0.12	0.92	0.46
FC5	0.75	0.35	0.12	0.92	0.35	0.25	0.25
FC6	0.92	0.46	0.03	0.92	0.75	0.35	0.75
CP5	0.17	0.46	0.03	0.75	0.17	0.25	0.46
CP6	0.17	0.46	0.03	0.75	0.17	0.25	0.46
TP9	0.17	0.12	0.03	0.25	0.46	0.25	0.46
TP10	0.25	0.12	0.03	0.35	0.12	0.12	0.46

Table 5. Entrainment at **15 min** (*Commercial Audio*). Kruskal-Wallis *p*-significance.

Electrode	Bands						
	Delta	Theta	Alpha	Beta	Gamma	Narrow 4 Hz	Narrow 14 Hz
Fp1	0.46	0.12	0.17	0.75	0.07	0.46	0.35
Fp2	0.25	0.07	0.17	0.92	0.12	0.92	0.60
F3	0.75	0.46	0.07	0.92	0.46	0.75	0.60
F4	0.75	0.75	0.03	0.92	0.25	0.75	0.46
C3	0.17	0.03	0.03	0.46	0.92	0.05	0.35
C4	0.46	0.05	0.05	0.46	0.60	0.05	0.46
P3	0.03	0.05	0.03	0.92	0.17	0.12	0.05
P4	0.03	0.03	0.03	0.92	0.25	0.07	0.46
O1	0.05	0.03	0.05	0.92	0.12	0.12	0.03
O2	0.08	0.08	0.08	0.69	0.14	0.14	0.89
F7	0.60	0.25	0.12	0.35	0.75	0.60	0.60
F8	0.60	0.25	0.12	0.35	0.75	0.60	0.60
T7	0.25	0.05	0.07	0.35	0.92	0.17	0.75
T8	0.25	0.07	0.12	0.75	0.75	0.05	0.46
P7	0.07	0.07	0.05	0.92	0.12	0.07	0.12
P8	0.05	0.05	0.05	0.60	0.12	0.05	0.92
Fz	0.60	0.60	0.05	0.46	0.75	0.75	0.35
Cz	0.25	0.05	0.05	0.17	0.92	0.46	0.92
Pz	0.03	0.03	0.03	0.25	0.12	0.07	0.35
FC1	0.92	0.07	0.05	0.46	0.07	0.03	0.92
FC2	0.75	0.35	0.07	0.92	0.75	0.25	0.75
CP1	0.12	0.03	0.03	0.60	0.07	0.12	0.05
CP2	0.07	0.03	0.03	0.12	0.46	0.12	0.35
FC5	0.25	0.46	0.05	0.46	0.25	0.35	0.92
FC6	0.46	0.35	0.03	0.75	0.46	0.75	0.25
CP5	0.05	0.05	0.03	0.75	0.07	0.12	0.12
CP6	0.05	0.05	0.03	0.75	0.07	0.12	0.12
TP9	0.12	0.35	0.03	0.35	0.07	0.12	0.92
TP10	0.25	0.05	0.03	0.35	0.35	0.05	0.75

Table 6. Entrainment at **20 min / final** (*Commercial Audio*). Kruskal-Wallis *p*-significance.

Electrode	Bands						
	Delta	Theta	Alpha	Beta	Gamma	Narrow 4 Hz	Narrow 14 Hz
Fp1	0.92	0.75	0.25	0.75	0.75	0.92	0.46
Fp2	0.92	0.75	0.17	0.75	0.75	0.75	0.92
F3	0.75	0.60	0.60	0.25	0.92	0.92	0.07
F4	0.75	0.35	0.25	0.92	0.46	0.92	0.17
C3	0.92	0.03	0.46	0.92	0.75	0.25	0.35
C4	0.75	0.03	0.25	0.35	0.92	0.92	0.46
P3	0.05	0.17	0.12	0.46	0.75	0.12	0.17
P4	0.07	0.07	0.12	0.25	0.92	0.12	0.75
O1	0.07	0.12	0.12	0.12	0.60	0.12	0.60
O2	0.08	0.08	0.14	0.08	0.69	0.08	0.50
F7	0.92	0.92	0.25	0.92	0.17	0.35	0.07
F8	0.92	0.92	0.25	0.92	0.17	0.35	0.07
T7	0.60	0.46	0.17	0.60	0.60	0.03	0.35
T8	0.46	0.25	0.46	0.75	0.92	0.46	0.46
P7	0.07	0.12	0.17	0.17	0.46	0.07	0.92
P8	0.17	0.05	0.12	0.46	0.60	0.12	0.75
Fz	0.75	0.92	0.35	0.60	0.75	0.60	0.35
Cz	0.75	0.17	0.12	0.25	0.92	0.46	0.25
Pz	0.05	0.03	0.07	0.35	0.46	0.05	0.35
FC1	0.35	0.03	0.60	0.05	0.60	0.03	0.03
FC2	0.35	0.92	0.12	0.75	0.46	0.92	0.35
CP1	0.46	0.12	0.05	0.92	0.92	0.12	0.25
CP2	0.17	0.05	0.12	0.92	0.75	0.12	0.75
FC5	0.75	0.75	0.35	0.92	0.92	0.17	0.35
FC6	0.75	0.92	0.35	0.92	0.92	0.92	0.75
CP5	0.25	0.25	0.17	0.92	0.60	0.12	0.92
CP6	0.25	0.25	0.17	0.92	0.60	0.12	0.92
TP9	0.17	0.35	0.05	0.17	0.46	0.17	0.25
TP10	0.12	0.25	0.03	0.75	0.75	0.12	0.60

Table 7. Entrainment at **5 min** (*Self-made Audio*). Kruskal-Wallis p -significance.

Electrode	Bands						
	Delta	Theta	Alpha	Beta	Gamma	Narrow 4 Hz	Narrow 14 Hz
Fp1	0.75	0.92	0.46	0.46	0.05	0.60	0.60
Fp2	0.75	0.75	0.46	0.75	0.12	0.75	0.46
F3	0.75	0.25	0.92	0.03	0.25	0.75	0.17
F4	0.25	0.17	0.92	0.12	0.03	0.92	0.35
C3	0.60	0.92	0.60	0.46	0.35	0.03	0.12
C4	0.35	0.75	0.60	0.25	0.35	0.25	0.92
P3	0.03	0.12	0.07	0.46	0.05	0.35	0.17
P4	0.07	0.60	0.46	0.75	0.05	0.92	0.60
O1	0.12	0.35	0.05	0.75	0.17	0.35	0.75
O2	0.35	0.69	0.89	0.35	0.35	0.69	0.14
F7	0.46	0.92	0.46	0.35	0.35	0.75	0.35
F8	0.46	0.92	0.46	0.35	0.35	0.75	0.35
T7	0.75	0.60	0.46	0.60	0.92	0.35	0.25
T8	0.75	0.46	0.60	0.92	0.60	0.92	0.92
P7	0.35	0.46	0.25	0.92	0.17	0.46	0.46
P8	0.35	0.92	0.92	0.46	0.17	0.92	0.60
Fz	0.46	0.17	0.46	0.05	0.03	0.60	0.35
Cz	0.92	0.35	0.35	0.17	0.03	0.35	0.17
Pz	0.12	0.35	0.25	0.46	0.17	0.46	0.25
FC1	0.35	0.92	0.46	0.03	0.25	0.03	0.25
FC2	0.12	0.12	0.46	0.17	0.05	0.05	0.75
CP1	0.75	0.17	0.25	0.46	0.07	0.75	0.25
CP2	0.60	0.46	0.35	0.75	0.05	0.92	0.75
FC5	0.35	0.75	0.60	0.25	0.25	0.05	0.46
FC6	0.35	0.46	0.92	0.75	0.92	0.12	0.60
CP5	0.35	0.35	0.25	0.92	0.17	0.46	0.35
CP6	0.35	0.35	0.25	0.92	0.17	0.46	0.35
TP9	0.92	0.60	0.60	0.92	0.07	0.46	0.46
TP10	0.46	0.60	0.60	0.75	0.60	0.75	0.75

Table 8. Entrainment at **10 min** (*Self-made Audio*). Kruskal-Wallis p -significance.

Electrode	Bands						
	Delta	Theta	Alpha	Beta	Gamma	Narrow 4 Hz	Narrow 14 Hz
Fp1	0.92	0.75	0.92	0.46	0.03	0.35	0.17
Fp2	0.60	0.92	0.75	0.17	0.12	0.46	0.35
F3	0.60	0.92	0.92	0.60	0.12	0.60	0.60
F4	0.25	0.92	0.75	0.12	0.03	0.92	0.46
C3	0.46	0.75	0.17	0.92	0.75	0.75	0.25
C4	0.75	0.60	0.92	0.75	0.07	0.35	0.60
P3	0.12	0.60	0.75	0.92	0.05	0.75	0.46
P4	0.35	0.46	0.60	0.46	0.12	0.75	0.60
O1	0.05	0.35	0.03	0.92	0.05	0.60	0.75
O2	0.08	0.50	0.14	0.50	0.22	0.50	0.50
F7	0.92	0.92	0.25	0.92	0.92	0.35	0.92
F8	0.92	0.92	0.25	0.92	0.92	0.35	0.92
T7	0.12	0.60	0.60	0.92	0.92	0.46	0.75
T8	0.17	0.75	0.92	0.60	0.92	0.75	0.92
P7	0.12	0.25	0.05	0.46	0.05	0.35	0.75
P8	0.17	0.46	0.35	0.60	0.05	0.75	0.92
Fz	0.25	0.75	0.75	0.25	0.03	0.60	0.25
Cz	0.92	0.60	0.75	0.60	0.05	0.25	0.75
Pz	0.25	0.75	0.92	0.60	0.25	0.75	0.92
FC1	0.75	0.60	0.92	0.75	0.25	0.25	0.75
FC2	0.35	0.46	0.60	0.60	0.05	0.25	0.92
CP1	0.92	0.75	0.92	0.75	0.17	0.75	0.75
CP2	0.75	0.60	0.92	0.60	0.12	0.60	0.92
FC5	0.60	0.46	0.25	0.05	0.35	0.60	0.25
FC6	0.35	0.92	0.60	0.92	0.25	0.92	0.92
CP5	0.12	0.60	0.12	0.92	0.05	0.75	0.46
CP6	0.12	0.60	0.12	0.92	0.05	0.75	0.46
TP9	0.07	0.60	0.12	0.75	0.25	0.75	0.46
TP10	0.25	0.92	0.35	0.60	0.60	0.60	0.35

Table 9. Entrainment at **15 min** (*Self-made Audio*). Kruskal-Wallis *p*-significance.

Electrode	Bands						
	Delta	Theta	Alpha	Beta	Gamma	Narrow 4 Hz	Narrow 14 Hz
Fp1	0.92	0.17	0.07	0.17	0.07	0.75	0.35
Fp2	0.60	0.35	0.25	0.17	0.25	0.60	0.60
F3	0.92	0.46	0.05	0.12	0.46	0.92	0.35
F4	0.75	0.92	0.12	0.25	0.75	0.60	0.92
C3	0.03	0.60	0.03	0.35	0.92	0.35	0.60
C4	0.25	0.60	0.03	0.46	0.12	0.60	0.46
P3	0.12	0.25	0.12	0.35	0.03	0.17	0.46
P4	0.12	0.12	0.12	0.75	0.03	0.12	0.92
O1	0.03	0.12	0.03	0.35	0.03	0.12	0.75
O2	0.22	0.22	0.08	0.89	0.08	0.22	0.69
F7	0.60	0.35	0.12	0.25	0.92	0.17	0.46
F8	0.60	0.35	0.12	0.25	0.92	0.17	0.46
T7	0.17	0.92	0.25	0.35	0.92	0.12	0.75
T8	0.05	0.75	0.46	0.46	0.60	0.17	0.35
P7	0.05	0.17	0.05	0.60	0.12	0.17	0.92
P8	0.12	0.35	0.12	0.92	0.07	0.12	0.75
Fz	0.75	0.46	0.12	0.17	0.12	0.75	0.60
Cz	0.07	0.60	0.12	0.35	0.05	0.92	0.07
Pz	0.12	0.12	0.25	0.35	0.03	0.12	0.35
FC1	0.92	0.35	0.07	0.07	0.75	0.60	0.17
FC2	0.75	0.35	0.05	0.12	0.60	0.92	0.75
CP1	0.12	0.60	0.12	0.35	0.12	0.25	0.12
CP2	0.12	0.12	0.05	0.46	0.03	0.17	0.17
FC5	0.25	0.60	0.05	0.25	0.92	0.75	0.17
FC6	0.12	0.75	0.05	0.35	0.25	0.75	0.92
CP5	0.12	0.60	0.07	0.46	0.17	0.35	0.75
CP6	0.12	0.60	0.07	0.46	0.17	0.35	0.75
TP9	0.05	0.35	0.05	0.75	0.17	0.25	0.46
TP10	0.07	0.60	0.12	0.35	0.92	0.35	0.35

Table 10. Entrainment at **20 min / final** (*Self-made Audio*). Kruskal-Wallis *p*-significance.

Electrode	Bands						
	Delta	Theta	Alpha	Beta	Gamma	Narrow 4 Hz	Narrow 14 Hz
Fp1	0.25	0.12	0.12	0.92	0.03	0.92	0.75
Fp2	0.35	0.46	0.17	0.60	0.46	0.60	0.75
F3	0.75	0.35	0.25	0.35	0.07	0.46	0.25
F4	0.35	0.92	0.35	0.17	0.03	0.60	0.46
C3	0.35	0.35	0.25	0.75	0.46	0.92	0.05
C4	0.25	0.92	0.35	0.35	0.03	0.60	0.75
P3	0.12	0.46	0.25	0.35	0.05	0.25	0.03
P4	0.12	0.25	0.25	0.75	0.03	0.25	0.25
O1	0.12	0.25	0.03	0.35	0.03	0.12	0.03
O2	0.14	0.22	0.08	0.69	0.22	0.22	0.69
F7	0.17	0.25	0.17	0.46	0.60	0.46	0.46
F8	0.17	0.25	0.17	0.46	0.60	0.46	0.46
T7	0.60	0.25	0.46	0.75	0.75	0.35	0.35
T8	0.17	0.92	0.60	0.46	0.60	0.60	0.92
P7	0.46	0.92	0.12	0.92	0.03	0.35	0.25
P8	0.07	0.35	0.17	0.92	0.03	0.25	0.75
Fz	0.35	0.35	0.12	0.46	0.25	0.92	0.46
Cz	0.35	0.60	0.12	0.46	0.25	0.35	0.12
Pz	0.17	0.25	0.25	0.35	0.03	0.17	0.05
FC1	0.25	0.35	0.35	0.46	0.75	0.35	0.35
FC2	0.75	0.92	0.25	0.60	0.25	0.92	0.60
CP1	0.35	0.75	0.35	0.75	0.05	0.25	0.03
CP2	0.35	0.46	0.35	0.75	0.05	0.25	0.17
FC5	0.46	0.60	0.17	0.12	0.60	0.75	0.03
FC6	0.12	0.46	0.35	0.60	0.25	0.92	0.60
CP5	0.25	0.60	0.12	0.46	0.03	0.60	0.12
CP6	0.25	0.60	0.12	0.46	0.03	0.60	0.12
TP9	0.12	0.25	0.17	0.35	0.60	0.12	0.07
TP10	0.07	0.92	0.12	0.35	0.35	0.25	0.75

Table 11. Entrainment at **5 min** (*Placebo audio*). Kruskal-Wallis *p*-significance.

Electrode	Bands						
	Delta	Theta	Alpha	Beta	Gamma	Narrow 4 Hz	Narrow 14 Hz
Fp1	0.17	0.05	0.35	0.25	0.25	0.17	0.35
Fp2	0.25	0.35	0.60	0.25	0.35	0.12	0.25
F3	0.25	0.12	0.92	0.46	0.92	0.60	0.25
F4	0.92	0.25	0.92	0.25	0.92	0.25	0.60
C3	0.60	0.12	0.92	0.25	0.60	0.17	0.46
C4	0.60	0.07	0.46	0.92	0.60	0.46	0.46
P3	0.92	0.46	0.60	0.46	0.92	0.75	0.46
P4	0.46	0.35	0.35	0.46	0.60	0.46	0.75
O1	0.60	0.75	0.92	0.60	0.46	0.46	0.75
O2	0.89	1.00	1.00	0.78	0.48	0.48	0.05
F7	0.35	0.07	0.75	0.46	0.75	0.25	0.46
F8	0.35	0.07	0.75	0.46	0.75	0.25	0.46
T7	0.60	0.60	0.46	0.35	0.75	0.75	0.05
T8	0.92	0.12	0.60	0.60	0.07	0.75	0.92
P7	0.75	0.92	0.75	0.07	0.75	0.92	0.75
P8	0.60	0.46	0.35	0.92	0.60	0.75	0.35
Fz	0.25	0.46	0.46	0.25	0.35	0.92	0.35
Cz	0.60	0.60	0.35	0.25	0.46	0.25	0.35
Pz	0.75	0.60	0.35	0.35	0.46	0.60	0.92
FC1	0.60	0.25	0.17	0.75	0.75	0.35	0.35
FC2	0.75	0.60	0.75	0.46	0.25	0.46	0.46
CP1	0.35	0.46	0.25	0.60	0.92	0.12	0.46
CP2	0.35	0.60	0.35	0.75	0.75	0.25	0.75
FC5	0.60	0.35	0.75	0.60	0.35	0.60	0.60
FC6	0.92	0.07	0.92	0.25	0.17	0.60	0.75
CP5	0.46	0.12	0.35	0.46	0.25	0.35	0.60
CP6	0.46	0.12	0.35	0.46	0.25	0.35	0.60
TP9	0.75	0.60	0.92	0.03	0.92	0.60	0.60
TP10	0.75	0.12	0.92	0.46	0.60	0.75	0.75

Table 12. Entrainment at **10 min** (*Placebo audio*). Kruskal-Wallis *p*-significance.

Electrode	Bands						
	Delta	Theta	Alpha	Beta	Gamma	Narrow 4 Hz	Narrow 14 Hz
Fp1	0.07	0.07	0.60	0.35	0.35	0.07	0.25
Fp2	0.05	0.05	0.35	0.05	0.17	0.05	0.35
F3	0.35	0.25	0.75	0.25	0.60	0.12	0.60
F4	0.46	0.35	0.75	0.92	0.46	0.25	0.92
C3	0.92	0.25	0.46	0.46	0.75	0.60	0.25
C4	0.92	0.12	0.46	0.75	0.92	0.75	0.25
P3	0.46	0.92	0.35	0.92	0.92	0.75	0.60
P4	0.92	0.25	0.12	0.92	0.25	0.46	0.60
O1	0.46	0.75	0.46	0.46	0.35	0.60	0.92
O2	0.12	1.00	0.21	1.00	0.58	0.33	0.40
F7	0.12	0.25	0.60	0.46	0.46	0.75	0.60
F8	0.12	0.25	0.60	0.46	0.46	0.75	0.60
T7	0.75	0.75	0.92	0.25	0.75	0.75	0.75
T8	0.92	0.05	0.60	0.35	0.17	0.75	0.60
P7	0.60	0.92	0.46	0.35	0.60	0.92	0.92
P8	0.75	0.75	0.35	0.92	0.03	0.92	0.60
Fz	0.60	0.60	0.75	0.92	0.92	0.25	0.60
Cz	0.35	0.75	0.12	0.75	0.46	0.75	0.92
Pz	0.75	0.35	0.17	0.60	0.35	0.60	0.60
FC1	0.75	0.92	0.60	0.75	0.60	0.25	0.60
FC2	0.92	0.75	0.75	0.75	0.17	0.25	0.92
CP1	0.60	0.60	0.35	0.46	0.46	0.60	0.35
CP2	0.75	0.75	0.25	0.92	0.92	0.60	0.75
FC5	0.92	0.75	0.75	0.25	0.25	0.60	0.35
FC6	0.25	0.25	0.75	0.92	0.92	0.05	0.60
CP5	0.60	0.12	0.35	0.46	0.75	0.92	0.46
CP6	0.60	0.12	0.35	0.46	0.75	0.92	0.46
TP9	0.75	0.75	0.92	0.17	0.92	0.75	0.92
TP10	0.75	0.46	0.75	0.60	0.75	0.60	0.46

Table 13. Entrainment at **15 min** (*Placebo audio*). Kruskal-Wallis *p*-significance.

Electrode	Bands						
	Delta	Theta	Alpha	Beta	Gamma	Narrow 4 Hz	Narrow 14 Hz
Fp1	0.92	0.35	0.60	0.17	0.92	0.12	0.35
Fp2	0.60	0.35	0.75	0.35	0.60	0.07	0.12
F3	0.35	0.25	0.46	0.03	0.35	0.60	0.03
F4	0.75	0.25	0.75	0.17	0.25	0.46	0.03
C3	0.46	0.12	0.25	0.35	0.17	0.25	0.35
C4	0.17	0.07	0.92	0.17	0.75	0.75	0.05
P3	0.92	0.12	0.05	0.07	0.17	0.25	0.46
P4	0.35	0.07	0.05	0.07	0.25	0.46	0.03
O1	0.46	0.17	0.07	0.07	0.17	0.17	0.46
O2	0.12	0.21	0.04	0.02	0.01	0.67	0.48
F7	0.35	0.35	0.35	0.17	0.75	0.75	0.25
F8	0.35	0.35	0.35	0.17	0.75	0.75	0.25
T7	0.60	0.25	0.46	0.60	0.92	0.75	0.25
T8	0.75	0.07	0.60	0.92	0.25	0.75	0.75
P7	0.92	0.17	0.07	0.17	0.12	0.12	0.05
P8	0.35	0.17	0.05	0.07	0.12	0.92	0.03
Fz	0.46	0.25	0.92	0.12	0.92	0.75	0.07
Cz	0.75	0.35	0.46	0.07	0.92	0.25	0.03
Pz	0.25	0.07	0.05	0.07	0.12	0.12	0.35
FC1	0.75	0.35	0.35	0.92	0.92	0.46	0.60
FC2	0.92	0.35	0.92	0.75	0.35	0.92	0.12
CP1	0.92	0.17	0.03	0.12	0.12	0.17	0.05
CP2	0.92	0.25	0.05	0.25	0.92	0.12	0.25
FC5	0.35	0.17	0.35	0.12	0.12	0.46	0.25
FC6	0.35	0.25	0.92	0.35	0.35	0.92	0.05
CP5	0.46	0.05	0.07	0.60	0.46	0.12	0.35
CP6	0.46	0.05	0.07	0.60	0.46	0.12	0.35
TP9	0.35	0.17	0.07	0.46	0.12	0.35	0.05
TP10	0.25	0.17	0.35	0.17	0.75	0.60	0.05

Table 14. Entrainment at **20 min / final** (*Placebo audio*). Kruskal-Wallis *p*-significance.

Electrode	Bands						
	Delta	Theta	Alpha	Beta	Gamma	Narrow 4 Hz	Narrow 14 Hz
Fp1	0.12	0.07	0.75	0.03	0.25	0.35	0.25
Fp2	0.35	0.25	0.92	0.25	0.25	0.07	0.35
F3	0.46	0.35	0.92	0.03	0.75	0.92	0.07
F4	0.75	0.60	0.35	0.17	0.35	0.92	0.25
C3	0.92	0.12	0.75	0.92	0.75	0.75	0.75
C4	0.46	0.17	0.46	0.60	0.92	0.92	0.60
P3	0.60	0.25	0.35	0.46	0.12	0.92	0.46
P4	0.35	0.25	0.17	0.35	0.17	0.75	0.46
O1	0.92	0.60	0.17	0.46	0.12	0.75	0.35
O2	0.78	0.48	0.09	0.67	0.03	1.00	0.67
F7	0.92	0.12	0.46	0.07	0.92	0.60	0.35
F8	0.92	0.12	0.46	0.07	0.92	0.60	0.35
T7	0.92	0.60	0.46	0.60	0.25	0.92	0.46
T8	0.35	0.35	0.35	0.25	0.25	0.92	0.25
P7	0.35	0.35	0.25	0.46	0.17	0.92	0.46
P8	0.35	0.46	0.17	0.60	0.12	0.75	0.92
Fz	0.46	0.46	0.92	0.17	0.35	0.92	0.46
Cz	0.46	0.35	0.12	0.07	0.60	0.46	0.03
Pz	0.35	0.46	0.25	0.35	0.25	0.75	0.75
FC1	0.60	0.35	0.35	0.75	0.92	0.92	0.12
FC2	0.75	0.60	0.75	0.75	0.25	0.92	0.60
CP1	0.46	0.35	0.25	0.17	0.05	0.60	0.92
CP2	0.46	0.35	0.25	0.25	0.12	0.75	0.75
FC5	0.46	0.46	0.75	0.46	0.25	0.75	0.46
FC6	0.92	0.25	0.92	0.60	0.92	0.92	0.60
CP5	0.92	0.12	0.35	0.75	0.75	0.75	0.92
CP6	0.92	0.12	0.35	0.75	0.75	0.75	0.92
TP9	0.92	0.75	0.25	0.75	0.75	0.60	0.46
TP10	0.75	0.25	0.25	0.35	0.60	0.92	0.75

4. Discussion

In this paper, effects of commercially available BBs and a self-made stimulation were examined. We could not find any significant difference in the cognitive tests. This may be due to several factors, including wrong types of cognitive task were used or short duration of stimulation. It is true that the tests used in this study did not cover the whole spectrum of cognitive tasks (for instance planning and problem solving were not analyzed), but the commercial stimulation is advertised as “perfect for any mental task requiring focus and concentration”, and the tests did require those capabilities.

We could not find either any significant difference in brain activity by means of EEG recording. It is possible that the size of the sample (6 per stimulation) was too small to examine group differences and/or the stimulation time was too short. The last possibility is the embedded noise with the stimulation. KASPRZAK (2011) reported significant changes using only BBs with no background sound. There were no side effects or adverse events noted by participants.

These results provide no evidence for improvements in cognitive function or changes in brain activity following binaural beat listening in a small sample of healthy adults after 20 min. It is important to consider the possibility that one session is insufficient to produce a measurable effect, and further studies including several sessions of listening should be considered.

Because BBAS is a safe, non invasive, and potentially useful modality to entrain brainwaves (KASPRZAK, 2011) and to improve attention (KENNEL *et al.*, 2010), this modality should be investigated farther using a larger sample.

Since subjects response can depend on baseline condition (ROSENFELD *et al.*, 1997), population characteristic including mental health, psychological profile, QEEG, age, gender, and other baseline variables should be specific clearly. Measurement of QEEG and relevant hormones before and after stimulation would help clinical outcomes and improve our understanding of the mechanism. Hormones such as glucocorticoids and melatonin fluctuate during the day and affect arousal and thus EEG.

Finally, future studies should follow participants for an extended period of time to determine the effectiveness of this therapy over the time.

In further experiments it is necessary also use simple stimulation with only one layer of BBs trying to observe the fast following response. The EEG analysis for this signal is a difficult selection; future studies will have to calculate trends in order to know what happens along time. Also it is important to evaluate new parameters like hemispheric lateralization and evoked potentials.

Acknowledgments

This research was undertaken with the support of *Centro de Acústica Aplicada y Evaluación No Destructiva (CAEND)*, Biomedical Technology Center (UPM) and Leonardo Torres Quevedo (CSIC Building).

We are grateful to Portuguese Society of Acoustics who organized VIII Iberoamerican Congress of Acoustics.

This paper was submitted at the VIII Ibero-American Acoustic Congress held on October 3 2012 in Évora (Portugal).

References

1. AFTANAS L.I., GOLOCHEIKINE S.A. (2002), *Non-linear dynamic complexity of the human EEG during meditation*, Neuroscience letters, **330**, 2, 143–6.
2. BARUŠS I. (2001), *The Art of Science: Science of the Future in Light of*, Journal of Scientific Exploration, **15**, 1, 57–68.
3. FOSTER D.S. (1990), *EEG and Subjective Correlates of Alpha-Frequency Binaural-Beat Stimulation Combined with Alpha Biofeedback*, 1–34.
4. KASPRZAK C. (2011), *Influence of Binaural Beats on EEG Signal*, Acta Physica Polonica, **119**, 986–990.
5. KENNEL S., TAYLOR A.G., LYON D., BOURGUIGNON C. (2010), *Pilot Feasibility Study of Binaural Auditory Beats for Reducing Symptoms of Inattention in Children and Adolescents with Attention-Deficit/Hyperactivity Disorder*, Journal of pediatric nursing, **25**, 1, 3–11.
6. LANE J.D., KASIAN S.J., OWENS J.E., MARSH G.R. (1998), *Binaural Auditory Beats Affect Vigilance Performance and Mood*, Physiology & Behavior, **63**, 2, 249–252.
7. LAVALLEE C.F., KOREN S.A., PERSINGER M.A. (2011), *A Quantitative Electroencephalographic Study of Meditation and Binaural Beat Entrainment*, The Journal of Alternative and Complementary Medicine, **17**, 4, 351–355.
8. OSTER G. (1973), *Auditory beats in the brain*, Scientific American, **229**, 4, 94–102.
9. OZIMEK E., KONIECZNY J., SONE T. (2008), *Binaural perception of the modulation depth of AM signals*, Hearing Research, **235**, 1-2, 125–133.
10. PADMANABHAN R., HILDRETH A.J., LAWS D. (2005), *A prospective, randomised, controlled study examining binaural beat audio and pre-operative anxiety in patients undergoing general anaesthesia for day case surgery*, Anaesthesia, **60**, 9, 874–877.
11. PÉREZ M., LAGO A. (2000), *Escalas Magallanes de Atención Visual*, Escalas Magallanes de Atención Visual, 30092.

12. REPARAZ C., PERALTA F., NARBONA J. (1996), *El test de percepción de diferencias (caras) como instrumento de medida de la atención sostenida*, Revista de ciencias de la educación, **166**, 265–280.
13. ROSENFELD J.P., REINHART A.M., SRIVASTAVA S. (1997), *The effects of alpha (10-Hz) and beta (22-Hz) “entrainment” stimulation on the alpha and beta EEG bands: individual differences are critical to prediction of effects*, Applied Psychophysiology and Biofeedback, **22**, 1, 3–20.
14. SCHWARZ D.W.F., TAYLOR P. (2005), *Human auditory steady state responses to binaural and monaural beats*, Clinical Neurophysiology, **116**, 3, 658–668.
15. SEDÓ M.A. (2004), *Test de las cinco cifras: una alternativa multilingüe y no lectora al test de Stroop*, Revista Española de Neurología, **38**, 9, 824–828.
16. SMITH J.C., MARSH J.T., BROWN W.S. (1975), *Far-field recorded frequency-following responses evidence for the locus of brainstem sources*, Electroencephalogr. Clin. Neurophysiol., **39**, 5, 465–472.
17. WAHBEH H., CALABRESE C., ZWICKEY H. (2007), *Binaural Beat Technology in Humans: A Pilot Study To Assess Psychologic and Physiologic Effects*, The Journal of Alternative and Complementary Medicine, **13**, 1, 25–32.

Controllability-Oriented Placement of Actuators for Active Noise-Vibration Control of Rectangular Plates Using a Memetic Algorithm

Stanisław WRONA, Marek PAWEŁCZYK

*Institute of Automatic Control, Silesian University of Technology
Akademicka 16, 44-100 Gliwice, Poland; e-mail: {Stanislaw.Wrona, Marek.Pawelczyk}@polsl.pl*

(received March 14, 2013; accepted November 4, 2013)

For successful active control with a vibrating plate it is essential to appropriately place actuators. One of the most important criteria is to make the system controllable, so any control objectives can be achieved.

In this paper the controllability-oriented placement of actuators is undertaken. First, a theoretical model of a fully clamped rectangular plate is obtained. Optimization criterion based on maximization of controllability of the system is developed. The memetic algorithm is used to find the optimal solution. Obtained results are compared with those obtained by the evolutionary algorithm. The configuration is also validated experimentally.

Keywords: active control, flexible structures, actuators placement, controllability Gramian, evolutionary algorithm, memetic algorithm.

1. Introduction

Structural sound sources are acoustic radiators of increasing significance for active noise control (ANC) systems (KOZUPA, WICIAK, 2010; MAZUR, PAWEŁCZYK, 2011; PAWEŁCZYK, 2008). The problem of actuators placement on a vibrating structure has been a point of interest in recent years. Their effect on sound radiation has been analysed by different authors (GÓRSKI, KOZUPA, 2012; LENIOWSKA, 2009; SZEMELA *et al.*, 2012). Misplaced actuators may result in lack of controllability, which deteriorates the performance of the system. In many practical applications there is also a limit to the number of actuators, so they need to reach the best possible performance. Therefore, their locations have to be carefully chosen.

Different techniques have been proposed over the years. A survey of actuator placement in various engineering disciplines until 1999 is presented in (PADULA, KINCAID, 1999). Later work in the area of actuator location on flexible structures is reviewed in (FRECKER, 2003).

There are two basic approaches to optimize actuators placement. One approach is primarily focused on selecting a control strategy, defining a performance index, and then simultaneously determining both the optimal model-based controller and actuators place-

ment. Performance of a linear quadratic regulator (LQR) controller was considered as an objective in (KUMAR, NARAYANAN, 2007). The spatial H_2 norm of the closed-loop system was used as the performance index for a genetic algorithm in (LIU *et al.*, 2006). A computational method to design an H_∞ controller and corresponding optimal actuators locations was presented in (ARABYAN, CHEMISHKIAN, 1998; CHEMISHKIAN, ARABYAN, 1999). However, in such an approach, optimality of the obtained solution is dependent on the choice of a control strategy.

Another approach is based on an open-loop system analysis, and therefore it is independent on controller choice. A Gramian controllability was taken as an objective in (SADRI *et al.*, 1999; HAN, LEE, 1999). Optimal placement of ten piezoelectric sensor/actuator pairs mounted on a cantilever plate using modified H_∞ norm was investigated in (HALE, DARAJI, 2012). A controllability-oriented approach and spillover effect reduction was presented in (PAWEŁCZYK, WRONA, 2013).

In this paper the controllability-oriented approach is adopted to solve the actuators placement problem. The proposed method is based on modeling the overall structure including position of actuators, and is totally independent of the control strategy. A fully-clamped isotropic rectangular plate is considered. A memetic

algorithm (MA) is proposed to be applied to find efficient locations for actuators. MA method similarly to evolutionary algorithm (EA), is well adapted in finding the global optimal solution for a complicated problem such as the locations of actuators. However, MA is characterized by improved procedures for local search and can lead to a faster convergence and a statistically better solution. Optimization criterion used in this paper is based on the Gramian matrix.

2. Plate modeling

In this section, the overall state model of a plate with actuators bonded to its surface is derived. The modeling is based on the Rayleigh-Ritz assumed mode shape method. Fundamental issues of this theory are recalled below to set a reference for further reading.

According to the Kirchhoff-Love plate theory (RAO, 2007), the equation of motion in Cartesian coordinates is:

$$D \left(\frac{\partial^4 w}{\partial x^4} + 2 \frac{\partial^4 w}{\partial x^2 \partial y^2} + \frac{\partial^4 w}{\partial y^4} \right) + m_s \frac{\partial^2 w}{\partial t^2} = f_a, \quad (1)$$

where

$$D = \frac{Eh^3}{12(1-\nu^2)}. \quad (2)$$

In (1) and (2) w is the plate transverse displacement; f_a is the total force generated by actuators; ∇^4 is the biharmonic differential operator; D is the flexural rigidity; E is the Young's modulus; ν is the Poisson's ratio; m_s is the mass per unit area of plate surface; and h is the plate thickness.

Considering only the transverse motion and neglecting the effect of rotary inertia, the kinetic energy of the plate T can be expressed as:

$$T = \frac{1}{2} \iint_S m_s \left(\frac{\partial w}{\partial t} \right)^2 dx dy, \quad (3)$$

where S is the surface of the plate. The strain energy U can be written as:

$$U = \frac{D}{2} \iint_S \left\{ \left(\frac{\partial^2 w}{\partial x^2} \right)^2 + \left(\frac{\partial^2 w}{\partial y^2} \right)^2 + 2\nu \frac{\partial^2 w}{\partial x^2} \frac{\partial^2 w}{\partial y^2} + 2(1-\nu) \left(\frac{\partial^2 w}{\partial x \partial y} \right)^2 \right\} dx dy. \quad (4)$$

The Rayleigh-Ritz method allows to find an approximate solution to a differential equation with given boundary conditions (LEISSA, 1969). It is based on an assumption that the solution can be expressed as a Ritz series:

$$w(x, y, t) = \sum_{i=1}^M \eta_i(x, y) q_i(t), \quad (5)$$

where q_i is the generalized displacement and η_i is the i -th Ritz function. The Ritz function needs to satisfy the geometric boundary condition, so for a rectangular plate it is assumed to be a product of the eigenfunctions of a one-dimensional bar u_n :

$$\eta_i(x, y) = u_n(x)u_m(y). \quad (6)$$

The Ritz functions determine, which geometry of the plate will be considered and what boundary condition will be adopted.

Then, the transversal displacement expressed as in (5) is substituted into kinetic and potential energy Eqs. (3) and (4):

$$T = \frac{1}{2} \sum_{i=1}^M \sum_{j=1}^M \left(\iint_S m_s \eta_i \eta_j dx dy \right) \dot{q}_i \dot{q}_j, \quad (7)$$

$$U = \frac{D}{2} \sum_{i=1}^M \sum_{j=1}^M \left\{ \iint_S \left[\frac{\partial^2 \eta_i}{\partial x^2} \frac{\partial^2 \eta_j}{\partial x^2} + \frac{\partial^2 \eta_i}{\partial y^2} \frac{\partial^2 \eta_j}{\partial y^2} + 2\nu \frac{\partial^2 \eta_i}{\partial x^2} \frac{\partial^2 \eta_j}{\partial y^2} + 2(1-\nu) \frac{\partial^2 \eta_i}{\partial x \partial y} \frac{\partial^2 \eta_j}{\partial x \partial y} \right] dx dy \right\} q_i q_j. \quad (8)$$

The superimposed dot denotes the time derivative. The kinetic and potential energies can be also written as functions of generalized displacement vector \mathbf{q} , mass matrix \mathbf{M} and stiffness matrix \mathbf{K} :

$$T = \frac{1}{2} \dot{\mathbf{q}}^T \mathbf{M} \dot{\mathbf{q}}, \quad (9)$$

$$U = \frac{1}{2} \mathbf{q}^T \mathbf{K} \mathbf{q}. \quad (10)$$

The superscript T denotes the transpose. The mass and stiffness matrices, \mathbf{M} and \mathbf{K} , depend on Ritz functions, and can be calculated as:

$$M_{ij} = \iint_S m_s \eta_i \eta_j dx dy, \quad (11)$$

$$K_{ij} = D \iint_S \left[\frac{\partial^2 \eta_i}{\partial x^2} \frac{\partial^2 \eta_j}{\partial x^2} + \frac{\partial^2 \eta_i}{\partial y^2} \frac{\partial^2 \eta_j}{\partial y^2} + 2\nu \frac{\partial^2 \eta_i}{\partial x^2} \frac{\partial^2 \eta_j}{\partial y^2} + 2(1-\nu) \frac{\partial^2 \eta_i}{\partial x \partial y} \frac{\partial^2 \eta_j}{\partial x \partial y} \right] dx dy. \quad (12)$$

Finally, the equation of a vibrating structure can be obtained:

$$\mathbf{M} \ddot{\mathbf{q}} + \mathbf{K} \mathbf{q} = \mathbf{Q}, \quad (13)$$

where \mathbf{Q} is the vector of generalized forces. In this paper, electrodynamic actuators are considered. Hence, for actuator positioning purpose, their action can be simplified and taken into account as a force acting on a point:

$$\mathbf{Q} = \iint_S \boldsymbol{\eta} f_a dx dy. \quad (14)$$

The harmonic solution of Eq. (13) gives the eigenvector matrix Φ and eigenfrequencies ω_i . Replacing \mathbf{q} by $\Phi \mathbf{v}$ and multiplying Eq. (13) on the left by Φ^T , it gives:

$$\ddot{\mathbf{v}} + \text{diag}(\omega_i^2) \mathbf{v} = \Phi^T \mathbf{Q}. \quad (15)$$

This equation can be written in a usual state-space form, using the state vector \mathbf{x} truncated at N modes as:

$$\mathbf{x} = [\dot{v}_1, \omega_1 v_1, \dot{v}_2, \omega_2 v_2, \dots, \dot{v}_N, \omega_N v_N]^T, \quad (16)$$

$$\frac{\partial}{\partial t} \mathbf{x} = \mathbf{A} \mathbf{x} + \mathbf{B} \mathbf{u} \quad (17)$$

with $\mathbf{A} = \text{diag}(\mathbf{A}_i)$, where

$$\mathbf{A}_i = \begin{bmatrix} -2\xi\omega_i & -\omega_i \\ \omega_i & 0 \end{bmatrix}. \quad (18)$$

Damping ratio ξ is determined experimentally. Matrix \mathbf{B} can be expressed as:

$$\mathbf{B} = [b_1, 0, b_2, 0, \dots, b_N, 0]^T, \quad (19)$$

where b_i is the i -th component of the vector $\Phi^T \mathbf{Q}$. Matrix \mathbf{B} contains as many columns as the number of actuators.

3. Optimization criterion for actuators locations

The chosen objective function to be minimized expresses control energy required to reach the desired state \mathbf{x}_{T_1} at time $t = T_1$:

$$E = \int_0^{T_1} \mathbf{u}^T(t) \mathbf{u}(t) dt. \quad (20)$$

For the initial state, \mathbf{x}_0 , the optimal solution requires the following energy transmitted from the actuators to the structure:

$$E_{\text{opt}} = (e^{\mathbf{A}T_1} \mathbf{x}_0 - \mathbf{x}_{T_1})^T \mathbf{W}^{-1}(T_1) (e^{\mathbf{A}T_1} \mathbf{x}_0 - \mathbf{x}_{T_1}), \quad (21)$$

where $\mathbf{W}(T_1)$ is the controllability Gramian matrix defined by:

$$\mathbf{W}(T_1) = \int_0^{T_1} e^{\mathbf{A}t} \mathbf{B} \mathbf{B}^T e^{\mathbf{A}^T t} dt. \quad (22)$$

To minimize control energy with respect to the actuators locations, a measure of the Gramian matrix should be maximized. It has been shown in the literature that instead of using $\mathbf{W}(T_1)$, a steady-state controllability Gramian matrix \mathbf{W}_c can be used for stable systems, when time tends to infinity (ANDERSON, MOORE, 1990):

$$\mathbf{W}_c = \int_0^{\infty} e^{\mathbf{A}t} \mathbf{B} \mathbf{B}^T e^{\mathbf{A}^T t} dt. \quad (23)$$

The steady-state controllability Gramian \mathbf{W}_c can be calculated by solving the Lyapunov equation:

$$\mathbf{A} \mathbf{W}_c + \mathbf{W}_c \mathbf{A}^T + \mathbf{B} \mathbf{B}^T = 0. \quad (24)$$

If the i -th eigenvalue of \mathbf{W}_c corresponding to i -th eigenmode is small, the eigenmode is difficult to control (it can be regulated only if a large control energy is available). To ensure controllability of initial N eigenmodes, the following criterion can be thus considered:

$$J = \min_{i=1, \dots, N} \lambda_i, \quad (25)$$

where λ_i is the i -th eigenvalue of the steady state controllability Gramian. Such criterion concerns maximization of controllability of the least controllable eigenmode.

As the number of actuators and considered eigenmodes increases, search space size expands and becomes more complex. Hence, memetic algorithms are proposed to solve the optimization problem.

4. Memetic algorithms

Evolutionary algorithms have proven to be a versatile and effective technique for solving nonlinear optimization problems with multiple optima (GOLDBERG, 1989). Their convergence properties has been discussed in (GREENHALGH, MARSHALL, 2000). However, they usually require evaluation of numerous solutions resulting in high computational cost. Memetic algorithms are hybrid forms of population-based approach coupled with separate individual learning. Memetic algorithms combine advantages of a global search, like for evolutionary algorithms, and local improvement procedures, which enhance converge to the local optima (NERI *et al.*, 2011). Because of complementary properties, they are particularly useful in solving complex multi-parameter optimization problems, such as the actuators placement.

As shown in Fig. 1, the memetic algorithm starts with a randomly generated population of candidate solutions called individuals. The fitness function is evaluated for each individual. A part of the existing population is selected for further reproduction dependent on the fitness value (individuals fitting better are

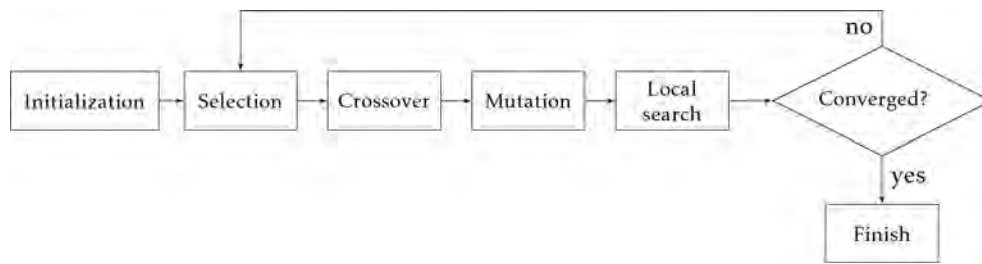


Fig. 1. Memetic algorithm flowchart.

more likely to be chosen). Children solutions are generated by applying one of crossover methods for two or more parents. To maintain genetic diversity, the mutation operator might be used dependent on a pre-defined probability. Then, a local search technique is employed to improve individual fitness. To maintain a balance between the degree of evolution (exploration) and individual improvement (exploitation), only a portion of the population individuals undergo the learning. Afterwards, a selection is performed, and the process is repeated until a certain termination criterion is met.

The optimization problem considered in this paper, consists of determining the efficient locations of fixed number of actuators. Optimization variables are actuators locations expressed as spatial coordinates. The size of the population is kept the same in each iteration step. Best individuals are kept unchanged in the next generation (elitist selection). The “Hill climbing” technique (NERI *et al.*, 2011) is assumed as the individual learning strategy. The termination criterion is satisfied if no improvement is found in the last m iterations, or the maximum number of iterations is reached.

5. Application for a fully-clamped square plate

In this section, application of the proposed method for optimal placement of 3 electrodynamic actuators on a fully-clamped square plate is presented. The objective is to ensure controllability of initial 6 eigenmodes, by maximizing criterion (25). Such assumptions make the analysis sufficiently general to consider both control complexity and application related aspects. Dimensions and characteristics of the plate and actuators are given in Table 1. Obtained eigenvalues of the controllability Gramian corresponding to eigenmodes are presented in Fig. 2c. Actuators locations found are shown in Fig. 2b.

Corresponding shapes and frequencies of the eigenmodes are presented in Fig. 4. Frequency responses of the plate due to excitation by individual actuators with a random signal were measured in 81 uniformly distributed points, depicted in Fig. 2a. The distance between measurement points, and therefore the number

Table 1. Mechanical and electrical properties of the plate and exciters.

Properties	Plate	Exciter EX1
Size [mm]	420x420	∅70
Thickness [mm]	3	19
Density [Kg/m ³]	2700	–
Mass [Kg]	1.428	0.115
Young modulus [GPa]	70	–
Poisson's ratio	0.35	–
Power handling [W]	–	5

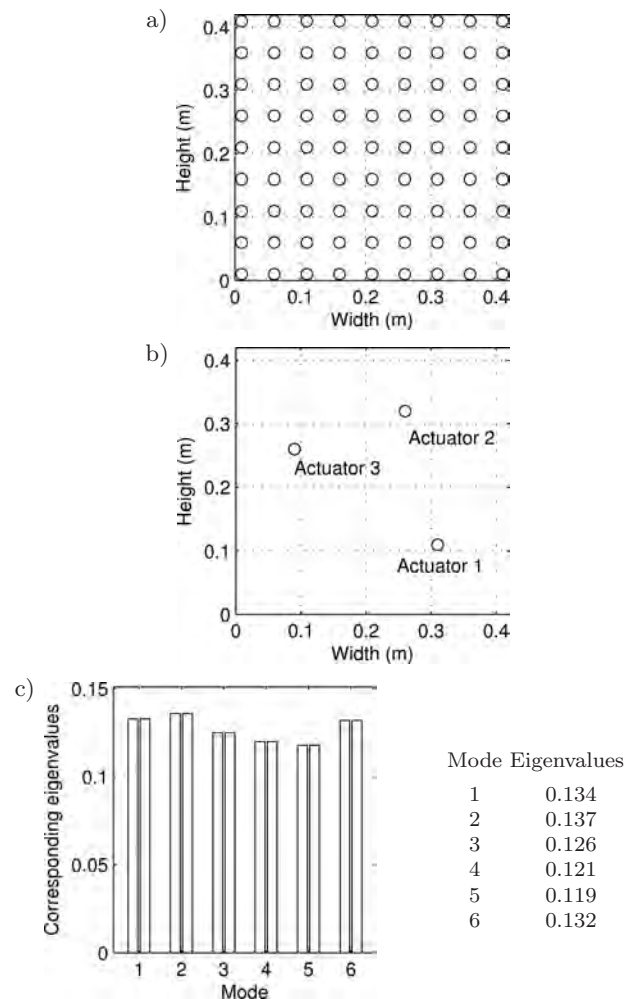


Fig. 2. Results of optimization: a) measurement points, b) actuator locations, c) eigenvalues.

of them, has been adopted to be considerably smaller than the distance between the nodes and anti-nodes of the plate eigenmodes in the frequency band consid-

ered. Results averaged over entire plate are presented in Fig. 3. For experimental verification the Polytec laser vibrometer PDV-100 has been used.

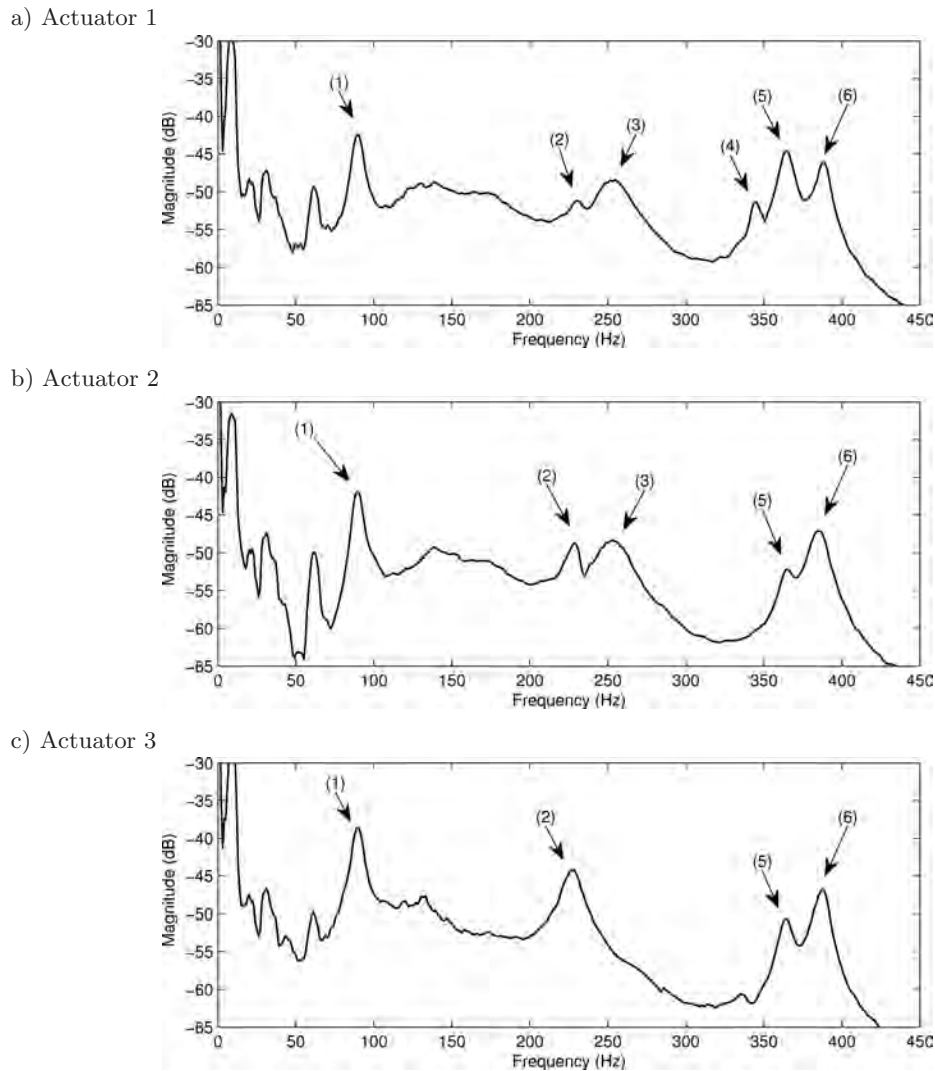


Fig. 3. Magnitudes of surface-averaged frequency responses of the plate due to excitation by individual actuators.

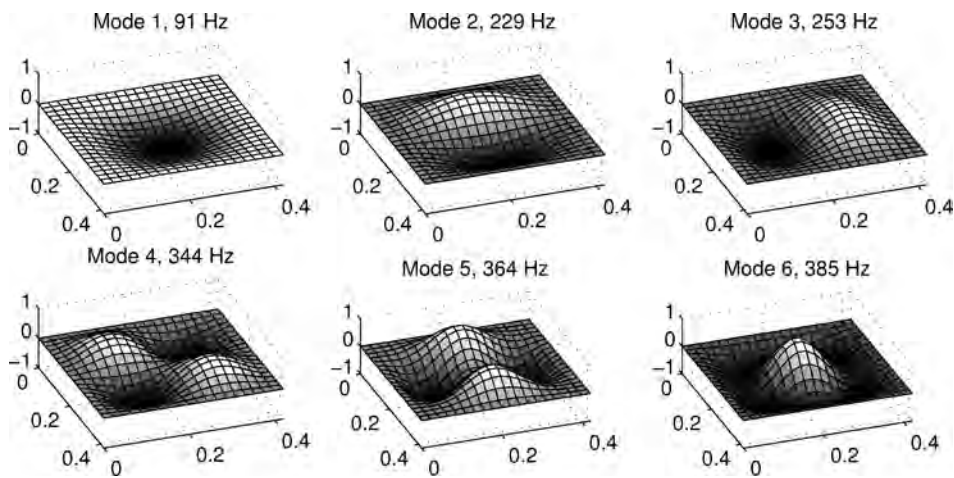


Fig. 4. The initial 6 eigenmodes shapes and frequencies (size of the plate is in [m], and the z-axis depict normalized amplitudes).

Particular eigenmode is considered controllable if the corresponding peak is distinguishable in the frequency response graph. As shown in Fig. 3, individual actuators complement each other. Every actuator excites the first mode, but e.g. the fourth mode is well excited only by the actuator 1. Hence, each desired eigenmode is controllable with an acceptable margin.

The results presented above demonstrate in detail the case of 3 actuators and initial 6 eigenmodes to be controlled. However, studies have also been performed for other quantities of actuators and frequency ranges considered. It follows from the analysis that the presented approach is suitable also for a wider frequency band. However, it has been noted that increasing frequency bandwidth for the same number of actuators results in decreased level of controllability, which is possible to achieve. On the other hand, for increasing the number of actuators while maintaining a constant frequency bandwidth, results in increasing the level of controllability. In practical applications usually there are limitations in the number of actuators that can be used. Thus, the frequency band, for which the algorithm is able to find efficient locations is also limited. An excessive extension of the band considered causes that the acquired locations will be a compromise between too many modes to be controlled and, as a result, none of them will be sufficiently controllable.

6. Comparison of evolutionary and memetic algorithms

In this section, performance of evolutionary and memetic algorithms in application to the problem of actuator placement is presented. Due to in-built local search procedures, MA involves more operations than EA for each generation. Extend of the additional computational load depends on adopted parameters and chosen procedures. For the study to be adequate, both algorithms should possess the same computational budget. Therefore, during the test, population in EA consisted of 90 individuals, while MA population had only 20 individuals. Such arrangement resulted in a similar average computation time. Maximum number of generations was set to 30. The probabilities for crossover, mutation and individual learning were 0.7, 0.05 and 0.0 for EA, and 0.5, 0.05 and 0.6 for MA, respectively. It was the best configuration found empirically for the specified problem. Details of the problem specific parameters are described in the previous section.

Both algorithms were started with randomly generated initial population, which affected strongly convergence rate. To obtain statistical measures of their performance, each algorithm was run 100 times. Each particular run is presented in gray in Fig. 5, for distribution of possible results to be visible. The average

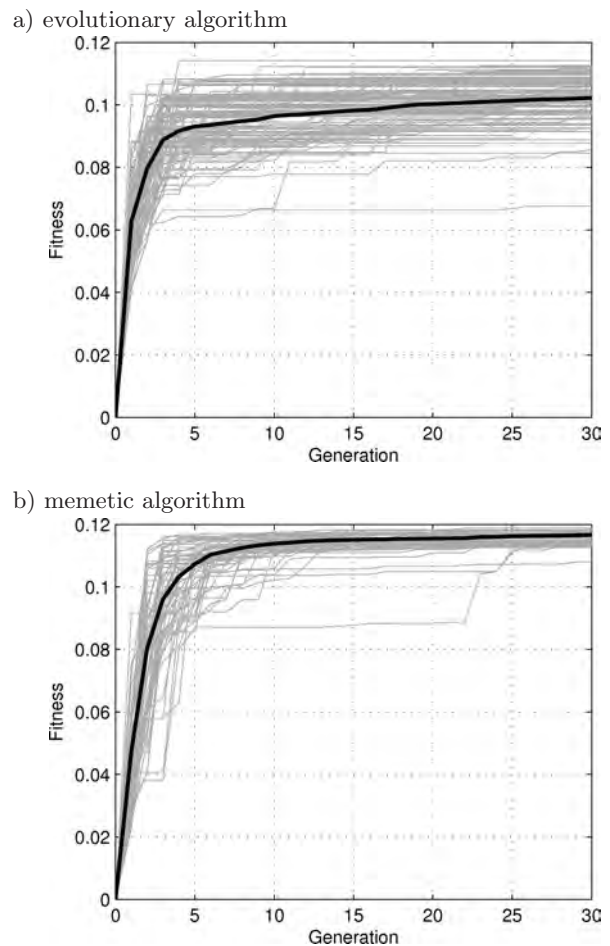


Fig. 5. Multiple runs of optimization algorithms.

result is shown as the bold black line. The summary of the characteristic values is given in Table 2.

Table 2. Comparison of characteristic values.

Properties	Evolutionary algorithm	Memetic algorithm
Runs	100	100
Generations	30	30
Population size	90	20
Crossover probability	0.7	0.5
Mutation probability	0.05	0.05
Individual learning probability	0.0	0.6
Best final fitness	0.114	0.119
Average final fitness	0.102	0.116
Worst final fitness	0.068	0.108

It follows from the analysis that both algorithms are capable of reaching similar level of best value of the fitness function. However, the EA best solution is worse than the MA average solution. This indicates that both of them could be used successfully for solving the opti-

mization problem, but MA provides a better solution. To ensure that obtained solution is near the global optimum, consistency of MA might also be considered as an advantage over EA. Less runs would be necessary in the case of MA, what indicates a better computational efficiency. Additionally, if more complicated structures of multiple plates and with more actuators are considered, benefits of using the MA algorithm shall be more significant (GARG, 2010).

7. Conclusion

A model of a rectangular plate with electrodynamic actuators bonded to its surface has been presented. The Reyleigh-Ritz method has been used to find a solution to a differential equation. Suitability of the model for other geometries and boundary conditions of plates has been pointed out. A controllability-oriented optimization criterion for placing the actuators has been developed, ensuring each mode of the structure to be controllable.

The proposed method has been used to find optimal locations of three electrodynamic actuators on a fully clamped aluminum square plate. Initial six eigenmodes of the plate have been taken into account. Results of an experimental verification confirmed high level of controllability of each mode considered. General features and limitations of the method presented has been outlined.

Performance of evolutionary and memetic algorithms in application to the optimization problem has been compared. The analysis confirmed suitability and efficiency of using memetic algorithms to find the optimal placement of actuators for an active noise-vibration control application. It has been pointed out that benefits of using memetic algorithms shall be more significant if more actuators and more complicated structures is considered.

The plate with correctly distributed actuators is ready to be applied for noise control problems. It is then a multi-output plant, which generally requires a multi-channel control system. However, with a bank of fixed-parameter filters it can be converted to a single output plant, what significantly reduces computational complexity of control systems, as shown in (MAZUR, PAWELCZYK, 2013b), particularly if the sound-radiating plate exhibits in practice a non-linear character due to improper fixing or properties of the actuators (MAZUR, PAWELCZYK, 2013a). For active control an LMS-based algorithm can be applied. However, contrary to the problem of electrical noise cancellation or speech enhancement (see, e.g. (LATOS, PAWELCZYK, 2010)), models of the plant paths including the specific actuators and their physical parameters are then required. These problems are of current interest of the authors.

Acknowledgments

The authors are indebted to two anonymous reviewers for their precious comments and suggestions, which helped improving the paper.

The research reported in this paper has been supported by the National Science Centre, decision no. DEC-2012/07/B/ST7/01408.

The authors would also like to thank EC Test System, Krakow, Poland, for providing Polytec laser vibrometer PDV-100 to experimentally validate obtained results.

References

1. ARABYAN A., CHEMISHKIAN S. (1998), *H_∞-optimal mapping of actuators and sensors in flexible structures*, Proceedings of the 37th IEEE Conference, 821–826.
2. ANDERSON B., MOORE J.B. (1990), *Optimal control: linear quadratic methods*, Prentice Hall, Englewood Cliffs, NJ, 357.
3. CHEMISHKIAN S., ARABYAN A. (1999), *Intelligent algorithms for H_∞-optimal placement of actuators and sensors in structural control*, Proceedings of the American Control Conference 1999, 1812–1816.
4. FRECKER M.I. (2003), *Recent advances in optimization of smart structures and actuators*, Journal of Intelligent Material Systems and Structures, **14**, 4-5, 207–216.
5. GARG P. (2010), *A Comparison between Memetic algorithm and Genetic algorithm for the cryptanalysis of Simplified Data Encryption Standard algorithm*, International Journal of Network Security & Its Applications, **1**, 1, 34–42.
6. GOLDBERG D.E. (1989), *Genetic algorithms in search, optimization, and machine learning*, Addison-Wesley Professional.
7. GÓRSKI P., KOZUPA M. (2012), *Variable Sound Insulation Structure with MFC Elements*, Archives of Acoustics, **37**, 1, 115–120.
8. GREENHALGH D., MARSHALL S. (2000), *Convergence criteria for genetic algorithms*, SIAM Journal on Computing, **30**, 1, 269–282.
9. HALE J.M., DARAJI A.H. (2012), *Optimal placement of sensors and actuators for active vibration reduction of a flexible structure using a genetic algorithm based on modified H_∞*, Journal of Physics: Conference Series, **382**, 1, 12036–12041.
10. HAN J.H., LEE I. (1999), *Optimal placement of piezoelectric sensors and actuators for vibration control of a composite plate using genetic algorithms*, Smart Materials and Structures, **8**, 2, 257–267.
11. KOZUPA M., WICIAK J. (2010), *Active vibration control of rectangular plate with distributed piezoelements excited acoustically and mechanically*, Acta Physica Polonica, **118**, 1, 95–98.
12. KUMAR K.R., NARAYANAN S. (2007), *The optimal location of piezoelectric actuators and sensors for vibration control of plates*, Smart Materials and Structures, **16**, 6, 2680–2691.

13. LATOS M., PAWELCZYK M. (2010), *Adaptive algorithms for enhancement of speech subject to a high-level noise*, Archives of Acoustics, **35**, 2, 203–212.
14. LEISSA A.W. (1969), *Vibration of plates*, NASA, Washington, DC, 41.
15. LENIOWSKA L. (2009), *Modelling and vibration control of planar systems by the use of piezoelectric actuators*, Archives of Acoustics, **34**, 4, 507–519.
16. LIU W., HOU Z., DEMETRIOU M.A. (2006), *A computational scheme for the optimal sensor/actuator placement of flexible structures using spatial H2 measures*, Mechanical Systems and Signal Processing, **20**, 4, 881–895.
17. NERI F., COTTA C., MOSCATO P. (2011), *Handbook of memetic algorithms*, Springer, 29.
18. MAZUR K., PAWELCZYK M. (2011), *Active noise-vibration control using the filtered-reference LMS algorithm with compensation of vibrating plate temperature variation*, Archives of Acoustics, **36**, 1, 65–76.
19. MAZUR K., PAWELCZYK M. (2013a), *Hammerstein nonlinear active noise control with the filtered-error LMS algorithm*, Archives of Acoustics, **38**, 2, 197–203.
20. MAZUR K., PAWELCZYK M. (2013b), *Active Noise Control with a single nonlinear control filter for a vibrating plate with multiple actuators*, Archives of Acoustics, **38**, 4, 537–545.
21. PADULA S.L., KINCAID R.K. (1999), *Optimization strategies for sensor and actuator placement*, NASA 19990036166.
22. PAWELCZYK M. (2008), *Active noise control – a review of control-related problems*, Archives of Acoustics, **33**, 4, 509–520.
23. PAWELCZYK M., WRONA S. (2013), *Optimal placement of actuators for active noise-vibration control with spillover effect suppression using a memetic algorithm*, Proceedings of 20th International Congress on Sound and Vibration.
24. RAO S. (2007), *Vibration of continuous systems*, Wiley.
25. SADRI A.M., WRIGHT J.R., WYNNE R.J. (1999), *Modelling and optimal placement of piezoelectric actuators in isotropic plates using genetic algorithms*, Smart Materials and Structures, **8**, 4, 490–498.
26. SZEMELA K., RDZANEK W.P., RDZANEK W.J. (2012), *The Acoustic Pressure Radiated by a Vibrating Circular Plate within the Fraunhofer Zone of the Three-Wall Corner Region*, Acta Physica Polonica – Series A General Physics, **121**, 1, 100.

Active Noise Control with a Single Nonlinear Control Filter for a Vibrating Plate with Multiple Actuators

Krzysztof MAZUR, Marek PAWEŁCZYK

Institute of Automatic Control, Silesian University of Technology
Akademicka 16, 44-100 Gliwice, Poland; e-mail: {Krzysztof.Jan.Mazur, Marek.Pawelczyk}@polsl.pl

(received March 14, 2013; accepted November 5, 2013)

Vibrating plates can be used in Active Noise Control (ANC) applications as active barriers or as secondary sources replacing classical loudspeakers. The system with vibrating plates, especially when nonlinear MFC actuators are used, is nonlinear. The nonlinearity in the system reduces performance of classical feedforward ANC with linear control filters systems, because they cannot cope with harmonics generated by the nonlinearity. The performance of the ANC system can be improved by using nonlinear control filters, such as Artificial Neural Networks or Volterra filters.

However, when multiple actuators are mounted on a single plate, which is a common practice to provide effective control of more vibration modes, each actuator should be driven by a dedicated nonlinear control filter. This significantly increases computational complexity of the control algorithm, because adaptation of nonlinear control filters is much more computationally demanding than adaptation of linear FIR filters.

This paper presents an ANC system with multiple actuators, which are driven with a single nonlinear filter. To avoid destructive interference of vibrations generated by different actuators the control signal is filtered by appropriate separate linear filters. The control system is experimentally verified and obtained results are reported.

Keywords: active noise-vibration control, active structural acoustic control, adaptive control, nonlinear-control.

1. Introduction

Vibrating plates are potentially very useful for Active Noise Control applications in industrial environments. The plates can be used as secondary sound sources, as replacement for classical loudspeakers, but also can be used as active barriers (FAHY, GARDONIO, 2007; HANSEN, SNYDER, 1997; RDZANEK, ZAWIESKA, 2003), where usually single or double plates (PIETRZKO, 2009) are placed between the noise source and the area where the noise sound pressure level (SPL) should be reduced. Rectangular plates are frequently used (ZAWIESKA, RDZANEK, 2007; GORSKI, KOZUPA, 2012), but also other plate shapes, including circular plates (ZAWIESKA *et al.*, 2007; RDZANEK *et al.*, 2011; LENIOWSKA, 2011) and triangular plates (BARAŃSKI, SZELA, 2008), are useful for some applications and are investigated in the literature. Also more complex structures like L-jointed plates, T-shaped plates (KEIRA *et al.*, 2005) or four connected plates (LIU *et al.*, 2010), are of scientific interest.

Plates are more resistant to harsh environment conditions than classical loudspeakers. However, plates are more difficult to control. The common problems include irregular multimodal response, the need to use multiple actuators on a single plate to effectively excite multiple plate modes, and a nonlinear response. The nonlinear response is caused by vibrations of not ideally clamped plate (EL KADRI *et al.*, 1999; SAHA *et al.*, 2005), but also might be caused by frequently used d33 effect of MFC patches if they are employed as actuators (STUEBNER *et al.*, 2009; MAZUR, PAWEŁCZYK, 2011a). In this paper, the latter problem is mitigated by using EX1 electrodynamic actuators. However, the former problem still needs to be approached, because it may significantly degrade performance of a linear feedforward ANC system. The degradation is especially visible for simple deterministic signals, when active control is expected to be very successful. For active control of such plants a feedback system could be used, which has inherited capability to compensate to some extent for plant nonlinearity. However, if a reference signal is

available in advance, a generally better performance can be obtained with a feedforward system, although it should have a nonlinear architecture. The nonlinear feedforward active noise control is more computationally demanding, than a linear control. Application of multiple actuators for a single plate additionally increases the number of required operations, and a dedicated control filter is used for each actuator.

This paper presents a solution with multiple actuators, which are driven by a single nonlinear ANC filter. The control signal being the output of such filter is then appropriately filtered by separate linear filters used to drive subsequent actuators. These filters are tuned to avoid destructive interference of vibrations, which might occur if control of the actuators were not coordinated.

2. Nonlinear feedforward control

There are many possible approaches to nonlinear feedforward control. For a simple and well modeled nonlinearity it can be possible to filter the control signal by an inverse model. This approach is commonly used for semi-active vibration control using MR dampers. However, for many plants it is very hard to find an appropriate inverse model for a required frequency band if the plant itself is nonminimum phase and with a delay. These are common problems for ANC applications. A popular alternative approach is to use black-box input-output models obtained with Artificial Neural Networks (HANSEN, SNYDER, 1997). Another approach, which can be employed for Active Noise/Vibration Control problems is to use nonlinear filters, linear with respect to parameters. A large number of algorithms fall into this category, including Volterra FXLMS (TAN, JIANG, 2001), FSLMS (DAS, PANDA, 2004; GEORGE, PANDA, 2012) and Generalized FLANN (GEORGE, PANDA, 2013).

For easier implementation, nonlinear filters, linear with respect to parameters, can be expressed as a sum of Hammerstein models with arbitrary nonlinear functions F_k (MAZUR, PAWEŁCZYK, 2011a; 2013):

$$u_c(i+1) = \sum_{k=1}^K W_{c,k}(z^{-1}) F_k(x(i), x(i-1), \dots, x(i-(N-1))), \quad (1)$$

where $u_c(i+1)$ is the value of the c -th control signal at the $i+1$ sample, $x(i)$ is the reference signal, $W_{c,k}(z^{-1})$ is the linear finite response filter for the c -th control signal and the k -th nonlinear function F_k , z^{-1} is the one-sample delay operator. The number of nonlinear functions is equal to K and the number of secondary paths is equal to C .

Figure 1 shows the block diagram of a multichannel control system with such nonlinear control filter. The bank of F_k nonlinear functions converts the reference

signal, $x(i)$, into a vector $\mathbf{x}(i) = [x_1(i), x_2(i), x_3(i)]^T$. This vector is next filtered by a bank of linear $W_{c,k}(z^{-1})$ FIR adaptive filters. These filters can be grouped into a matrix of FIR filters $\mathbf{W}(z^{-1})$:

$$\mathbf{W}(z^{-1}) = \begin{bmatrix} W_{1,1}(z^{-1}) & W_{1,2}(z^{-1}) & \cdots & W_{1,K}(z^{-1}) \\ W_{2,1}(z^{-1}) & W_{2,2}(z^{-1}) & \cdots & W_{2,K}(z^{-1}) \\ \vdots & \vdots & \ddots & \vdots \\ W_{C,1}(z^{-1}) & W_{C,2}(z^{-1}) & \cdots & W_{C,K}(z^{-1}) \end{bmatrix}. \quad (2)$$

Outputs of $W_{c,k}(z^{-1})$ adaptive control filters form a vector of control signals $\mathbf{u}(i) = [u_1(i), u_2(i), \dots, u_C(i)]^T$. The signals are then used to drive a vector of secondary paths $\mathbf{S} = [S_1, S_2, \dots, S_C]^T$. The adaptation algorithm uses the vector of reference signals $\mathbf{x}(i)$ and the scalar error signal $e(i)$ to adapt weights of $\mathbf{W}(z^{-1})$ control filters, as described in the following Section. The P stands for the primary path in the ANC system.

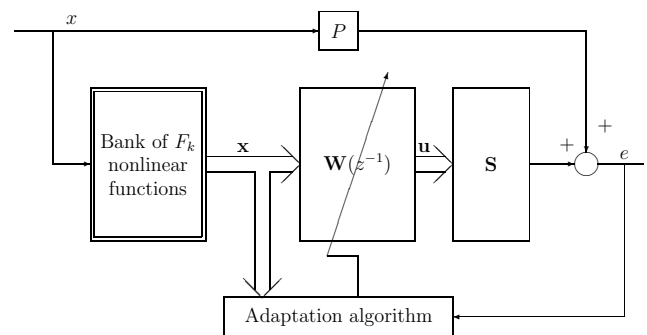


Fig. 1. Multichannel ANC system with Hammerstein nonlinear control filters.

3. Adaptation of control filter parameters

When the filters are linear with respect to parameters the classical adaptive control adaptation algorithms, like LMS, Affine Projection or RLS, with appropriate modifications to improve convergence properties can be employed. Otherwise, more complex algorithms such as genetic algorithms (GÓRSKI, MORZYŃSKI, 2013) or memetic algorithms should be employed.

The Normalized Leaky LMS algorithm takes the form (ELLIOTT, 2001):

$$\mathbf{w}_{c,k}(i+1) = \alpha \mathbf{w}_{c,k}(i) - \mu \frac{\mathbf{x}_{c,k}^*(i)}{\sum_{c=1}^C \sum_{k=1}^K \mathbf{x}_{c,k}^{*T}(i) \mathbf{x}_{c,k}(i) + \zeta} e_c^*(i), \quad (3)$$

where $0 \ll \alpha < 1$ is the leakage coefficient, μ is the convergence coefficient, and ζ is a parameter protecting against division by zero in case of lack of

excitation. In (3) $\mathbf{x}_{c,k}^*(i) = [x_{c,k}^*(i), x_{c,k}^*(i-1), \dots, x_{c,k}^*(i-(M-1))]^T$ is a vector of regressors of the reference signal for the LMS algorithm, M is the order of an FIR model of the secondary path. For notation simplicity it is assumed that orders of all secondary paths are the same. The symbol $e_c^*(i)$ stands for the error signal for the c -th secondary path. The error signal, $e(i)$, is to be minimized in the square sense by the LMS algorithm. Some additional modifications to the LMS algorithm, like variable step size, can also be used to enhance convergence properties (BISMOR, 2012).

In contrary to electrical noise cancellation or speech enhancement (see, e.g. (LATOS, PAWEŁCZYK, 2010)) for active noise/vibration control applications the filter outputs drive the secondary path (acousto-electric or vibro-acousto-electric), the algorithm must be mod-

ified to guarantee convergence (PAWEŁCZYK, 2008). The most popular modification is filtration of the reference signal by a model of the secondary path, what results in obtaining the well-known Filtered-x LMS algorithm (ELLIOTT, 2001; KUO, MORGAN, 1996). Figure 2 shows a block diagram of the multichannel FXLMS algorithm, when used for adaptation of nonlinear filters as in (1). The ANC error signal is used as the error signal for the LMS algorithm $e_c^*(i) = e(i)$.

Because each reference signal must be filtered by models of corresponding secondary paths, the Filtered-x structure involves a number of numerical operations for such application, where multiple reference signals are generated from a single reference with a bank of F_k filters. The Filtered-error LMS (FELMS) algorithm is more appropriate in that case (Fig. 3). In the FELMS

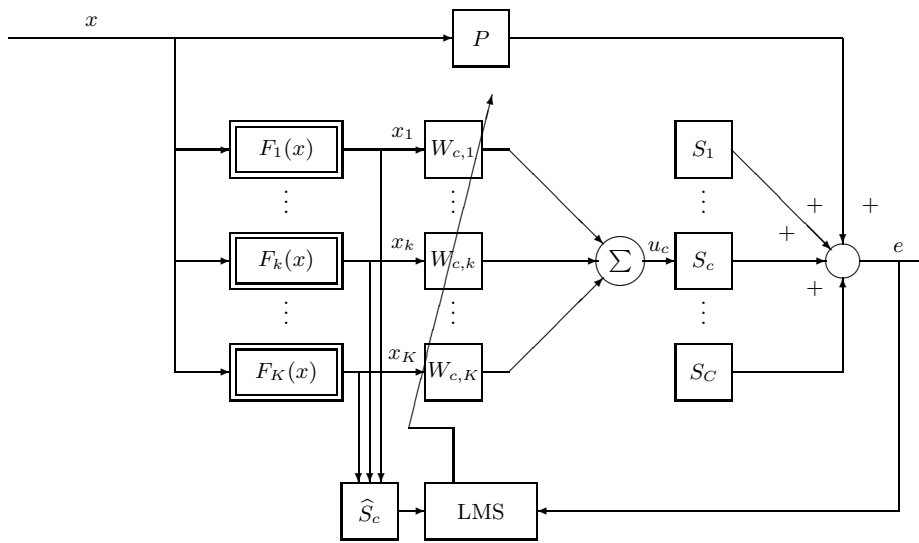


Fig. 2. An excerpt of the ANC system with Hammerstein nonlinear control filters and multichannel FXLMS algorithm for the c -th control channel.

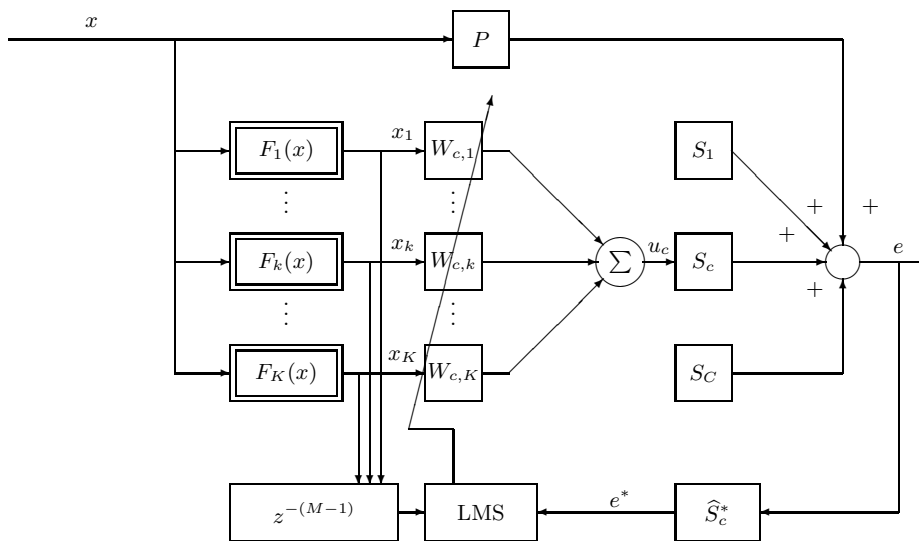


Fig. 3. An excerpt of the ANC system with Hammerstein nonlinear control filters using FELMS algorithm for the c -th control channel.

algorithm the multiple reference signals are simply delayed $x_{c,k}^*(i) = x_k(i - (M - 1))$, but the error signal is obtained as:

$$e_c^*(i) = \hat{s}_c(i)^T \mathbf{e}(i), \quad (4)$$

where

$$\hat{s}_c(i) = [\hat{s}_{c,M-1}(i), \hat{s}_{c,M-2}(i), \dots, \hat{s}_{c,0}(i)]$$

is a time-reversed model of the c -th secondary path,

$$\mathbf{e}(i) = [e(i), e(i - 1), \dots, e(i - (M - 1))]^T$$

is a vector of regressors of the error signal.

4. Control of multiple actuators with a single nonlinear filter

The Filtered-error structure reduces the number of numerical operations needed for filtering every reference signal by a secondary path model. However, when multiple actuators are used for the same plate, multiple nonlinear control filters are involved. This significantly increases computational cost. Such problem can be reduced by using a single nonlinear control filter. However, the same output cannot be used to drive all

actuators because of potential destructive interference of vibrations generated by different actuators. The control signals for different actuators should be properly filtered for a positive interference to occur.

Figure 4 shows the resulting structure. The output of nonlinear ANC control filter is filtered by the E_c filter dedicated for each actuator. Dependent of E_c filter choice, the filtration of the error signal by \hat{H}^* filter might be required. However, in the proposed system such filter is avoided, because the E_c filters are tuned to linearize the total secondary path phase response.

Because the secondary path models may change in time, for instance they strongly depend on plate temperature (MAZUR, PAWELCZYK, 2011b), E_c filters are made adaptive. Figure 5 shows the control system used for adaptation of E filter weights (MAZUR, PAWELCZYK, 2013). This system compares the obtained actual response to the response of desired secondary path model H , and updates the weights appropriately. When the desired path have a linear phase response, filtration by \hat{H}^* is not needed and delaying the reference signals by D steps, where D is the delay of the desired path H , is sufficient for convergence.

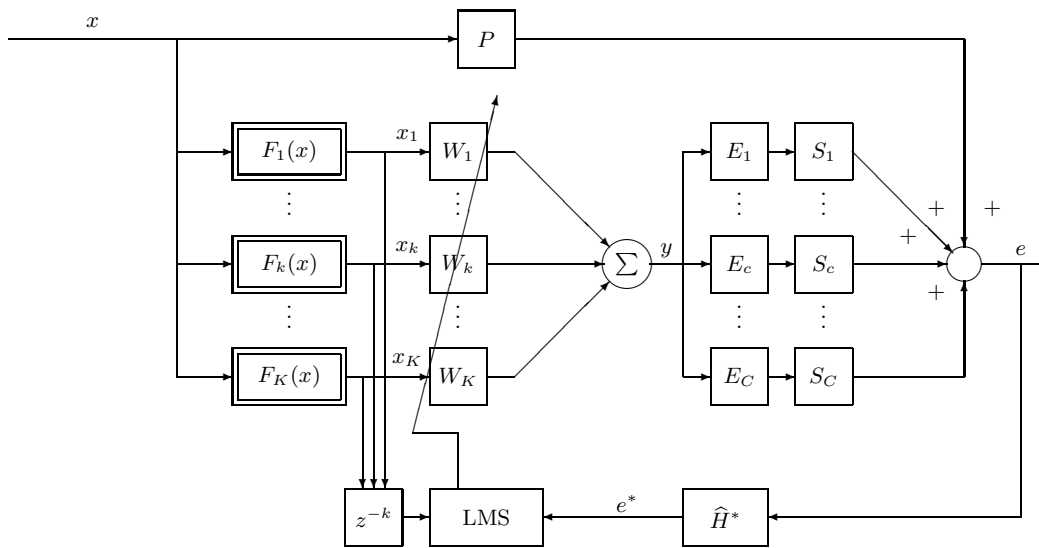


Fig. 4. ANC system with Hammerstein nonlinear control filters using single nonlinear control filter.

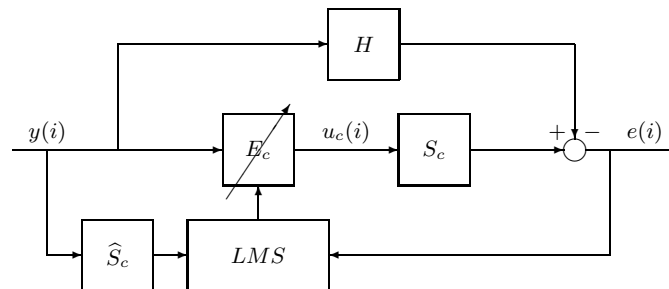


Fig. 5. Single-channel adaptive sound radiation control system.

Table 1 shows the asymptotic computational complexity of basic steps for the proposed algorithm and for the control system with separate per-actuator nonlinear filters, with FXLMS and FELMS adaptation algorithm. The order notion, O , is used. In case of per-actuator nonlinear filters with FXLMS adaptation algorithm each step have asymptotic computational complexity proportional to the number of channels multiplied by the number of nonlinear functions and the order of FIR filters. The FELMS adaptation algorithm reduces the computational complexity of the filtration by the secondary path model. In the proposed algorithm there is only one nonlinear filter, and the computational complexity does not depend on the number of actuators. The computational complexity of added additional steps does not depend on the number of nonlinear functions, and the overall asymptotic computational complexity is reduced from $O(KCA)$ to $O(KA + CA)$, where $A = \max(N, M, N_E, N_K)$.

Table 1. Asymptotic computational complexity of presented algorithms.

	NFXLMS	NFELMS	proposed algorithm
Nonlinear filter			
Output calculation	$O(KCN)$	$O(KCN)$	$O(KN)$
Reference/error filtration	$O(KCM)$	$O(CM)$	$O(M)$
Filter adaptation	$O(KCN)$	$O(KCN)$	$O(KN)$
Linear per-actuator filters			
Output calculation	–	–	$O(CN_E)$
Reference/error filtration	–	–	$O(CM_E)$
Filter adaptation	–	–	$O(CN_E)$

5. Experimental results

The control system has been applied to reduce noise transmitted through a fully-clamped aluminum plate of dimensions $400 \text{ mm} \times 500 \text{ mm} \times 1 \text{ mm}$ from a small enclosure to a laboratory room (Fig. 6). The noise was generated by a loudspeaker located in the enclosure, and the goal of the control system was to reduce sound pressure level at specified area around an error microphone in the laboratory room.

Three NXT EX-1 actuators (of 5 W power) were mounted on the plate (see Fig. 6). Positions of the actuators were chosen to maximize the minimal eigenvalue of the controllability Gramian matrix for first 25 plate modes (see Fig. 7) (WRONA, PAWELCZYK, 2013).

Both the nonlinear ANC filter and per-actuator linear control filters were implemented on a single microprocessor system (Fig. 8). However, for larger systems, where many vibrating plates are used, those separate

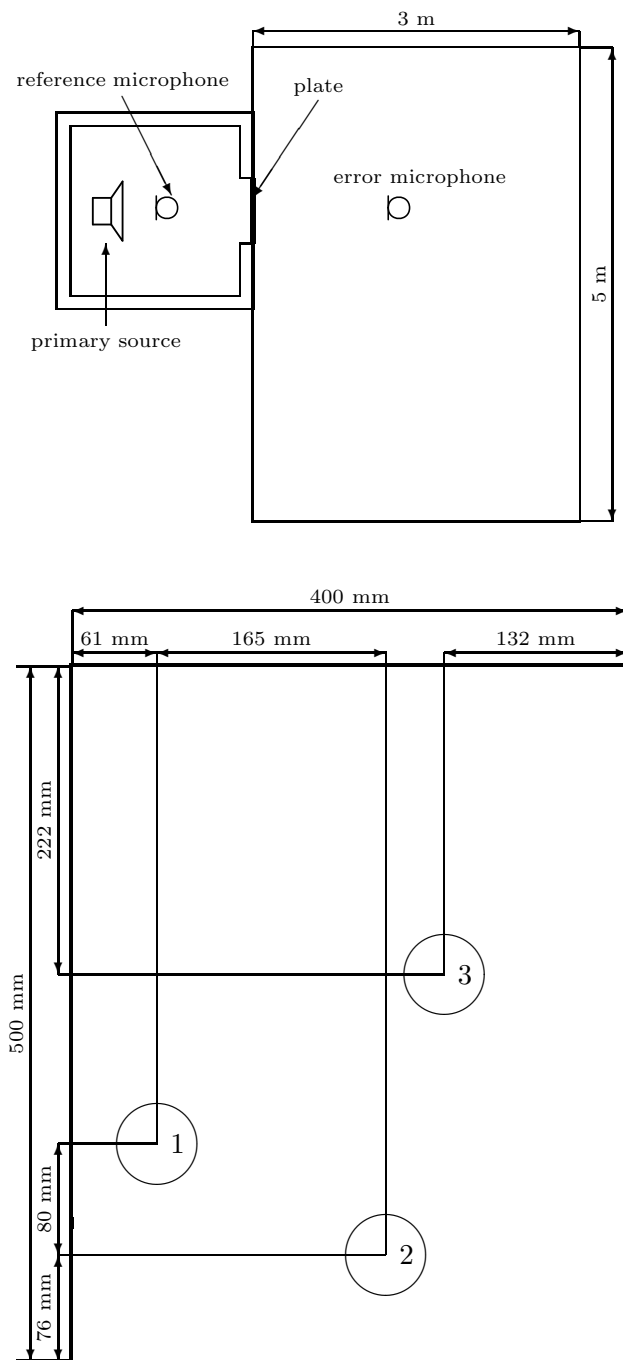


Fig. 6. Laboratory setup (top) and EX-1 actuators installed on the plate (bottom).

functions can be implemented on separate microprocessor systems and the $y(i)$ control signal(s) is then passed between those systems.

The error and reference microphones were connected to 16-bit ADCs with synchronous sampling by using microphone amplifiers and 8th order Butterworth low-pass anti-aliasing filters with 600 Hz cut-off frequency. The sampling frequency was set to 2 kHz (0.5 ms sampling period). Four 16-bit ZOH DACs with synchronous sampling were used to control loudspeaker

in the enclosure and three EX-1 actuators. As reconstruction filters, 8th order Butterworth low-pass filters with 600 Hz cut-off frequency were used. The DACs

and ADCs sampling processes were not synchronous – the DAC outputs were updated just after ADC conversion, after approximately $1.44 \mu\text{s}$.

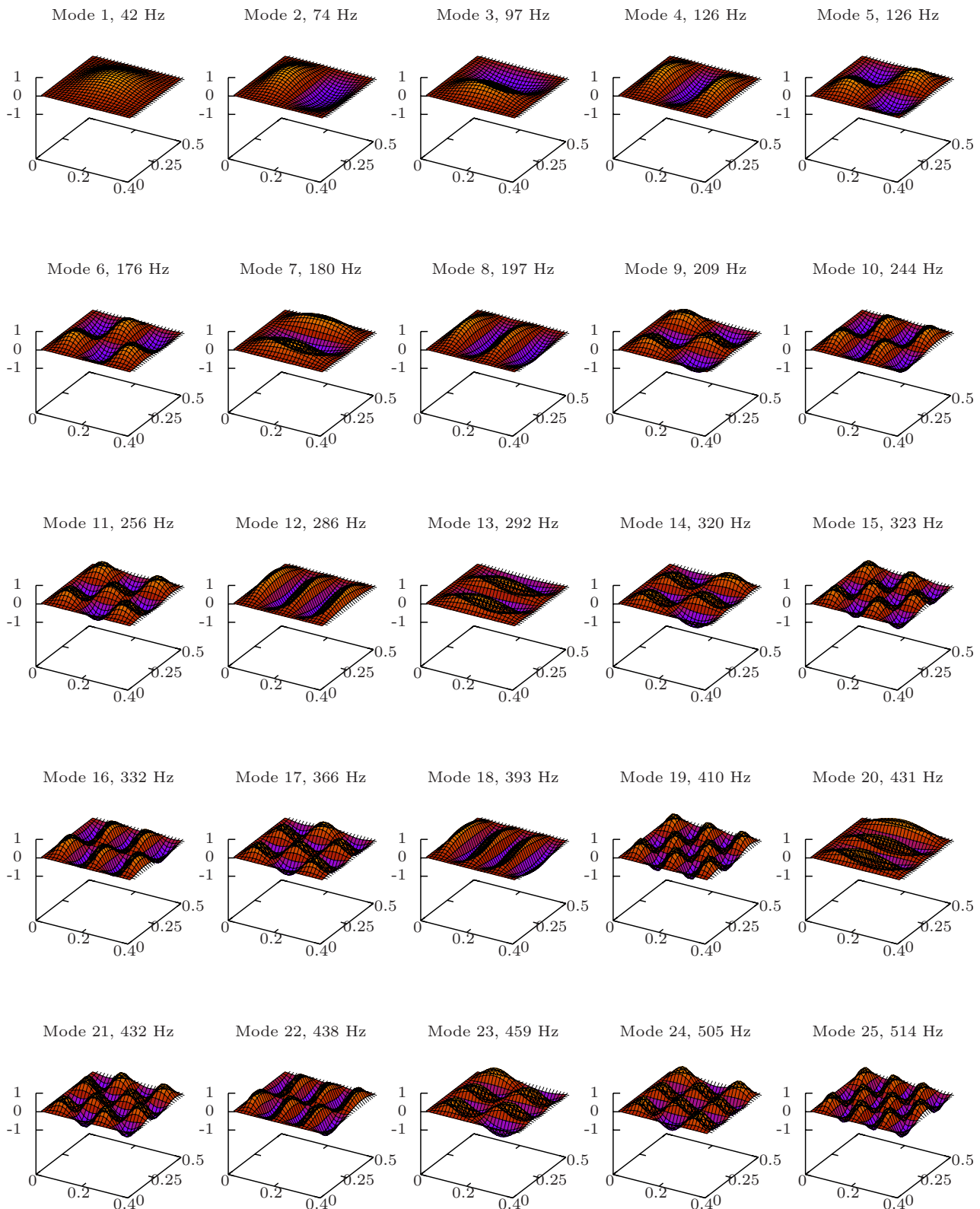


Fig. 7. First 25 mode shapes for used $0.5 \text{ m} \times 0.4 \text{ m}$ plate. The vertical axis shows the vibration amplitude normalized to $[-1, 1]$ range.

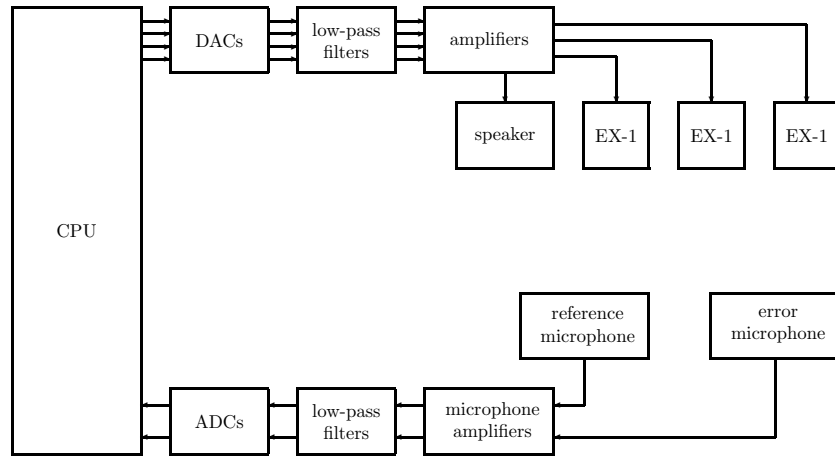


Fig. 8. Implementation of the ANC system.

The system presented in Fig. 4 was used as the nonlinear control system. The desired secondary path response H was equal to z^{-16} . The order of the E linear filters was set to $N_E = 256$. The order of control filter was set to $N = 256$. The parameters of NLMS adaptation algorithm were set to $\alpha = 1$, $\mu = 0.05$, $\zeta = 10^{-12}$. The first 5 functions of trigonometric expansion used in the FSLMS algorithm were used as the F_k functions:

$$\begin{aligned}
 F_1(x) &= x, & F_2(x) &= \sin(\pi x), \\
 F_3(x) &= \cos(\pi x), & F_4(x) &= \sin(2\pi x), \\
 F_5(x) &= \cos(2\pi x).
 \end{aligned} \tag{5}$$

Figure 9 shows the Power Spectral Density (PSD) of the error microphone signal for classical linear feedforward FXLMS ANC system, for different levels of 155 Hz tonal noise. For comparison, PSD of the noise

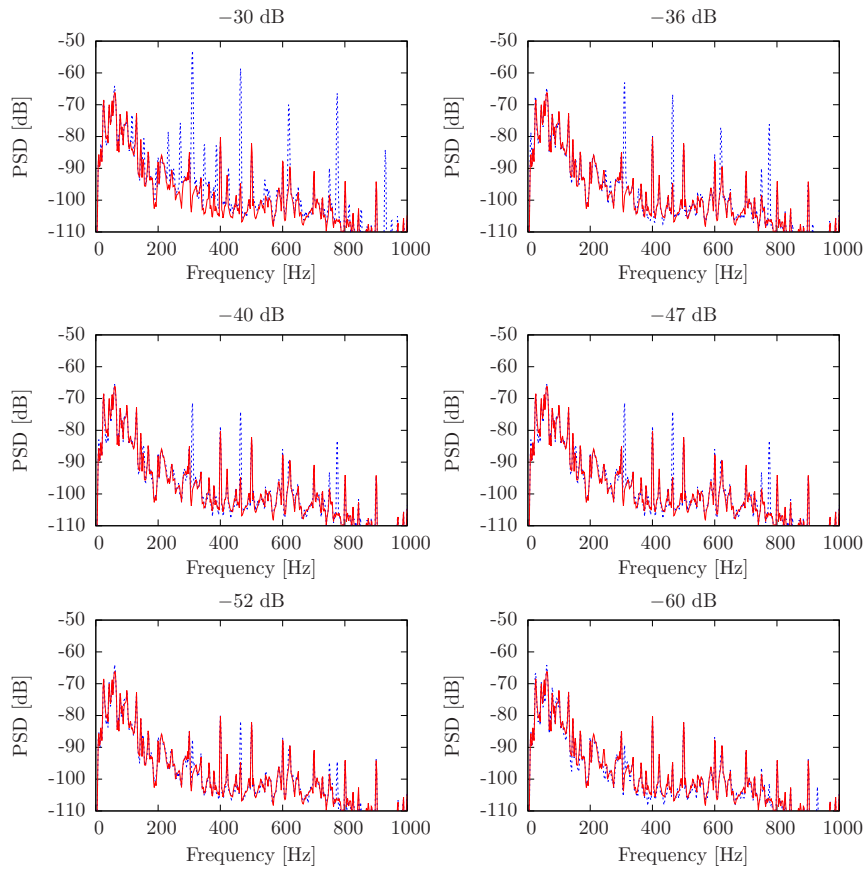


Fig. 9. PSD of error microphone signal for FXLMS ANC system for different levels of 155 Hz tonal noise and noise floor level.

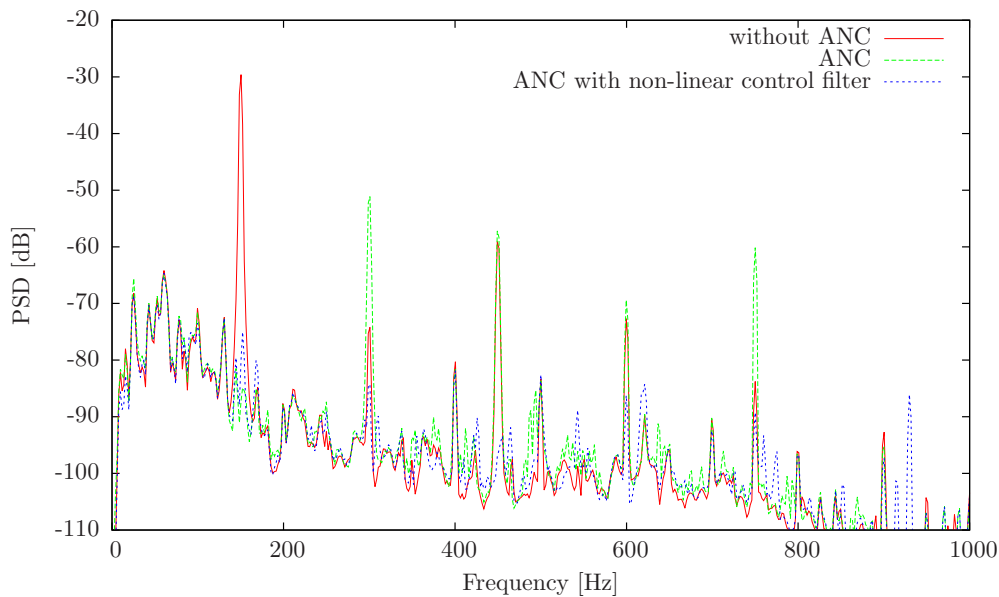


Fig. 10. PSD of error microphone signal for different control strategies for 155 Hz tonal noise.

floor signal (without the primary noise and with disabled ANC) is included in each plot. The PSD of the primary noise (without ANC but with the noise floor) is not plotted for clarity of the figures, but above each plot the power of 155 Hz tone without ANC is presented.

For small noise powers the nonlinear artifacts are not visible or they have powers comparable to the noise floor power. For higher powers, -30 dB and -36 dB, the harmonics are clearly visible and they limit the noise reduction level.

The performance of the proposed nonlinear control system for the 155 Hz tone is shown in Fig. 10. The FXLMS ANC achieves 18.9 dB reduction of the SPL. However, because the human hearing system is more sensitive to higher frequencies, the harmonics caused by the nonlinearity are even heard as louder. After A-weighting the SPL reduction of the FXLMS system is only 11.0 dB. The nonlinear feedforward control system provides 28.3 dB reduction of the SPL and even 30.6 dB when A-weighted.

6. Conclusions

By using linear filters dedicated for each actuator bonded to a single plate, it is possible to use only one nonlinear control filter to efficiently drive all the actuators. The nonlinear filters are very computationally demanding, and reduction of their number saves computational load, which can be spent for implementing more complex filters.

The per-actuator linear control filters were used also to linearize phase response of the secondary paths. This allowed for application of the FELMS, simplified even to the Delayed LMS algorithm for adaptation

of nonlinear control filter weights. This provides additional reduction of numerical operations. Efficiency of the proposed approach is particularly evident, when considering A-weighted noise reduction results.

Acknowledgments

The authors are indebted to two anonymous reviewers for their precious comments and suggestions, which helped improving the paper.

The research reported in this paper has been supported by the National Science Centre, decision no. DEC-2012/07/B/ST7/01408.

References

1. BISMOR D. (2012), *LMS algorithm step size adjustment for fast convergence*, Archives of Acoustics, **37**, 1, 31–40.
2. BRAŃSKI A., SZELA S. (2008), *Improvement of effectiveness in active triangular plate vibration reduction*, Archives of Acoustics, **33**, 4, 521–530.
3. DAS D.P., PANDA G. (2004), *Active mitigation of non-linear noise Processes using a novel filtered-s LMS algorithm*, IEEE Transactions on Speech and Audio Processing, **12**, 3, 313–322.
4. EL KADIRI M., BENAMAR R., WHITE R.G. (1999), *The non-linear free vibration of fully clamped rectangular plates: second non-linear mode for various plate aspect ratios*, Journal of Sound and Vibration, **228**, 2, 333–358.
5. ELLIOTT S. (2001), *Signal Processing for Active Control*, London 2001, Academic Press.
6. FAHY F., GARDONIO P. (2007), *Sound and Structural Vibration*, Second edition, Elsevier, Oxford.

7. GEORGE N.V., PANDA G. (2012), *A robust filtered-s LMS algorithm for nonlinear active noise control*, Applied Acoustics, **73**, 836–841.
8. GEORGE N.V., PANDA G. (2013), *Advances in active noise control: A survey, with emphasis on recent nonlinear techniques*, Signal Processing, **93**, 363–377.
9. GÓRSKI P., KOZUPA M. (2012) *Variable Sound Insulation Structure with MFC Elements*, Archives of Acoustics, **37**, 1, 115–120.
10. GÓRSKI P., MORZYŃSKI L. (2013), *Active Noise Reduction Algorithm Based on NOTCH Filter and Genetic Algorithm*, Archives of Acoustics, **38**, 2, 185–190.
11. HANSEN C.H., SNYDER S.D. (1997), *Active Control of Noise and Vibration*, E & FN Spon, London.
12. KEIRA J., KESSISOULOVA N.J., NORWOOD C.J. (2005), *Active control of connected plates using single and multiple actuators and error sensors*, Journal of Sound and Vibration, **281**, 73–97.
13. KUO S.M., MORGAN D.R. (1996), *Active Noise Control Systems*, John Wiley & Sons, Inc., New York.
14. LATOS M., PAWELCZYK M. (2010), *Adaptive Algorithms for Enhancement of Speech Subject to a High-Level Noise*, Archives of Acoustics, **35**, 2, 203–212.
15. LENIOWSKA L. (2011), *An Adaptive Vibration Control Procedure Based on Symbolic Solution of Diophantine Equation*, Archives of Acoustics, **36**, 4, 901–912.
16. LIU C., LI F., FANG B., ZHAO Y., HUANG W. (2010), *Active control of power flow transmission in finite connected plate*, Journal of Sound and Vibration, **329**, 4124–4135.
17. PAWELCZYK M. (2008), *Active noise control – a review of control-related problems*, Archives of Acoustics, **33**, 4, 509–520.
18. MAZUR K., PAWELCZYK M. (2011a), *Feed-forward compensation for nonlinearity of vibrating plate as the sound source for active noise control*, Mechanics and Control, **30**, 3, 146–150.
19. MAZUR K., PAWELCZYK M. (2011b), *Active noise-vibration control using the filtered-reference LMS algorithm with compensation of vibrating plate temperature variation*, Archives of Acoustics, **36**, 1, 65–76.
20. MAZUR K., PAWELCZYK M. (2013), *Hammerstein nonlinear active noise control with the Filtered-Error LMS algorithm*, Archives of Acoustics, **38**, 2, 197–203.
21. PIETRZKO S.J. (2009), *Contributions to Noise and Vibration Control Technology*, AGH University of Science and Technology Press, Kraków.
22. RDZANEK W.P., SZEMELA K., PIECZONKA D. (2011), *Acoustic Pressure Radiated by a Circular Membrane Into the Quarter-Space*, Archives of Acoustics, **36**, 1, 121–139.
23. RDZANEK W.P., ZAWIESKA W.M. (2003), *Vibroacoustic analysis of a simply supported rectangular plate of a power transformer casing*, Archives of Acoustics, **28**, 2, 117–125.
24. SAHA K.N., MISRA D., GHOSAL S., POHIT G. (2005), *Nonlinear free vibration analysis of square plates with various boundary conditions*, Journal of Sound and Vibration, **287**, 1031–1044.
25. STUEBNER M., SMITH R.C., HAYS M., OATES W.S. (2009), *Modeling the nonlinear behavior of Macro Fiber Composite actuators*, Behavior and Mechanics of Multifunctional Materials and Composites 2009, Proceedings of the SPIE, **7289**, 728913–728918.
26. TAN L., JIANG J. (2001), *Adaptive Volterra filters for active control of nonlinear noise processes*, IEEE Transactions on Signal Processing, **49**, 8, 1667–1676.
27. WRONA S., PAWELCZYK M. (2013), *Controllability-oriented placement of actuators for active noise-vibration control of rectangular plates using a memetic algorithm*, Archives of Acoustics, **38**, 4, 529–536.
28. ZAWIESKA W.M., RDZANEK W.P. (2007), *The influence of a vibrating rectangular piston on the acoustic power radiated by a rectangular plate*, Archives of Acoustics, **32**, 2, 405–415.
29. ZAWIESKA W.M., RDZANEK W.P., RDZANEK W.J., ENGEL Z. (2007), *Low frequency estimation for the sound radiation efficiency of some simply supported flat plates*, Acta Acustica United with Acustica, **93**, 3, 353–363.

Technical Notes

Evaluation of Two Alternative Procedures for Measuring Airflow Resistance of Sound Absorbing Materials

Romina del REY⁽¹⁾, Jesus ALBA⁽¹⁾, Jorge P. ARENAS⁽²⁾, Jaime RAMIS⁽³⁾

⁽¹⁾ *Research Institute for Integrated Coastal Zone Management-IGIC,
Universitat Politècnica de Valencia
Grao de Gandia 46730 (Valencia), Spain*

⁽²⁾ *Institute of Acoustics, Univ. Austral de Chile
Campus Miraflores, PO Box 567, Valdivia, Chile; e-mail: jp Arenas@uach.cl*

⁽³⁾ *Department of Physics, System Engineering and Signal Theory, Univ. of Alicante
Mail Box 99; 03080 Alicante, Spain*

(received February 26, 2013; accepted May 27, 2013)

It is well known that sound absorption and sound transmission properties of open porous materials are highly dependent on their airflow resistance values. Low values of airflow resistance indicate little resistance for air streaming through the porous material and high values are a sign that most of the pores inside the material are closed. The laboratory procedures for measuring airflow resistance have been standardized by several organizations, including ISO and ASTM for both alternate flow and continuous flow. However, practical implementation of these standardized methods could be both complex and expensive. In this work, two indirect alternative measurement procedures were compared against the alternate flow standardized technique. The techniques were tested using three families of eco-friendly sound absorbent materials: recycled polyurethane foams, coconut natural fibres, and recycled polyester fibres. It is found that the values of airflow resistance measured using both alternative methods are very similar. There is also a good correlation between the values obtained through alternative and standardized methods.

Keywords: material characterization, airflow resistance, sound absorbing materials, eco-friendly materials.

1. Introduction

Presently, there exists a wide range of sound absorbing materials. This is due not only to technological advances in the field, but also to the importance of reducing noise pollution for health and environmental concerns. For this reason, current research focuses on the application of sound absorbing materials in different environments, with the goal of improving acoustic comfort, as well as searching for alternative fabrication methods of sound absorbing materials. Furthermore, an enormous importance is given to the development of *eco-materials*. These eco-materials are an alternative to the conventional materials for actual and future applications (NICK *et al.*, 2002; ASDRUBALI, 2006).

The great majority of sound absorbing materials, independent of the composition, are of the porous and/or fibrous type. There are many studies about

the absorption mechanisms of the acoustic energy in the interior of porous materials, differentiating the distinctive mechanisms in function of the type of pore of which the material is composed (ARENAS, CROCKER, 2010).

Various studies have proposed physical-mathematical models to interpret the acoustic behavior in porous sound absorbing materials. The majority of these models are based on describing the characteristic wave impedance and the propagation constant in function of the frequency, given the physical properties of the materials, such as the porosity, tortuosity, or airflow resistance (ALBA *et al.*, 2011).

The airflow resistance is the resistance experienced by air as it passes through a material. This property is directly related to the capacity of the material to absorb sound energy. Thus, the value of this magnitude is used as an input variable in prediction models in the

frequency domain, of which the majority is based on empirical expressions.

In the works published on the topic, airflow resistance values measured by the same producers of absorbent materials can be found. On the other hand, other authors present empirical formulas for the determination of the airflow resistance of fibrous materials using values such as the bulk density of the material and diameter of the fibres. BIES and HANSEN (1980), presented a formula of this type for the case of fibres with a relatively uniform diameter and with small quantities of binder, such as rockwool and fibreglass. Subsequently, GARAI and POMPOLI (2005), modified this formula for the specific case of polyester fibres.

The airflow resistance in Rayls or in kNs/m can be obtained in the laboratory in a standardized form (ISO, 1991). The standardized testing procedure is based on the passing of airflow through the sample. This airflow should be unidirectional, controlled, and constant. Also, it is necessary to determine the differential pressure created across the sample under study. Another procedure is one where the airflow is alternated. In this case, it is necessary to determine the alternate component of the pressure in the volume that is occupied by the sample. Both methods are described in the ISO standard. The second procedure (method B) consists in a piston connected to a motor and coupled with a circular tube and a sample holder. This procedure not only requires complex equipment, but also it is necessary to work at a very low frequency, in some cases around 2 Hz, leading to performance problems in microphones that register the signal at such low frequencies. It is also difficult to achieve a controlled unidirectional laminar airflow. The recommended velocity of the airflow that passes through the material sample is between 0.5 mm/s and 4 mm/s.

Given the complexity of the standardized method, some alternative experimental procedures have been described by different authors. For example, STINSON and DAIGLE (1983) presented the fundamentals of an electronic system to measure the airflow resistance in an absorbent porous material using a variable capacitance pressure transducer. A procedure for measuring the airflow resistance was also proposed by WOODCOCK and HODGSON (1992) using the inversion of the DELANY and BAZLEY (1970), expression of the characteristic impedance as a function of airflow resistivity. Another technique was proposed by SEBAA *et al.* (2005) who used the physical property that in low frequencies the resistivity to the flow has a significant influence on the sound waves reflected. The flow resistivity was estimated, solving an inverse scattering problem for the waves reflected by a homogeneous isotropic porous material with a rigid skeleton. Subsequently, an extension of this work was presented using an acoustic transmissivity method to determine flow resistivity (FELLAH *et al.*, 2006).

Indirect methods for obtaining airflow resistance have also been developed based on measurements in an impedance tube and two side-mounted microphones (PICARD *et al.*, 1998; PANNETON, OLYN, 2006). DOUTRES *et al.* (2010) evaluated the macroscopic non-acoustical properties measuring the acoustical properties using a three-microphone impedance tube in the frequency bands where the material behaves as an equivalent fluid. These methods (using either two or three microphone positions) yield good results, although minimization of errors has to be done through accurate calibration procedures.

In particular, the method described by INGARD and DEAR (1985) is an indirect way for obtaining the value of the airflow resistance of sound absorbing materials at certain frequencies. This method is used in the area of acoustic characterization of materials as an alternative to the standardized method. The measuring device in this indirect model is based on an impedance tube, device which is more sensitive than the one described in the standardized model. This method was subsequently modified by REN and JACOBSEN (1993) who replaced the position of microphones and the rigid termination for a completely absorbent one. Also, introduction of the concept of dynamic flow impedance identified that the real part (flow resistance) represents the frictional retardation to flow and the imaginary part (flow reactance) is attributable to the effective mass density of the fluid. This study also analyzed the measurement errors and optimization of the arrangement given by Ingard and Dear.

MCINTOSH *et al.* (1990) analyzed the Ingard and Dear technique. They measured the complex flow impedance under low- and high-intensity levels and showed that finite sample lengths have an effect on the accuracy of the measurements. They demonstrated that a sample length much less than a wavelength is required for good finite amplitude flow impedance measurement. IANNACE *et al.* (1999) compared airflow resistivity measurements using both the Ingard and Dear technique and steady-state airflow method. They confirmed that both methods give compatible results for thin layers of loose granular materials. Another variation of the method included the change of position of the two microphones at the front of the sample (PICARD *et al.*, 1998). In this configuration, the method was applied to the particular case of stratified rockwool samples.

Another alternative way of measurement in order to estimate the airflow resistance value is a recently proposed method by DRAGONETTI *et al.* (2011). From a structural point of view, the developed by this method device is quite simple and does not present the low frequency limitation unlike the standardized method. The results of Dragonetti *et al.* were compared to the standardized method B (ISO, 1991) with good correlation.

Given that the method proposed by DRAGONETTI *et al.* (2011) is part of a recent study, it is useful to implement it to evaluate its performance in different types of materials including recycled porous ones. The main objective of this study is to compare the experimental airflow results obtained by the Dragonetti *et al.* method to those obtained by the method of INGARD and DEAR (1985) and the standardized method. The two alternative methods are similar in the use a loudspeaker and two microphones. This study presents measurements of airflow resistance for three distinct families of eco-materials. The measuring devices that are described in these two references were reproduced by the authors.

2. Two simple alternative methods

2.1. Ingard and Dear method

In this method the airflow resistance is measured using a closed cylindrical tube with a perfectly rigid termination, a loudspeaker at the other end, and a pair of microphones. Figure 1 (top) shows the schematics of the measuring device. The sample of the absorbent material of thickness d is inserted in the middle of the tube. The distance between the posterior face of the sample material and the rigid termination is l . One of the microphones is located to measure the sound pressure directly in front of the absorbent material (p_1). The other microphone is located in front of

the rigid termination that closes the tube (p_2). The loudspeaker emits a low frequency pure tone signal chosen to produce an odd number of quarter wavelengths throughout the distance $l+d$ from the rigid termination to the sample material. It should satisfy the condition $\lambda \gg 1.7D$, where D is the inner diameter of the tube and λ is the wavelength of sound. Also, $l + d = (2n - 1)\lambda/4$, whereas n is a whole number.

Assuming that the losses in the tube are negligible, that the microphones are calibrated to have the same sensibility, and that the flow reactance is small at low frequencies, the airflow resistance σ is determined by the equation

$$\sigma = \rho c 10^{(L_{p_1} - L_{p_2})/20}, \tag{1}$$

where ρ is the average air density, c is the speed of the sound in the tube, and L_{p_1} and L_{p_2} are the pressure levels that correspond to the pressure measurements p_1 and p_2 , respectively.

However, the measurement process is facilitated with the use of a dual channel FFT analyzer and a sound source generating a broadband stationary random noise inside the tube. In this case, the airflow resistance is calculated as a function of frequency using the absolute value of the imaginary part of the transfer function between the microphone signals, i.e. (INGARD, DEAR, 1985)

$$\sigma = \rho c \left| \text{Im} \left(\frac{p_1}{p_2} \right) \right|. \tag{2}$$

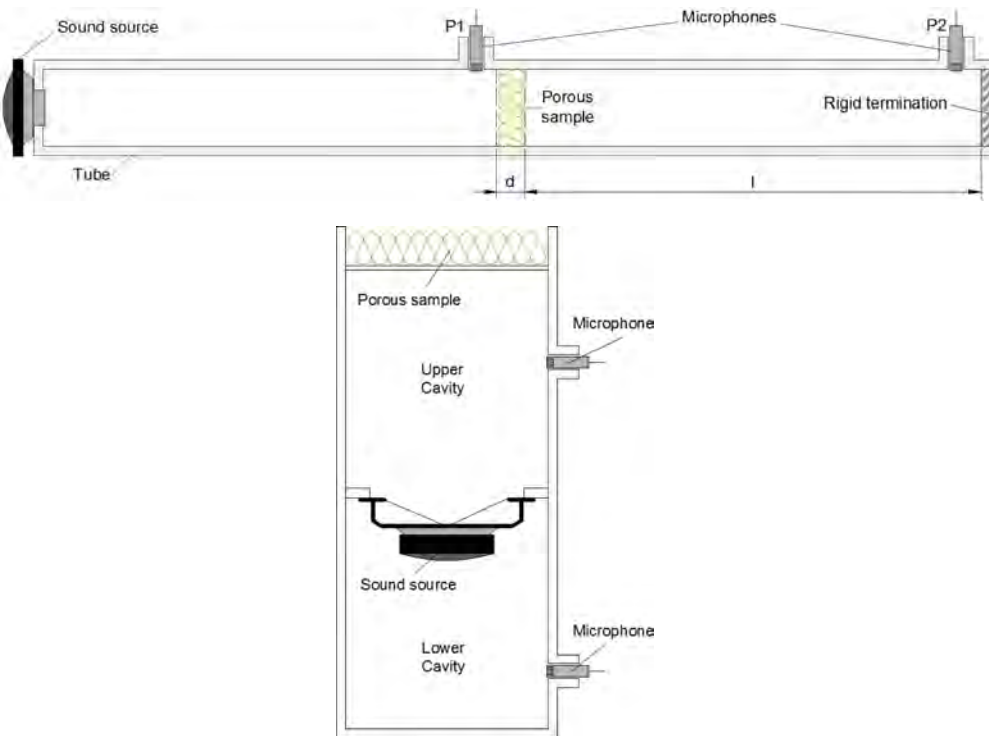


Fig. 1. Schematic diagram of the two measuring devices; top: INGARD and DEAR (1985) and bottom: DRAGONETTI *et al.* (2011).

Thus, it is possible to read the numerical value of the airflow resistance at frequencies where the length is an odd number of quarter wavelengths, i.e. looking for the minima of this function. Then, by extrapolating towards a zero frequency value, the “DC” airflow resistance is estimated (MCINTOSH *et al.*, 1990).

2.2. Dragonetti *et al.* method

The study by DRAGONETTI *et al.* (2011) includes a detailed description of an analogy between the prototype designed and an equivalent electrical circuit which permits the mathematical analysis of the behavior of the sound pressure in both cavities of the measuring device. Figure 1 (bottom) shows the schematic of the measuring device. In particular, in the case of low frequencies, the airflow resistance value can be obtained easily from the transfer function (H) between the microphones situated in both cavities of the device, which is given by

$$\sigma = \frac{\text{Im}(H)}{-\omega C_{dw}d}, \quad (3)$$

where ω is the circular frequency, d is the sample thickness, $\text{Im}(H)$ is the imaginary part of the transfer function H between the sound pressure measured in the upper and lower cavity given by

$$H = \frac{p_{up}}{p_{dw}}, \quad (4)$$

C_{dw} is the acoustic compliance of the lower cavity given by

$$C_{dw} = \frac{V_{dw}}{\gamma P_0 S}, \quad (5)$$

S is the cross sectional area of the porous sample, P_0 is the atmospheric pressure, γ is the specific heat ratio (approximately 1.41 for air), and V_{dw} is the compressible air volume in the lower cavity.

As it can be seen, once calibrated, the device in Fig. 1 provides a simple way to determine the value of airflow resistivity. The appropriate seals of each part of the device are essential to avoid air leaks, which helps to obtain consistent results. In this case, the calibration process is very important due to the effective volumes of both cavities. This calibration process is detailed in the study by DRAGONETTI *et al.* (2011).

3. Constructed measuring devices

3.1. Ingard and Dear device

The measuring device described by INGARD and DEAR (1985) was designed and built by the authors of this study (RAMIS *et al.*, 2010). The apparatus consists of a cylindrical, polymethylmethacrylate (PMMA) tube with a 40 mm diameter, wall thickness of 5 mm, and 169 cm in length. One end of the tube is equipped with a high frequency compression driver

(Beyma CP800TI) with a throat diameter of 49 mm, which permits emission without considerable distortion at 100 Hz. The other end is closed with a rigid, highly sound-reflective termination. The distance between the first microphone and the rigid termination was 0.845 m. This value was chosen to be one quarter wavelength at 100 Hz, approximately. The two microphones used are of 1/2 inch, and mounted flush into the tube wall. Figure 2 (top) shows a photograph of the constructed device.

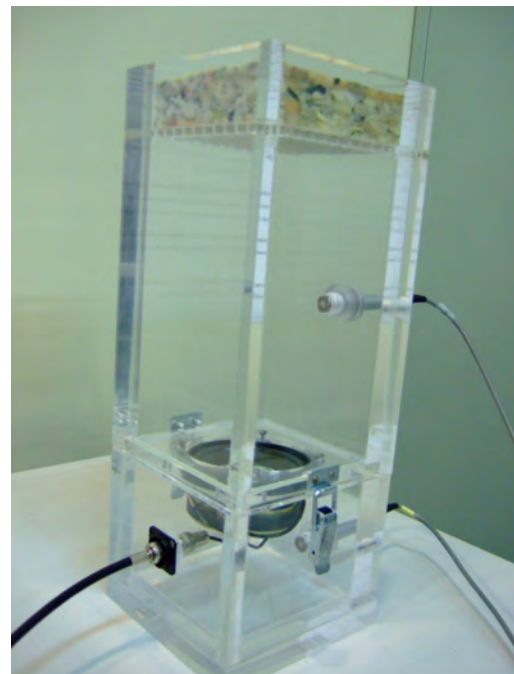
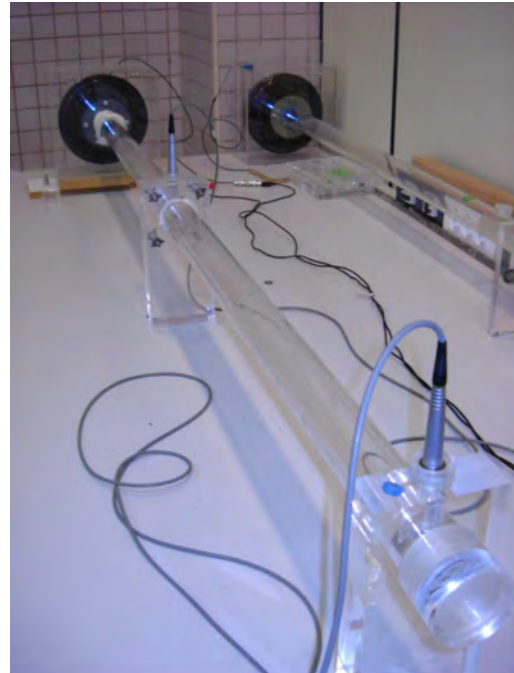


Fig. 2. Photographs of the constructed measuring devices; top: INGARD and DEAR (1985); bottom: DRAGONETTI *et al.* (2011).

3.2. Device of Dragonetti et al.

The device is designed and built with the goal of characterizing new sound-absorbing eco-materials, corresponding to the one described in the reference (DRAGONETTI *et al.*, 2011) and is shown in Fig. 2 (bottom).

The device described in the reference, as well as the device designed for this study are constructed with polymethylmethacrylate (PMMA) with a 20 mm thickness. In both cases, the volume of the upper and lower cavities is 2.30 and 0.99 litres, respectively. The upper part of the device is composed by a perforated grate where the study sample is held. The design considers circular perforations of 8.5 mm in diameter, with separations of 10.4 mm on both the horizontal and vertical axis. With this, the perforated area of the sample holder is 64.7%. It is necessary, in line with the reference prototype, to have at least 50% of the surface perforated, with a diameter of perforation of at least 3 mm. Noteworthy is that the method proposed by DRAGONETTI *et al.* (2011) is based on the adaptation of the standard (ISO, 1991), particularly the method B that is based on alternate airflow.

The microphones in both cases are 1/2 inch and the diameter of the speaker used (Fonestar UT-354) is 3 inches wide. This speaker has a good response in the range of frequencies used in this study.

4. Eco-materials studied

Three distinct eco-materials families were studied: recycled polyurethane foams, materials elaborated from coconut fibres, and recycled polyester fibres. While fabricating each of the materials, the use of toxic resins was avoided. The binding agent used, as in the case of polyester, was the thermofusion of the fibres. The three types of eco-materials have been

studied as sound absorbing materials in earlier works (DEL REY *et al.* 2011a; 2011b; 2012). The recycled foam has an average pore diameter of 150 μm . The coconut and polyester fibre materials have a mean value of the fibre diameter 250 μm and 36 μm , respectively.

In Fig. 3, microscopic images are shown from these three families of materials. The distribution of pores in the interior of each type of material can be appreciated, although the images are not of the same scale. It can be easily seen that the recycled foam corresponds to a cellular type porous material, and that the vegetable fibres of the coconut and the recycled polyester (PET) are porous materials of the fibrous type (ARENAS, CROCKER, 2010).

5. Results

Tests of eco-materials were carried out with alternative methods to those described in the ISO standard. Also, the same materials were tested in concordance with the ISO standard (1991) in an external laboratory in Portugal. The tests were conducted based on the method B of alternated airflow. For all the methods three samples of each eco-material were tested and the average of these three measurements was calculated.

In the case of the Ingard and Dear method, the transfer function is measured between the two microphone positions on the constructed prototype. The airflow resistance value is obtained by looking for the minima of the modulus of the imaginary part of this function and extrapolating towards a zero frequency value. To subsequently obtain the flow resistivity, the value is multiplied by the air impedance and divided by the thickness of the sample. Measurements considered sound pressure levels of 126 dB at the rigid termination, corresponding to velocity amplitudes of approximately 0.144 m/s on the front side of the material



Fig. 3. Microscopic detail of the composition of each of the eco-materials studied (images are not of the same scale); left: Recycled foam; middle: Coconut fibres; right: Recycled polyester fibres.

sample at 100 Hz. Figure 4 shows an example of the values measured for a polyester fibre with a density of 10 kg/m^3 and thickness 4 cm (denoted as I400-40). As expected, minima are observed at 100, 300, 500, 700, and 900 Hz, approximately.

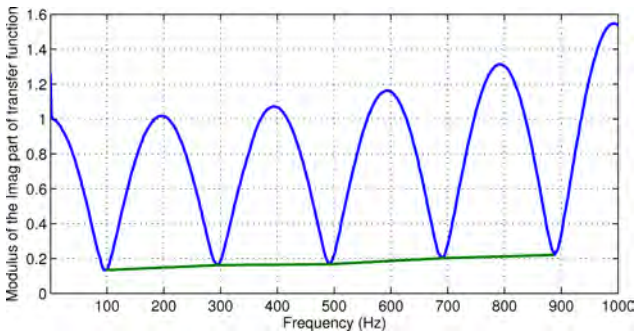


Fig. 4. Example of the values measured for a polyester fibre sample using the Ingard and Dear method.

Figure 5 shows the results measured from the imaginary part of the transfer function H as a function of

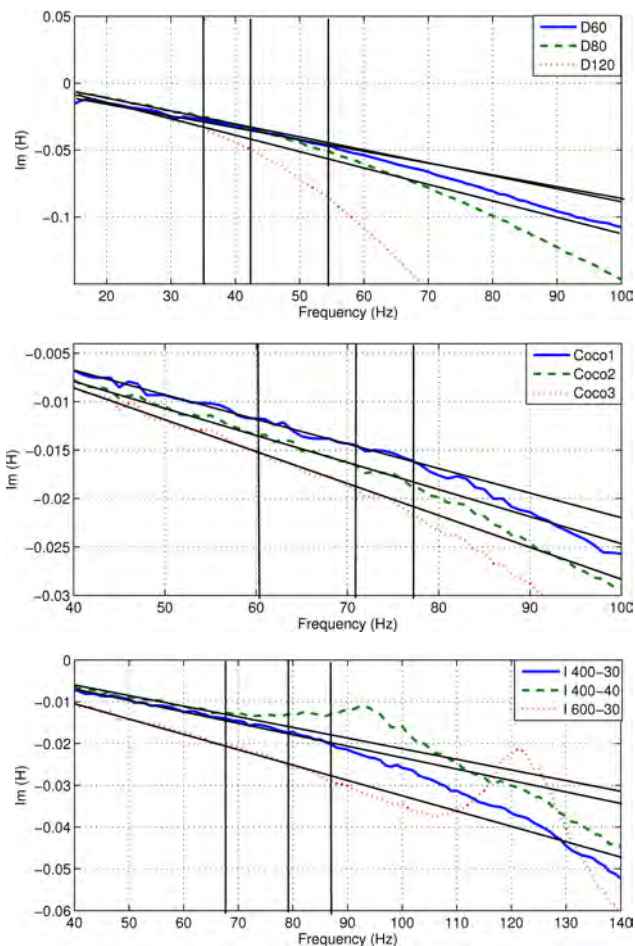


Fig. 5. Results of $\text{Im}(H)$ as a function of frequency for three types of porous eco-materials; top: recycled foam, middle: coconut fibres, bottom: recycled polyester fibre. The vertical lines indicate the relevant upper frequency limits.

frequency for the three families of eco-materials studied in concordance with the method of Dragonetti *et al.* To ensure a constant velocity for each frequency, the sound pressure level inside the lower cavity was 111 dB, corresponding to an approximately airflow velocity amplitude of 0.5 mm/s at the lowest frequency considered in this study. The plots in Fig. 5 give information about the limit on frequencies of Eqs. (3) and (5). The valid frequency limit is that in which the values can be approximated to a straight line. This frequency limit depends on intrinsic parameters of the porous material, such as the tortuosity and porosity values (DRAGONETTI *et al.*, 2011). In the samples studied in this test and for the frequency ranges considered, this dependence is shown clearly in Fig. 5 (bottom).

Figure 6 shows the average values of the airflow resistivity (airflow resistance divided by the sample thickness) in function of the frequency for each of the eco-material samples.

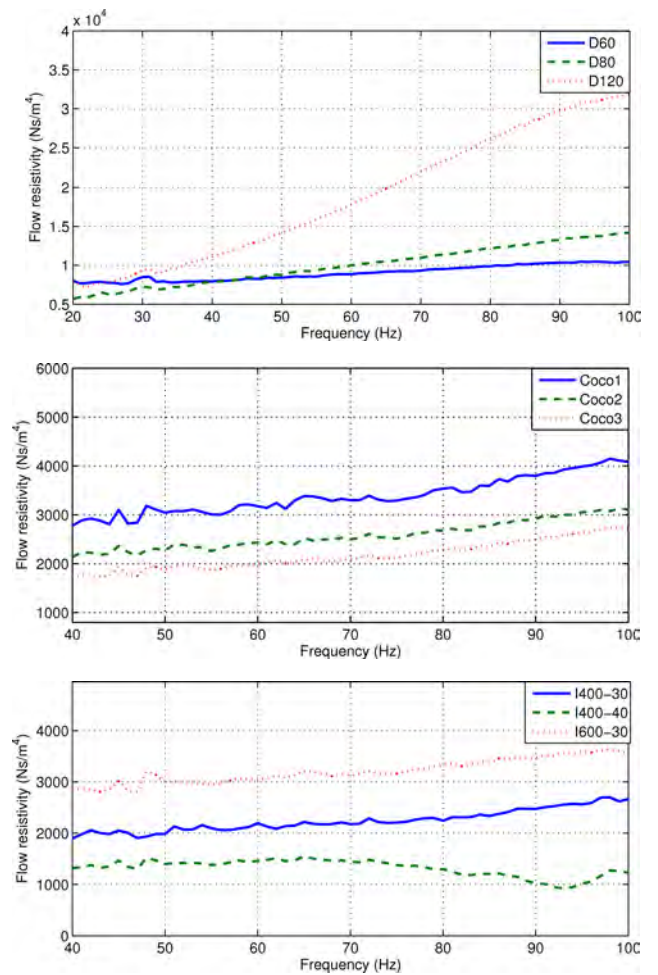


Fig. 6. Flow resistivity as a function of frequency for three types of porous eco-materials; top: recycled foam, middle: coconut fibres, bottom: recycled polyester fibre.

Table 1 presents the values obtained from all tested samples with both alternative indirect methods and the results according to the standard. Density, thick-

Table 1. Results of the airflow resistivity measured by different methodologies for the eco-material samples. The values in parenthesis indicate the standard deviation.

Material	Density [kg/m ³]	Thickness [cm]	Airflow resistivity [kNs/m ²]		
			Dragonetti <i>et al.</i>	Ingard and Dear	ISO 9053:1991 Method B
Recycled foam D60	61	3.2	9.2 (1.8)	9.0 (1.1)	6.1 (0.1)
Recycled foam D80	86	3.1	10.9 (4.4)	14.6 (0.7)	13.2 (0.1)
Recycled foam D120	135	3.1	21.0 (5.0)	13.5 (0.5)	35.6 (0.8)
Coconut fibres Coco1	128	1.9	3.1 (0.4)	2.8 (0.5)	2.6 (0.1)
Coconut fibres Coco2	100	2.9	2.3 (0.2)	1.9 (0.1)	1.9 (0.1)
Coconut fibres Coco3	83	4.2	1.8 (0.2)	1.5 (0.2)	1.2 (0.1)
Recycled polyester fibre I400-30	14	3.0	2.2 (0.4)	1.7 (0.1)	1.5 (0.7)
Recycled polyester fibre I400-40	10	4.0	1.4 (0.2)	1.3 (0.1)	1.1 (0.2)
Recycled polyester fibre I600-30	20	3.3	2.7 (0.2)	2.3 (0.5)	2.4 (0.3)

ness, average values of the airflow resistivity, and standard deviation are shown.

Analyzing the experimental results, it is important to note several findings in particular. In the case of the polyester fibre samples, which are lighter and homogenous in composition, both indirect methods offer similar values and very low levels of error. Also, these values are similar to the ones obtained with the ISO standard. It is important to emphasize that the testing with this type of light materials is more comfortable with these indirect techniques than with the standard one. With the indirect techniques, it was easier to cut and adapt the sample correctly. However, in the case of the standard, it is necessary to increase the precautions. As a result, for these types of samples the use of the two alternative indirect methods seems very adequate.

For the coconut fibre samples, there is also a good coincidence between the results of the tested methods and the standardized method. The density of the coconut is greater than that of the polyester, the distribution of the fibres is less homogeneous, and there are more differences between the diameters of the fibres. The errors in this case are not only due to the method but also to the composition of the materials, which increases the dispersion of the results. For these types of materials, both proposed methods appear adequate.

With respect to the recycled foams, larger divergences are observed. In the first place, the data of the indirect methods are similar to D60 but it is not the case for higher densities. These materials present high heterogeneity in their composition. It is assumed that these foams contain pieces of recycled foam of different types, which means that each sample can have quite a different composition. It is only possible to control the density and thickness, as factors that the samples share. In this sense, if the indirect methods are valid they can offer an estimation of airflow resistivity which can change due to the inhomogeneous composition.

It is important to highlight the value of the sample D120. In the case of the Dragonetti *et al.* method, the error increased upon the increasing density of the samples. In the case of the Ingard and Dear method, the errors increased due to the construction of the tube where indirect transmissions appear to reduce the difference between the pressure levels, thus reducing the value of airflow resistivity.

6. Conclusions

This study presented the results of airflow resistance for three families of eco-materials, measured by two alternative methods to the ISO standard. It is possible to observe the dependency of frequency range on the thickness of the samples and nature of the material measured. In general, it was possible to observe that both alternative methods give similar values. In the case of the coconut fibres, the values measured using the Ingard and Dear method are closer to the values measured with the ISO standard, while the values obtained by the Dragonetti *et al.* method slightly overestimate the values of airflow resistivity. This also occurs in the case of the recycled polyester fibres.

In the case of the materials of recycled foams, larger differences are noted, which is explained by the inhomogeneity of this type of recycled material. It appears reasonable that the test of eco-materials with the ISO standard does not guarantee a reliable measured value of airflow resistivity. In this sense, the indirect techniques of Dragonetti *et al.* and of Ingard and Dear appear useful, facilitating in many situations the testing procedure. In other cases it can serve as a control measurement for estimating the range in which this parameter can move. In every case, it can be concluded that the alternative methods are a viable option to the more complex, standardized procedures.

Acknowledgments

This project has been made possible thanks to the FONDECYT Project 1110605 and the grant GV/2012/066 Projects I+D for emerging research groups. The authors would like to thank Dr. Luis Godinho from the Department of Civil Engineering of University of Coimbra (Portugal) for his help with the experimental work and the ISO data reported in Table 1 of this paper.

References

- ALBA J., DEL REY R., RAMIS J., ARENAS J.P. (2011), *An inverse method to obtain porosity fibre diameter and density of fibrous sound absorbing materials*, Archives of Acoustics, **36**, 3, 561–574.
- ARENAS J.P., CROCKER M.J. (2010), *Recent trends in porous sound absorbing materials for noise control*, Sound and Vibration, **44**, 7, 12–17.
- ASDRUBALI F. (2006), *Survey on the acoustical properties of new sustainable materials for noise control*, Proceedings of Euronoise, Tampere, Finland.
- BIES D.A., HANSEN C.H. (1980), *Flow resistance information for acoustical design*, Applied Acoustics, **13**, 5, 357–391.
- DELANY M.E., BAZLEY E.N. (1970), *Acoustical properties of fibrous absorbent materials*, Applied Acoustics, **3**, 2, 105–116.
- DEL REY R., ALBA J., BERTO L., SANCHIS V. (2011a), *Absorbent Acoustic Materials based in Natural Fibers*, ACUSTICUM 2011 EAA, Aalborg, Denmark.
- DEL REY R., ALBA J., RAMIS J., SANCHIS V. (2011b), *New absorbent acoustics materials from plastic bottle remnants*, Materiales de Construcción, **61**, 204, 547–558.
- DEL REY R., ALBA J., ARENAS J.P., SANCHIS V. (2012), *An empirical modelling of porous sound absorbing materials made of recycled foam*. Applied Acoustics, **73**, 604–609.
- DOUTRES O., SALISSOU Y., ATALLA N., PANNETON R. (2010), *Evaluation of the acoustic and non-acoustic properties of sound absorbing materials using a three-microphone impedance tube*, Applied Acoustics, **71**, 6, 506–509.
- DRAGONETTI R., IANNIELLO C., ROMANO A.R. (2011), *Measurement of the resistivity of porous materials with an alternating air-flow method*, Journal of the Acoustical Society of America, **129**, 2, 753–764.
- FELLAH Z.E.A., FELLAH M., SEBAA N., LAURIKS W., DEPOLLIER C. (2006), *Measuring flow resistivity of porous materials at low frequencies range via acoustic transmitted waves*, Journal of Acoustic Society of America, **119**, 1926–1928.
- GARAI M., POMPOLI F. (2005), *A simple empirical model of polyester fibre materials for acoustical applications*, Applied Acoustics, **66**, 12, 1383–1398.
- IANNACE G., IANNIELLO C., MAFFEI L., ROMANO R. (1999), *Steady-state air-flow and acoustic measurement of the resistivity of loose granular materials*, Journal of the Acoustical Society of America, **106**, 3, 1416–1419.
- INGARD K.U., DEAR T.A. (1985), *Measurement of acoustic flow resistance*, Journal of Sound and Vibration, **103**, 4, 567–572.
- ISO (1991), 9053:1991. Acoustics – Materials for acoustical applications. Determination of airflow resistance, International Organization for Standardization, Geneva.
- MCINTOSH J.D., ZUROSKI M.T., LAMBERT R.F. (1990), *Standing wave apparatus for measuring fundamental properties of acoustic materials in air*, Journal of the Acoustical Society of America, **88**, 4, 1929–1938.
- NICK A., BECKER U., THOMA W. (2002), *Improved acoustic behavior of interior parts of renewable resources in the automotive industry*, Journal of Polymers and the Environment, **10**, 3, 115–118.
- PANNETON R., OLYN X. (2006), *Acoustical determination of the parameters governing viscous dissipation in porous media*, Journal of the Acoustical Society of America, **119**, 4, 2027–2040.
- PICARD M.A., SOLANA P., URCHUEGUIA J.F. (1998), *A method of measuring the dynamic flow resistance and the acoustic measurement of the effective static flow resistance in stratified rockwool samples*, Journal of Sound and Vibration, **216**, 3, 495–505.
- RAMIS J., ALBA J., DEL REY R., ESCUDER E., SANCHIS V. (2010), *New absorbent material acoustic based on kenaf's fibre*, Materiales de Construcción, **60**, 299, 133–143.
- REN M., JACOBSEN F. (1993), *A method of measuring the dynamic flow resistance and reactance of porous materials*, Applied Acoustics, **39**, 265–276.
- SEBAA N., FELLAH Z.E.A., FELLAH M., LAURIKS W., DEPOLLIER C. (2005), *Measuring flow resistivity of porous material via acoustic reflected waves*, Journal of Applied Physics, **98**, 084901.
- STINSON R., DAIGLE A. (1983), *Electronic system for the measurement of flow resistance*, Journal of the Acoustical Society of America, **83**, 2422–2428.
- WOODCOCK R., HODGSON M. (1992), *Acoustic methods for determining the effective flow resistivity of fibrous materials*, Journal of Sound and Vibration, **153**, 1, 186–191.

Latest Developments in International Standardization of Whole-Body and Hand-Arm Vibration

Martin LIEDTKE, Jörg RISSLER, Uwe KAULBARS

Institute for Occupational Safety and Health of the German Social Accident Insurance (IFA)
Alte Heerstraße 111, 53757 Sankt Augustin, Germany; e-mail: martin.liedtke@dguv.de

(received March 13, 2013; accepted September 23, 2013)

Latest developments in international standardization of whole-body and hand-arm vibration are presented. In addition, two German projects are presented that might have impact on international work programs in the next years.

Keywords: standards, whole-body vibration, hand-arm vibration.

1. Introduction

International standards concerning whole-body vibration (WBV) and hand-arm vibration (HAV) are prepared by ISO/TC 108/SC 4 and CEN/TC 231 who are working together under the regulations of the VIENNA AGREEMENT 2001. Currently, there are 83 published standards and amendments in the program of both committees. This paper introduces some aspects of the latest developments in the work of these two committees.

In the first section, two German projects are introduced that affect WBV and HAV, and that are likely to have some impact on international work programs. The next section contains comments on projects for WBV, followed by a section dealing with HAV-projects.

As far as current projects are concerned, the information given here reflects only the momentary state of the discussion, and there is no guarantee that the final standards will actually contain the outlined concepts.

2. DIN projects affecting WBV/HAV with probable impact on ISO and CEN

Two projects of the German Institute for Standardization (DIN) are dealing with the measurement of vibrations from a more general point of view. The first one addresses the question of the uncertainty of measurement. The second is dealing with qualifications of measurement personnel.

As far as the uncertainty of vibration measurements is concerned, a DIN working group is prepar-

ing a guide (Technical Report) that summarizes the information available in standards. Starting with the GUM, ENV 13005:1999, ISO/BIPM, the principles of the evaluation of uncertainty are given in the main part of the future guide; annexes are dealing with common situations for WBV, HAV, emission measurements of (hand-held) machinery, and measurements of vibration in the environment (immissions).

Another issue that affects both WBV and HAV is the qualification of the measurement personnel. In this case, the existing standards concerning qualifications of measurement personnel in the field of machinery surveillance are taken as a basis to develop a similar scheme of qualification levels for the personnel of WBV and HAV laboratories.

3. International WBV-projects

In the field of WBV, the measurement standard ISO 2631-1:1997 is currently under revision. Two further projects investigate the measurement of posture together with WBV ISO/TR 10687:2012 and the effect of shock on WBV exposure ISO 2631-5:2004.

3.1. WBV measurement ISO 2631-1

ISO 2631-1:1997 amended in 2010, is concerned with the measurement of WBV and evaluation of the effects of WBV with regard to health, comfort and perception, and motion sickness. Minor technical revisions with regard to health have been incorporated in the amendment of 2010. For example, the defini-

tion of the daily exposure $A(8)$ of the DIRECTIVE 2002/44/EC has been addressed, where the daily exposure $A(8)$ is expressed as the equivalent continuous acceleration over an eight-hour period, calculated as the highest (rms) value. The $A(8)$ cannot be expressed by the VDV.

Currently, the literature concerning health and comfort effects is being reviewed. There are arguments in the literature to simplify and revise the section on comfort. The section on health effects, on the other hand, still reflects in large parts the available knowledge and will most likely not be revised thoroughly. The structure of future revisions will depend on the amount of changes. One possibility is to rewrite ISO 2631-1 with its current structure, another is to take some parts out of ISO 2631-1 and establish them as new parts of ISO 2631.

3.2. Posture and WBV: ISO/TR 10687

The aim of ISO/TR 10687:2012 is to define variables that should be reported whenever posture has to be described within a WBV context. The document lists several body angles which are defined by points on the surface of a subject. The definition is descriptive in the main part of the Technical Report and a mathematical definition is given in an informative annex. A pictorial description of the lateral flexion of lumbar and thoracic spine is given in Fig. 1. Apart from the definition of body angles, the Technical Report requires the user to collect further information regarding musculoskeletal load: whether or not a helmet is worn, whether or not armrests are used, etc.

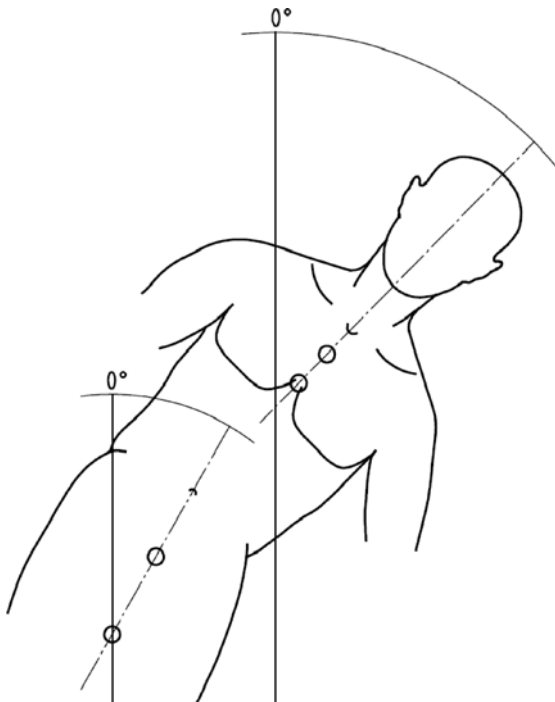


Fig. 1. Lateral flexion of lumbar and thoracic spine.

3.3. Shock ISO 2631-5

The effect of shock in the context of WBV is addressed in ISO 2631-5:2004. The idea of the existing standard is to define a dose based on peaks of a transfer function of an acceleration time series. The transfer function in z -direction is defined by a neuronal network trained at a special set of acceleration time series. In the x - and y -direction, the transfer function is produced by a single-degree-of-freedom lumped parameter model. Due to this different evaluation of the vibrational axes and some other theoretical drawbacks, this standard is currently under revision.

At the moment, two methods are in the discussion which will apply to different excitation regimes: unweighted acceleration time series with peaks above or below 9.81 ms^{-2} . Both methods retain the underlying idea of a dose based on peak values of a transfer function. The method for smaller peaks has already been published as a specification (Technical Report) in Germany: DIN SPEC 45697:2012-06.

4. International HAV-projects

The following three subsections are concerned with standardization projects in the field of HAV. The assessment of coupling forces is presented, followed by the development in emission standards and, finally, the ideas concerning a revision of the frequency weighting for neurological and vascular effects.

4.1. Standards governing coupling forces for hand-arm vibration

ISO 5349-2:2001 requires measurement to be performed directly at the point of transmission to the hand-arm system for precise determining of the vibration stress upon the hand-arm system caused by a hand-held or manually guided machine or control element. Since this is not possible for technical reasons, the vibration is measured on the handle of the machine or the control element.

Where measurement is performed on the handle of the machine, the result of the measurement and the stress upon the hand-arm system are influenced considerably by the coupling of the hand to the machine or control element. Stronger coupling results in a drop in the acceleration values measured at the handle, since more energy is transmitted to the hand-arm system. The stress also increases with rising coupling. Equally, it is necessary for measurement purposes to differentiate between various forces acting upon the hand-arm system.

To address this issue, DIN V 45679, which was published as long ago as 1998, describes not only the frequency weighting, but also a further weighting that is dependent upon the coupling force.

ISO 15230, published in 2007, purposefully addresses the parameters of interaction between the hand and the machine and sets out measurement methods and the requirements applicable to instruments. However, it does not state procedures for evaluating the data.

The German proposal for a supplement containing an evaluation method to be added to ISO 15230 has been rejected. This resulted in development of a CEN Report on the European standardization level, published in 2012 in the form of CEN/TR 16391. Besides dealing with the recommendations made in DIN 45679 concerning evaluation, the report contains guidance on the selection of machines and training of the user for the purpose of reducing the transmitted vibration and thereby the stress caused by it.

The revised version of DIN 45679 published in 2013 contains the provisions in ISO 15230 and the evaluation method to CEN/TR 16391. An English version of the standard is in preparation.

4.2. Standards for measuring hand-arm vibration emissions

Conversion of the measurement method in the ISO 5349-1 basic standard from one to three axes of measurement necessitated revision of the ISO 8662 series of standards governing the measurement of emission values.

Whereas earlier standards governing emissions were developed only with regard to high reproducibility of the measured values and for comparison of machines within a group, the new ISO 28927 series contains more realistic operating conditions for the group of machines concerned for the purpose of risk assessment.

Owing to the standardization work conducted in parallel by CEN and CENELEC, deviations in the provisions concerning the measurement locations for electrically driven machines in IEC 60745-1 required an alternative measurement location to be specified rather than the one measurement location previously defined in the CEN standards (ISO 20643). As a result of these changes, adaptation was also required of the basic standard (ISO 20643). This in turn required new measurement locations for the workplace measurements. An amendment to ISO 5349-2 gives examples of the newly specified alternative measurement locations.

4.3. Standard for a new frequency weighting for hand-arm vibration

In response to a request by France, the preliminary work item (PWI) was discussed at the meeting of WG 3 of ISO/TC 108/SC 4 in September 2008. The results of the enquiry showed that the existing

frequency weighting in ISO 5349-1 enjoyed recognition and general use, both in legislative texts and in many standards. The group was therefore unanimous in ruling out a change in this weighting in the immediate future. The group agreed however to define a supplementary frequency weighting which would give better consideration to the neurological and vascular effects. In June 2011, a workshop on the subject was held in conjunction with the Conference on Hand-Arm Vibration in Canada. A draft alternative frequency weighting that had been drawn up by the Canadian head of the project was discussed at the meeting of the WG 3 held in Nancy in September 2012 and is to be completed by the next meeting in September 2013 in the form of ISO 18570. Under discussion is a new supplementary curve with a flat frequency range between the cut-off frequency of 200 Hz and 400 Hz (BRAMMER, PITTS, 2012).

References

- BRAMMER A., PITTS P. (2012), *Frequency Weighting for Vibration-induced White Finger Compatible with Exposure-response Models*, Industrial Health, **50**, 397–411, 2012, NIOSH Japan https://www.jstage.jst.go.jp/article/indhealth/50/5/50_MS1383/_pdf.
- CEN/TR 16391, *Mechanical vibration and shock – Hand-transmitted vibration – Influence of coupling forces at the hand-machine interface on exposure evaluation*.
- DIN SPEC 45697:2012-06, *Mechanische Schwingungen und Stöße – Verfahren zur Bewertung stoßhaltiger Ganzkörper-Vibrationen*.
- DIN V 45679, *Mechanical vibration – Measurement and evaluation of coupling forces for assessment of vibration exposure of the hand-arm system*.
- DIN 45679, *Mechanische Schwingungen – Messung und Bewertung der Greif- und Andruckkräfte zur Beurteilung der Schwingungsbelastung des Hand-Arm-Systems*.
- DIRECTIVE 2002/44/EC of 25 June 2002 on the minimum health and safety requirements regarding the exposure of workers to the risks arising from physical agents (vibration) (sixteenth individual Directive within the meaning of Article 16(1) of Directive 89/391/EEC).
- GUM, ENV 13005:1999, ISO/BIPM *Guide to the expression of uncertainty in measurement*.
- ISO 2631-1:1997, *Mechanical vibration and shock – Evaluation of human exposure to whole-body vibration – Part 1: General requirements*.
- ISO/TR 10687:2012, *Mechanical vibration – Description and determination of seated postures with reference to whole-body vibration*.
- ISO 2631-5:2004, *Mechanical vibration and shock – Evaluation of human exposure to whole-body vibration – Part 5: Method for evaluation of vibration containing multiple shocks*.

11. ISO 5349-2:2001, *Mechanical vibrations – Measurement and evaluation of human exposure to hand-transmitted vibration – Part 2: Practical guidance for measurement at the workplace.*
12. ISO 15230:2007-08-31, *Mechanische Schwingungen und Stöße. Ankopplungskräfte der Hand an Maschinengriffen bei Einwirkung von Hand-Arm-Schwingungen.*
13. ISO 5349-1 basic standard, *Mechanical vibration – Measurement and evaluation of human exposure to hand-transmitted vibration – Part 1: General requirements.*
14. ISO 8662, *Hand-held portable power tools. Measurements of vibrations at the handle.*
15. ISO 28927, *Hand-held portable power tools – Test methods for evaluation of vibration emission.*
16. IEC 60745-1, *Hand-held motor-operated electric tools – Safety – Part 1: General requirements.*
17. ISO 20643, *Mechanical vibration – hand-held and hand-guided machinery – Principles for evaluation of vibration emission.*
18. ISO 5349-2:2001/DAM 1:2013, *Mechanical vibrations – Measurement and evaluation of human exposure to hand-transmitted vibration – Part 2: Practical guidance for measurement at the workplace.*
19. ISO 18570, *Mechanical vibration – Frequency weighting characteristics for hand-transmitted vibration.*
20. VIENNA AGREEMENT (Agreement on technical co-operation between ISO and CEN (2001). The text of the Vienna agreement is available at: <http://www.cen.eu/boss/supporting/Reference%20documents/cooperation/Pages/default.aspx>

An Objective and Subjective Study of Noise Exposure within the Frequency Range from 10 kHz to 40 kHz

Bożena SMAGOWSKA

Central Institute for Labour Protection – National Research Institute
Czerniakowska 16, 00-701 Warszawa, Poland; e-mail: bosma@ciop.pl

(received April 8, 2013; accepted October 14, 2013)

The paper consists of study results of exposure to high frequency noise at metalworking workplaces. The study was carried out using objective methods (measurements of parameters characterizing the noise) and subjective studies (questionnaire survey). Metalworking workplaces were located in a steel structure (e.g. deck gratings) of the manufacturing plant. The results are equivalent sound pressure levels in the 1/3 octave frequency bands with center frequencies from 10 kHz to 40 kHz in reference to an 8-hour workday equal to approximately 81–105 dB at most of the tested workplaces and exceed permissible values. The questionnaire survey of annoyance high frequency noise (i.e. in the audible frequency and low ultrasound range) was conducted among 52 operators of machines. Most of the workers describe the noise as: buzzing, insistent, whistling and high-pitched squeaky. Respondents specify the noise levels occurring at workplaces as: loud, impeding communication, highly strenuous and tiring.

Keywords: ultrasonic noise exposure, metalworking workplaces.

1. Introduction

The broadband noise containing high audible frequencies (10–16 kHz) and low ultrasonic frequencies (20–40 kHz) at workstations is in Poland defined as ultrasonic noise. The assessment of ultrasonic noise exposure is based on (equivalent and maximum) sound pressure levels in the 1/3 octave band (the central frequencies are in the range from 10 kHz to 40 kHz) (Regulation of the Minister of Labour and Social Policy of 29 November 2002). The main sources of ultrasonic noise in the working environment are the so-called low frequency ultrasonic technological devices, including washers, welders, drills, soldering tools and galvanizing pots (SMAGOWSKA, 2013). Apart from the above-mentioned technological devices, in which the ultrasonic vibrations constitute the working factor, ultrasonic noise arises also as an unintentional result of the work of many machines and devices. The existence of ultrasonic components of significant sound pressure levels has been found in the work of devices where phenomena of aerodynamic (flow or outflow of compressed gas) or mechanical character (big rotational speed of machine elements) occur (SMAGOWSKA, 2010; 2012). This refers to compressors, blowpipes, valves,

pneumatic tools and high-speed machinery (planers, millers, circular saws and some textile machinery).

The results of exposure to ultrasonic noise may affect the workers hearing organ (hearing losses) and the non-hearing parts of the body (PAWLACZYK-ŁUSZCZYŃSKA *et al.*, 2007; SMAGOWSKA, MIKULSKI, 2012). For the prevention of adverse effects of ultrasonic noise exposure and related hearing losses, Maximum Admissible Intensities¹ (MAI) have been determined (Regulation of the Minister of Labour and Social Policy of 29 November 2002).

This paper contains measurement and assessment results of exposure to ultrasonic noise from the so-called non-technological noise sources at metal workplaces. The assessment was carried out using objective methods (measurements of parameters characterizing noise within the frequency range covering sounds and ultrasonics of frequencies from 10 kHz to 40 kHz) and subjective studies (questionnaire survey). The test results are presented below.

¹MAI – admissible exposure limits of a health-damaging factor are established as exposure levels adjusted to the properties of respective factors, so that the impact of the factor on an employee during his work activity should not bring about adverse consequences on the state of his health or on that of future generations.

2. Admissible values of ultrasonic noise in Poland

The admissible values of ultrasonic noise in respect of health protection of workers, valid in Poland, are specified in the Regulation of the Minister of Labour and Social Policy of 29 November 2002 (Regulation of the Minister of Labour and Social Policy of 29 November 2002). On the basis of measurements, the physical parameters characterizing ultrasonic noise are identified as follows:

- the equivalent sound pressure level in the 1/3 octave band with central frequency, f , from 10 kHz to 40 kHz, referred to an 8-hour working day, $L_{feq,8h}$, or to the working week, $L_{feq,w}$, both in dB; the reference to a working week is exceptionally used in case of the irregular ultrasonic noise influence on the human organism in certain days of the week or when an employee works in a number of days a week different from 5),
- maximum sound pressure levels in 1/3 octave band with the central frequency, f , from 10 kHz to 40 kHz, L_{fmax} in dB.

Admissible equivalent sound pressure levels at workstation referred to 8-hour working day and maximum sound pressure levels in 1/3 octave bands consists Table 1.

Table 1. Admissible equivalent sound pressure levels at a workstation referred to 8-hour working days and maximum sound pressure levels in 1/3 octave bands.

Central frequency of 1/3 octave bands f [kHz]	Admissible equivalent sound pressure levels $L_{feq,8h,dop}$ [dB]	Maximum admissible sound pressure levels $L_{fmax,dop}$ [dB]
10; 12.5; 16	80 (77^1)(75^2)	100
20	90 (87^1)(85^2)	110
25	105 (102^1) (100^2)	125
31.5; 40;	110 (107^1)(105^2)	130

¹ Admissible values of equivalent ultrasonic noise sound pressure levels for pregnant women (Regulation of the Council of Ministers of 10 September 1996).

² Admissible values of equivalent ultrasonic noise sound pressure levels for juveniles (Regulation of the Council of Ministers of 24 August 2004).

3. Results of measurements and assessment of ultrasonic noise at selected metalworking workplaces

The equivalent sound pressure levels in 1/3 octave bands with the central frequency, f , from 10 kHz to 40 kHz, $L_{feq,8h}$ and maximum sound pressure levels in 1/3 octave bands with the central frequency, f ,

Table 2. Values of equivalent sound pressure levels at workplaces.

No.	Machine	Activity	The equivalent sound pressure level $L_{feq,8h}$ in 1/3 octave bands in reference to an 8-hour workday, in dB						
			10	12.5	16	20	25	31.5	40
1.	Plate saw – Tyro	cutting of deck gratings	96.6	86.7	81.5	88.3	80.4	79.5	74.1
2.	Plate saw – automatic drive	cutting of deck gratings	89.0	100.2	96.0	86.2	89.4	86.0	87.2
3.	Plate saw – hand drive	cutting of deck gratings	84.7	75.2	75.2	82.7	73.2	76.3	67.4
4.	Plate saw – Trennjaeger	cutting of deck gratings	94.1	104.8	93.8	91.9	94.1	87.2	86.6
5.	grinder for sharpening	sharpening of circular saw's teeth	81.1	79.4	80.6	48.5	74.9	73.0	70.2
6.	welding machine – ESAB	burning out a shape on the grating with oxygen-acetylene mixture	81.1	78.1	79.2	80.7	82.4	84.2	85.8
7.	welder SCI 1500	submerged arc	74.5	72.4	70.9	67.8	65.6	65.0	62.8
8.	Johnson' rotary cutter	cutting of iron plate (m. – platform 1)	91.0	76.3	81.5	80.9	70.9	67.7	61.3
9.	Johnson' rotary cutter	cutting of iron plate (m. control pulpit)	82.5	68.5	75.5	76.0	64.3	61.4	56.9
10.	Johnson' rotary cutter	cutting of iron plate (m. – platform 2)	86.1	75.2	82.7	84.4	82.8	67.4	67.9
11.	arc welder	carbon-arc air gouging	102.8	102.1	100.1	98.9	98.2	98.0	96.9
12.	machine for plasma cutting – Plasmatome 20HPO	cutting of deck gratings of plasma burner	78.5	93.7	83.8	86.2	91.5	92.7	96.2
13.	welding line EVGZ	termal welding of deck grating	82.7	84.7	85.5	84.4	84.2	85.0	84.3

Table 3. The values of maximum sound pressure levels at workplaces.

No.	Machine	Activity	The maximum sound pressure level $L_{f \max}$, in 1/3 octave bands, in dB						
			10	12.5	16	20	25	31.5	40
1.	Plate saw – Tyro	cutting of deck gratings	108.2	97.2	94.4	102.8	92.6	91.8	89.0
2.	Plate saw – automatic drive	cutting of deck gratings	99.6	114.1	109.9	94.7	103.3	100.0	101.4
3.	Plate saw – hand drive	cutting of deck gratings	108.0	99.4	97.6	104.4	94.4	94.5	88.5
4.	Plate saw – Trennjaeger	cutting of deck gratings	106.5	120.3	105.9	104.1	107.1	100.0	99.6
5.	grinder for sharpening	sharpening of circular saw's teeth	85.3	83.1	84.0	81.3	77.9	76.1	73.3
6.	welding machine – ESAB	burning out a shape on the grating with oxygen-acetylene mixture	88.4	85.9	85.7	86.5	88.7	91.1	93.5
7.	welder SCI 1500	submerged arc	72.7	76.3	73.3	70.5	69.8	68.5	67.2
8.	Johnson' rotary cutter	cutting of iron plate (m. – platform 1)	101.4	83.8	90.5	88.3	86.2	75.2	66.1
9.	Johnson' rotary cutter	cutting of iron plate (m. control pulpit)	85.8	73.0	79.4	86.0	75.1	63.7	65.1
10.	Johnson' rotary cutter	cutting of iron plate (m. – platform 2)	94.1	85.7	87.6	91.8	90.4	72.2	75.0
11.	arc welder	carbon-arc air gouging	121.8	121.2	120.4	119.8	118.4	117.3	116.3
12.	machine for plasma cutting – Plasmatome 20HPO	cutting of deck gratings of plasma burner	84.2	103.0	92.4	96.0	102.2	104.3	107.1
13.	welding line EVGZ	termal welding of deck grating	90.3	91.9	93.1	92.6	92.4	94.2	94.3

from 10 kHz to 40 kHz $L_{f \max}$ have been measured at selected metalworking workplaces. The measurements of the noise parameters were taken in places where the employee's stay during work (i.e. at a distance between 0.5 m and 1.5 m from the noise source, depending on the workplace type). The studies were carried out during the following operations: cutting of deck gratings, sharpening of circular saw's teeth, burning out a shape on the grating with an oxygen-acetylene mixture, submerged arc and plasma arc welding, cutting of a metal sheet with rotary shears, carbon-arc air gouging of joints, and pressure welding of deck grating. The results of measurements of the noise parameters are presented in Tables 2 and 3.

The values of equivalent sound pressure levels in 1/3 octave frequency band with the central frequency, f , from 10 kHz to 40 kHz, in reference to an 8-hour workday are within the range of 81–105 dB at most of the tested workplaces. In most cases, the excess of MAI values for ultrasonic noise occurs for this parameters. The operation of submerged arc welding is the only exception (measured levels are within the 63–75 dB range during operating the welder SCI 1500). The highest equivalent sound pressure levels are measured during the carbon-arc air gouging of joints; they are equal to 97–103 dB. The measured maximum sound pressure levels in 1/3 octave bands of frequencies from 10 kHz to 40 kHz vary between 64 and 122 dB. Allowable val-

ues of this parameter are exceeded in 1/3 octave bands of 10 kHz, 12.5 kHz and 16 kHz during the following activities: cutting of deck gratings, cutting of metal sheets and carbon-arc air gouging of joints. The highest equivalent sound pressure levels occur during carbon-arc air gouging of joints and vary in this case within the range of 116–122 dB.

4. Questionnaire survey results

The questionnaire survey was conducted for 52 operators of machines used in the manufacturing of the aforementioned deck gratings. This was performed in order to carry out the subjective assessment of noise exposure at workplaces. The tested group consisted of men; the group's average period of working was approximately 11 years. The average age experience within the surveyed group equalled to 40 years. About 95% of the surveyed workers were employed on a full-time basis.

92% of the respondents stated that they are exposed to noise constantly. The noise was characterized by the majority of workers as: droning, insistent, creaking, whistling and squeaky, whereas slightly fewer people described it as roaring and wheezing. Male respondents unequivocally considered the Sound Pressure Level (SPL – in the survey “noise level”) at their

workplaces as: not nuisance, tolerable, loud, impeding communication, high bothersome and tiring. Figure 1 shows survey results for the workers subjective assessment of the ‘noise level’ at their workplaces. About 50% of responses confirmed that the “noise level” is: loud, impeding communication, high bothersome and tiring.

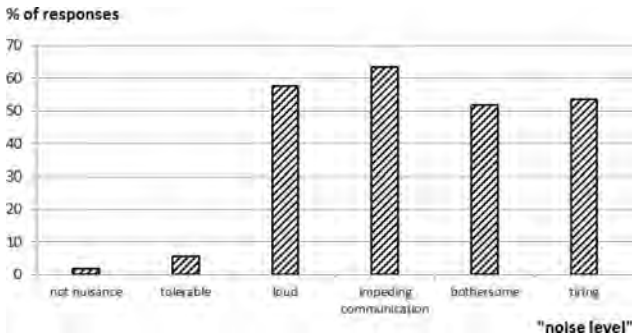


Fig. 1. Employees subjective assessment of the “noise level” at workplaces for the production of deck grating.

Figure 2 presents survey results for the employees’ subjective assessment of the degree of annoyance of the level of noise at workplaces for the production of deck grating. The following terms received the largest number of points on the scale representing the degree of annoyance of noise: horrible, enormous, persistent, and intense.

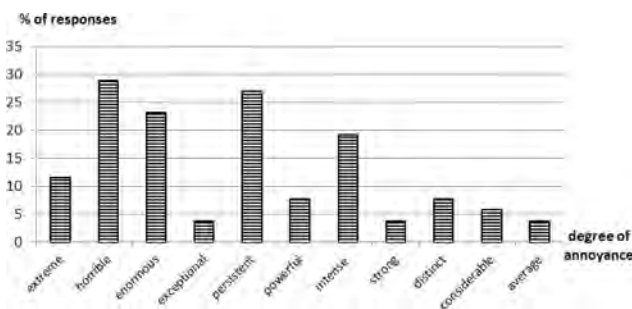


Fig. 2. Employees’ subjective assessment of the degree of annoyance of the level of noise at workplaces for the production of deck grating.

Audiometric tests are performed at least once every two years, what was confirmed by the respondents, in their subjective appraisal. 17% of the interviewee considered the state of their hearing as defective. 21.2% of the employees have a nuisance in hearing normal speech, whereas in case of a whispering voice these difficulties were noticed by 50% of respondents. 26.9% of the questionnaire people suffer tinnitus, 19.2% claim to understand very loud speech. All interviewed people have and wear hearing protector devices (alternatively): earmuffs (9.6%), earplugs (61.5%) and custom-made earplugs (96.2%). The most often enumerated machines and devices used

at their workplace are: acetylene-oxygen torch, pneumatic tool, grinder, plasma cutting processes, cutting with acetylene-oxygen torches and gas metal arc welding.

5. Summary

The results of measurements and the assessment of high frequency noise at selected metalworking workplaces confirmed that during operating these devices and machines the workers are exposed to an occupational risk of ultrasonic noise. The results have proved a large diversity of risk at workplaces of different types of machines. The highest values characterizing this hazard factor occur most often within the operating frequency of the equipment. In case of non-technology ultrasonic noise sources, they exceed the ultrasonic noise MAI values in three primary 1/3 octave bands of central frequencies: 10 kHz; 12.5 kHz and 16 kHz. Due to the fact that these frequency bands overlap clearly with the upper range of audible sound frequencies, the risk of the occurrence of hearing damage is assessed as high.

The results of the subjective test confirmed the annoyance of exposure to this type of noise in the environment. In the relation between objective and subjective results of exposure to this hazard factor in the work environment, it is necessary to take appropriate preventive actions (technical organizational and medical actions) (Regulation of the Minister of Health and Social Policy of 30 May 1996 Regulation of the Minister of Economy and Labour of August 5, 2005). Devices emitting high frequency noise should be equipped by the manufacturers with means of technical protections against noise (soundproof and isolation casings shields or silencers) (DOBRUCKI *et al.*, 2010). In the case when those ways of noise limitations at workplaces are impossible, the employer should fit the workers with hearing protections or plugs. When the measurements of noise parameters in reference to an 8-hour workday the MAI values are exceeded, a properly time of work or even a full stop of activity should be implemented as well as employees’ rotation. Technical and organizational activities have to be used at the same time with medicine prevention. A preliminary and periodic medical care should be provided.

Acknowledgments

This paper has been based on the results of a research task carried out within the scope of the second stage of the National Programme “Improvement of safety and working conditions” supported partly in 2011–2013 – within the scope of research and development – by the Ministry of Science and Higher

Education/National Centre for Research and Development. The Central Institute for Labour Protection – National Research Institute is the Programme’s main coordinator.

References

1. DOBRUCKI A., ŻÓŁTOGÓRSKI B., PRUCHNICKI P., BOLEJKO R. (2010) *Sound-Absorbing and Insulating Enclosures for Ultrasonic Range*, Archives of Acoustics, **35**, 2, 157–164.
2. PAWLACZYK-ŁUSZCZYŃSKA M., DUDAREWICZ A., ŚLIWIŃSKA-KOWALSKA M. (2007), *Theoretical Predictions and Actual Hearing Threshold Levels in Workers Exposed to Ultrasonic Noise of Impulsive Character-A Pilot Study*, JOSE, **13**, 4, 409–418.
3. *Regulation of the Minister of Health and Social Policy of 30 May 1996 on conducting the medical examination of employees, range of medical prevention and medical decisions given on the purposes specified in the Labour Code* [in Polish: *Rozporządzenie MZiOS z dnia 30 maja 1996 w sprawie przeprowadzania badań lekarskich pracowników, zakresu profilaktycznej opieki zdrowotnej nad pracownikami oraz orzeczeń lekarskich wydawanych dla celów przewidzianych w Kodeksie Pracy*], Journal of Laws of 1996 No 69, item 332 as amended; Journal of Laws of 1997 No 60, item 375; Journal of Laws of 1998 No 159, item 1057; Journal of Laws of 2001 No 37, item 451.
4. *Regulation of the Council of Ministers of 10 September 1996, on the list of works prohibited to women* [in Polish: *Rozporządzenie Rady Ministrów z dnia 10 września 1996 r. w sprawie wykazu prac wzbronionych kobietom*], Journal of Laws of 1996 No 114, item 545 as amended; Journal of Laws of 2002 No 127, item 1092.
5. *Regulation of the Minister of Labour and Social Policy of 29 November 2002 on the maximum admissible concentration and intensities for agents harmful to health in the working environment* [in Polish: *Rozporządzenie Ministra Pracy i Polityki Socjalnej z dnia 29 listopada 2002 r. w sprawie najwyższych dopuszczalnych stężeń i natężeń czynników szkodliwych dla zdrowia w środowisku pracy*], Journal of Laws No 217, item 1833, as amended; Journal of Laws No 212 item 1769 of 28 October 2005.
6. *Regulation of the Council of Ministers of 24 August 2004, on the list of works prohibited to juveniles and the conditions of their employment for performance of some of these works* [in Polish: *Rozporządzenie Rady Ministrów z dnia 24 sierpnia 2004 r. w sprawie wykazu prac wzbronionych młodocianym i warunków ich zatrudnienia przy niektórych z tych prac*], Journal of Laws of 2004 No 200, item 2047 as amended; Journal of Laws of 2005 No 136, item 1145.
7. *Regulation of the Minister of Economy and Labour of 5 August 2005 on safety and hygiene at work for works related with exposure to noise or mechanical vibrations* [in Polish: *Rozporządzenie Ministra Gospodarki i Pracy z dnia 5 sierpnia 2005 r. w sprawie bezpieczeństwa i higieny pracy przy pracach związanych z narażeniem na hałas lub drgania mechaniczne*], Journal of Laws No 157, item 1318.
8. SMAGOWSKA B. (2010), *Ultrasonic noise at workstations with machinery and devices with air compression* [in Polish with an abstract in English: *Hałas ultradźwiękowy na stanowiskach maszyn i urządzeń ze sprężonym powietrzem*], Bezpieczeństwo Pracy, **7–8**, 38–41.
9. SMAGOWSKA B. (2012), *Ultrasonic noise at selected workstations of textile machines – occupational risk assessment* [in Polish with an abstract in English: *Hałas ultradźwiękowy na stanowiskach pracy maszyn włókienniczych – ocena ryzyka zawodowego*], Przegląd włókienniczy – włókno, odzież, skóra, **2**, 42–46.
10. SMAGOWSKA B. (2013), *Ultrasonic noise sources in the work environment*, Archives of Acoustics, **38**, 2, 169–176.
11. SMAGOWSKA B., MIKULSKI W. (2012), *Lab research on the influence of ultrasonic noise on human cognitive skills and psychomotor capability* [in Polish with an abstract in English: *Badania laboratoryjne wpływu hałasu ultradźwiękowego na funkcje poznawcze i sprawność psychomotoryczną człowieka*], Bezpieczeństwo Pracy, **5**, 24–26.

Influence of Material Used for the Regenerator on the Properties of a Thermoacoustic Heat Pump

Bartłomiej KRUK

*Chair of Acoustics and Multimedia, Faculty of Electronics, Wrocław University of Technology
Janiszewskiego 7/9, 50-372 Wrocław Poland; e-mail: bartlomiej.kruk@pwr.wroc.pl*

(received October 5, 2012; accepted October 24, 2013)

Research in thermoacoustics began with the observation of the heat transfer between gas and solids. Using this interaction the intense sound wave could be applied to create engines and heat pumps. The most important part of thermoacoustic devices is a regenerator, where process of conversion of sound energy into thermal or *vice versa* takes place. In a heat pump the acoustic wave produces the temperature difference at the two ends of the regenerator. The aim of the paper is to find the influence of the material used for the construction of a regenerator on the properties of a thermoacoustic heat pump. Modern technologies allow us to create new materials with physical properties necessary to increase the temperature gradient on the heat exchangers. The aim of this paper is to create a regenerator which strongly improves the efficiency of the heat pump.

Keywords: thermoacoustics, heat pump, engines, traveling wave.

1. Introduction

Thermoacoustics refers to a physical phenomenon by which a temperature difference can create and amplify sound waves and *vice versa*: the sound wave causes the formation of the temperature difference between the two heat exchangers. The principle of operation equipment involves the use of a cyclic interaction between the acoustic waves and gas particles. Under the influence of an acoustic wave, gas particles oscillate near the equilibrium position causing perturbations of pressure and displacement. In thermoacoustic devices, the acoustic wave is brought to interact with the porous structure, called regenerator. The regenerator is made of a material with a much higher heat capacity compared to the gas medium through which the sound wave propagates. The function of regenerators in thermoacoustic systems is an exchange and temporary storage of heat. A thermoacoustic layout can be generally divided into two segments:

- the part containing a thermodynamic regenerator, two heat exchangers and a thermal buffer column;
- the acoustic system that provides adequate conditions for the acoustic wave (a waveguide and sound source).

The people who worked as glassblowers were the first to observe the thermoacoustic effect. They no-

ticed that the heated pipes for blowing glass made sounds. In 1777, Byron Higgins observed that placing the flame at both ends of an open tube resulted in the appearing of an audible sound. Another described example of this phenomenon is the P.L. Rijke pipe reported in 1859 (WARD, SWIFT, 1996). He observed that placing hot metal at the bottom of both ends of an open tube leads to an emergence of strong oscillations of gas molecules. The tube generates a sound only at the vertical orientation. Rijke's tube closed at one end can generate a sound if the end is heated. This phenomenon was observed by a German physicist Sondhauss. Currently the Sondhauss Tube is known as the first heat engine (transformation of thermal energy into the acoustic wave – mechanical work).

After discovering the phenomena mentioned above, it was also found that they are reversible, i.e. acoustic vibrations can be produced by the heat flow, or *vice versa* – a heat flow can be produced by acoustic vibrations.

2. Classification of thermoacoustic devices

Devices in thermoacoustics can be classified according to the type of operation (engines, heat pumps),

used materials (regenerators, stacks), and with respect to the type of acoustic wave (standing and running waves). According to Garrett thermoacoustic devices can be divided in the following way:

- engines with a standing wave;
- heat pumps working with a travelling wave;
- engines with a travelling wave;
- heat pumps working with a standing wave.

2.1. Classification of devices with respect to the type of wave

Waves can be classified according to the phase difference between the sound pressure p and the acoustic velocity v (DOBRUCKI, 2007). CEPERLEY (1979; 1982) reasoned why running waves are more appropriate in thermoacoustic processes. Thermoacoustic devices based on a travelling wave feature an advantage that the pressure and velocity are in phase while the wave passes through the regenerator (BACKHAUSE, 2002). The gas enters a cycle of compression, heating, expansion and cooling, similar to the cycles in Stirling or Carnot engine.

Because the pores in the regenerator are small, as compared with the thermal penetration depth parameter ($r_h \ll \delta_\kappa$), the thermal contact between the particles of gas and the regenerator elements will be almost perfect (SCHUTTE, 2009). As a result, there is a constant exchange of heat between the gas and the material that takes place over a vanishingly small temperature difference, which causes a slight increase in entropy.

Figures 1 and 2 explain why the hydraulic radius r_h must be substantially smaller than δ_κ . If the thermal contact is poor ($r_h \simeq \delta_\kappa$), heating and cooling are delayed and the device using traveling waves works ineffectively. The ineffective work of the thermoacoustic device contributes to the shifting of 2 and 4.

This phenomenon can be used to make the work of a thermoacoustic device more efficient, provided that the traveling wave is changed into a standing wave.

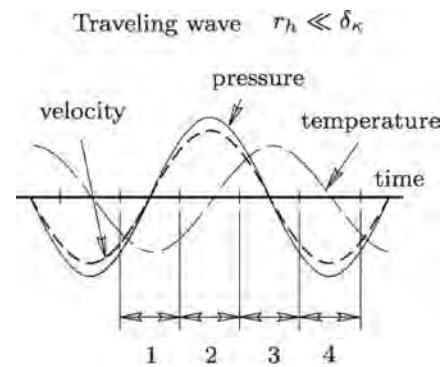


Fig. 1. Pressure and acoustic velocity as a function of time for a travelling wave ($r_h \ll \delta_\kappa$).

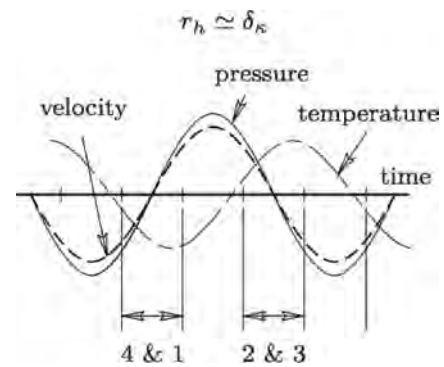


Fig. 2. Pressure and acoustic velocity as a function of time for a traveling wave ($r_h \simeq \delta_\kappa$).

If the wave propagates in the direction of the temperature gradient, the system works as an engine. However, if the propagation direction is opposite to the gradient of temperature, the system works as a heat pump.

3. Measurement arrangement

The measurement setup is shown in Fig. 3. Since the measurements are time-consuming, the measurement position is fully automated. The whole measurement is being controlled by a computer with software created in LabView.

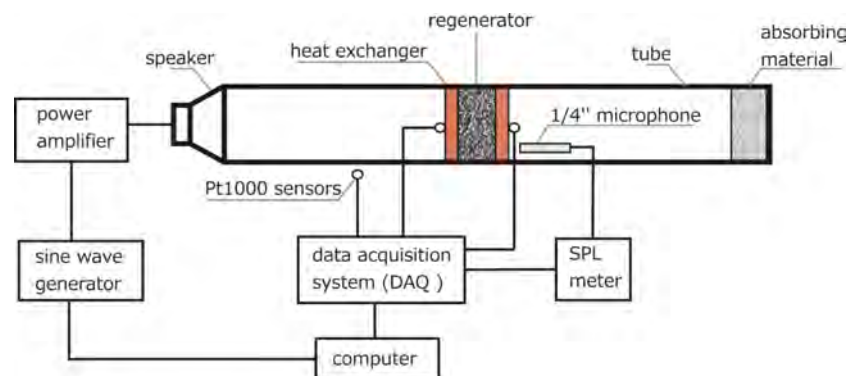


Fig. 3. Measurement arrangement.

The materials used to build the regenerator were supplied by the University of Twente (Netherlands). The following materials have been tested: aluminum, steel, politetrafluoroethylene (PTFE), rockwool, glasswool.

The material shown in Fig. 4 is made of aluminum molded foam.



Fig. 4. Left – aluminum, right – enlargement of the material.

The material shown in Fig. 5 was cut from a grid made of steel wire with the diameter of 0.01 mm.

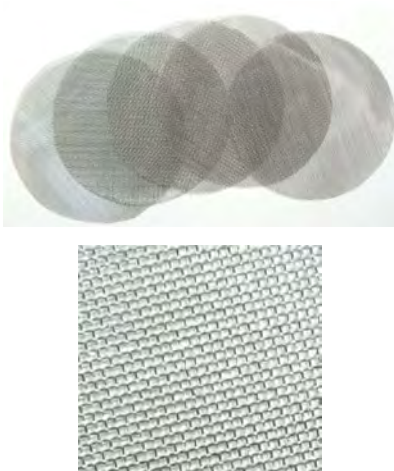


Fig. 5. Top – steel, bottom – enlargement of the material.

The material shown in Fig. 6 was made of politetrafluoroethylene. For the improvement of the thermoacoustic properties of the material, there have been drilled holes with the diameter of 0.01 mm. If these holes are closed the material will lose its improved properties.

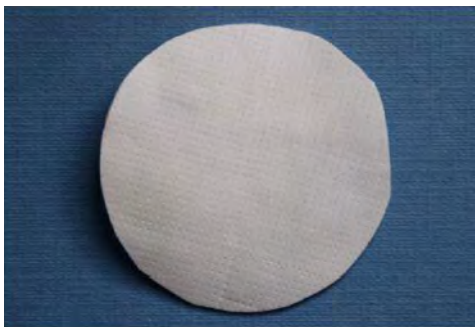


Fig. 6. Material – politetrafluoroethylene.

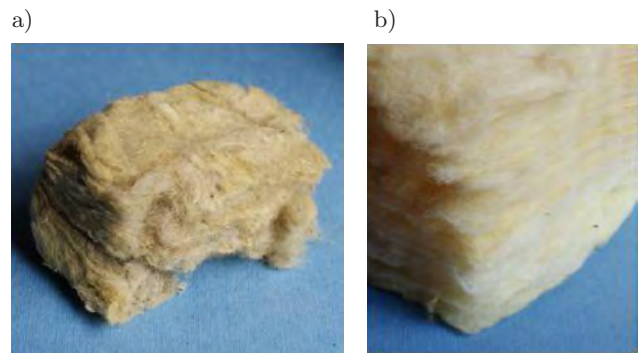


Fig. 7. Material: a) rockwool, b) glasswool.

A heat exchanger is a piece of equipment built for an efficient heat transfer from one medium to another. In the described thermoacoustic heat pump, heat exchangers are used to inject and remove heat from the system. Heat exchangers are made of copper. This material features very good thermal conductivity characteristics necessary for efficient operation of the entire device. The heat exchanger is shown in Fig. 8.



Fig. 8. Heat exchanger.

A modular design allows to create regenerators of any thickness. It allows to verify the influence of thickness on the differences in temperature between hot and cold heat exchangers. The example regenerator module is shown in Fig. 9.

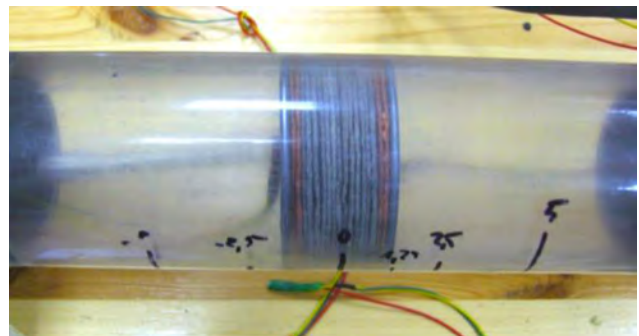


Fig. 9. Regenerator module – aluminum width 2005 mm.

4. Results

A single measurement point should take about 5.5 minutes to assure the stabilization of temperature on

the heat exchangers. The sound pressure level was measured with a 1/4" microphone at the cold heat exchanger. The measurements were carried out for the pressure level of 140 dB. In order to match the impedance at the end of the waveguide, the absorbing material with absorption coefficient close to unity is attached to its end.

Removal of the absorbing material of the pipe causes formation of standing waves. That is the reason

why for frequencies above 150 Hz the device does not work properly. This relationship is shown in Fig. 10.

Figure 11 shows the dependence of the absorption coefficient on the frequency.

The temperature difference between the hot and cold ends of the heat exchanger is shown in Fig. 12.

One can see the importance of the regenerator in the thermoacoustic device but a more important thing is the particular material it was made of.

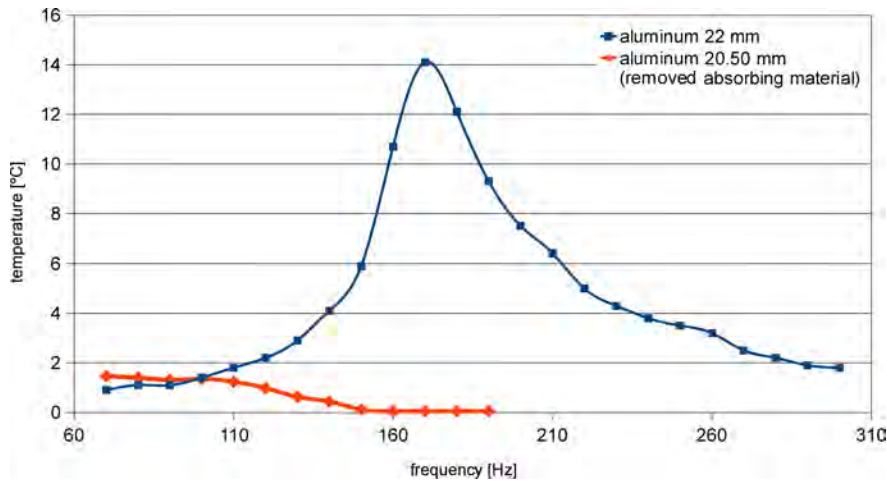


Fig. 10. Temperature gradient as a function of the frequency depending on the impedance matching waveguide.

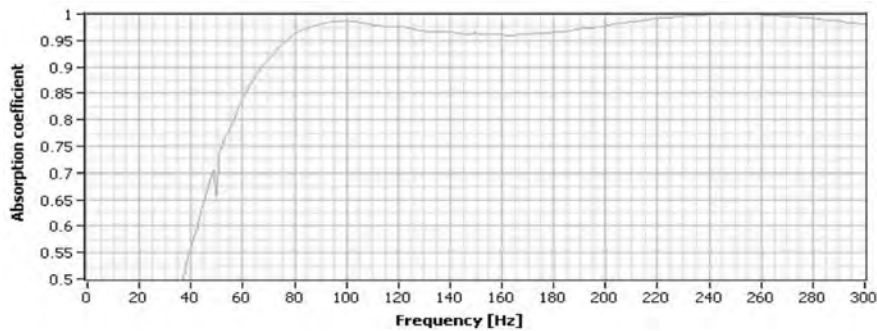


Fig. 11. Dependence of the absorption coefficient on the frequency for the absorbing material at the end of a tube.

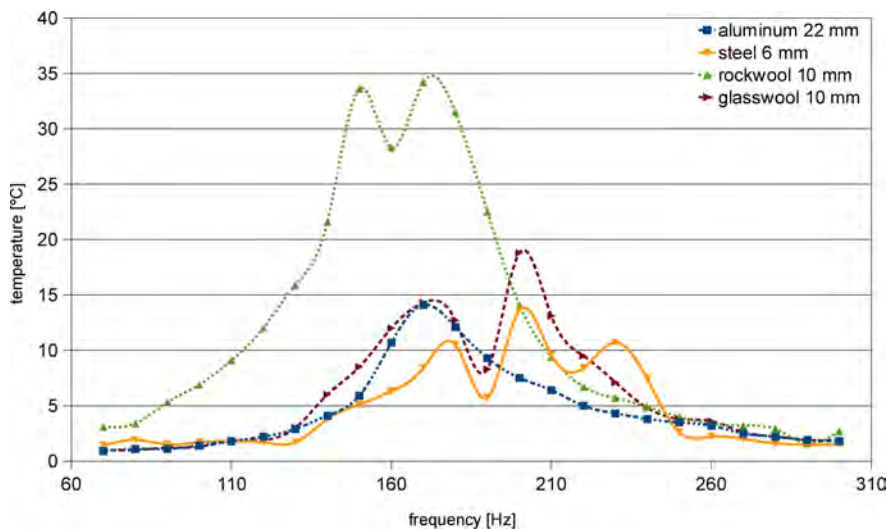


Fig. 12. Temperature gradient as a function of the frequency depending on the material of the regenerator.

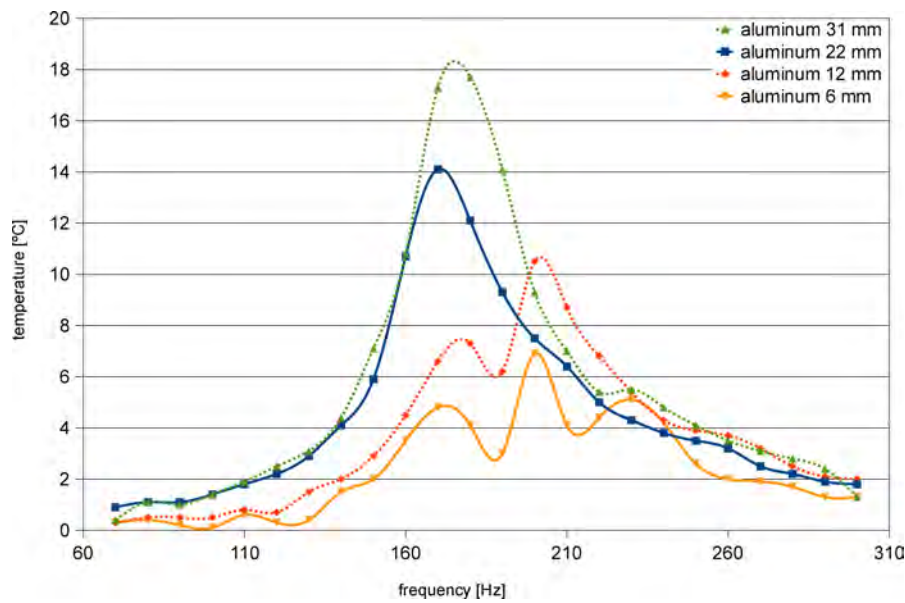


Fig. 13. Temperature gradient as a function of the frequency, depending on the width of the regenerator, material – aluminum.

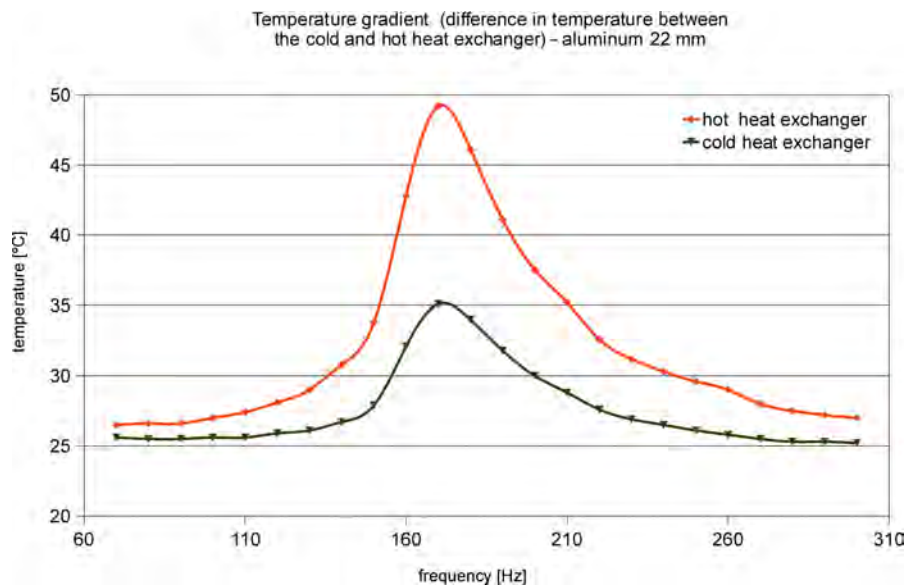


Fig. 14. Regenerator temperature as a function of the frequency.

Figure 13 presents the results of the temperature gradient as a function of the frequency depending on the width of the regenerator. One can see the relation between the width of the regenerator and the frequency bandwidth where maximum temperature differences appear.

Figure 14 shows the temperature of the hot and cold heat exchangers as a function of the frequency.

5. Conclusions

Comparing the present results with the data obtained before the modification of the measuring ar-

rangement (JANOWICZ, 2011; DOBRUCKI *et al.*, 2012) significantly important differences can be observed. These differences result from a change of an acoustic pressure level place (the measurement of pressure on the cold heat exchanger) and the use of accurate measuring devices (for example: the use of PT1000, which has greater sensitivity and accuracy as compared to k-type thermocouples used in previous measurements). In Table 1 the results obtained in the study by JANOWICZ (2011) are presented.

The maximum values of temperature differences between the hot and cold heat exchangers for the tested materials are summarized in Table 2.

Table 1. Summary of the results – JANOWICZ (2011).

material	width [mm]	f [Hz]	t_2-t_1 [°C]
aluminum	6.0	280	5.8
steel	6.0	280	9.8
glasswool	40	280	4
rockwool	23	280	18

Table 2. Summary of the results.

material	width [mm]	f [Hz]	t_2-t_1 [°C]
aluminum	31	180	17
	22	170	14.1
	12	200	10.5
	6	200	6.9
steel	6	200	6.9
glasswool	18.8	200	18.8
rockwool	10	170	34.2
PTFE	10	120	3.4

Comparing the results it can be seen that the implemented modifications significantly improved the obtained temperature gradients.

As it can be seen the best properties were obtained for aluminum and mineral wool: the temperature differences at both ends of the regenerator reached the value of 34°C. Much worse properties were observed for PTFE and glasswool, for which at frequencies higher than 120 Hz, the temperature changes could not be observed. This is caused by the lack of transparency for an acoustic wave.

These studies are the beginning of work on a heat pump. In the future the results may support the construction of a thermoacoustic engine. In order to optimize the geometric dimensions of the regenerator, it is necessary to measure the gas flow resistivity of compared materials.

The results can be used to create the optimal material needed to build the regenerator. At the present state the temperature differences in the heat exchanger may reach the value of about 35°C.

References

1. BACKHOUSE S., SWIFT G. (2002), *New varieties of thermoacoustic engines*, LA-UR-02-2721, 9th International Congress on Sound and Vibration, July 2002.
2. CEPERLAY P.H. (1979), *A pistonless Stirling engine – the traveling wave heat engine*, J. Acoust. Soc. Am., **66**, 1508–1513.
3. CEPERLAY P.H. (1982), *Resonant travelling wave heat engine*, US Patent 4, 355, 517.
4. DOBRUCKI A. (2007), *Electroacoustic transducers* [in Polish: *Przetworniki elektroakustyczne*], WNT, Warszawa.
5. DOBRUCKI A., JANOWICZ K., OWCZAREK P. (2012), *Research on materials used in thermoacoustic device with travelling wave*, Proceedings International Conference Euronoise, pp. 811–814, Prague.
6. JANOWICZ K. (2011), *Maximization of the intensity of an acoustic wave in the thermoacoustic engine – analysis of arrangement and experiments* [in Polish], MSc. thesis, Wrocław University of Technology.
7. KRUK B. (2012), *Influence of material used for regenerator on properties of a thermoacoustic heat pump with traveling wave*, Proceedings on 59th Open Seminar of Acoustics, pp. 133–136, Boszkowo.
8. SCHUTTE A. (2009), *Thermoacoustics-Numerical modeling and experimental validation*, MSc. thesis, University of Twente.
9. WARD B., SWIFT G. (1996), *Design Environment for Low-Amplitude ThermoAcoustic Engines*, LA-CC-93.
10. ŻMUDZKI S. (1993), *Stirling engine* [in Polish: *Silniki Stirlinga*], WNT, Warszawa.

In Memoriam

Professor Marian URBAŃCZYK



1948–2013

Polish acoustical community mourns the loss of Professor Marian Urbańczyk who passed away on July 10, 2013.

Professor Marian Urbańczyk was born on February 2nd, 1948, in Katowice (Poland). There he attended the Silesian Technical College (Śląskie Techniczne Zakłady Naukowe), where he was a student of the electrical engineering and electronics class and in 1967 completed his secondary education with school-leaving examination and a honorary mention. In 1973, he graduated successfully (again with distinction) from the Faculty of Electrical Engineering at the Silesian University of Technology (Politechnika Śląska) in Gliwice. The same year he has joined the SUT's Institute of Physics as a university teacher at the newly created Faculty of Mathematics and Physics. The late Professor Urbańczyk remained connected with the Institute until 2009, from 2007 to 2009 performing the function of its Deputy Director for Students' Affairs.

The scope of the Professor's scientific interest comprised electronics of solid state, metrology, and technical physics, with special attention paid by him to acoustics, including acoustoelectronic systems and their applications in technology and metrology.

In 1981, Marian Urbańczyk delivered his doctor's dissertation concerning technical acoustics at the Institute of Fundamental Problems of Technology Polish Academy of Sciences (IPPT PAN) in Warsaw. In the year 1999, he was granted the post-doctoral degree (habilitation) by the Council of the Faculty of Electronics at the Wrocław University of Technology. In 2012, Marian Urbańczyk was made full professor by the President of Poland.

The Silesian University of Technology in Gliwice remained the scene of Professor Urbańczyk's scientific activity to the very end of his life.

Since September 1, 2009, Professor had been working at the Department of Optoelectronics at the SUT's Faculty of Electrical Engineering, acting as its Deputy Director.

Professor Marian Urbańczyk was a promoter of several doctor's dissertations and numerous master theses. In the framework of his didactic work, he has organized many students' laboratories and workshops. He was also the author of a wide variety of teaching curriculums (syllabuses). The late Professor Urbańczyk was highly valued both by his students and co-workers.

Professor Marian Urbańczyk was an unquestionable authority in the field of technical acoustics,

metrology, and electronics, and an internationally acknowledged author (and co-author) of more than 200 scientific publications, nearly 50 of them having been included in the ISI list. His papers were published in highly-ranked journals and frequently cited by other authors. He was also the co-author of numerous patents and patent applications.

The Professor was a member of Scientific Committees of many conferences, both domestic and international.

Professor Marian Urbańczyk was a member of many international and Polish scientific societies, including the European Acoustical Association (EAA), the International Optical Engineering Society (SPIE), the Polish Acoustical Society (PTA), the Photonic Society of Poland, the Polish Physical Association (PTF), and the Polish Association of Sensor Technology (PTTS).

Since 1975, Professor Urbańczyk was a member of the Polish Acoustical Society (PTA), elected later the Member of the Main Board of this organization and

the Chairman (Local President) of the Board of Upper Silesia Branch of the PTA.

The Professor acted also as a co-organizer of annual international conferences, including the Winter School on Wave and Quantum Acoustics and the Workshop on Acoustoelectronics.

For his scientific achievements, Professor Urbańczyk has been awarded state orders, medals, and scientific rewards.

Professor Urbańczyk's death is an irreparable loss to the Silesian University of Technology, the Polish Acoustical Society, and the whole Polish scientific community.

Professor Marian Urbańczyk was an extraordinary person, always very kind-hearted and understanding for others. For those who knew him personally, he was a Friend and a Master.

And as the Friend and the Master we will retain him in our fond memory.

Tadeusz Pustelny

In Memoriam

Professor Mikołaj ŁABOWSKI



1935–2013

Mikołaj Łabowski, Professor Emeritus at the Institute of Acoustics, Adam Mickiewicz University in Poznań, passed away on the 18th of October, 2013.

Professor Mikołaj Łabowski was born on the 17th of December, 1935, in Florynka in the southern part of Poland. He graduated from the Faculty of Mathematics, Physics and Chemistry of the Adam Mickiewicz University receiving his Master of Science degree in physics in 1962. Eight years later he obtained his PhD title from the same university. In 1981, on the basis of the book “Ultra- and hypersonic properties of selected liquids and critical mixtures” he obtained the degree of habilitated doctor. The President of Poland awarded him the titles of Associate Professor in Physics in the year 1991 and Full Professor in 1999.

From 1985 to 1987, Mikołaj Łabowski held the post of Vice-Dean for Students’ Affairs at the Faculty of Mathematics and Physics of the Adam Mickiewicz University. In the years 1996–1999, he was the Director of the University’s Institute of Acoustics. He held many posts in the Polish Acoustical Society, of which he was a Honorary Member. He always served with advice and assistance in scientific matters to the Committee of Acoustics of the Polish Academy of Sciences.

Professor Łabowski was an outstanding scientist, one of the founders of ultrasonic physics in Poland. After returning from scholarship in the Lomonosov University in Moscow, he became an expert in the field of ultrasonic studies of liquids and liquid mixtures. His groundbreaking works on ultrasonic properties of critical binary mixtures opened up new perspectives in the research of dynamic phenomena in the vicinity of critical temperatures. Professor Łabowski’s outstanding scientific achievements were recognized by rewarding him the Minister of Education Prize in the years 1981 and 1987.

Throughout his whole professional career associated with the Adam Mickiewicz University in Poznań, Professor Łabowski has published over 100 papers, mostly in renowned international scientific journals, and carried out an intensive teaching activity. Through his profound knowledge and enthusiasm, Professor Mikołaj Łabowski continuously inspired colleagues and collaborators and decisively shaped the development of ultrasonic physics in Poznań.

With the death of Professor Mikołaj Łabowski, Polish acoustics has lost a great researcher, teacher, and scholar.

Tomasz Hornowski

Calendar of events

Conferences

Conferences in Poland

XLII Winter School on Vibroacoustical Hazards Suppressions, 3–7 March 2014, Szczyrk
<http://ogpta.polsl.pl/oddzial/>

XLIII Winter School on Wave and Quantum Acoustics, 3–7 March 2014, Szczyrk, <http://ogpta.polsl.pl/oddzial/>

XXXI Symposium on Hydroacoustics, May 13–16, 2014, Świnoujście, <http://www.sha2014.pl/>

LXI Open Seminar on Acoustics, 7–12 September 2014, Kraków, <http://www.osa2014.agh.edu.pl>

International Conferences

5–9 May, Providence, USA 167th Meeting of the Acoustical Society of America
<http://www.acousticalsociety.org>

1–5 June, Nara, Japan 11th International Congress on Noise as a Public Health Problem (ICBEN 2014)
<http://www.icben2014.com/>

22–27 June, island of Rhodes, Greece 2nd International Conference and Exhibition on Underwater Acoustics
<http://www.uaconferences.org>

6–10 July, Beijing, China 21th International Congress on Sound and Vibration (ICSV21)

7–12 September, Krakow, Poland Forum Acusticum 2014
<http://www.fa2014.pl/>

6–10 October, Prague, Czech Republic 11th European Conference on Non Destructive Testing
<http://www.ecndt2014.com/>

27–31 October, Indianapolis, USA 168th Meeting of the Acoustical Society of America
<http://www.acousticalsociety.org>

29–31 October, Murcia, Spain TECNIACUSTICA 2014 MURCIA, 45th Spanish Congress on Acoustics, 8th Iberian Congress on Acoustics, European Symposium on Smart Cities and Environmental Acoustics
<http://www.sea-acustica.es>

16–19 November, Melbourne, Australia Internoise 2014
<http://www.internoise2014.org>

FROM THE EDITORIAL BOARD

The Editorial Committee wishes to express many thanks and appreciation to all the reviewers, listed below, for their valuable opinions concerning papers submitted to the Archives of Acoustics in 2013:

Jan Adamczyk	Jędrzej Kociński	Dariusz Pleban
Danuta Augustyńska	Piotr Kokowski	Anna Preis
Andrzej Balcerzak	Janusz Kompała	Andrzej Rakowski
Wojciech Batko	Peter Kopcansky	Zbigniew Ranachowski
Alexandra Bendixen	Danijel Korzinek	Wojciech P. Rdzanek
Romuald Bolejko	Krzysztof Kosala	Daniel Recasens
David Bradley	Bożena Kostek	Enrique Riera
Adam Brański	Vasyl Kovalchuk	Tomira Rogala
Peter Bury	Janusz Kowal	Barbara Rudno-Rudzińska
Jorge Camacho	Piotr Krzyworzeka	Krzysztof Rudno-Rudziński
Czesław Cempel	Radosław Kucharski	Bjoern Schuller
Ireneusz Czajka	Andrzej Kulowski	Brian Seymour
Zbigniew Dąbrowski	Lucyna Leniowska	Aleksander Sęk
Juan J. del Coz Diaz	Marcin Lewandowski	Jan Sikora
Andrzej Dobrucki	Adam Lipowczan	Ewa Skrodzka
Raffaele Dragonetti	Wojciech Łapka	Manuel Sobreira Seoane
Szymon Drgas	Piotra Łobacz	Lars Söderholm
Zbigniew Engel	Jacek Marszał	Marek Szary
Stefan Ernst	Philippe Martin	Joanna Szczucka
Wiesław Fiebig	Mirosław Meissner	Krzysztof Szemela
Neville Fletcher	Wojciech Michalski	Krzysztof Szlifirski
Ignacy Gloza	Witold Mikulski	Antoni Śliwiński
Zdzisław Gosiewski	Marianna Mirowska	Ewa Świercz
Tadeusz Gudra	Andrzej Miśkiewicz	Kazuo Tanabe
Fusheng Han	Rafał Młyński	Jarosław Tęgowski
Ji-Huan He	Robert Mores	Marian Urbańczyk
Edward Hojan	Leszek Morzyński	Stefan Weyna
Urszula Jorasz	Paweł Mrówka	Jerzy Wiciak
Mariusz Kaczmarek	Józef Nizioł	Jacek Wierzbicki
Tadeusz Kamisiński	Barbara Okoń-Makowska	Arnold Wilczyński
Julius Kaplunov	Vincent Pagneux	Taichi Yazaki
Maciej Karpiński	Ryszard Panuszka	Paulo H.T. Zannin
Cezary Kasprzak	Marek Pawełczyk	Adam Zieliński
Piotr Kielczyński	Andrzej Pawelek	Tomasz Zieliński
Maurycy J. Kin	Małgorzata Pawlaczyk-Łuszczczyńska	Edward Zorębski
Piotr Kleczkowski	Krystyna Pawlas	Bronisław Żółtógórski
Zygmunt Klusek	Janusz Piechowicz	

43rd Winter School on Wave and Quantum Acoustics

10th Winter Workshop on Molecular
Acoustics, Relaxation and Calorimetric
Methods (MAR&CM)

10th Winter Workshop on Acoustoelectronics (AE)

19th Winter Workshop on Photoacoustics
and Thermal Waves Methods (PA&TWM)

2014.03.03 - 2014.03.07
Hotel "META", Szczyrk POLAND
<http://ogpta.polsl.pl>

XLII Szkoła Zimowa Zwalczania Zagrożeń Wibroakustycznych (SZ ZZW)

Głównym organizatorem konferencji jest:
Oddział Górnośląski
Polskiego Towarzystwa Akustycznego



<http://ogpta.polsl.pl>

2014.03.03 - 2014.03.07
Hotel "META"
Szczyrk Beskidy POLAND

Świnoujście, May 13-16, 2014



XXXI SYMPOSIUM ON HYDROACOUSTICS

House of Creative Work of the Polish Academy of Science
H. Sienkiewicza 18
72-600 Świnoujście

Organizers:

The Committee on Acoustics of the Polish Academy of Sciences -
Section of Underwater Acoustics, Ultrasound and Medical Acoustics
Polish Acoustical Society - Gdansk Division
Gdansk University of Technology
Polish Naval Academy in Gdynia

www.sha2014.pl

AIMS AND SCOPE

Archives of Acoustics, the peer-reviewed quarterly journal publishes original research papers from all areas of acoustics like:

- acoustical measurements and instrumentation,
- acoustics of musics,
- acousto-optics,
- architectural, building and environmental acoustics,
- bioacoustics,
- electroacoustics,
- linear acoustics,
- noise and vibration,
- nonlinear acoustics,
- psychoacoustics,
- physical and chemical effects of sound,
- physiological acoustics,
- speech processing and communication systems,
- speech production and perception,
- transducers,
- ultrasonics,
- underwater acoustics,
- quantum acoustics.

INFORMATION FOR AUTHORS

ARCHIVES OF ACOUSTICS the journal of Polish Academy of Sciences (a quarterly founded in 1976), publishes original papers concerning all fields of acoustics. Basically, the papers should not exceed 40 000 typographic signs (about 20 typewritten pages).

Submitted papers must be written in good English.

Follow this order when typing manuscripts: Title, Authors, their affiliations and e-mails, Abstract, Keywords, Main text, Acknowledgments, Appendix, References, Figure Captions and then Tables.

Special care must be attached to the following rules:

1. Text should be submitted with double-lined spacing and preferably in a 12 point font size. The text should be in single-column format.
2. The title of the paper should be as short as possible.
3. Full names and surnames should be given.
4. The full postal address of each affiliation, including the country name should be provided. Affiliations should contain the full postal address, as well as an e-mail address of one author designated as corresponding author.
5. The text should be preceded by a concise abstract (less than 200 words).
6. Keywords should be given. It is also desirable to include a list of notations.
7. The formulae to be numbered are those referred to in the paper, as well as the final formulae. The formula number should be written on the right-hand side of the formula in round brackets.
8. All notations should be written very distinctly.
9. Vectors should be denoted by semi-bold type. Trigonometric functions are denoted by sin, cos, tan and cot, inverse trigonometric functions – by arcsin, arccos, arctan and arccot; hyperbolic functions are denoted by sinh, cosh, tanh and coth.
10. References in the text (author(s) and year of publication) are to be cited between parentheses.
11. All cited works within the text must be included in the References Section, and arranged in alphabetical order by authors' last name. Number them from 1 to n.
12. Acknowledgments should be included in a section before the references.
13. Items appearing in the reference list should include the surname and the initials of the first name of the author, the full title of the paper/book in English followed by the information on the original paper language.
In case of a book, the publisher's name, the place and year of publication should be given.
In case of a periodical, the full title of the periodical, consecutive volume number, current issue number, pages, and year of publication should be given; the annual volume number must be semi-bold so as to distinguish it from the current issue number.
14. For more information on references see <http://acoustics.ippt.pan.pl/Instructions.pdf>

Each manuscript is initially evaluated by the Editor and then allocated to an Associate Editor according to specific subject area. Upon receiving the Associate Editor's list of potential reviewers, the Editorial Office forwards it to reviewers. The Editor and the Associate Editors make the final recommendation. Their opinions are the basis for the Editorial Committee to determine whether the paper can be accepted for publication or not.

The Word or L^AT_EX source and pdf files of the final version of articles will be requested after acceptance for publication. High-quality illustrations (format bitmap (gif, jpg) or PostScript, with resolution no lower than 300 dpi) should be sent along with the manuscript.

After publication CD-ROM containing PDF version of article will be sent to authors.

*EDITORIAL BOARD
ARCHIVES OF ACOUSTICS*

SUBSCRIPTION

Subscription orders for "Archives of Acoustics" may be sent to:

Editorial Office "Archives of Acoustics"
Pawińskiego 5B, 02-106 Warszawa, Poland
phone: (48-22) 826 12 81 ext. 206
fax (48-22) 826 98 15
e-mail: akustyka@ippt.pan.pl

Information about subscription are available in <http://acoustics.ippt.pan.pl>

Instructions for citation and bibliographic references

References in the text (author(s) and year of publication) are to be cited between parentheses.

1. Direct quotations should be between quotation marks.

2. Indirect quotations (i.e. when the author's idea is explained but not directly quoted) do not use quotation marks or italics.

Examples:

- a. The research of mufflers was started by Davis (1954).
- b. To increase the muffler's acoustical performance, the assessment of a new acoustical element – a reverse-flow mechanism with double internal perforated tubes – was proposed and investigated by this author (Munjaj, 1987),

3. When an author or group of authors has more than one publication in the same year a lower case letter is added to the date.

Example:

In two recent studies (Rakowski, 1993a; 1993b) it was suggested that...

4. Multiple author citation:

a. Two authors: both names should be listed in each citation.

Example: (Rakowski, Miyazaki, 2007)

b. Three or more authors: use the first author's name and "*et al.*"

Example: (Dobrucki *et al.*, 2005)

5. To cite a document produced by an organization, the first time write out the name of the organization in full and give the acronym or abbreviation in square brackets. For subsequent references you may use the acronym or abbreviation.

Example:

First time: Sanitary politics (United Nations High Commissioner for Refugees [UNHCR], 2006, p. 35)...

Then: Established politics (UNHCR, 2006, p. 45)...

In the reference list write the full name of the organization.

6. When a source has no identified author, cite the first two or three words of the title (in italics if it is a book, between quotation marks if it is an article) followed by the year and the page.

Examples:

In the recent book (*Encyclopedia of Physics*, 1993, p. 164)...

In the article ("*The relation of pitch ...*", 1979, p. 67) it is held that...

The in-text reference should match the start of the reference in the bibliography/reference list.

7. Using quotations in the text may also be as it is shown in the following examples:

Examples:

a. "Field measurements of bistatic scattering strength (BSSS) are difficult and expensive to acquire at sea, in real conditions." (Blondel, Pace, 2009, p. 101)

b. Blondel and Pace (2009) held that "field measurements of bistatic scattering strength (BSSS) are difficult and expensive to acquire at sea, in real conditions" (pp. 101)

8. To cite a work that was discovered in another work, observe the following examples:

a. Brown (1967), cited by Smith (1970, p. 27), found...

b. It was found (Brown, 1967, cited by Smith, 1970, p. 27) that...

9. To cite e-mail messages:

If necessary, cite them within the body of the text as a personal communication.

Example:

a. ...and this point was conceded (S. Weyna, personal communication, August 22, 2001), ...

Presenting bibliography/reference list

General matters

a. Reference list should be arranged alphabetically by author surname. Put all the entries in one long alphabetical list. Do not list books, journal articles, websites, etc. in separate sections. Number them from 1 to n.

Example:

- 1.
- 2.
- 3.

b. When an author or group of authors has more than one publication in the same year a lower case letter is added to the date. This letters will be used when citing this source in the text.

Example:

- Zou D., Crocker M.J (2009a), *Response of a plate to PZT actuators*, Archives of Acoustics, **34**, 1, 13–23.
Zou D., Crocker M.J (2009b), *Sound power radiated from rectangular plates*, Archives of Acoustics, **34**, 1, 25–39.

c. Book, encyclopedia and article titles should be italicized.

1. Books

Author, initials (year), Title of the book [language of publication – if other than English], Edition, if later than the first, Publisher, Place of publication.

Examples:

- American Psychological Association (2001), *Publication manual of the American Psychological Association*, 5th Ed., Washington D.C. [Author].
- Encyclopedia of Physics* (1993), 2nd edition, McGraw-Hill, New York.
- Varshneya A. (1944), *Fundamentals of inorganic glasses*, p. 111, Academic Press, New York.
- Moore M.H., Estrich S., McGillis D., Spelman W. (1984), *Dangerous offenders: the elusive target of justice*, Harvard University Press, Cambridge.
- Strunk W., White E.B. (1979), *The elements of style*, 3rd Ed., Macmillan, New York.
- Engel Z., Piechowicz J., Stryczniewicz L. (2003), *The fundamentals of industrial vibroacoustics* [in Polish], WIMIR AGH, Kraków.
- Nowicki A. (1995), *Basics of Doppler Ultrasonography*, [in Polish:] *Podstawy ultrasonografii dopplerowskiej*, PWN, Warszawa.

List up to six (6) authors. If there are seven (7) or more, list the surname and initials of the first one and then “et al.”

2. Edited book

Editor, initials (Ed.), (year), Title of the book, Edition if later than the first one, Volumes if there are more than one, Publisher, Place of publication.

Examples:

- Crocker M.J. [Ed.], (2007), *Handbook of Noise and Vibration Control*, John Wiley & Sons, Inc., New York.
- Klinke R., Hartman R. [Eds.], (1983), *Hearing – physiological bases and psychophysics*, Springer, Berlin, Heidelberg, New York, Tokyo.

3. Chapter in edited book

Author of chapter, initials (year), Title of chapter, [in:] Title of the book, Name of the Editor/s Initials [Ed.], pp. start and end of chapter page numbers, Publisher, Place of publication.

Example:

- Rakowski A. (1991), *Context-dependent intonation variants*, [in:] *Music, language, speech and brain*, Sundberg J., Nord L., Carlson R. [Eds.], pp. 203–211, MacMillan Press, London.
- Berlincourt D.A., Curran D.R., Jaffe H. (1964), *Piezoelectric and Piezomagnetic Materials and Their Function in Transducers*, [in:] *Physical Acoustic*, Mason W.P. [Ed.], vol. 1, part. A, pp. 169–270, Academic Press, New York.

4. Journal article

Author, initials (year), Title of the article [language of publication – if other than English], Title of the journal, Volume number (bold face), issue number, start and end page numbers of article.

Write directly page numbers (not preceded by p. or pp.),

Examples:

- Houtsma A. (2007), *Experiments on pitch perception: Implications for music and other processes*, Archives of Acoustics, **32**, 475–490.
- Sek A., Moore B. C. J. (1995), *Frequency discrimination as a function of frequency, measured in several ways*, Journal of the Acoustical Society of America, **97**, 2479–2486.
- Ranachowski P., Rejmund F., Pawelek A., Piątkowski A. (2005), *Studies of cordierite material under compressive load at different temperatures and after thermal shock* [in Polish], Ceramics, **89**, 101–115.

5. Conference paper in published proceedings

Example:

- a. Rakowski A., Miśkiewicz A. (2002), *Pitch discrimination of low-frequency tones*, Proceedings of 7th International Conference on Music Perception and Cognition , pp. 538–540, Sydney.

6. Dissertations in congresses and meetings (unpublished)

Example:

- a. Tucker S. (2003) , *An ecological approach to the classification of transient underwater acoustic events: perceptual experiments and auditory models*, Ph.D. Thesis, Department of Computer Science, University of Sheffield.
- b. Salamon R. (2009), *Contemporary military sonar system*, Dissertation presented during the 56th Open Seminar on Acoustics, OSA 2009, Goniądz, Poland.

7. Electronic sources

Author, initials (year), Title, Retrieved month, day, year, from Internet address.

If no date is shown on the document, authors should use n.d. (no date)

If the author is not given, authors should begin the reference with the title of the document.

If a document is part of a large site such as a university or a government department's website, give the name of the parent organization and the relevant department before the web address.

Examples:

- a. Cox T. (n.d.), *Sound quality*, from www.acoustics.salford.ac.uk/res/cox/sound_quality/
- b. Deciding your future (2000), Retrieved September 5th, 2001, from University of Portsmouth, Careers Service: www.port.ac.uk/departments/careers/plancareer/deciding-your-future.htm
- c. Alexander J., Tate M.A. (2001), *Evaluating web resources*, Retrieved August 21st, 2001, from Widener University, Wolfgram Memorial Library: www2.widener.edu/Wolfgram-Memorial-Library/webevaluation/webeval.htm

Authors should not write the web address (URL) within the text of the paper, it should appear only in the reference list/bibliography. To cite this source within the text they should use the author's name (if the reference has one) or the first few words of the website title.

8. Audiovisual sources: music

Author, initials (Date of copyright), Title of the song. On Title of the album [medium of recording], Location: Label (Recording date if different from copyright date)

Example:

- a. Puccini G. (1990), *Nessun dorma*, On Carreras Domingo Pavarotti in concert [CD], Decca, London.